Differential toxicity of two murine endothelial cells to ROS duress:
Understanding oxidative stress-induced blood-brain barrier dysfunction

By

Olufemi Akinyinka Alamu

M.B; B.s., MSc Anatomy

A thesis submitted in partial fulfilment of the requirement for the degree of

Doctor of Philosophy

Faculty of Science, Department of Medical Bioscience

University of the Western Cape

Cape Town, South Africa

Supervisors: Prof David W Fisher, And Prof Okobi E Ekpo

January 2020

Abstract

The blood-brain barrier (BBB) is a critical interface between the blood circulation and brain tissue which performs critical selection of circulating molecules that gain access to the brain tissue. Its unique ability to adjust to changes in the constituents of the blood circulation confer in the BBB a dynamic nature enabling changes in its properties to suit the homeostatic needs of the brain.

Dysfunction of the BBB has been established to be pivotal to the initiation and/or maintenance of an array of neurological disorders, most of which involve the production of excess reactive oxygen species (ROS) and oxidative stress in their pathophysiology. Thus, clinical trials of exogenous antioxidant agents have been proposed and initiated, with most results being inconclusive. Extensive studies of the impact, capacity and plasticity of endogenous antioxidants in the cells that constitute the blood-brain barrier, especially the brain endothelial cells, therefore, became necessary for the rational choice, timing, and the mode of application of antioxidants in the management of oxidative stress-mediated neurological diseases.

In the present study, incremental hydrogen peroxide (H_2O_2) concentrations were dosed in cell culture medium to simulate OS and gauge the capacity of the brain endothelial cell (BECs) models of the BBB to resist ROS toxicity, the contribution of endogenous antioxidants to this resistance and to study the morphological changes in ROS-mediated BBB dysfunction.

Two types of mammalian endothelial cells, b.End5 and bEnd.3, commonly used for *in vitro* studies of the blood-brain barrier, were selected for use in this study. A combination of spectrophotometry, fluorescent microscopy, trypan blue exclusion method and flow cytometry were used to assess cell viability, cellular glutathione (GSH) content, cell cycle changes, cellular death by apoptosis and necrosis in BECs exposed to incremental H_2O_2 concentrations for 24hr. Exogenous antioxidants were variably administered to study the effects of externally incident antioxidants when the cells were under H_2O_2 exposure.

Results showed that b.End5 cell line significantly tolerated higher concentrations of H_2O_2 than the bEnd.3 cell line. GSH contents for both cell lines were fairly similar under physiological conditions but after exposure to H_2O_2, b.End5 cells demonstrated higher resistance to GSH depletion than the bEnd.3 cell line, although the two cell lines were obtained from the same animal species. Along incremental concentrations of H_2O_2, increased cell proliferation, cell necrosis and apoptosis and cell cycle arrest were observed concurrently. At H_2O_2 concentrations that defined OS, live cells were depleted in b.End5 cells used while there was significant increases in apoptotic and necrotic cells with apoptotic cells as the significant

majority comparatively. Cell cycle studies showed arrest of cell division at the G2/M phase of the cell cycle at higher concentrations of H_2O_2. Application of exogenous antioxidants ameliorated the H_2O_2-induced cellular depletion as well as improved recovery in cellular viability following withdrawal of H_2O_2 after 24hr exposure.

It was conclusive that apoptotic pathway of cellular death is a major pathway of BECs response to OS. Also, there was differential H_2O_2 toxicity and GSH *de novo* synthesis capacity between the b.End5 and bEnd.3 cell lines despite their common origin from the same animal species and their possession of similar contents of endogenous antioxidant GSH under physiological conditions.

This finding calls for more caution for the choice of cellular models for specific studies of the BBB to ensure that results obtained are reproducible, reliable and sufficiently conclusive. Furthermore, our results tend to suggest that the processes responsible for the endothelial component of BBB dysfunction under conditions of oxidative stress occur concurrently and include increased proliferation, necrotic and apoptotic cell death as well as cell cycle arrest. Additionally, study suggests that the clinical administration of antioxidants could be an appropriate intervention for the alleviation of neurological diseases.
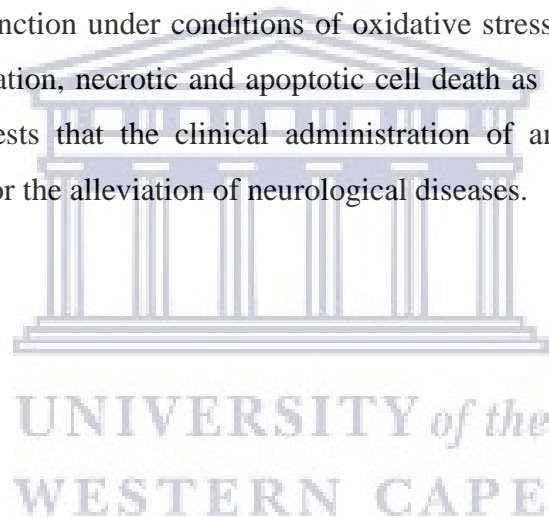
Keywords

Reactive oxygen species, oxidative stress, b.End5, bEnd.3, necrosis, apoptosis, proliferation, cell cycle, flow cytometry, glutathione, antioxidants, blood-brain barrier, degenerative neuropathy.

Declaration

I declare that '' *Differential toxicity of two endothelial cells of murine origin to ROS duress: Understanding oxidative stress-induced blood-brain barrier dysfunction.*'' is my original work that has not been submitted before for any degree or examination in any other university. During review of published data and literature, all the sources I have used or quoted have been indicated and acknowledged by complete references.

Olufemi Akinyinka Alamu   Signature _____

January 2020

Acknowledgements

I wish to return all glory to the Almighty God who has been my Ultimate source of inspiration and strength through the journey to the completion of this work; had the Lord not been there, I would have had nothing. His Holy Name be for ever exalted.

My profound gratitude goes to my ever listening and supportive Supervisor, and Co-supervisor, Prof. David W. Fisher and Prof. Okobi E. Ekpo, for motivating and encouraging me to finish the work under their thorough and effective supervision. I am genuinely indebted to Prof. DW Fisher for his guidance, inspiration and encouragement throughout the difficult times in the course of this project. God will reward you excellently for all your efforts. Furthermore, I am most grateful to Prof. O Ekpo for providing me with the link to Prof. Fisher without which I would not have had this great opportunity to come under his supervision.

I would also like to thank Prof. Emmanuel Iwuoha, Dr Tesfaye Waryo and Dr Unathi Sidwaba for the opportunity offered me to learn and attempt to fabricate an aptasensor for the detection and assay of glutathione in the Sensor Lab, Chemical Science Building, University of the Western Cape. Though, the aim was incompletely fulfilled, techniques learnt remained invaluable and will hopefully be applied in my future research projects.

I wish to show appreciation to my laboratory colleagues and companions who have one way or the other offered advises, observations and input that have contributed immensely to the final success of this project. I must say thank you to Mrs. Mariam Abobaker-Rado, Miss Shireen Mentor, Mrs. Hanan Abd-Elwahab, and Mr Omar Zabeda for not just being colleagues in the Neurobiology lab, Department of Medical Bioscience but also family. I wish to show appreciation also to my friends and companions in the Department of Medical Bioscience who made my stay in the department a wonderful one, Mr Hassan Ghanaim, Miss Tarryn Weber, Miss Eurinah Harris, Mr Kenau Pearce, Mr Yanga Mnyamana, Mr Robben Boysen, Miss Palesa Makoti, Mr Akeel Morris, and others that space would not permit me to mention.

I am also grateful to my colleagues from Ladoke Akintola University, Ogbomoso Nigeria, for their companionship, Dr Ayoola Isaac Jegede, and Dr Olubunmi Simeon Oyekunle. Similar expression of my gratitude for the company of other colleagues from Nigeria, Dr Sylvester Ifeanyi Omoruyi and Dr Adaze Enogieru. My loyalty and gratitude also goes to the following

friends who have contributed to my joyful stay during my study period in Cape Town: Dr Albert O. Amosu, Dr Popoola Olugbenga, Dr James Ayuk, Dr Agbele Kehinde, Dr Sunday T Vodah, Dr Okuntade O. Japhet, Dr Oladipo David, and Dr Kolajo Akinyede.

I am grateful for the support of my immediate and close family members throughout my stay far away from home to complete the work of this study, starting from my dad and mum, Mr. and Mrs. Joseph Olalekan Alamu, and my siblings Mr. and Mrs. Ayodele Olalekan, Mr. and Mrs. Adewumi Alagabi, Mr. Abimbola Olalekan, Mr. and Mrs. Taiwo Folusho Alamu, Mr. and Mrs. Kehinde Olumide Alamu; my lovely aunt and her family Mrs. MA Ogunwole and finally my Cape Town family who gave me immense family support throughout my entire stay to study in the city of Cape Town, Mr. and Mrs. Tunbosun Eluyoye. God bless you all.

Finally, my deepest and sincere appreciations go to my sweetheart, Mrs. Grace Olubunmi Alamu and our lovely children Miss. Olubusayo Opeyemi and Mr. Oludamilare Akintunde Alamu for their immense support and understanding throughout this whole period spent far away from home. Your encouragement and reassurance kept me going through the trying period of my stay in Cape Town. The Lord bless you ceaselessly.
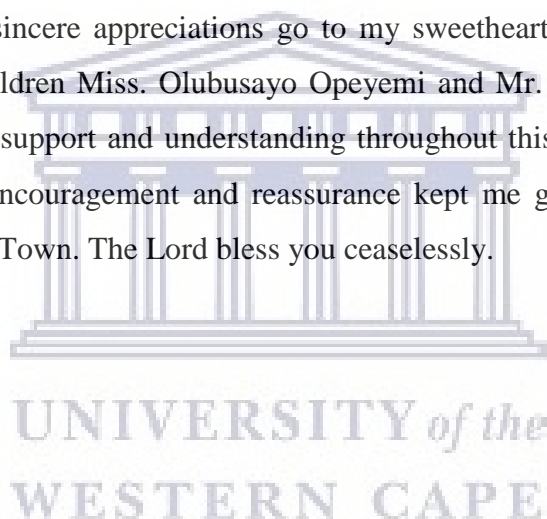
Dedication

I dedicate this work to the Almighty God who has given me the inspiration and sustenance to start and complete the work of this project. Additionally, I dedicate the work of this project to the following important people in my life:

My dad and mum, Joseph Olalekan Alamu, and Comfort Morenike Alamu, who supported me in their prayers for the success of this work; My Spouse, Grace and my children Busayo and Damilare who bore the pains of staying without me throughout the duration of this programme.

List of Publications/conferences

Article

Olufemi Alamu, Mariam Rado, Okobi Ekpo, and David Fisher (2020). Differential Sensitivity of Two Endothelial Cell Lines to Hydrogen Peroxide Toxicity: Relevance for in Vitro Studies of the Blood-Brain Barrier (Accepted), *Cells* MDPI.

Book Chapter

Fisher D, O. Alamu (2020). The relationship between the blood-brain barrier, degenerative neuropathy and oxidative stress. In: Martin CR, Preedy VR, editors. Oxidative Stress and Dietary Antioxidants in Neurological Diseases. San Diego: Academic Press.

Conference Presentation

a. Defining Oxidative Stress at the blood-brain barrier: a quantitative approach: First Conference of Biomedical and Natural Sciences and Therapeutics (CoBNeST, 7-10 October 2018) Stellenbosch

Table of contents

List of Figures

List of Tables

List of Abbreviations

CNS; Central nervous system

BBB; Blood-brain barrier

NCD; Non communicable disease

DALY; Disability adjusted life years

WHO; World health organisation

AD; Alzheimer's disease

PD; Parkinson's disease

MS; Multiple sclerosis

ROS; Reactive oxygen species

OS; Oxidative stress

NDD; Neurodegenerative disease

AO; antioxidants

GSH; Glutathione

GSSG; Glutathione disulphide

PCR; Polymerase chain reaction

HRP; Horse-radish peroxidase

TJ; Tight junction

ATP; Adenosine triphosphate

CSF; Cerebrospinal fluid

NVU; Neuro-vasculo-glial unit

ISF; Interstitial fluid

ECs; Endothelial cells

PCs; Pericytes

SMCs; Smooth muscle cells

ECM; Extracellular matrix

BM; Basement membrane

GDNF; Glial cell line-derived neurotrophic factor

VEGF; Vascular endothelial growth factor

JAM; Junctional adhesion molecule

ZO1; Zona occludens 1

Pgp; P-glycoprotein

GLUT1; Glucose transporter 1

NAA; Neutral amino acids

EAAT; Excitatory amino acid transporter

ECF; Extracellular fluid

NKCC1; Sodium-potassium-chloride cotransporter 1

NHE1; Sodium-hydrogen exchanger 1

NBCn1; Sodium-bicarbonate cotransporter 1

AE2; Anion exchanger 2

DHA; Docosahexaenoic acid

EPA; Eicosapentaenoic acid

1   CHAPTER ONE

1.1   Introduction

The blood-brain barrier, BBB, is a partition between the blood circulation and the central nervous tissue and a structure that must be traversed by molecules in order to gain access to the interior of the central nervous system, CNS (Daneman & Prat, 2015). It presents a dynamic interface between the circulating blood and the central nervous tissue capable of modifying the ease of passage across it in response to signals from both blood circulation and the CNS (Daneman & Prat, 2015). It selects the constituents of the circulating blood that is transported into central nervous tissue, a function which it performs when it selectively prevents the passage of some molecules while showing preference for selected others (Abbott *et al.*, 2010). Abnormality of this barrier function has been reportedly implicated in the development and/or propagation of several neurological diseases (Abdullahi *et al.*, 2018; Chakraborty *et al.*, 2017) including stroke and neurodegenerative diseases (degenerative neuropathies) such as Alzheimer and Parkinson's diseases. These neurological disorders are classified by the World Health Organization (WHO) into non-communicable diseases (NCD) which together contribute about 54% to the global burden of diseases in 2010, when estimated using disability-adjusted life years (DALY) as the metric (Chin & Vora, 2014). DALY, is defined as the sum of the years of life lost due to premature mortality and years lived with disability (Murray *et al.*, 2012). WHO in 2010 reported stroke to be the second leading global cause of premature death and disability (Chin & Vora, 2014). Stroke is defined as acute focal neurological dysfunction caused by focal infarction at a single or multiple sites of the brain and retina (Kasner & Sacco, 2013). However, neurological disorders such as Alzheimer's disease (AD) and other dementias, Parkinson disease (PD), epilepsy and multiple sclerosis (MS), are categorized differently as stroke (Chin & Vora, 2014). Combination of neurologic disorders and cerebrovascular accident contribute 7.1% of the total global burden of disease in 2010 (Murray *et al.*, 2012). Within this combined estimates of the global burden of neurologic disorders and cerebrovascular disease as reported in 2010, haemorrhagic stroke (35.7%) and ischemic stroke (22.4%) contribute the largest portions of DALY. In addition, the burden of neurodegenerative diseases is reported to be growing at an alarming rate: between 1990 and 2016, number of deaths attributed to Parkinson's and Alzheimer's diseases and other dementias almost doubled (Collaborators, 2019). About 26.6 million people suffers from Alzheimer's disease in 2006 and this prevalence is projected to quadruple by 2050 (Collaborators, 2019)

due to the likelihood of more aged people to live longer with the disease because of advancement in the modalities of treatment. Aging is an important contributing risk factor in the development of neurodegeneration and BBB disruption has been reported to occur early in the aging human brain (Erdő *et al.*, 2017). Research evidence has indicated that a higher incidence of age-related neurodegeneration begins in the hippocampus, a brain region associated with cognitive functions (Takeda *et al.*, 2014). Additional reports from quantification of regional BBB permeability in the living human brain have also indicated an age-dependent BBB breakdown in the hippocampus, a brain region affected early in AD (Nissanka & Moraes, 2018).

1.2   Background of the study

Importantly, a number of the neurological disorders especially the neurodegenerative diseases (NDDs) have been linked to both oxidative stress (OS) and a dysfunctional BBB (Rosenberg, 2012). The BBB dysfunction observed in neurodegenerative diseases has in turn been severally linked to OS-induced brain endothelial cellular changes (Freeman & Keller, 2012; Krizbai *et al.*, 2005). OS is the cellular status which results when there is an imbalance between the cellular generation and neutralization of reactive oxygen species (ROS), either due to excessive ROS production or inadequacy of endogenous cellular antioxidants (Sies *et al.*, 2017).

Though several studies have documented the presence of OS in the earlier stages of most NDDs, it is difficult to say if OS is a cause or consequence of the neurodegenerative process. However, in the treatment and/ or alleviation of these disorders, use of antioxidants are being considered and clinical trials are ongoing (Barnham *et al.*, 2004; Jomova *et al.*, 2010; Mecocci & Polidori, 2012). Surprisingly, despite several clinical trials the overall clinical benefit of antioxidant in the treatment and/or alleviation of neurological disorders remains inconclusive (Galasko *et al.*, 2012). In view of the ongoing search for antioxidants with promising effects in the treatment of BBB dysfunction-linked NDDs, it is of considerable importance to first look inward and investigate the capacity of the endogenous antioxidant systems within the cellular components of the BBB to respond by buffering both endogenous and exogenous production of ROS, and the possible manipulation of such systems for the protection of the BBB in conditions that induces ROS production. The central component of the BBB are the endothelial cells of the brain capillaries which functions are modulated by supporting cells in contiguous interaction (Abbott *et al.*, 2010).

1.3   Rationale of the study

To date, the functions and structure of the BBB have been studied using both *in vivo* model using different experimental animals, and *in vitro* models of the BBB (Coronado-Velázquez *et al.*, 2018). The *in vitro* models often engage the use of endothelial cells of animal origin such as mouse, rat, and bovine with the intent to harmonize findings obtainable from animal models of same species (Campisi *et al.*, 2018). However, most of the *in vitro* models have not been characterized for their ability to mount up adaptive responses under the condition of accumulating ROS which are features necessary for the definition of OS as well as features that characterize changes in OS responsible for the observation of abnormal permeability under OS conditions. Researchers have hence used arbitrary concentrations of selected ROS to study cellular changes in brain endothelial cells of identical origin to study diverse changes under conditions of OS (Cao, Dai, *et al.*, 2019; Song *et al.*, 2014). It is therefore necessary to characterise commonly used endothelial cells for their suitability for use as models for specific investigations pertaining to the nature of the BBB. In this study, it is reinforced that OS affects the cells of the BBB by limiting their viability with regards to physiological functioning and survival as well as their ability to proliferate and replace lost cells (Li *et al.*, 2012).

1.4   Problem statements

The capacity of virtually all of the brain endothelial cell models for *in vitro* studies of the BBB to survive under condition of accumulating ROS and /or OS has not been well studied. This has created unnecessary murkiness in the appraisal and /or harmonisation of data obtainable from the studies using the different cells because scientists just assign arbitrary concentrations of ROS molecules to the cells in the different studies. The characteristics of the endogenous antioxidant systems within brain endothelial cell models have not been well studied to evaluate how they respond to keep the cell in oxidative eustress when encountering redox challenges. Furthermore, the responses in brain endothelial cells to ROS and OS that culminate in BB dysfunction has not been completely understood.

1.5   Aim of the study

This study aims to utilize selected *in vitro* models to study the response of the endothelial cells of the BBB to ROS of variable strength with regards to cell survival or death and how these effects impact on the understanding of BBB dysfunction. Furthermore, specific ROS

concentrations suitable for the definition of OS were determined. Established *in vitro* models utilizing mouse-derived cells were used and cultured cells were exposed to selected ROS molecule of varying concentrations and parameters in the cultured cells in relation to cell survival which impact on BBB integrity were recorded. First the capacity of the cultured cells to survive exposure to escalating ROS strength was determined. In addition, attempts were made to experimentally enhance the survival capacity of the cells by application of selected exogenous antioxidants (AO). Then, the presence of a selected endogenous antioxidant was determined and quantified with and without ROS treatments. Furthermore, at redox conditions where cellular survival was lost and cells became depleted in culture, the mechanisms for cell depletion were carefully studied in line with existing mechanisms for cellular death. The findings were interpreted in line with existing information regarding the functionality of the BBB.

1.6   Objectives of the study

The objectives of this study were drawn in 4 parts:

1.6.1   Cell viability/survival

- The ROS-buffering capacity of two blood-brain barrier endothelial cell-line models were determined and compared
- A possible protective effect of an exogenous antioxidant on the ROS-buffering capacity of each of the cell-line models were determined

1.6.2   Endogenous antioxidant protection

- The presence of endogenous antioxidant, GSH, in the two cell-line models were detected and defined
- Quantification and comparison of the cellular GSH content in the two model cells and determination of the baseline oxidative status of each cell in normal culture using the GSH:GSSG ratio were done.
- Quantitative tracking of the response of endogenous cellular GSH in each cell during exposure to escalating ROS concentration was done.

1.6.3   Mechanisms of endothelial cell inhibition during escalating ROS exposure

- Necrosis

- Apoptosis:
  - Mitochondrial involvement:
    - Mitochondrial depolarization assays:
      I. Fluorescence microscopy
      II. Flow cytometry
- Cell cycle study by flow cytometry

1.6.4 Determination of the ROS level that quantitatively defines OS for each model.

1.7 Significance of the study

This study is important in that it provided some mechanistic insights into the negative impact of ROS and/or OS on the BBB functionality which clearly forms a critical component of neurodegenerative process as well as other neurological diseases. It has also defined the reproducible concentration of ROS in selected cell line that is suitable for modelling OS.

1.8 Scope

This work was designed to utilise cellular approaches to the measure of viability and chemical quantification and detection of cellular antioxidants. Measurement and characterisation of cellular deaths with a probe into selected mechanisms involved in cell death were experimentally carried out. Because known concentrations of ROS were incident on the cells in culture, measurement of ROS in the cells was not undertaken. Additionally, the work does not cover measurement of changes in ribonucleic acid by PCR methods as well as western blot analysis of protein expression changes.

1.9 Chapter summary

In this chapter, the work of this project is introduced with details of what constitute health challenges globally with some statistics of the volume of the problem with regards to this health challenges. The background to this study is clearly stated with regards to how the problems have been scientifically approached and limitations to the depth of the current solutions available. Why this study is necessary and the possible merits of the work when completed were clearly stated. The next chapter will present discussion on relevant existing work with respect to ROS and OS-mediated BBB dysfunction and the role of antioxidants

2 CHAPTER TWO: Literature review

2.1 Introduction

In this chapter, a broad range of topics with respect to existing scientific reports pertaining to the blood-brain barrier physiology and pathophysiology, reactive oxygen species and oxidative stress and the role they play in impacting diverse changes in cellular physiology and pathophysiology will be discussed. Additionally, antioxidants and their uses, classification, adverse effects of their use and specific antioxidants will be reviewed.

The chapter will be discussed in four parts that will include, Introduction to the blood-brain barrier, historical background, and location of the BBB, anatomical description of the BBB and the physiological functions of the BBB. Reactive oxygen species will be introduced and discussed with respect to the production and sources of ROS, the concept of oxidative stress, the impact of ROS on cellular signalling, BBB regulation and its role in neurological disorders with component of BBB dysfunction. General introduction to antioxidants will be discussed and the antioxidant therapy in neurologic diseases will be reviewed. The concluding section of the chapter will critically reviewed existing reports on the nature and historical background of glutathione, its homeostasis in the cell, and its role in cellular redox signalling. The chapter will then be summarised.

2.2 Introduction to the blood-brain barrier

2.2.1 Historical Background

The over twelve decades history of dye injections studies by the German scientist, Paul Ehrlich, heralded our current knowledge of the concept of what is now known as the blood-brain barrier (Ribatti *et al.*, 2006). He had reported, in 1885, the exclusion of the brain and spinal cord from staining following parenteral injections of a variety of vital dyes in adult animals (Ehrlich, 1885). He concluded that the CNS has a low or no affinity for vital dyes.

Biedl and Kraus (1898) and Lewandowsky (1900) postulated the existence of a barrier at the level of cerebral vasculature when they observed presence and absence of neurological symptoms on the CNS when cholic acids and sodium ferrocyanide were respectively injected intraventricularly and intravenously (Biedl & Kraus, 1898; Lewandowsky, 1900). Lewandowsky in 1900 then introduced the term "blood-brain barrier"

In 1909 and 1913, Goldman further demonstrated the presence of a barrier using Trypan Blue dye. He demonstrated that the brain stained blue on intraventricular injection of Trypan blue but unstained on intravenous injection which demonstrated the presence of a barrier between the brain and the peripheral blood circulation (Edwin E Goldmann, 1909; Edwin Ellen Goldmann, 1913).

Between 1913 and the 1960s, the structural definition of the blood-brain barrier remained unclear mostly due to the limited resolution of the light microscope which does not clearly resolve the thickness of a cerebral endothelial cell. However, with the development of the electron microscope in 1931, the definition of ultrastructural features of blood vessels became possible.

In the late 1960s was the site of the mammalian BBB localized. Some light microscopy (LM) studies had indicated the passage of a macromolecular tracer, horseradish peroxidase (HRP) into the brain parenchyma (Westergaard, 1977). HRP is a glycoprotein with a molecular weight of 40,000 which is demonstrable by both light and electron microscopy (Krzyzowska-Gruca, 1966). Karnovsky, 1967, had demonstrated that HRP injected intravenously into mice passed freely out of capillaries in cardiac and skeletal muscles (Karnovsky, 1967). Reese and Karnovsky, 1967, were the first to demonstrate at ultrastructural level that the endothelium of the mouse cerebral capillaries constitutes a structural barrier to the HRP (Reese & Karnovsky, 1967). The barrier is made up of the plasma membrane and the cell body of endothelial cells and of tight junctions (TJs) between adjacent cells. The TJs completely obliterate the narrow cleft between adjacent cells. It was found that HRP was able to pass into the interendothelial spaces only up to the first luminal interendothelial TJs in cerebral capillaries, but not beyond. Pinocytotic vesicles were found to be uncommon and not involved in the transport. Similar results were obtained using tracers with molecular weights much smaller than HRP such as microperoxidase with molecular weight of 1,900 and diameter of 2nm and even lanthanum ion with ionic radius of 0.115nm (M. Brightman & Reese, 1969; Feder, 1971). The TJs enable the active exclusion of specific solutes from the interstitial fluid while facilitating the transfer of other solutes from plasma to CNS fluid.

At about the same time, Brightman (1965, 1968) showed that either ferritin or HRP injected into the intraventricular space passed between ependymal cells into the brain interstitium and through the astrocyte endfeet gap junctions into the area of the basement membrane, where the tracers were then stopped by the endothelial cells (M. W. Brightman, 1965, 1968). These

30

findings supplement those of Reese and Karnovsky, showing that the anatomical site of the BBB was neither the astrocytic endfeet nor the basement membrane, but rather the endothelium itself.

The study of the BBB further advanced in the 1970s when techniques for isolation of brain microvessels became introduced and leading into the subsequent isolation of BBB plasma membranes for biochemical and radio-receptor studies (Pardridge, 1998). Brain capillaries are isolated by either mechanical or enzymatic homogenization but these isolates so derived were found to be non-metabolically viable in that they have very low ATP levels (Lasbennes & Gayet, 1984). Because isolated brain capillaries feature an intact membrane preparation of the BBB, they are suitable for experiments that cannot be done with other methodologies.
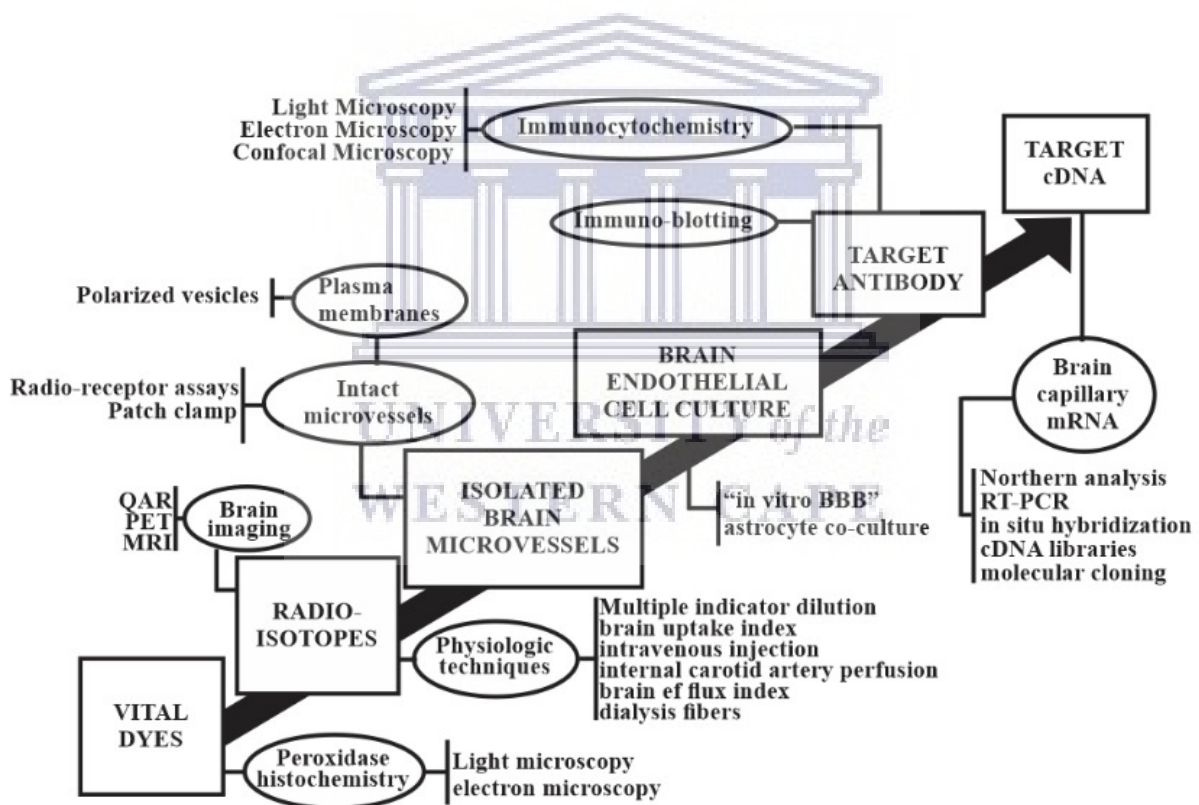
Figure 2.1: Linear evolution of blood-brain barrier research methodology from vital dyes to molecular biology (Pardridge, 1999).

Despite increased, multifaceted understanding of the nature of the BBB to date, however, the manipulation of the BBB for prevention, alleviation and treatment of CNS disorders has remained challenging

Plating of brain capillary endothelial cells began in the 1980s culminating in the development of early *in vitro* BBB models (Bowman *et al.*, 1983; DeBault *et al.*, 1979). Furthermore, it was found that tissue culture grown endothelial cells lack many of the characteristics of the *in vivo* BBB which deficiency was subsequently addressed by endothelial-astrocyte co-cultures. In the 1990s, biochemical and molecular biological analysis of BBB properties began with the production of target specific cDNAs and antibodies for the study of proteins and mRNAs in isolated microvessels (Boado & Pardridge, 1991).

.

2.3 Importance of the blood-brain barrier

The functions of the CNS depends on the excitability of its neurons which involves the generation of electrochemical impulses that enable the neurons to generate, transmit and integrate nervous signals. The dependence on electrical and chemical signals for the generation of nervous impulses in the CNS demands for critical regulation of the local composition of ions around conducting segments of neurons. This demand was, arguably, a major drive for the development of mechanisms for the maintenance of the homeostasis within the neural microenvironment (Abbott, 1992). This function, is brought about by cells at three critical interfaces that form barriers which tightly regulate blood-CNS exchange. These barriers include the blood-brain barrier (BBB), the blood-CSF barrier and the arachnoid barrier (Abbott *et al.*, 2010). The BBB, localized to the brain microvascular endothelial cells provides a comparably larger surface areas than the other two barriers and forms the largest site for the blood-CNS exchange (Abbott *et al.*, 2010; Nag & David J, 2005). It exhibits barrier function that is mechanical, transport and metabolic in nature: the mechanical barrier is localized to tight junction between the endothelial cells that line the brain microvessels while the transport barrier is dependent on the presence of various specific membrane transporters and vesicular mechanisms within the brain microvascular endothelial cells and the metabolic barrier consists of metabolizing enzymes that modify molecules in transit (Abbott *et al.*, 2010; Liebner *et al.*, 2018; Serlin *et al.*, 2015). The functions and properties of the BBB though mostly reside in the endothelial cells, are regulated by the paracrine influence of other cells contributing to the BBB such as pericytes, astrocytic endfeet, glial cells, neural cells and immune cells, in what is referred to as the neuro-glio-vascular (NGV) unit (Daneman & Prat, 2015).

Functions of the BBB includes the regulation of ionic milieu within the CNS, protection of the CNS from surge of plasma neuro-excitatory glutamate such as occurs after a meal, it prevents

entrance of macromolecules and neurotoxins while permitting the entrance of nutritional molecules such as glucose and amino acids.

In regulating the composition of important ions within the millieu of the CNS it utilizes specific ion channels transporter to maintain stable ionic composition for normal synaptic impulse generation and conduction. The mammalian plasma potassium concentration approximates 4.5mM while that of CSF and brain ISF is maintained at approximately 2.5-2.9mM. It is reported that the CSF and brain ISF potassium concentration remained unchanged following meal, exercise and when potassium is imposed experimentally (Abbott *et al.*, 2010; Hansen, 1985). Furthermore, calcium and magnesium ion concentrations as well as pH are also well regulated at the BBB (Nischwitz *et al.*, 2008).

2.4   Location of the blood-brain barrier

The blood-brain barrier is anatomically localized in the capillaries of the brain. The brain receives blood supply from the carotid and vertebral vessels and within the parenchyma of the brain divides into smaller vessels of capillary bore, usually single endothelial layer thick. This presents the level of tissue exchanges, as also found elsewhere in the body. However, at the capillary level in the brain the endothelial cells exhibit peculiar phenotype responsible for the characteristics that culminates in the barrier properties of these capillaries.

2.5   Structure of the blood-brain barrier

The micro-vessels of the brain consist of two main cell types, the endothelial cells (ECs) that line the blood vessels while adherent to a basement membrane and the mural cells that sleeves the abluminal surface of the ECs. Mural cells collectively refer to pericytes (PCs) and vascular smooth muscle cells (SMC). While PCs are mural cells of micro-vessels, SMCs are found in arteries and veins. Though the BBB properties are conferred by the ECs, they are stimulated and maintained by intricate interactions with the mural cells, immune cells, glial cells, and neural cells in the complete set up known as the neuro-vasculo-glial unit (NVU) (Abbott *et al.*, 2010; Daneman & Prat, 2015).

2.6   Endothelial Cells of the BBB

The ECs of the BBB are modified simple squamous epithelial cells that line the walls of blood capillaries. They exhibit polarity in that they present two surfaces, one which rests on a

basement membrane called the abluminal surface and the other which relates to the circulating blood referred to as the luminal surface. They are held together by tight junctions, which tightly restrict paracellular transit of solutes, and adherent junctions (Abbott *et al.*, 2010; Liebner *et al.*, 2018). Other properties of BBB ECs include exhibition of extremely low rates of transcytosis which limits vesicular transcellular transit of molecules and cells. These two barrier systems functionally polarized the EC into distinct luminal and abluminal membrane compartments regulating the movement of molecules between the blood and the brain(Daneman & Prat, 2015). Exclusion of some lipophilic molecules from the brain, while selectively transporting similar molecules of obligatory importance, is achieved by the expression of two modalities of transporters which appear to sort molecules as either wanted or unwanted (Daneman & Prat, 2015; Serlin *et al.*, 2015). Efflux transporters transport lipophilic molecules which can normally freely diffuse through the cell membrane back into the blood. The highly specific nutrient transporters ferry specific nutrients across the BBB into the CNS and also remove specific waste products from the brain into the blood. Other properties of the brain ECs include possession of higher mitochondrial density than ECs elsewhere in the body used for ATP generation needed to drive the ion gradient that is crucial to transport functions. Expression of extremely low levels of leukocyte adhesion molecules also greatly restrict the access of immune cells from the circulation (Daneman *et al.*, 2010). Furthermore, presence of metabolic enzymes which alter the physical properties of molecules in transit the EC constitute the metabolic or enzymatic barrier by influencing its reactivity, solubility and transport properties (Haddad-Tóvolli *et al.*, 2017). These barriers facets combine to afford the ECs a dynamic regulation of the CNS homeostasis (Daneman & Prat, 2015; Haddad-Tóvolli *et al.*, 2017; Serlin *et al.*, 2015).

2.7   Mural Cells of the BBB

Mural cells in micro-vessels that form the BBB include the pericytes (PCs) which form an incomplete enclosure around the endothelial walls. They are localized to the abluminal surface of the microvascular endothelial tube, embedded in the basement membrane (BM) (Gürsoy-Özdemir & Tas, 2017). PCs contains contractile proteins which serves to control the diameter of the capillaries by their contractile activities. Embedded in the BM which separates them from the ECs they have no direct contact with the ECs (Daneman & Prat, 2015). At discrete points described as peg- and -socket junctions, however, their processes do form cellular adhesion with the ECs mediated by adhesion molecule N-cadherin (Daneman & Prat, 2015).

Other endothelial-pericyte adhesions that have been documented include adhesion plaques, gap junctions and tight junctions. In addition to a higher density of PCs in CNS microvasculature than elsewhere in the body, CNS PCs have a neural crest origin whereas elsewhere in the body PCs are of mesodermal origin (Shepro & Morel, 1993). Their roles include regulation of angiogenesis, deposition of extracellular matrix (ECM), wound healing, regulation of immune cell infiltration and blood flow regulation in response to neural signals and also possibly as multipotent stem cells of the CNS (Armulik *et al.*, 2011). Well documented also is their regulatory role on BBB development as well as the maintenance of its function in adulthood and aging (Armulik *et al.*, 2010; Daneman & Prat, 2015).

2.8 Basement Membrane of the BBB

The basement membrane (BM) forms the outer covering of the vascular tube and has two layers including the vascular layer and the outer parenchymal layer (Daneman & Prat, 2015; Sorokin, 2010). It is crucial to the morphological and functional polarity of the ECs into apical (luminal) and basolateral (abluminal) cell domains. The vascular layer is secreted by the ECs and PCs while the parenchymal BM is secreted by astrocytic endfeet that extend to the vasculature (Daneman & Prat, 2015). The secreted molecular components of the BM include type IV collagens, laminin, nidogen, heparin sulphate, proteoglycans and other glycoproteins (Daneman & Prat, 2015). The vascular and parenchymal layers differ in composition: the vascular layer contains laminins α4 and α5 while the parenchymal layer contains α1 and α2 (Sorokin, 2010; C. Wu *et al.*, 2009) . The BM serves as an anchor for signalling processes at the vasculature as well as provide additional barrier against access of the neural tissue by transiting molecules (Sorokin, 2010). Disruption of the BM by matrix metalloproteinases has been documented as an important component of several neurological disorders (Montagne *et al.*, 2017; Yang & Candelario-Jalil, 2017).

2.9 Role played by astrocytes

Astrocytes are glial cells with polarized cellular processes. The endfeet of their basal processes ensheath the vascular tube containing the BBB and are in direct contact with the basement membrane. The astrocytic endfeet binds to the BM through protein interaction between dystroglycan-dystrophin-agrin binding and by this linkage a process that regulates water homeostasis in the CNS is established (Daneman & Prat, 2015; Noell *et al.*, 2011; Wolburg *et al.*, 2011). They feature proteins such as dystroglycan, dystrophin, and aquaporin 4. Astrocytes

couple neuronal circuits to the blood vessels and by so doing relay signals that regulate blood flow in response to neuronal activity. They are also recognized as important stabilizer of the BBB phenotype (Daneman & Prat, 2015; Daneman *et al.*, 2010). Astrocytes are key elements in the initiation and maintenance of the mature phenotype of the BBB through their endfeet which surround brain capillaries and are thus brought into close proximity and contact with the ECs. This arrangement brings about crosstalk that enhance the phenotypic differentiation of both cell types (Erickson & Banks, 2018). Astrocytic secreted growth factors such as VEGF, glial cell line-derived neurotrophic factor (GDNF), basic fibroblast factor (bFGF) and ANG-1 also provide additional contribution to the BBB phenotype (Cabezas *et al.*, 2014).

2.10 Tight Junctions of the BBB

The integrity of adjacent brain ECs contact is largely contributed by the tight junctions which therefore is responsible for the barrier to macromolecules and polar solutes. The BBB features extremely tight, 'tight junctions' known as *zonulae occludentes* which greatly limits transfer of polar solutes through paracellular pathways between the ECs from the circulating blood plasma to the brain extracellular fluid (Abbott *et al.*, 2010). Adherens junctions (AJs) and tight junction (TJs) are the junctional complexes that bind adjacent ECs. AJs feature cadherin proteins which extend across intercellular cleft and are linked bilaterally into adjacent cells cytoplasm by the scaffolding proteins alpha, beta and gamma catenins. This molecular organization serves to give structural support that holds the cells together and is essential for the formation of tight junctions (Abbott *et al.*, 2010). The tight junctions are made up of additional complex of proteins that also span the intercellular cleft which include occludin and claudins, and junctional adhesion molecules (JAMs). Occludin and claudins are further linked to a number of cytoplasmic proteins which serve scaffolding and regulatory functions. These include the zonula occludens proteins ZO1, ZO2, ZO3 and cingulin (Abbott *et al.*, 2010). Twenty known isoforms of claudin have been reported of which claudin-3 and claudin-5 have been reported to be the most critical to the integrity of the BBB (Abbott *et al.*, 2010). The tight junctions of the BBB responds to locally produced and circulating factors which may alter the paracellular permeability. The barrier functions of the TJs not only depend on the expression of claudin and occludin that span the intercellular cleft but also on the arrangement and interaction of these proteins. Furthermore, the expression of occludin and JAMs also impact on the formation and function of tight junctions (Abbott *et al.*, 2010; Dermietzel *et al.*, 2007). Ions, other polar solutes, such as hexose sugars, vitamins, amino acids, nucleoside

monocarboxylic acids and macromolecules are greatly restricted in passage across the paracellular diffusional pathway due to the TJs. The restriction of ionic passage is responsible for the high *in vivo* trans-endothelial electrical resistance of the blood-brain barrier, estimated at about 1800 ohm cm^2 (Abbott *et al.*, 2010; Butt *et al.*, 1990). Regulation of the strength of the tight junctions is related to the linkage of the intracellular scaffold proteins ZO1, ZO2 and ZO3 with both the junctional molecules claudin and occludin and intracellular actin and cytoskeleton (Wolburg *et al.*, 2009). Several factors have been reported to modulate TJ assembly and thus the strength of the TJs and barrier permeability of the BBB. These include variation in intra/extracellular calcium concentration, vasoactive agents, and cytokines from associated cells of the brain microvessels such as astrocytes, microglia and nerve terminals which are contiguous with the endothelial extracellular matrix/basal lamina (Abbott *et al.*, 2006).

Many of the BBB properties such as the formation of TJs, and polarized expressions of transporters in the luminal and abluminal endothelial membranes were induced by endothelial interactions with astrocytes, pericytes and neurons (Abbott *et al.*, 2006; Nakagawa *et al.*, 2009)
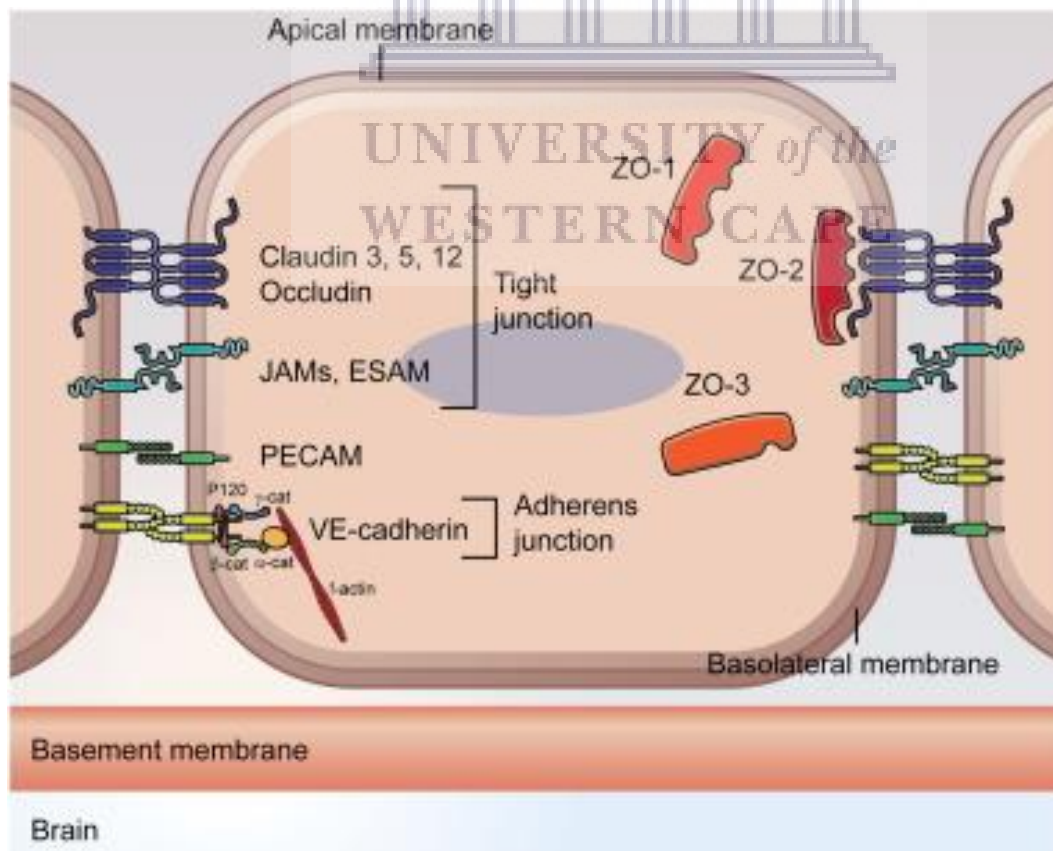
Figure 2.2: Structure of the BBB junctional complex.

Diagram illustrates tight junction and adherent junction. The tight junction consists of occludin and mainly claudin-3 and 5 which span the intermembrane space by binding to each other on each side and are anchored to intracellular actin and cytoskeleton by scaffolding proteins of the zonula occludentes 1, 2, and 3 and cingulin. Adherent junction consists of intercellular VE-cadherin which are also anchored intracellularly to actin cytoskeleton by the α, β and ɣ-catenins. The adherens junction provide structural integrity and attachment between the cells and promote formation of the TJ (Weiss *et al.*, 2009).

2.11 Transport functions of the BBB

There are several mechanisms for BBB permeability just as there are various molecules that are of obligatory importance to the brain while other molecules are necessarily excluded or effluxed from the brain to achieve CNS homeostasis. The TJs play important role in the restriction of transfer of molecules across the BBB. Important factors affecting transfer of molecules include the size of the molecules and its hydrophilic/lipophilic characteristics, though these physico-chemical properties are not always absolute determinants of CNS penetration. Lipid-soluble molecules can passively diffuse through the BBB into the brain at a rate which correlate with its lipid solubility (Abbott *et al.*, 2010). Hydrophilic nutrients are transported mostly actively by specific transporters while most protein cannot diffuse across the BBB. However, some proteins cross by receptor-mediated transport, such as transferrin, insulin, insulin-like growth factor, and low density lipoproteins (LDLs) (Weiss *et al.*, 2009). Furthermore, a large panel of lipophilic molecules, mostly xenobiotics, are actively transported out of the brain against concentration gradient by the *ATP Binding Cassette* (ABC) family of membrane transporters using ATP hydrolysis. The most active ABC-transporters at the BBB are P-glycoprotein (Pgp), multidrug resistance proteins (MRPs) and the breast cancer resistance protein (BRCP) (Weiss *et al.*, 2009). A summary of the major pathways of transport across the BBB include:

1. Trans-cellular or transmembrane diffusion,
   a. Involving passive diffusion of molecule with high lipophilicity and small molecular sizes across brain EC membranes along concentration gradient and usually with no energy expenditure.
   b. Active transfer via active transporters which are ATP-dependent/independent integral membrane proteins that can transport molecules against their concentration gradients. They are of two functional type which include carrier-mediated

transporters, and active efflux transporters (such as *p*-glycoprotein) which transfer drugs and other molecules out of the brain. These proteins are further classified into two: carrier proteins carrying specific molecules, and ion channels which form narrow pores through which ions can pass (Fong, 2015). Ion channels mediate passive transport of ions spontaneously down their gradients while carrier proteins either mediate passive (or facilitated diffusion) or active transport coupled to ATP hydrolysis (Fong, 2015). The latter is the route of transfer for xenobiotics and several other cell processes such as inflammation, cell detoxification, lipid trafficking and hormone secretion (Fong, 2015).

2. Endocytosis and exocytosis (vesicular transport) which involves the internalization of molecules by brain endothelial cells into intracellular vesicles which are then released on opposite cell surfaces.

3. Extracellular/paracellular transfer which is highly negligible due to restriction by TJs.

Common substances trafficking across the BBB include water, blood gases such as O_2 and CO_2, glucose, amino acids, ions/electrolytes such $[Na^+]$, $[K^+]$ and $[HCO_3^-]$ and lipids that are critical to brain survival and function.

2.12 Transport of specific substances critical to brain homeostasis

2.12.1 Transfer of water, O_2, CO_2 and major nutrients across the BBB

Substances of highest fluxes in and out of the brain mostly across the BBB are collectively water, glucose, O_2, CO_2 and amino acids (Hladky & Barrand, 2016). Experimental data using trace water measurements showed that a single pass of blood flow perfusing the brain delivers 70-90% of water in the perfusing blood across the BBB into the brain tissue (Takagi *et al.*, 1987). However, this influx is balanced all over the brain by an almost equal efflux primarily supported by a finding of nearly similar concentration of water on the two sides of the interfaces. It is estimated that a 1000 fold smaller than the unidirectional movement of water approximates the total net flow of water into the brain across the blood-brain interfaces (Hladky & Barrand, 2016; Takagi *et al.*, 1987). Given the observation of high unidirectional flow of water across the BBB, it follows that water molecules can easily move across the BBB. It has been considered that water fluxes could be osmotically driven and osmotic water permeability measurements has been used to estimate the osmotic gradient sufficient for fluid secretion of 0.1µl g^{-1} min^{-1} corresponding to 200ml day^{-1} in a human brain. As little as 0.4mM NaCl concentration difference could be sufficient to drive such magnitude of flow. Because of the

small value of this osmotic force, it is proposed that nothing else than osmotic force is needed to drive the net flux of water across the BBB (Fenstermacher, 1984; Hladky & Barrand, 2016). This is further supported by water permeability measurement lying within possible range of water permeability for protein-free lipid bilayers (Fettiplace & Haydon, 1980) and the lack of detectable *in vivo* aquaporin expression in brain EC (Haj-Yasein *et al.*, 2011). Aquaporin appearance in cultured cells is thus thought to be due to de-differentiation but not an indication of normal situation within the brain (Dolman *et al.*, 2005). Furthermore, the permeability of the EC membranes may be further amplified by the presence of transporters and other proteins such as GLUT1 which is known to be highly expressed in the brain endothelium and is known for increasing the osmotic water permeability of membranes in other types of cells (MacAulay & Zeuthen, 2010).

The bulk of glucose metabolism in the brain involves complete oxidation with consumption of specific amount of O_2 and production of same daily amount of CO_2 and metabolic water. The diffusion distances are small and so O_2 and CO_2 easily diffuse across the membranes of the BBB endothelial cells. They can thus be transferred to and from the circulating blood driven by their concentration gradients (Hladky & Barrand, 2016).

2.12.2 Transport of glucose and amino acids

The human brain consumes about 0.6 moles of glucose per day which must cross the BBB (Hladky & Barrand, 2016). About 20% of glucose in circulating blood plasma is estimated to be extracted by the brain (Hladky & Barrand, 2016). A saturable glucose transporter, GLUT1 is expressed both on the luminal and abluminal membranes of the brain ECs which passively transport glucose across the BBB (Hladky & Barrand, 2016). Both influx and efflux of glucose occur concurrently but with a net influx sustained by the concentration gradient between the blood and the brain interstitial fluid(ISF) (Hladky & Barrand, 2016). The fate of the glucose after crossing the EC is such that it enters the astrocytic endfeet and from this site some of this glucose could be transported back through the ECs to contribute to the efflux. Substantial amounts of the GLUT1 transporters are also reported to exist within brain ECs cytoplasm. These are localized to the vesicular membranes and acts as reservoir of the GLUT1 transporter. Glucose supply to the brain is increased during sustained neural activity and this requires an increase in glucose transfer among other changes (Paulson *et al.*, 2010). Increase in glucose transport, in part, reflect the redistribution of GLUT1 from the cytoplasmic vesicles to the plasma membranes of the ECs (Pardridge, 1993).

The BBB tightly restricts influx of some amino acids such as the neurotransmitters glutamate and glycine while it allows the rapid, passive but saturable influx of many others including all essential amino acids (Mann *et al.*, 2003). The rate of amino acid influx is balanced by a nearly equal efflux. This efflux from the brain is against concentration gradient across the abluminal membrane of the ECs and is powered by the coupled movement of Na^+ (Hawkins *et al.*, 2006). There is a polar distribution of amino acid transporters in the ECs and this helps to mediate amino acid homeostasis in the brain. There exists two facilitative neutral amino acids (NAA) transporters on both the luminal (blood-facing) and the abluminal (brain-facing) membranes which serve to provide the brain with essential AAs. In the abluminal membranes of brain ECs exists 4 Na^+-dependent transporters of NAA (neutral amino acid) which actively transfer every naturally occurring NAA from the ECF to ECs onward to the circulation. The Na^+-dependent carriers on the abluminal membrane mediate the maintenance of the NAA concentrations in the brain ECF at approximately 10% those of the plasma. Additional features of the abluminal membrane is the presence of at least 3 Na^+-dependent systems transporting acidic AAs (EAAT, excitatory amino acid transporter) and a Na^+-dependent system transporting glutamine. Facilitative transporters of glutamine and glutamate are found only in the luminal membrane of the BBB. Taken together, this organization ensures the net removal of acidic and nitrogen-rich AAs from the brain and accounts for the low level of glutamate penetration into the CNS (Hawkins *et al.*, 2006).

2.12.3 Transport of Ions

The BBB plays the principal role in the long-term regulation of the ionic composition of the brain interstitial fluid (ISF). Though astrocytes are very important in the short term control of ISF ionic composition but they cannot set or determine the long-term composition. The net transfers of inorganic ions across the BBB are small and related to the net rate of fluid transfer from the brain parenchyma.

Estimates of the net transfer of Na^+ concomitant with fluid transfer from the brain parenchyma falls below the Na^+ movements into the ECs that is coupled to amino acids reabsorption. This suggests that the ECs of the BBB are certainly capable of active transport of Na^+ sufficient to support the estimated rate of fluid transfer. Research data has shown that the ECs of the BBB are capable of active transport of Na^+ but in very low net amount that lend difficulties to the detection of ion fluxes and the expression of the transporters that mediate its transfer (Hladky & Barrand, 2016). All the molecular components required for ions secretion with concomitant

amount of fluid are present at the BBB. There exist also an energy source needed to drive secretion due to relatively high number of mitochondria in the ECs of the BBB which is estimated to occupy 5-10% of the endothelial cell volume(Hladky & Barrand, 2016). Hydrostatic pressure difference cannot explain the magnitude of water transfer between blood in the cerebral microvessels and the brain ISF as it does between blood and peripheral tissues because of the functional difference between the brain microvessels and peripheral tissue in that the former have much lower permeability to Na^+ and Cl^-. Thus any pressure that will filter water across the BBB would leave solute behind and wash away solute on the brain side. This will lead to increased solute concentration difference and build-up of osmotic pressure that will eventually stop net fluid transfer across the barrier. It follows therefore that at the BBB, there must be transport of solutes, with water accompanying, either by simple diffusion through the lipid bilayers of the EC membranes or via specific proteins such as GLUT1. *In vivo measurement* of ion fluxes across the BBB has been carried out using tracer ions, however, it has been largely impossible to measure net fluxes. Inferences has had to be made from measurements of changes in the content of parenchyma (both intra and extracellular), and allowance for exchange between the ISF and CSF (Hladky & Barrand, 2016). That the influx of Na^+ across the BBB does not occur by transcellular route and hence does not involve the Na-pump or the NKCC1 is supported by strong documentary evidence, however, there is further need to clearly confirm the route of passage as paracellular (Hladky & Barrand, 2016). Plasma [K^+] is maintained higher than that in the CSF and ISF (which are closely similar) and this suggests the existence of an active process that maintains lower concentrations of K^+ in CSF and ISF such as active transport of K^+ from the ISF to the blood across the BBB (Hladky & Barrand, 2016). It has been documented that approximately four-fifth of K^+ entry to the brain was via the BBB while the rest is from the choroid plexus (Hladky & Barrand, 2016). Control of ISF [K^+] when there are long-term changes in plasma [K^+] has two components of influx, with one at a rate that is independent of plasma [K^+] ([K^+]$_{plasma}$) while the other is proportional to [K^+]$_{plasma}$.. When the plasma potassium concentrations are within normal range, the two components of the influx remain almost equal. With increase in the influx when there is high plasma potassium, the amount of potassium in the brain showed no variation with variation in plasma level. Thus it is conclusive that because the volume of brain tissue is larger relative to that of CSF and that parts of the brain are farther from the ventricular and subarachnoid CSF, it is unlikely that the control of the [K^+]$_{ISF}$ of the brain is secondary to control of the CSF by the choroid plexuses. It is therefore noteworthy that the maintenance of nearly constant [K^+]$_{ISF}$ requires some mechanisms for increasing efflux from ISF to blood during increased [K^+]$_{plasma}$.

Further research data support the efflux of K^+ from brain to blood being due to activity of a Na^+-pump. Activation of the Na^+-pump by external K^+ in isolated cerebral microvessels has been documented to occur over a range of $[K^+]$ encountered in ISF (Schielke *et al.*, 1990). The presence of ion transporters in the BBB has been well supported by research data and four ion transporters have been identified and localized primarily to one membrane or the other. These include the Na^+/K^+-ATPase, otherwise known as the Na^+-pump, NKCC1 (Na-K-Cl cotransporter 1), NHE1 and NHE2 (Na/hydrogen exchanger 1 and 2 respectively).

Additional evidence exists for the presence and activity of AE2 (anion exchanger 2), NBCn1 (Na-HCO_3 cotransporter 1 and NBCe1 (electrogenic Na-HCO_3 cotransporter 1) (Daneman *et al.*, 2010). A number of different studies have localized the Na^+/K^+-ATPase otherwise known as the Na^+-pump in the membranes of BBB ECs (Del Pino *et al.*, 1995; Hladky & Barrand, 2016). This is the key transporter that couples metabolic energy to ion transport at the BBB and is preferentially localized to the abluminal surface of the brain ECs, though 25% of its activity is reportedly luminal. Expression of three different α subunits and two β subunits of the sodium pump have been reported at the BBB and this allows for the possibility of six different pumps (Zlokovic *et al.*, 1993). The exact sidedness of the sodium pump however, remains largely controversial though it provides clues as to the direction of movement of Na^+ at the BBB. In addition to the sodium pump, the expression of other
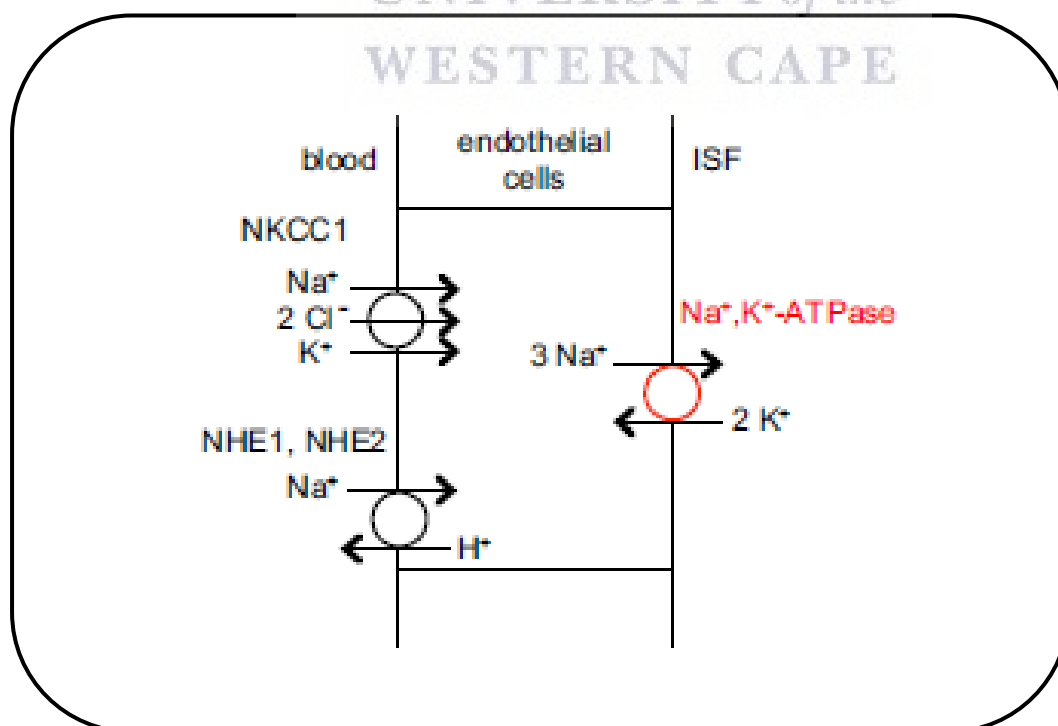
Figure 2.3: Ion transporters localised to the membranes of ECs of the BBB.

The Na$^+$/K$^+$-ATPase and Na$^+$/H$^+$-exchangers, NHE1 and NHE2 are also present on opposite sides of the cells but at lower densities (Hladky & Barrand, 2016).

ion transporters has also been reported at the blood–brain barrier and the deployment of several techniques for the identification and localization have revealed a panel of ion transporters in cultured brain endothelial cells as well as in brain slices. These include the NKCC1 and NHE1 and 2, identified by bumetanide binding assays and immuno-electron microscopy; HCO$_3^-$ transporters, Cl$^-$/HCO$_3^-$ exchanger AE2 and Na$^+$-HCO$_3^-$ cotransporters NBCe1 and NBCn1 detected at mRNA levels in brain ECs (Hladky & Barrand, 2016). The localization of these transporters to one or other of the brain endothelial cell surfaces is, however, not yet achieved (Hladky & Barrand, 2016).

2.12.4 Lipid and membrane-vesicle transport across the brain endothelium

The cell membrane regulate most major life processes as many important life processes takes place in, on, or attached to cell membranes. Docosahexaenoic acid (DHA) and eicosapentaenoic acid (EPA) are fatty acids within the membrane bilayer, which are attached as structural components to the larger phospholipid membrane molecular building blocks by ester bonds. These fatty acids interact in the membrane with other fatty acids to enhance membrane fluidity and DHA and EPA have been considered the most efficient of all major membrane fatty acids imparting fluidity to the cell membrane (Levental & Levental, 2019) which in turn enhance membrane biochemical efficiency. Thus adequate levels of DHA and EPA in membrane systems will support cell survival, growth and renewal (Schönfeld & Reiser, 2019).

Endothelial low rate of transcytosis is one of the barriers presented at the blood-brain interface. The regulation of this modality of barrier has been scientifically reported to involve the *Mfsd2a* (major facilitator superfamily domain containing 2a) gene, which encodes a transmembrane protein that is specific to the ECs of the BBB (Nguyen *et al.*, 2014). Additionally, the presence of this gene in the ECs of the BBB also facilitates the transport of certain essential lipids from blood to the brain tissue which are quite crucial to brain growth and development. *Mfsd2a* is a member of the major facilitator superfamily of secondary active transporters which are proteins that couple the transport of an ion down its electrochemical gradient with the transport of another molecule against its concentration gradient. Essential lipids such as omega-3 fatty

acids, particularly docosahexaenoic acid (DHA) are transported across the BBB by the transporters coded by the *Mfsd2a* gene. Deficiency of this fatty acid in the brain of growing animals has shown to cause proven reduction in brain size and cognitive defects, the findings which are similar to results obtained in *Mfsd2a* knock-out animals. Research data has further shown that DHA molecules are only transported across the BBB when attached to lysophosphatidylcholine ((LPC) (Nguyen *et al.*, 2014). Further, evidence also showed that Mfsd2a-mutant mice that exhibit poor BBB transport of DHA also showed increased BBB endothelial cell transcytosis which correlate with increased transcytosis also observed in animals with reduced density of pericytes (Ben-Zvi *et al.*, 2014). This finding suggests that the expression of the transporter gene depends on the presence of pericytes.
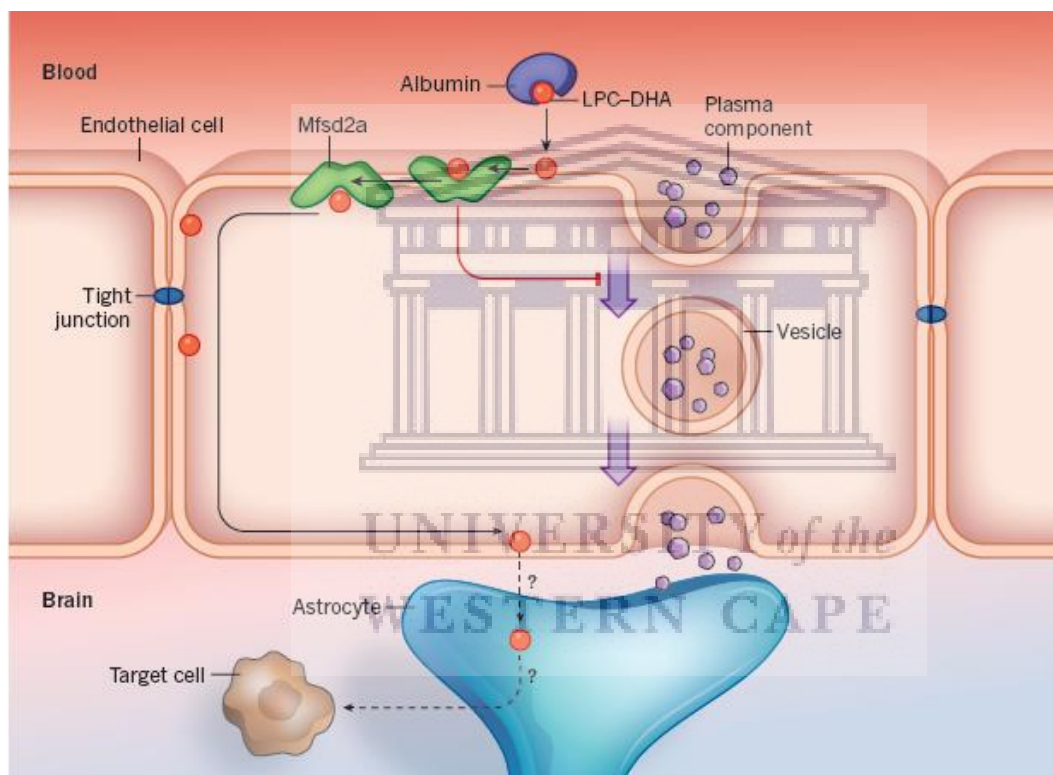
Figure 2.4: Lipid and membrane-vesicle transport across the brain endothelium. Lysophosphatidylcholine and Docosahexaenoic acid are transported in the bloodstream bound to protein albumin. On reaching the BBB, the complex is released from albumin and is adsorbed into the outer lipid leaflet of the EC membrane. The LPC-DHA complex then binds to Mfsd2a which transfers it to the inner membrane lipid leaflet thus potentially bypassing the tight junctions between endothelial cells to reach the brain-facing side of the EC membrane. Mfsd2a inhibits transcytosis in the ECs, a mechanism for the transport of some plasma contents including proteins and cells. The specific target for the DHA as well as the mechanism for its

transfer through the astrocytic endfeet which completely wraps the ECs are, however, unknown (Sweeney *et al.*, 2018).

Taken together, the major facilitator superfamily domain containing 2a protein is an important transporter protein that is specifically expressed in the BBB which serves the double function of transporting essential lipids required for brain development as well as suppressing vesicular transcytosis across the ECs of the BBB.

2.13 Experimental Models of the Blood-Brain Barrier

The BBB under physiological conditions exhibit a relative impermeability to many therapeutic drugs limiting their reach to the CNS in therapeutically potent concentrations, and presenting a major barrier to the treatment of CNS disorders. However, it shows abnormally increased permeability in a large number of neurological disorders such as brain tumours, brain trauma and degenerative neuropathies(Sweeney *et al.*, 2018). The dual nature of the BBB in pathology and therapeutics has generated considerable scientific and industrial interest pertaining to the understanding of the nature of the BBB in health and diseases. This consequently has necessitated the development of several experimental models of the BBB which are mainly based on the culture of brain endothelial cells, *in vitro* (Wilhelm *et al.*, 2011). The *in vitro* models target the mimicry of the *in vivo* anatomical BBB and researchers have utilized monocultures of endothelial cells, bi-culture with either astrocytes or pericytes or tri-culture platforms (Kaisar *et al.*, 2017). In monoculture platforms, ECs are cultured on a support (that mimic the basement membrane) such as collagen-coated culture flask under static conditions. An alternative way of monoculture is to culture the ECs on transwell setup on a microporous semi-permeable membrane that allows exchange of solutes, including cell-derived factors between the basolateral and the apical compartment separated by the insert membrane (Kaisar *et al.*, 2017). Cell migration and drug transport assays can be performed using this model and ECs derived from various sources has been successfully used such as mouse, bovine, rat, porcine and human-derived ECs (Patching, 2017). Due to the absence of modulatory effects of neighbouring cells as obtained *in vivo,* these monoculture models lacks the ability to maintain barrier properties over a long term period (Kaisar *et al.*, 2017). The need for further improvement led to the development of the bi- and tri-culture platforms. The effectiveness of the models are characterized using measurements of the trans-endothelial electrical resistance, TEER (a measure of impedance to current flow across the barrier), low permeability and the

expression of membrane transporters and surface proteins (Kaisar *et al.*, 2017). TEER is a functional parameter measured in derived units as Ohms (Ω) x cm$^{2.}$

In the bi-culture platform, a non-contact method can be used in which astrocytes are cultured at the bottom of the well and this allows for the exchange of diffusible factors across the transwell membrane to the ECs which are cultured on the apical chamber of the insert. In the contact method, astrocytes are cultured on the basolateral surface of the transwell membrane while ECs are cultured on the apical aspect. This allows for close proximity between the two cell types, however, the thickness of the intervening insert membrane is far higher than obtained in the *in vivo* basement membrane and thus limits cell-cell contact. This gives the non-contact method some advantage over this method (Kaisar *et al.*, 2017).

In tri-culture models, ECs and pericytes are cultured opposite each other on the apical and basolateral surfaces of the transwell insert respectively while astrocytes are cultured at the bottom of the well. Tri-cultures consisting of ECs, neurons and pericytes/astrocytes have also been used to model the NVU, however, the greater the complexity of these models the more challenging becomes their maintenance (Patching, 2017).

Cell types utilised in the various BBB models are either used as primary cells or immortalised cells. Mice are popularly used in CNS research and accordingly mouse brain endothelial cells BBB models have been developed and this has improved reproducibility while transitioning between *in vitro* and *in vivo* (Kaisar *et al.*, 2017). The integrity of the *in vitro* BBB model is characterized by TEER measurement and values compared with the *in vivo* values reported to be in the range of 1800-2000 Ω.cm^2 (Butt *et al.*, 1990). Several BBB models have been made from freshly prepared mouse brain endothelial monocultures or co-culture with pericytes and/or astrocytes. Furthermore, primary cell models from various animal sources exhibit variable TEER: primary rat BMECs exhibit higher TEER than mouse-derived BMECs in either monoculture or bi- and/or triple culture and primary bovine or porcine-derived ECs exhibit even higher TEER values (see table (Kaisar *et al.*, 2017))

Table 2-1: Table shows the sources, primary cell types, platforms and models of the BBB with their respective TEER characteristics- adapted from Kaisar et al 2017 (90).

Cell Source	Mouse				Rat		Bovine	Porcine	
Cell type	Primary BMEC				Primary BMEC		Primary BMEC	Primary BMEC	
Culture type	Mono-culture	Co-culture			Co-culture		Co-culture	Co-culture	
		With murine pericytes	With immortalized mouse astrocytes	With rat astrocytes	With rat astrocytes	Triple culture with rat astrocytes and pericytes	With rat astrocytes	With rat astrocytes	Triple culture with rat/porcine astrocytes and pericytes
BBB model design	EC on top of transwell inserts	EC on top of transwell insert and pericytes on the bottom well	EC on top and astrocytes on the bottom of transwell insert	EC on top and astrocytes on bottom well	EC on top of transwell insert and astrocytes on bottom well	EC on top, pericytes on bottom of transwell insert and astrocytes on bottom well	-	EC on top of transwell insert and astrocytes on bottom well	EC on top, pericytes on bottom of transwell and astrocyte on bottom well
Approximate TEER/Ω.cm^2	≈50-150	≈150	80	≈200	300->600	400	600-1800	800	>100

Table 2-2. Table shows the sources, immortalised cell types, platforms and models of the BBB with their respective TEER characteristics - adapted from Kaisar et al 2017 (90).

Cell Source	Mouse			Rat		Human		
Culture type	Monoculture			Monoculture	Co-culture	Monoculture	Co-culture	
Cell Type	bEND.3	b.END5	Immortalized Mouse Cerebral EC (cEND)	RBE4	RBE4 with rat glial cells	Immortalized human brain endothelial cells (hCMEC/D3)	With astrocytes or pericytes	Tri-culture with astrocytes and pericytes
Approximate TEER/Ω.cm^2	60-70	40-50	400	>100	-	40-50	50-60	>40

Despite the useful insights provided by the static *in vitro* models of the BBB into its role in CNS disease initiation and/or progression as well as drug delivery, static transwell models are devoid of fluidic shear stress (Gastfriend *et al.*, 2018). It has been scientifically proven that both astrocytic factors as well as shear stress are the two most important factor for the phenotypic differentiation of the BBB ECs (Booth & Kim, 2012). In order to overcome this challenge dynamic or flow based co-culture systems have been developed (Booth & Kim, 2012). These consist of three-dimensional, hollow fibre structure that enable co-culturing of ECs with glia, and with the ECs exposed to shear stress (Gastfriend *et al.*, 2018). They therefore, provide platforms to study the effects of shear stress on the BBB properties. Furthermore, they provide platforms for physiologically crucial arrangement of the different NVU cell types and also the possibility of real cell-cell contact. However, microfluidic set up requires specialized equipment and expertise for their construction (Gastfriend *et al.*, 2018).
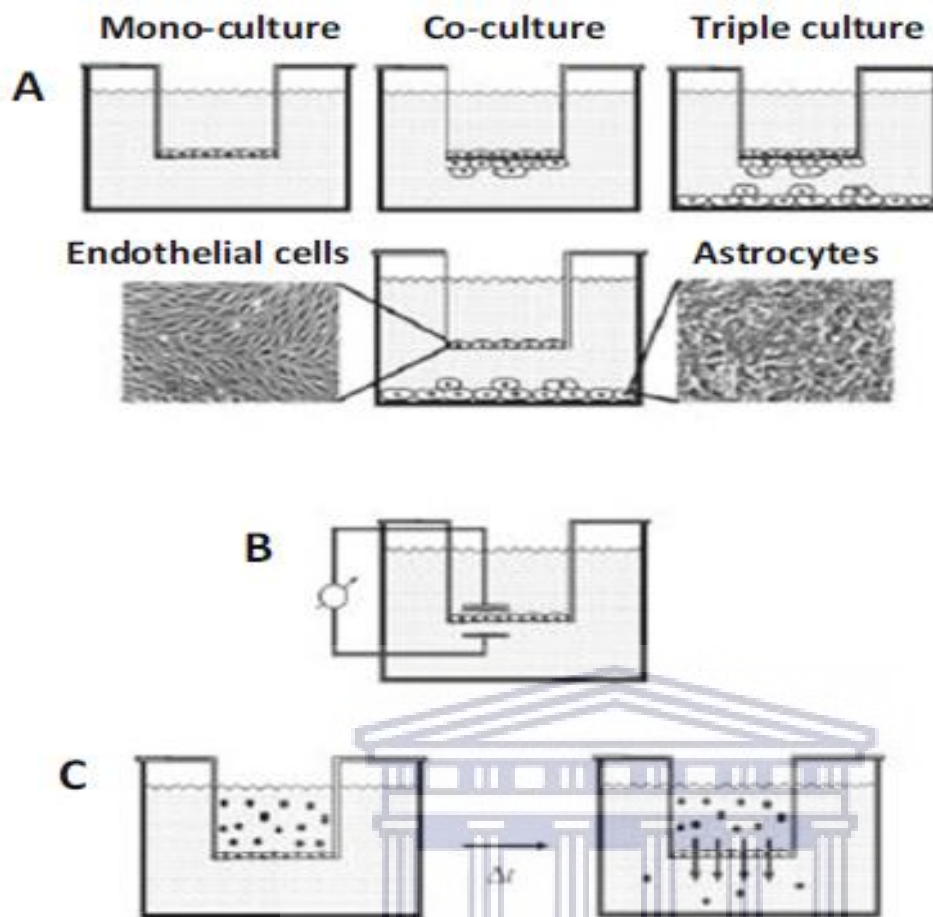
Figure 2.5: Basic cell culture *in vitro* models of the blood-brain barrier.

(A) Shows static BBB models using culture inserts in a monoculture, co-culture and triple culture platforms. (B) Shows measurement of TEER of brain EC monolayers grown in cell culture insert using a pair of electrode. (C) Illustrates flux of tracer compounds or drugs from apical compartment to the basolateral compartment across brain endothelial monolayer that can be measured at given intervals to calculate endothelial permeability coefficients (Patching, 2017).
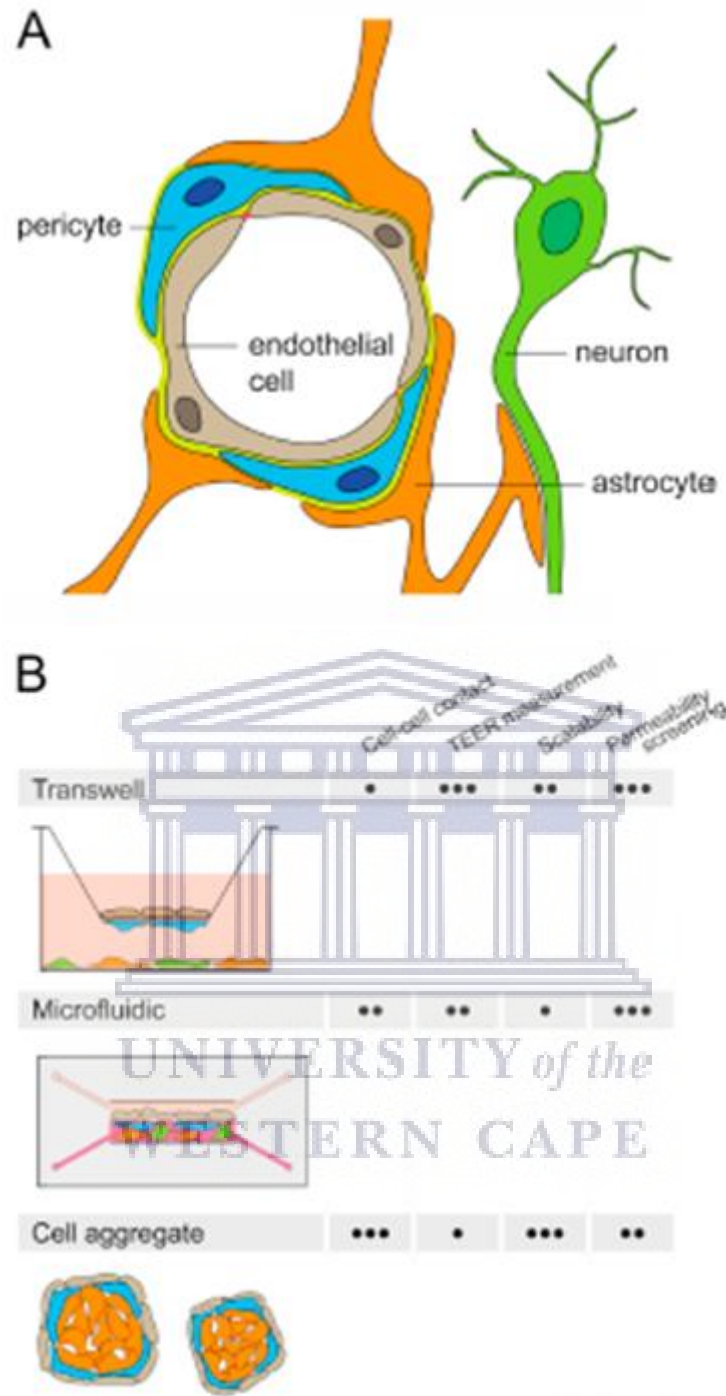
Figure 2.6: Basic illustration of the in vivo BBB and the various in vitro models.
(A) Illustrates the basic arrangement of the cells in the in vivo BBB. (B). Summarises the gains
in the various in vitro systems (Gastfriend *et al.*, 2018).

2.14 Reactive Oxygen Species

2.14.1 Introduction to ROS

Knowledge of free radicals dates back to over a century past when they were unexpected to feature in biological systems due to their high reactivity with consequential short half-life (Lushchak, 2014).

Down the century, several hypothesis proposing roles for free radicals in all oxidation reactions pertaining to organic molecules were nullified, however, they serve as sources of motivation for further studies on the role of free radicals in biological systems (Lushchak, 2014). Further studies later established the presence of free radicals in biological systems and proposed further their involvement in various biological processes and aging. From this point, knowledge steadily expanded of free radical involvement in life processes. However, for a long time it was grossly misconceived that free radicals in biological systems play only deleterious roles and thus considered as damaging species. This view was further reinforced with the discovery of superoxide dismutase enzyme, which protects living cells against free radicals, about the same time (Lushchak, 2014). Several physiological roles played by free radicals were discovered in the latter half of the 20th century. These include the use of free radicals by cells of the immune system to neutralize infectious invaders (Allen & Criss, 2019), production of nitric oxide in endothelial cells regulating vascular tone (Someya *et al.*, 2019) and the regulating effects of hormones such as insulin on the levels of free radicals (Guzmán *et al.*, 2019). These discoveries challenged the previously existing bio-damaging view of free radicals and led to the suggestion that free radicals are regulators of metabolic pathways.

The study of ROS in biological systems is ever advancing but remains one of the most complicated field of study in regard of the following challenges: the species are chemically unstable and thus highly reactive which therefore exist in low concentration in their steady states; they are involved in diverse reactions; their distribution in time and space within and outside the cells are not well understood; their presence and quantity depends on the physiological state of an organism; and finally, there is paucity of technical tools for reproducible evaluation of their absolute or relative levels. Reactive oxygen species were though, once considered to contribute only toxic effects to living systems but their beneficial effects have since been acknowledged.

2.14.2 Free radicals, or ROS? What do we actually deal with?

The interchangeable use of the two terms is common, however, ROS includes both radical and non-radical species (Lushchak, 2014). Reactive oxygen species (ROS) are highly reactive intracellular chemical species containing O_2 (Glasauer & Chandel, 2013). They are more chemically reactive then O_2 and they reacts with biological targets such as lipids, proteins and DNA (Glasauer & Chandel, 2013). All living organisms with complete adaptation to aerobic life converts over 90% of their consumed oxygen to water via reactions involving the electron transport chain (ETC) (Glasauer & Chandel, 2013). In animal cells the ETC is localized to the inner mitochondrial membrane (Letts & Sazanov, 2017). During ETC reactions four-electron reduction of molecular oxygen is coupled with oxidative phosphorylation and energy production in the form of ATP (Glasauer & Chandel, 2013). In the same system and concomitantly, much less than 10% of consumed oxygen gets reduced via one-electron successive pathways leading to the formation of superoxide anion radical from molecular oxygen (Glasauer & Chandel, 2013). This is further followed by one-electron reduction and simultaneous acceptance of two protons to yield hydrogen peroxide (Glasauer & Chandel, 2013). Because this latter compound is not a free radical yet more reactive than molecular oxygen, it conveniently fits into the designation of ROS. When hydrogen peroxide accepts one more electron, split up products are produced in the form of hydroxyl radical and hydroxyl anion. The hydroxyl radical further react with one more electron and proton to produce water molecule. These basic reactions proceed in biological systems often enhanced by removal of hydrogen ions from different compounds such as proteins, lipids and nucleic acids which often results in initiation of chain reactions (Glasauer & Chandel, 2013). The superoxide radical (O_2^-), hydrogen peroxide (H_2O_2), and hydroxyl radical ($HO\cdot$) are collectively called ROS whereas hydrogen peroxide is not a free radical. Furthermore, ROS does not only include the aforementioned but also various peroxides such as lipid peroxide, and peroxides of proteins and nucleic acids (Kim *et al.*, 2015). Different ROS shows diversity in their specificity and preference for the different biological targets due to their differences in reactivity. In addition, their homeostatic regulation is related to several other reactive species such as reactive carbonyl (glyoxal, methyglyoxal), reactive nitrogen species (nitric oxide, peroxynitrite), reactive sulphonyl species and so forth. Superoxide is produced from oxidative phosphorylation as a result of one electron reduction of molecular O_2. Once formed, it becomes soon converted to hydrogen peroxide by superoxide dismutases (SODs) enzymes. Unlike the superoxide radical, H_2O_2 is diffusible across the cell membranes into all cellular compartments where it can

modulate cell signalling. Hydrogen peroxide in the presence of metal ions such as copper, becomes converted into the highly reactive hydroxyl radical which is highly toxic to the cell.
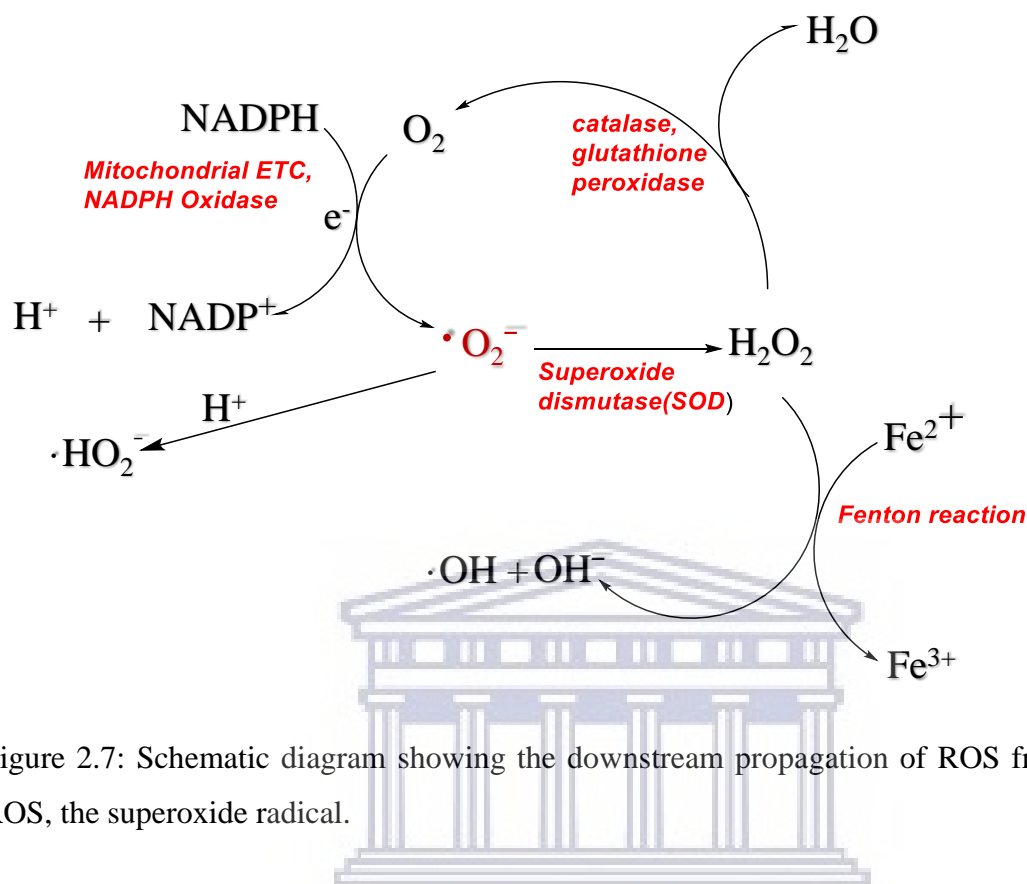
Figure 2.7: Schematic diagram showing the downstream propagation of ROS from primary ROS, the superoxide radical.

The superoxide radical is the primary ROS form generated from various cellular mechanisms such as the mitochondrial oxidative phosphorylation, NADPH oxidases activities, endoplasmic reticulum stress, and ultra-violet radiation. Further metabolic processing converts the superoxide to the various downstream ROS such as hydrogen peroxide and the more reactive hydroxyl radical.

2.14.3 Cellular sites of ROS generation

The main sources of cellular ROS include mitochondria and the NADPH family of oxidases (Nox). Within the cell in general, they are generated by both endogenous and exogenous sources: endogenous generation involves mitochondrial production of superoxide with chain propagation of downstream ROS. It has been estimated that about 2% of the total amount of oxygen consumed in the mitochondrial is diverted to the production of superoxide in the mitochondrial electron transport chain (ETC)(Circu & Aw, 2010). In the mitochondria, eight sites that generate ROS has been identified, however, only 3 of these sites have been well characterized which are complex I, II, and III of the mitochondrial respiratory chain localized

within the inner mitochondrial membrane (Glasauer & Chandel, 2013). In these 3 complexes O_2^- radical is generated by one-electron reduction of molecular O_2 and then moved into the mitochondrial matrix where it undergoes enzymatic conversion into H_2O_2 by SOD2. In addition, complex III has the ability to generate O_2^- directly into the intermembrane space from where it can transit into the cytosol via voltage-gated anion channels. It then undergoes enzymatic conversion to H_2O_2 in the cytosol by SOD1 (Glasauer & Chandel, 2013).
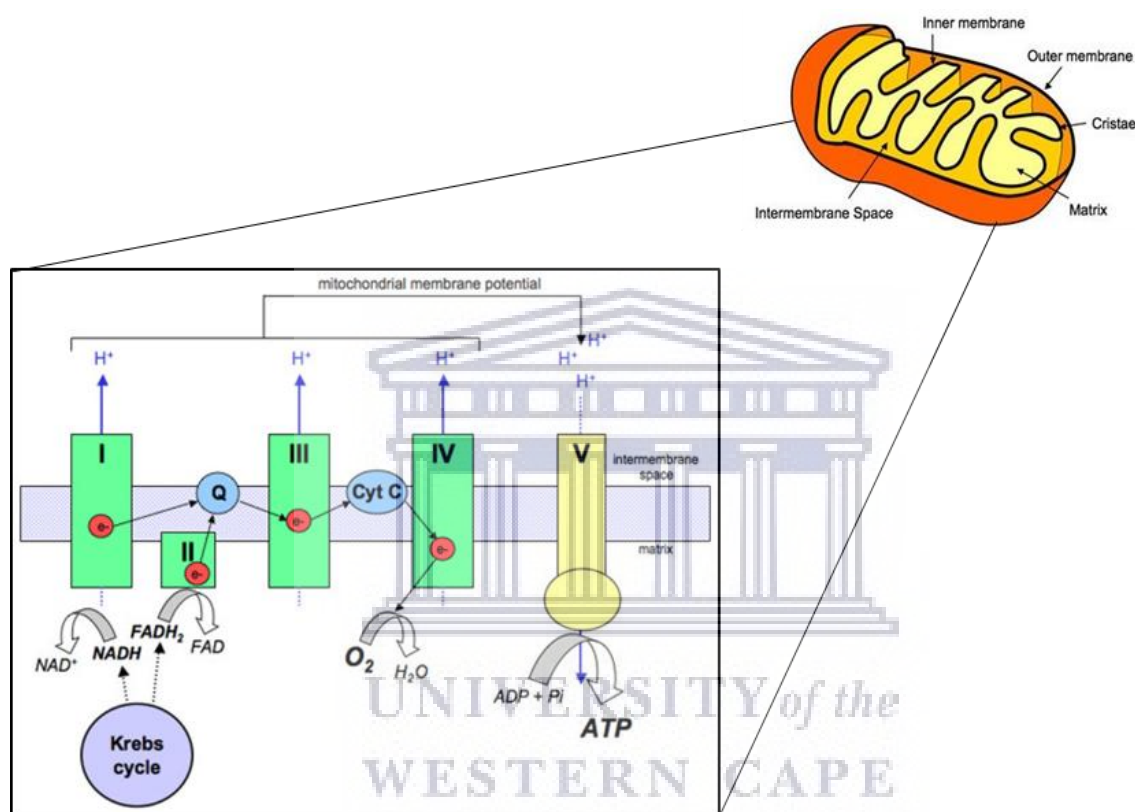
Figure 2.8: The electron transport chain (ETC) in the mitochondria is the major site of oxidative phosphorylation in mammalian cells.

The ETC is a series of electron transporters in the inner mitochondria membrane which transfer electrons from NADH and $FADH_2$ to molecular O_2. At the same time protons are pumped from the mitochondrial matrix to the intermembrane space while O_2 is reduced to form water.

NADPH oxidases (Nox) are primarily found in the plasma membrane but are also present on other membranes such as the endoplasmic reticulum (ER) and the mitochondria. They function solely in the production of ROS (Glasauer & Chandel, 2013; Schröder, 2019). In Nox-derived ROS production, NADPH donates electron to the centre of Nox catalytic subunit which then generate O_2^- by one-electron reduction of molecular O_2. The generated O_2^- soon get

enzymatically converted to H_2O_2 by cytosolic SOD1 (Glasauer & Chandel, 2013). Seven Nox enzymes have been characterized in the human cells which include Nox1-Nox5 and Duox1 and Duox2 (Schröder, 2019). Nox2 is involved in host defence and consists of 2 membrane-bound subunits (Nox2 and p22phox) and 4 cytosolic subunits (p47phox, p67phox p40phox and Rac2). ROS production by Nox2 is activated when the subunits assemble and this assembly is tightly controlled thereby avoiding accidental activation. While killing microbial invader, however, potential harm is incident by Nox-derived ROS on the cell within which it is maximally activated, as well as on the surrounding cells and tissues. Furthermore, Nox2-derived ROS is not limited to host defence but also prolonged and/or 'permanent' effects leading to extended manifestations such as vascular reactivity (Schröder, 2019). Mechanism of prolonged or permanent 'mild' activation of Nox2 include ROS-induced ROS formation. This involves mitochondrial-derived ROS phosphorylating p47phox, via activation of protein kinase C (pkC), thereby causing the assembly of the active Nox2 complex (Schröder, 2019). The mechanism of vascular relaxation involves the effect of NO formed by endothelial nitric oxide synthase (eNOS). The O_2^- derived from Nox2 activation reacts with NO to form $ONOO^-$ and this reaction attenuates the level of bioactive NO and thus attenuates vascular relaxation. In addition, O_2^- and $ONOO^-$ can attack polyunsaturated fatty acids (PUFA) in the cell membranes of vascular endothelial cells to yield advanced lipid peroxidation end products (ALEs) such as 4-hydroxynonenal (4-HNE) which are potential modifiers of protein function (Dalleau *et al.*, 2013; Schröder, 2019). Nox2 in addition to its expression in leukocytes are significantly expressed in endothelial cells and has been established to be of critical importance in endothelial cell redox pertubations. Other sources of ROS include the cytosolic xanthine oxidase and the cytochrome P_{450} monooxygenases localized in the endoplasmic reticulum.

2.14.4 Homeostasis of ROS

In living cells levels of ROS are maintained low but never abolished and this is achieved by presence of systems that that regulate the dynamics of production and elimination of ROS (Sies *et al.*, 2017). Production of ROS can be viewed from the angle of metabolism involving the mitochondrial oxidative reactions that release ROS as by product, as waste product of vital cellular reactions and on the other hand, as a result of cellular response to stimulation by xenobiotics, cytokines, bacterial invasion and inflammation. In the latter group cellular ROS production is directed at anabolic and catabolic processes, for cellular defense or as part of signal transduction pathway (Zhang *et al.*, 2016). It is critical for the cell to keep in check the amount of ROS accumulation within it and this critical role is provided by the presence series

of antioxidant proteins and molecules within the cell. The major antioxidant proteins found within cells include the superoxide dismutases (SOD), glutathione and glutathione peroxidase (GPx), glutathione S-transferase (GST) and other molecules that play important roles in cellular antioxidation (Marengo *et al.*, 2016). Superoxide dismutases (SODs) catalyse the first stage in the neutralization of ROS by enzymatic conversion of O_2^- to H_2O_2 which can then be further broken down to water by catalase, glutathione and glutathione peroxidase (GPx) (Wang *et al.*, 2018). There are different isoforms of SOD localized to different compartments of the cell which is suggestive of the need for critical control of ROS balance within the cell (Wang *et al.*, 2018). Importance of SOD is underscored by the finding of increased evidence of oxidative damage such as membrane lipid peroxidation, protein carbonylation and DNA fragmentation in cells that have significant loss of SOD activities (Wang *et al.*, 2018). Glutathione has the ability to react directly and neutralize various ROS as well as act as cofactor for the GPx-dependent ROS buffering (Baxter *et al.*, 2015). Disorders of glutathione homeostasis in the central nervous system has been associated with a variety of neurological disorders (Baxter *et al.*, 2015).

2.14.5 ROS involvement in cellular signalling

ROS when kept within physiological range in the cell act as signalling molecule in several cellular processes by exerting regulatory influences on cellular signalling pathways such as NF-kB, MAPKs, Keap1-Nrf2-ARE, PI3K-Akt, Protein Kinase, Ca^{2+} and Ubiquitination/Proteasome signalling pathways (Zhang *et al.*, 2016).

2.14.5.1 ROS modulation of the NF-kB signalling pathway

NF-kB is a transcription factor that act in several cellular processes such as cell proliferation, differentiation, autophagy, cellular adhesion, senescence and apoptosis (Panahi *et al.*, 2018). Defective NF-kB signalling has been reported to be associated with diseases such as cancer, arthritis, asthma, degenerative neuropathies and heart diseases (Chauhan *et al.*, 2018; Galani *et al.*, 2019; Hutami *et al.*, 2018). ROS has been reported to activate NF-kB complex via several mechanisms which include inhibiting the phosphorylation of IkBα subunit which when phosphorylated, it undergoes degradation and allows NF-kB to translocate to the nucleus of the cell where it activates transcription of target genes (Zhang *et al.*, 2016). Also, ROS targets other regulatory subunits of the NF-kB complex with resultant activation of NF-kB signalling (Zhang *et al.*, 2016). Other mechanisms of ROS on the NF-kB signalling system is the disturbance of

the ubiquitination and degradation of IkB and inactivation of Ubcl2 with consequent activation of NF-kB (Zhang *et al.*, 2016).

2.14.5.2 ROS modulation of MAP Kinase pathway

The mitogen-activated protein kinase (MAPK) cascades include several kinases such as the extracellular signal-related kinase (ERK1/2), the c-Jun N-terminal kinases (JNK), the p38 kinase (p38) and the big MAP kinase 1 (BMK1/ERK5) (Zhang *et al.*, 2016). These provide intracellular signal transduction pathways for the modulation of cellular processes such as growth, differentiation, cell cycle, cell survival and cell death (Gräb & Rybniker, 2019; Xie *et al.*, 2019; Yang *et al.*, 2015). They share certain properties such as their serine/threonine kinase nature as well as the cascade of their intra- and extracellular activation which leads to the phosphorylation of their various substrate proteins directly involved in the modulation of cellular activities (Kidger & Keyse, 2016). The ERK pathway for example, is normally activated by growth factors such as epidermal growth factor, EGF, platelet-derived growth factor, PDGF and cytokines such as interleukin-1β, IL-1β, and tumour necrosis factor-α, TNF-α and its activation is via stimulation of tyrosine kinase receptors (Su *et al.*, 2016). Activation leads to the subsequent activation of several transcription factors. ROS as a signalling molecule has, however, been reported to activate the tyrosine kinase receptors of EGF and PDGF, without the actual ligands, to stimulate the activation of the ERK pathway (Lin *et al.*, 2018). The mechanism for ROS activation of the ERK pathway is cell specific; in commensal bacteria, ERK pathway is activated by ROS inactivation of dual-specific phosphatase 3 (DUSP3) by oxidation on its Cys-124 residue. DUSP14 knockout also resulted in ERK activation (Lin *et al.*, 2018; Wentworth *et al.*, 2011). However, in some other cells, exposure to H_2O_2 causes phosphorylation and activation of phospholipase C-gamma (PLC-γ) which leads to the generation of inositol triphosphate (IP3) and diacylglycerol (DAG)(Zhang *et al.*, 2016). IP3 generated is capable of triggering the release of Ca^{2+} from intracellular stores and thus increased intracellular Ca^{2+} which mediates the activation of several intermediates leading to the subsequent activation of the ERK pathway (Zhang *et al.*, 2016).

2.14.5.3 ROS modulation of Keap1-Nrf2-ARE signalling

Another important signalling pathway modulated by ROS is the Keap1-Nrf2-ARE signalling pathway (Zhang *et al.*, 2016). Nuclear Factor Erythroid 2-related factor 2 (Nrf2) is transcriptional regulator of genes involved in cellular processes such as cell metabolism, proliferation, immune response and antioxidant defence (Silva-Islas & Maldonado, 2018). Nrf2

activity is normally kept repressed in the cytoplasm by its main regulator, Kelch-like ECH-associated protein 1 (Keap1) which is an adapter protein of Cullin 3 (Cul3) ubiquitin E3 ligase complex (Silva-Islas & Maldonado, 2018; Zhang *et al.*, 2016). Keap1 represses Nrf2 by its sequestering, ubiquitination, and proteasomal degradation (Deshmukh *et al.*, 2017; Silva-Islas & Maldonado, 2018). Nrf2 activation is normally induced by OS which oxidizes some cysteine residues in Keap1 causing decreased Nrf2 ubiquitination with consequent increase in its nuclear translocation and activation. Nrf2 once translocated to the nucleus induces antioxidant response element (ARE) genes for antioxidant defence (Deshmukh *et al.*, 2017; Silva-Islas & Maldonado, 2018).

2.14.5.4 ROS modulation of PI3-Akt pathway

ROS also modulate the phosphoinositide-3-kinase-Akt (PI3-Akt) signalling pathway which is involved in the regulation of critical cellular functions such as protein synthesis, cell cycle progression, cell proliferation, apoptosis, autophagy, and drug resistance reactive to growth factors (PDGF, VEGF), hormone (PGE_2) and cytokine (IL-17, IL-6 and IL-2) stimulation (Ahn *et al.*, 2012; Cantrell, 2001; Zhang *et al.*, 2016). Activation of PI3K is initiated, for example, when growth factor binds to its receptors leading to its direct stimulation of class 1A PI3Ks that are bound via their regulatory subunit or adapter molecules such as the insulin receptor substrate (IRS) proteins. Upon activation, the active PI3K catalyses the cascade that produces phosphatidylinositol 3, 4, 5-triphosphate (PIP3) from phosphatidyl inositol 4, 5-biphosphate (PIP2) (Thapa *et al.*, 2019). The membrane-localized PIP3 is a signalling molecule that recruits and activate proteins such as the phosphoinositide-dependent protein kinase (PDK) and protein kinase B (Akt) serine/threonine kinases. Activated PDK and Akt subsequently promotes the activation of their target genes such as p53, mTOR1 (mammalian target of rapamycin 1), BAD (bcl2-associated agonist of cell death), FOXO (forkhead box protein class O) and GSK3 (glycogen synthase kinase 3) (Thapa *et al.*, 2019).

ROS reportedly activate PI3K directly to amplify its downstream cascade as well as concurrently inactivate its negative regulator and inhibitor of Akt activation, phosphatase and tensin homolog (PTEN), by oxidizing cysteine residues within the active centre (Kim *et al.*, 2018). Additionally, ROS is able to drive PTEN into the proteolytic degradation pathway via promotion of phosphorylation by casein kinase II on PTEN (Lee *et al.*, 2018). Also, protein phosphatase 2A (PP2A) which is a potential inhibitor of Akt/PKB is made to interact with

Akt/PKB with subsequent short-term activation of Akt/PKB at low levels of ROS after oxidation of the disulphide bridges in Akt/PKB (Lee *et al.*, 2018).

2.14.5.5 ROS interaction with calcium ion signalling pathway

Ca^{2+} signalling is central to a variety of cellular processes and functions such as contraction, secretion, metabolism, gene expression, cell survival and cell death (Raffaello *et al.*, 2016). Ca^{2+} homeostasis within the cell is maintained by dynamic balance between processes that increase cytoplasmic Ca^{2+} and those that deplete it (Marchi & Pinton, 2016). Cytoplasmic Ca^{2+} is increased by influx from extracellular medium and intracellular stores such as sarcoplasmic and endoplasmic reticulum (SR/ER) while it is depleted by processes such as efflux across the plasma membrane and sequestration into the mitochondria (Marchi & Pinton, 2016). The mechanisms for Ca^{2+} uptake into the cytoplasm involve the inositol 1, 4, 5-triphosphate receptor (IP_3R), the ryanodine receptor (RyR) and the nicotinic acid-adenine dinucleotide phosphate which mediate Ca^{2+} release from ER and SR, and also voltage-dependent Ca^{2+} channels (VDCC) and store-operated Ca^{2+} channel (SOC), which mediate Ca^{2+} influx from extracellular matrix (Arias-del-Val *et al.*, 2019; Grillo *et al.*, 2019; Lewis, 2019; Park & Suh, 2018). On the other hand, mechanisms for depletion of cytoplasmic Ca^{2+} include the plasma membrane Ca^{2+} ATPase (PMCA) which mediates the extrusion of Ca^{2+} across the plasma membrane, the sarcoplasmic/endoplasmic reticulum Ca^{2+} ATPase (SERCA), which returns Ca^{2+} into the ER/SR, Na^+/Ca^{2+} exchanger (NCX) which clears out Ca^{2+} by exchanging it with Na^+ and the mitochondrial Ca^{2+} uniporter (MCU) which ferries Ca^{2+} into the mitochondria (Brini & Carafoli, 2011; Kamer & Mootha, 2015; Kiess & Kockskämper, 2019). Current scientific evidence have demonstrated a cross influence between ROS and Ca^{2+} signalling systems in a variety of cellular processes (Görlach *et al.*, 2015). Several research studies have indicated that Ca^{2+} modulates both processes of ROS generation and ROS clearance thus tilting the cellular redox balance into either oxidized or reduced state (Görlach *et al.*, 2015; Montezano *et al.*, 2018).

Cellular ROS is generated from both mitochondrial and extra-mitochondrial sites. In the mitochondrion, Ca^{2+} primarily promote the synthesis of ATP and ROS by stimulating enzymes of the Krebs cycle and oxidative phosphorylation (Niedzwiecka *et al.*, 2018). The mitochondrial respiratory chain is the main source of physiological ROS, superoxide, production and this specie is both spontaneously and enzymatically dismutated to produce H_2O_2, catalysed by SOD (Sies *et al.*, 2017). Increase in ROS generation occurs when Ca^{2+} activates 3 dehydrogenases of the TCA cycle, specifically, pyruvate dehydrogenase, isocitrate

dehydrogenase, and oxoglutarate dehydrogenase as well as other enzymes such as ATP synthase (complex V) and the adenine nucleotide translocase (Antony *et al.*, 2018). In addition to the modulation of mitochondrial ROS generating enzymes, Ca^{2+} also regulate some extra-mitochondrial ROS generating enzymes such as Nox and nitric oxide synthase (NOS) under both physiological and pathological conditions (Görlach *et al.*, 2015). Concomitantly, Ca^{2+} also mediates ROS clearance mechanisms by regulating the antioxidant defence system (Feno *et al.*, 2019). These it does by direct activation of antioxidant enzymes such as catalase and glutathione reductase, by upregulation of SOD and induction of mitochondrial GSH release early in Ca^{2+} -induced mitochondrial permeability transition pore (mPTP) opening (Zhang *et al.*, 2016). Indirect activation of catalase, on the other hand, can occur via a ubiquitous Ca^{2+} -binding protein, calmodulin (CaM), with resultant decrease in cellular H_2O_2 levels (Zhang *et al.*, 2016). Other mechanisms by which ROS modulate Ca^{2+} signalling include oxidation of Cys thiol of Ca^{2+} channels/pumps/exchangers involving RyR, IP_3R, SERCA, PMCA, and NCX (Forman *et al.*, 2010). Content of multiple reactive Cys thiols which influence channel gating/assembly is a feature of the RyR/IP_3R and many of the regulatory proteins that form complex with it (Zhang *et al.*, 2016). When the RyR/IP_3R undergoes thiol oxidation by ROS, enhanced intersubunit binding and blockade of binding of the negative regulator, calmodulin, occur which results in the general increase in channel activity and thus promotion of Ca^{2+} efflux (Zhang *et al.*, 2016). Similarly, SERCA pumps also contain numerous Cys residues which on ROS oxidation causes inhibition of SERCA activity and consequent decreases in Ca^{2+} influx from the cytoplasm to the ER (Forman *et al.*, 2010). Other pumps include PMCA which, can be reversibly inactivated by ROS by altering the Tyr^{589}, Met^{622}, and Met^{831} residues; NCX, which activity can be both stimulated or decreased because while H_2O_2 generated from the xanthine/xanthine oxidase system enhances NCX activity, oxidants species from hypoxanthine/xanthine oxidase decrease it activity (Zhang *et al.*, 2016). Voltage-dependent calcium channel also undergoes alteration in activity due to interaction with ROS (Zhang *et al.*, 2016).

Other signalling pathways that involve ROS include signalling through the mitochondrial permeability transition pore (mPTP)(Maryanovich & Gross, 2013; Sánchez *et al.*, 2011), protein kinase (Eisenberg-Lerner & Kimchi, 2012; Kruk *et al.*, 2013), and the ubiquitination/proteasome system (Reyskens & Essop, 2014; Segref *et al.*, 2014).

2.15 The role of ROS in blood-brain barrier regulation

Reactive oxygen species has been reported to play critical roles in modulating a number of mechanisms involved in the regulation of BBB integrity (Cai *et al.*, 2016; Coelho-Santos *et al.*, 2016; Tzeng *et al.*, 2019). Some of the pathway of BBB regulation that are modulated by ROS include Ca^{2+}signal-mediated control of TJ assembly and disassembly (Chen *et al.*, 2016), TJ assembly regulation via protein kinase C (PKC) (Kalsi *et al.*, 2019), TJ and basement membrane degradation via protein tyrosine kinases (PTK) and matrix metalloproteinases (MMP) activation (Haorah *et al.*, 2007) and cellular Src kinase (c-Src)-mediated activation of caveolin-1 that causes increased trans-endothelial transport across the BBB (Coelho-Santos *et al.*, 2016).

ROS and other substances that alter cellular Ca^{2+} metabolism (Görlach *et al.*, 2015) such as alcohol (which also generate ROS), through activation of MLCK (Citi, 2019), cause TJ protein phosphorylation and dysfunctional BBB. Ca^{2+} is a second messenger in the regulation of BBB permeability and both intra- and extracellular Ca^{2+} is an important component of TJ regulation. When cultured endothelial cells are exposed to Ca^{2+}-free medium, that is low extracellular Ca^{2+}, both reversibly increased permeability and decline in TEER measurement were observed. Putative mechanism include: failure of calcium binding to its sites on cadherin extracellular domains causing conformational changes at TJ complexes and subsequent barrier dysfunction, and initiation of signalling cascades causing disassembly and/or redistribution of ZO-1 and occludin away from apical/lateral borders. The redistribution of ZO-1 is suggestive of changes in the endothelial cell contractile machinery mediated by activation of myosin light chain kinase (MLCK) of which inhibition by MLCK inhibitor (ML-7) brought about abolition of ZO-1 redistribution.

Protein kinase C (PKC) is another regulator of TJ assembly which on activation by increased intracellular Ca^{2+} causes dysregulated barrier properties (Rakkar & Bayraktutan, 2016). PKC play important role in endothelial TJ complex assembly/disassembly. Two classic forms of PKC (alpha and beta) can be activated by hydrogen peroxide have been reported to be mostly involved in TJ disassembly (Konishi *et al.*, 1997). Intracellular Ca^{2+} therefore, also play important role in the regulation of barrier function. Increased intracellular Ca^{2+}, which could occur either through Ca^{2+} channel or release from intracellular stores, activates signalling

cascades that specify posttranslational TJ distribution as well as transcriptionally regulate TJ expression (Chen *et al.*, 2016).

Phosphorylation is a mechanism for the regulation of transmembrane and accessory proteins of the TJ (Shigetomi & Ikenouchi, 2017). Serine and threonine phosphorylation of occludin controls its intracellular distribution and subsequent barrier properties (Van Itallie & Anderson, 2018). Localization of hyperphosphorylated occludin to intercellular junction is critical to maintenance of barrier junction (Van Itallie & Anderson, 2018). Decline in occludin phosphorylation such as due to inhibition of PKC, has been reported to correlate to a rapid fall in TEER (Bolinger *et al.*, 2016). Similarly, claudins' phosphorylation has also been implicated in the regulation of paracellular permeability (Van Itallie & Anderson, 2018). Tight junction phosphorylation or dephosphorylation status is stimulus dependent, (such as inflammatory cytokines, OS, or growth factors), as well as the amino acid residues where phosphorylation occurs (such as serine, threonine or tyrosine) (Van Itallie & Anderson, 2018). OS associated with alcohol metabolism in BMVEC has been reported to lead to phosphorylation of occludin and claudin-5 and redistribution of TJ protein in an *in vitro* brain endothelium model (Haorah *et al.*, 2005). ROS thus has the ability to oxidize certain residues of important signalling molecules which potentiate them for easy phosphorylation (Zhang *et al.*, 2016). Furthermore, by residue oxidation, ROS causes inhibition or deactivation of phosphatases, such as PTEN, thereby sustaining long term phosphorylation and thus activation of important signalling molecules that regulate BBB integrity, such as PKC and MLCK (Zhang *et al.*, 2016).
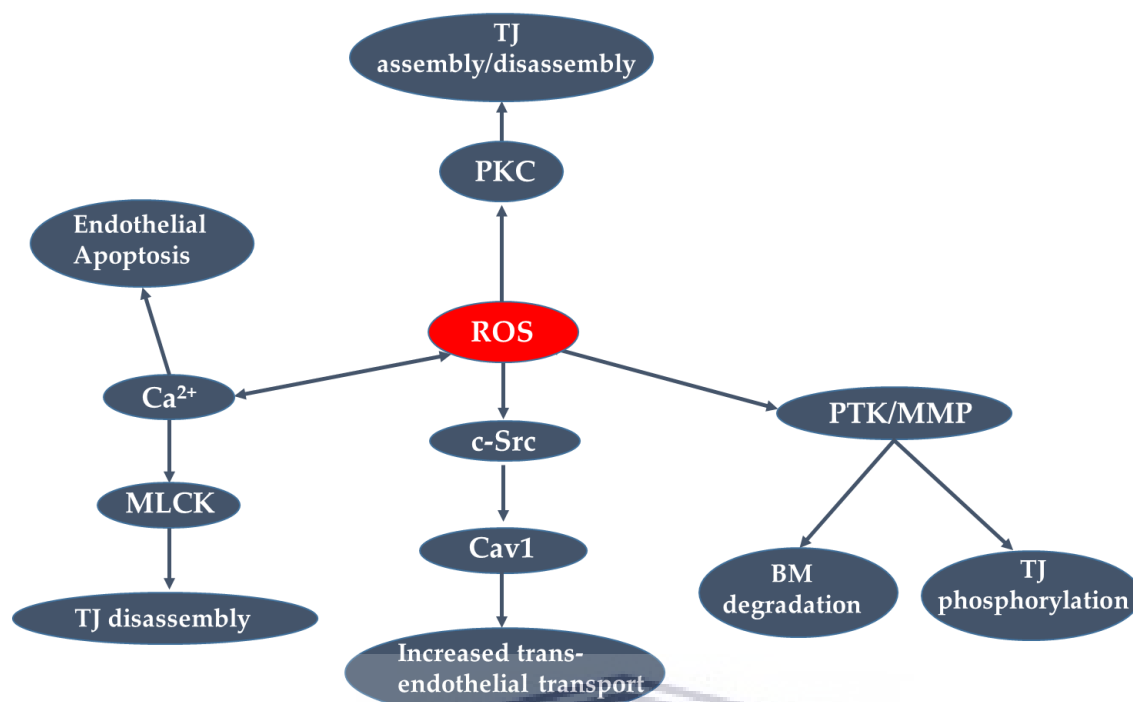
Figure 2.9: The regulation of the BBB properties by ROS.

ROS-mediated regulation of the BBB via modulation of molecular signals that regulate important components of the barrier system. ROS can modulate TJ assembly/disassembly, alter the components and integrity of the BBB basement membrane and alter the vesicular transport system within endothelial cells of the BBB.

2.16 ROS in BBB dysfunction-associated neurological conditions:

2.16.1 Contribution of BBB dysfunction to the pathogenesis of neurodegenerative diseases (NDDs)

Fluxes of molecules between the peripheral circulation and the CNS and *vice versa* is finely controlled by the BBB which is composed primarily of endothelial cells, which in turn is regulated by astrocytes and pericytes. Through the interactions between EC and astroglial cells at the BBB, homeostasis of the brain metabolism is maintained (Abbott *et al.*, 2010; Daneman & Prat, 2015; Liebner *et al.*, 2018). The BBB is sensitive to OS damage and disruption, which in turn compromises the homeostasis of neural function and may be responsible for triggering neural pathogenesis.

2.16.2 Effects of Aging and Oxidative Stress

Aging is an important contributing risk factor in the development of neurodegeneration and BBB disruption, occurring early in the aging human brain. Research has indicated that a higher

incidence of neurodegeneration begins in the hippocampus, a brain region associated with cognitive functions (Erdő *et al.*, 2017; Takeda *et al.*, 2014). Magnetic resonance imaging (MRI) quantification of regional BBB permeability in the living human brain indicated an age-dependent BBB breakdown in the hippocampus, a brain region affected early in AD (Bhat *et al.*, 2015; Fischer & Maier, 2015; Nissanka & Moraes, 2018). The cognitive impairment associated with hippocampal BBB breakdown correlates with injury to BBB-associated pericytes. (Abbott *et al.*, 2010; Blesa *et al.*, 2015). The association of the stage at which the BBB breaks down and whether it causatively impacts cognitive impairment, is however, unsettled.

There is increasing evidence to support the contribution of BBB breakdown in the pathogenesis of NDDs such as PD, AD, ALS (amyotrophic lateral sclerosis), and MS (multiple sclerosis) as well as typical neurovascular disorders such as stroke and vascular dementia (Cheignon *et al.*, 2018; Fischer & Maier, 2015; Tramutola *et al.*, 2017). One of the implications of a number of vascular disorders such hypertension, cerebrovascular disorder and dysfunctional BBB is the increased permeability associated with neurodegeneration. Data from mouse transgenic models with BBB breakdown studies supports the initiation and or contribution to neurodegeneration by accumulation of circulating proteins, free iron, iron-containing hemosiderin and/or plasmin in the CNS neurons (Zhao, Nelson, *et al.*, 2015). Emerging research regarding the overlap between the pathogenesis of vascular dementia (VaD) and AD are now available from epidemiological studies that revealed that vascular risk factors such as diabetes mellitus (DM), hypertension and atherosclerosis play important role in the progression of AD but the mechanisms of these associations are yet unclear. Putative theories include the possibility that the cerebrovascular damage induced by these diseases could cause impaired cognitive function (Takeda *et al.*, 2014). Examining the effects of hypertension on pathological amyloid accumulation in mouse brain models demonstrated Aβ deposition in the hypertensive brain which was associated with impaired BBB integrity. There is also evidence that some antihypertensive drugs restored cerebrovascular dysfunction via reduction of OS and improved cognitive function in AD mouse model (Takeda *et al.*, 2014). Another study using diabetic AD mouse models showed that co-existence of diabetic condition could lead to accelerated Aβ-related vascular alterations which was associated with induction of receptors for advanced glycation end-products (RAGE) in the cerebral blood vessels. Many studies suggest that cerebrovascular dysfunction does not only play a role in vascular dementia but also in AD brain (Takeda *et al.*, 2014).

2.16.3 Immuno-genetic Factors

ApoE-Ɛ4 is a strong genetic factor for sporadic AD although the mechanism of how it impacts on AD pathogenesis is not clear. The ApoE-Ɛ4 allele increases the accumulation of senile plaques in AD subjects as well as cognitively normal people. Recent findings showed that ApoE regulates cerebrovascular function via the cyclophilin A-nuclear factor-κB-matrix metalloproteinase-9 pathway in pericytes (Yang & Candelario-Jalil, 2017). Some evidence are available to support the compromise of BBB integrity in AD preceding the development of amyloid plaques and cognitive impairment. Thus, functional changes in the BBB could be one of the earliest signs of AD (Elahy *et al.*, 2015; Takeda *et al.*, 2014). It was also demonstrated that Aβ immunization therapy can restore BBB integrity in some mouse models and improve typical AD brain pathological features such as plaques and microgliosis. This suggests the possibility of a BBB-focused strategy for AD treatment (Dickstein *et al.*, 2006).

Post-mortem tissue analysis of AD brain showed evidence of BBB damage including accumulation of blood-derived proteins in the hippocampus and cortex of human subjects with AD and ALS, and degeneration of BBB-associated pericytes, which indicated BBB breakdown (Takeda *et al.*, 2014; Zhao, Nelson, *et al.*, 2015). Tight junction protein function and transmembrane components are also affected in neurodegenerative disorders: occludin being vulnerable to degradation by MMPs, while the molecular connections of adherens junctions and TJPs to the actin cytoskeleton are also disrupted by tau leading to tau-induced neurotoxicity. TJPs are also reported to be involved in RAGE-mediated Aβ cytotoxicity to the BBB endothelial cells with subsequent damaged BBB structural integrity (Erdő *et al.*, 2017).

There is early development of neurovascular dysfunction in AD associated with accumulation of Aβ peptide and NFTs in the brain (Deane & Zlokovic, 2007). Depending on the stage of the disease, AD affects all cell types of the NVU including EC and mural cells, glial and neurons (Deane & Zlokovic, 2007; Zhao, Nelson, *et al.*, 2015). Faulty Aβ clearance from the brain leads to elevated Aβ in the brain of patients with sporadic AD (Deane *et al.*, 2009; Festoff *et al.*, 2016; Zhao, Nelson, *et al.*, 2015). Research data has shown from various animal models that Aβ is cleared from the brain primarily by trans-vascular clearance across the BBB (Deane *et al.*, 2009; Deane *et al.*, 2003; Deane *et al.*, 2008). The molecular mechanism involves the Aβ produced in the brain binding to LRP1 (low density lipoprotein receptor-related protein-1) at the abluminal side of the BBB leading to its rapid internalization into endothelial cells and subsequent clearance through the blood (Chakraborty *et al.*, 2017; Garcia-Castillo *et al.*, 2017).

PICALM (phosphatidylinositol-binding clathrin assembly protein) plays critical role in the molecular mechanism of Aβ clearance by directing the internalization, trafficking and sorting of LRP1- Aβ complexes for exocytosis at the luminal side of the BBB (Garcia-Castillo *et al.*, 2017; Zhao, Nelson*, et al.*, 2015; Zhao, Sagare*, et al.*, 2015). Aβ is then cleared in the plasma by binding to soluble plasma LRP1 and subsequent transport via blood to the excretory organs (kidney and liver) (Erdő *et al.*, 2017; Zhao, Nelson*, et al.*, 2015). Other contributions to CNS clearance of Aβ peptide include enzymatic degradation by neprilysin, an insulin degrading enzyme, MMPs plasmin and tissue plasminogen activator (Saraiva *et al.*, 2016; Zhao, Nelson*, et al.*, 2015; Zhao, Sagare*, et al.*, 2015). Recent research data has suggested that PICALM variants as well as mutation of Clusterin (CLU, apoJ) are also associated with the pathogenesis of sporadic AD (Zhao, Nelson*, et al.*, 2015; Zhao, Sagare*, et al.*, 2015).

2.16.4 Role of OS in the development of Neurodegenerative Diseases

OS is a condition of unbalanced cellular and /or tissue redox states to which the brain is especially vulnerable because of its high oxygen demand, possession of abundant peroxidation-susceptible lipid cells and modest content of antioxidant and related enzymes (Cobley *et al.*, 2018; Kim *et al.*, 2015). Neurodegenerative disease (NDD) is a heterogeneous groups of neurological disorders characterized by a slow progressive neuronal loss (Kim *et al.*, 2015). Although the definitive cause of neurodegenerative disease is yet uncertain, OS has been strongly implicated in playing a critical role in its initiation as well as progression. NDD has been strongly linked with aging and has thus been largely described as a disease of abnormal aging (Wang *et al.*, 2014). Alzheimer's disease, Parkinson's disease, Huntington's disease and Friedreich's ataxia are well known examples of NDD. The critical role played by OS has been reported in the pathogenesis of virtually all these diseases and thus OS appears to be a common denominator in their pathogenesis. Several mechanisms of OS regarding the initiation and/or its propagation have been reported for NDDs, especially for Alzheimer's disease (AD) and Parkinson's disease (PD) (Cheignon *et al.*, 2018; Fischer & Maier, 2015; Tramutola *et al.*, 2017; Wang *et al.*, 2014).

2.16.5 OS as an early event in the initiation and progression of Alzheimer's disease

The evolution of AD incorporate an intermediate transient phase of mild cognitive impairment (MCI) during which there is no significant increase in senile plaques or neurofibrillary tangles (NFTs). Data from MCI subjects provided strong correlated evidence that OS usually precedes the development of clinically demonstrable AD (Tramutola *et al.*, 2017; Wang *et al.*, 2014).

Significantly, elevated levels of oxidized biomolecular markers of OS, compared with age-matched control subjects, were found in MCI subjects (Montagne *et al.*, 2015; Montagne *et al.*, 2017). Furthermore, in the urine, plasma and CSF of MCI subjects elevated levels of specific isoprostanes were found, while CSF levels of markers such as Aβ peptides and tau protein remain unchanged compared to controls with age-matched subjects (Kim *et al.*, 2015; Montagne *et al.*, 2015; Wang *et al.*, 2014). Evidence of significantly increased levels of protein peroxidation and oxidative modification of specific proteins in the hippocampus, superior and middle temporal gyri of MCI subjects have been documented (Tramutola *et al.*, 2017). Furthermore, several other studies also showed significant decreased levels of non-enzymatic antioxidants such as uric acid, vitamin C, E and A, zeaxanthin, ß-cryptoxanthin and α-carotene as well as reduced activity of antioxidant enzymes such as SOD, glutathione peroxidase and glutathione reductase in MCI subjects (Kim *et al.*, 2015; Takeda *et al.*, 2014). Levels of some of these biomolecules, especially the isoprostane (8,12-iso-iPF2α-VI) correlated with the severity of AD (Wang *et al.*, 2014). All these findings preceding the neuropathological findings in AD suggest that OS is a very early contributor to AD and is likely to play a critical role in the progression of the disease and probably other NDDs.

2.17 Sources of excess ROS production in NDDs

In spite of the tell-tale evidence of OS pathology in the brain, neither the specific origin of increased ROS nor the mechanisms for dysfunction of endogenous antioxidant system or the disturbance of redox balance in AD and other NDDs is certain. However, both extracellular and subcellular accumulation of Aβ peptide and the presence of trace metal ions such as copper and iron have been suggested to cause increased ROS production (Kim *et al.*, 2015; Tramutola *et al.*, 2017). Further, reduced activities of α-secretase can cause decrease in β and ɣ-secretase activities which can further enhance Aβ peptide accumulation (Wang *et al.*, 2014). As the mitochondria is itself vulnerable to OS, increased ROS is associated with oxidation of mitochondrial proteins resulting in consequent mitochondrial dysfunction and energy production failure. Mitochondrial dysfunction and disordered glucose metabolism have been supported by overwhelming research data as a critical factor in the pathogenesis of AD (Bhat *et al.*, 2015; Tramutola *et al.*, 2017; Wang *et al.*, 2014). Glucose is the primary source of energy in the brain and oxidation of enzymes involved in glucose metabolism and the consequent decline in glucose metabolism has been documented in AD (Shokouhi *et al.*, 2013; Tramutola *et al.*, 2017; Wang *et al.*, 2014). Research data are also available to support the hypothesis that

the oxidation of crucial metabolic enzymes such as pyruvate kinase, phosphoglucomutase-1, enolase-1, triose phosphate isomerase, ATP-synthase, glyceraldehyde-3 phosphate dehydrogenase, malate dehydrogenase (Tramutola *et al.*, 2017), leads to the reduced activities of these enzymes. Parallel observations points to decreased neuronal expression of genes encoding for subunits of the mitochondrial respiratory chain; reduced complex IV activity observed in the hippocampus and platelets of AD subjects (Kim *et al.*, 2015; Tramutola *et al.*, 2017; Wang *et al.*, 2014). The overall result is a dysfunctional glucose metabolism and reduced ATP generation in the AD brain which further leads to increased mitochondrial ROS generation. Furthermore, Aβ-induced mitochondrial dysfunction has also been reported as a cause of impaired calcium homeostasis in AD brain (Kim *et al.*, 2015). This may be associated with intracellular calcium overload and decreased calcium reuptake which is related to increased ROS, and the opening of the permeability transition pore (PTP) which is an important step in the ferrying of pro-apoptotic molecules across the mitochondria into the cytosol, triggering subsequent apoptosis. In PD, accumulation of α-synuclein aggregates which interferes with vesicular dopamine storage, leading to a build-up of cytosolic dopamine which interacts with trace metal ions such as iron to generate ROS (Blesa *et al.*, 2015; Nissanka & Moraes, 2018). Further, supporting this school of thought, is a number of reports indicating the metabolism of dopamine into semiquinones, auto-oxidation into ROS, as well as the deficiency of complex I enzyme of the mitochondrial respiratory chain (Blesa *et al.*, 2015; Kim *et al.*, 2015; Tramutola *et al.*, 2017).

2.18 Evidence of OS involvement in development of NDDs

Research has demonstrated that an increase in oxidized biomolecules generated by ROS as well as changes in cellular content of antioxidant molecules is measurable as corroborative evidence of OS in several NDDs including AD and PD. This method of measuring oxidized biomolecules is adopted due to the difficulty in measuring ROS specifically, which are usually short-lived. In addition, they are kept at modestly low concentrations by a dynamic balance between the rates of cellular production and neutralization by endogenous antioxidants, leaving empirically either excessive ROS production or impaired antioxidant systems to cause OS. Alterations in the levels of antioxidants and antioxidant enzyme activities were also reported in AD and other NDDs (Wang *et al.*, 2014). Significantly low plasma levels of antioxidants such as glutathione, albumin, lycopene, bilirubin, vitamin A, C and E, were reported in AD patients compared to age-matched control subjects (Wang *et al.*, 2014). Furthermore, different

brain areas in AD also showed significant decreases in the activity of endogenous antioxidant enzymes such as superoxide dismutase (SOD), catalase, glutathione peroxidase and heme-oxygenase despite increased gene expression of some of these enzymes (Kim *et al.*, 2015; Wang *et al.*, 2014).

2.19 Antioxidants.

2.19.1 What are antioxidants?

An antioxidant (AO) is defined as any substance that, when present at low concentrations compared to an oxidisable substrate, significantly delays or prevents oxidation of that substrate (Halliwell, 1990; Halliwell & Gutteridge, 1995). Cellular source of AO include both endogenous molecules such as enzymatic and non-enzymatic cellular constituents that helps to protect the cells against oxidative stress, and exogenous molecules such as dietary compounds that have AO capabilities. Given the critical role OS has been scientifically documented to play in the initiation and progression of neurological, and a number of other diseases (Butterfield, 2018; Paloczi *et al.*, 2018), it becomes rational to propose the use of exogenous antioxidants for the amelioration of the cumulative cellular damage due to oxidative stress.

Several distinct dietary compounds with antioxidant properties have been identified and studied such as polyphenols (flavonoids), β-carotene, vitamin C and vitamin E (α-tocopherol) (Freyssin *et al.*, 2018; Zhang *et al.*, 2018).

2.19.2 Endogenous Cellular Antioxidants: Classification

Mammalian cells are equipped with a full complement of antioxidant system which help to neutralize reactive species thus keeping their total cellular concentration within physiological range (Zhang *et al.*, 2016). Cellular antioxidants are classified into two broad categories, enzymatic or first-line and non-enzymatic or second-line antioxidants which act via catalysis of free radical neutralization (Aslani & Ghobadi, 2016; Carocho & Ferreira, 2013; Ighodaro & Akinloye, 2018). Enzymatic antioxidants are sub-classified into primary and secondary types of which the primary types are the most effective (Aslani & Ghobadi, 2016). Primary enzymatic antioxidants include glutathione peroxidase (GPx), catalase (CAT), superoxide dismutases (SOD) and peroxiredoxins (Prxs) (Aslani & Ghobadi, 2016). These enzymes neutralize reactive species and free radicals or prevent their formation and usually require cofactors for their enzymatic activity, except for peroxiredoxins (Aslani & Ghobadi, 2016; Ighodaro & Akinloye, 2018). The secondary enzymatic class of cellular antioxidants consist of

enzymes which help to regenerate and thus supportive of other endogenous antioxidants (Aslani & Ghobadi, 2016). This class includes glutathione reductase which helps to reduce glutathione disulphide and thereby regenerate glutathione, and glucose-6-phosphate dehydrogenase which helps to regenerate NADPH (Aslani & Ghobadi, 2016).

Non-enzymatic antioxidants occur as either metabolic, that are generated via metabolic pathways and are thus endogenous or as nutrients antioxidants which are exogenously introduced into the cells as constituents of foods or dietary supplements (Carocho & Ferreira, 2013; Mirończuk-Chodakowska *et al.*, 2018). Metabolic non-enzymatic antioxidants include thiol antioxidants, such as glutathione (GSH), thioredoxins (Trx) and glutaredoxin (Grx), lipoic acid (LA), melatonin, coenzyme-Q (CoQ), uric acid (UA), bilirubin and metal chelating agents such as transferrin (TF), ferritin (FT), caeruloplasmin (CP), lactoferrin (LTF), albumin (ALB), myoglobin (MB), and metallothioneins (MTs) (Aslani & Ghobadi, 2016; Mirończuk-Chodakowska *et al.*, 2018).
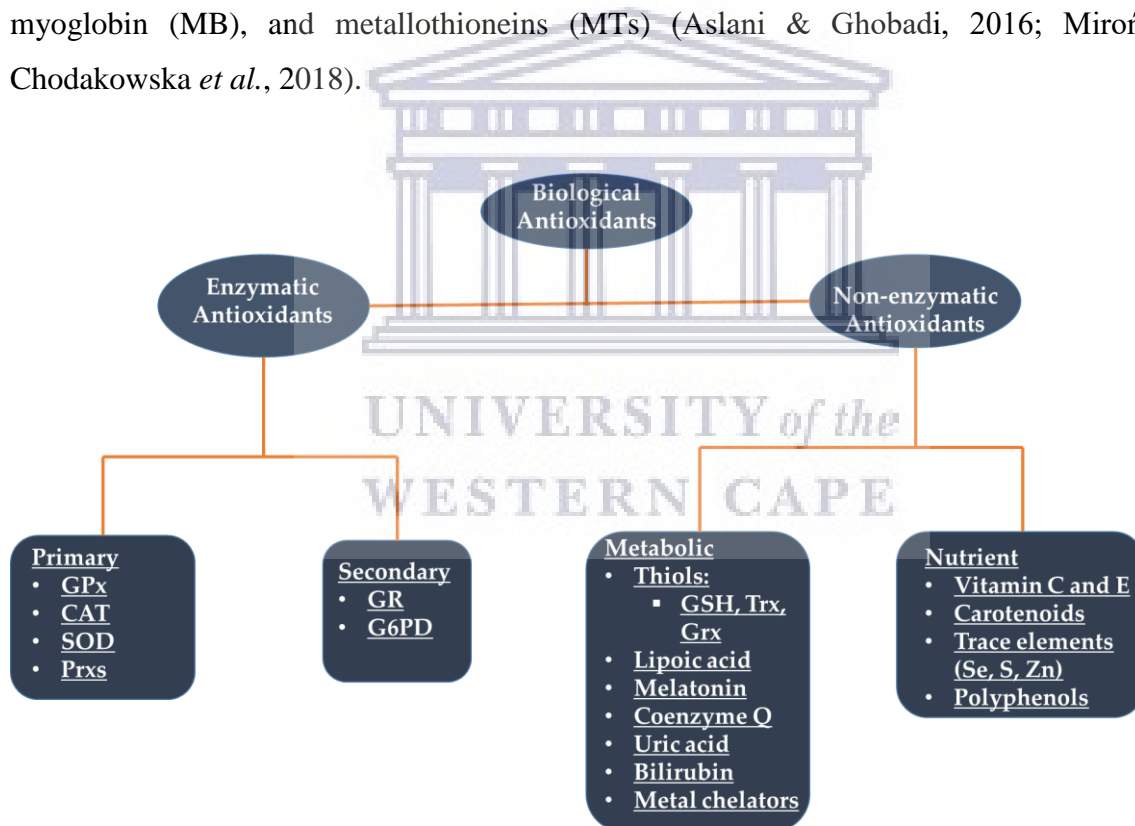
Figure 2.10: Classification of endogenous cellular antioxidants.

Enzymatic antioxidants neutralises oxidants through enzymatic conversion into non-reactive substances and are further subdivided into primary and secondary subtypes. Non-enzymatic antioxidants are either derivatives of cellular metabolic reactions or essential nutrient substances (Aslani & Ghobadi, 2016; Ighodaro & Akinloye, 2018; Mirończuk-Chodakowska *et al.*, 2018).

71

2.20 Antioxidant therapy in neurologic diseases

2.20.1 Evidence of the ameliorative effects of dietary antioxidants on neurodegenerative diseases

2.20.1.1 Dietary Polyphenols

Epidemiological and clinical studies have demonstrated that polyphenols and flavonoids exert a protective effect against neurodegenerative diseases (Samieri, 2018). Several authors have reported that diets enriched with fruits and vegetables rich in antioxidants (carrots, blueberries, strawberries, spinach) can produce beneficial effect in old rats against age-related decline in cognitive functions (Nissanka & Moraes, 2018). Polyphenols are naturally present in fruits, and vegetables (olive oil, red wine, tea) with flavonoids being the largest group of the polyphenols with more than 2000 distinct flavonoids known (Ramassamy, 2006). They naturally occur as glycosylated, hydroxylated and methoxylated phenol derivatives (Xie & Chen, 2013). The glycosylated form either contains glucose or rhamnose as the sugar moiety (Ramassamy, 2006). By glycosylation the chemical, physical and biological properties of the flavonoids are moderated as well as their absorption by the small intestine (H. Cao & Chen, 2012). Their antioxidant potency is related to the number of hydroxyl group present such that the most potent of flavonoids contains 3-6 hydroxyl groups (Chen *et al.*, 2018). There is paucity of data on bioavailability of phenolics after oral intake, however, the increase in the serum antioxidant levels following consumption of food and beverages rich in polyphenols have been reported (Oh & Shahidi, 2018). Taken together, these findings suggest that the consumption of polyphenolic compounds could have beneficial effects against oxidative stress-induced damages.

2.20.1.2 Ameliorative effects of dietary polyphenols

For the purposes of this chapter we discussed the widely used exemplar of exogenous AOs, green tea. The flavonoids in green tea has attracted considerable research interest because of its potential to prevent or treat cancer (Ramassamy, 2006; Sakaki *et al.*, 2019). Bioactive constituents of green tea include flavonoids (catechins and their derivatives) and it constitutes about 30% of the dry weight of a leaf (Sakaki *et al.*, 2019). Analysis of green tea using HPLC yields mainly epigallocatechin-3-galate (EGCG) as the polyphenolic constituent (more than 60% of total catechins) (Sakaki *et al.*, 2019). Other compounds in green tea are the flavonols

(quercetin, kaempferol and rutin), caffeine, phenolic acids, and theanine (Sakaki *et al.*, 2019; Zhang *et al.*, 2018).

Reports from nutritional and epidemiological studies as well as animal model of PD revealed risk reduction for Parkinson's disease by the consumption of teas with high AO content such as green and black teas. These effects have been ascribed to EGCG, the most potent component of green tea (Bastianetto *et al.*, 2006; Pan *et al.*, 2003). Green tea compounds also act as chelator of ferric ion which could also explain the green tea-induced-protection against MPTP (Bastianetto *et al.*, 2006) since MPTP is known to increase iron levels in the Substantia Nigra Pars compacta of mice, rats and monkeys. While there is no significant benefit with regard to tea consumption in AD, several *in vitro* studies showed that green tea could protect against Aβ-induced neuronal damages (Bastianetto *et al.*, 2006; Singh & Ghosh, 2019).

In the last decade, studies have provided multiple confirmation that EGCG is able to regulate the proteolytic processing of amyloid-precursor protein in both *in vivo* and *in vitro* studies (Singh & Ghosh, 2019). In neuronal cell cultures, it promotes the non-amyloidogenic α-secretase pathway (Singh & Ghosh, 2019) and reduces the formation of Aβ fibrils (Singh & Ghosh, 2019). EGCG-mediated promotion of neuronal protection has also been linked to its ability to modulate a number of intracellular signalling pathways such as MAPK, protein kinase C, and phosphatidylinositol-3-kinase (PI3K) (Ramassamy, 2006; Rodríguez-Morató *et al.*, 2018). These pathways play important roles in neuronal protection against a variety of oxidative insults and are essential to cell survival (Zhang *et al.*, 2016). EGCG also lowers the expression of the pro-apoptotic genes Bax, Bad, cell cycle inhibitor Gadd45, Fas ligand and tumor necrosis factor-related apoptosis ligand (TRAIL) in SH-SY5Y neuroblastoma cells (Levites *et al.*, 2002).

Beneficial effects were mediated via antioxidant potential, through modulation of different pathways such as signalling cascades, anti-apoptotic processes, and synthesis or degradation of Aβ peptide (Ramassamy, 2006)

2.20.2 Over-indulgence of exogenous antioxidants: Reductive Stress

In redox reactions, two or more atoms undergo changes in their oxidation states (Viswanathan & Razul, 2020). The oxidation state of an atom is defined as the "charge of this atom after ionic approximation of its heteronuclear bond". This definition describes all atoms in a poly-elemental molecule as ions and thus a change in the charge on an ion in a molecule implies a

change in the oxidation state of that molecule (Nič *et al.*, 2009). In cells are complex networks of metabolic and signalling pathways and their components such as metabolites, enzymes and their regulatory components, ROS and other nucleophiles, antioxidant components, protein thiols and redox couples. These together constitute the cellular redox system (Lee & Loscalzo, 2020). When products and/ or by-products of redox reactions cross the structural barriers of cellular and subcellular compartments they alter their redox environments. Oxidative stress attacks nucleic acids, proteins, lipids and carbohydrates in cellular and subcellular compartments (Lee & Loscalzo, 2020).

Under physiologic conditions the redox system within the cells and the entire body is maintained at a redox balance by the action of the endogenous antioxidant system that neutralizes excess ROS. Under pathologic conditions resulting from redox imbalance, the endogenous antioxidant system either fails to contain the challenge of ROS production or the rate of ROS production becomes excessive (Kim *et al.*, 2015). Research data has supported the use of exogenous antioxidant (such as vitamin C and vitamin E, and polyphenols) supplementation of diet as beneficial in the treatment and/or amelioration of diseases conditions mechanistically impacted by redox imbalance (Sakaki *et al.*, 2019). However, several reports have documented the adverse effects of exogenous AO treatment on cellular physiology which include modulatory effects on cell signals involved in critical cell functions as proliferation, senescence, cell growth, and apoptosis (Zhang *et al.*, 2016). The overzealous use of antioxidants therefore, has the potential to impact negatively on the normal and beneficial effects of ROS in biologic systems which can lead to undesirable conditions of reductive stress (Mentor & Fisher, 2017). Furthermore, because the beneficial effects of antioxidant clinical trials on many clinical conditions has largely yielded modest benefit, some authors have suggested the over-use of exogenous AOs may indeed cause a 'pro-oxidant' effect (reductive stress) (Mentor & Fisher, 2017).

2.21 Glutathione

Glutathione, GSH, is the most abundant non-protein thiol (γ-glutamyl-cysteinyl-glycine) in animal cells and it exists in two forms as oxidized glutathione or glutathione disulphide (GSSG) and reduced/free glutathione (GSH) with only GSH showing antioxidant activity (Guilford & Hope, 2014). The biological functions of GSH is conferred by its unique gamma-glutamyl bond between the glutamate and cysteine residues and also by the presence of a free thiol group (Li *et al.*, 2012). During cellular redox buffering, GSH is utilized to neutralize ROS with a

resultant by product GSSG that lacks antioxidant capability (Guilford & Hope, 2014) and the GSH/GSSG system is the major redox couple in animal cells (Wu *et al.*, 2004).

Production of GSH is brought about via two mechanisms, *de novo* synthesis and GSSG recycling. GSH is synthesized, *de novo,* from glutamine, cysteine and glycine in a reaction catalysed sequentially by two cytosolic enzymes, γ- glutamyl cysteine ligase (GCL) and glutathione synthetase (GS) (Guilford & Hope, 2014; Wu *et al.*, 2004). The synthesis of GSH is primarily regulated by GCL activity, cysteine availability and GSH feedback inhibition. Alternatively, GSH can be obtained by the reduction of GSSG via the reaction catalysed by glutathione reductase (GSR) (Guilford & Hope, 2014; Wu *et al.*, 2004) as well as transmembrane cellular enrichment via interorgan exchange (Li *et al.*, 2012). In the GSR reaction NADPH is utilized in reducing one molecule of GSSG to produce two molecules of GSH. Pathological situations exist that inhibit the *de novo* GSH synthesis leaving cells to source for GSH mainly via the recycling of GSSG (Morris *et al.*, 2013).

GSH plays critical roles in cellular redox balance, and regulation of cellular events such as gene expression, DNA and protein synthesis, cell proliferation and apoptosis, signal transduction, cytokine production, immune response and protein glutathionylation (Sies, 1999).

Deficiency of GSH contributes to OS which promotes aging and the pathogenesis of many diseases including neurological diseases such as seizure, Alzheimer's disease, Parkinson's disease, stroke and several others. Several of these neurological diseases incorporate BBB dysfunction in their pathogenesis (Paloczi *et al.*, 2018). New knowledge on the role of brain endothelial GSH metabolism in BBB dysfunction is critical for the development of effective strategies to improve care of these diseases.

2.21.1 Historical Background

2.21.1.1 *The discovery of glutathione*

Glutathione discovery dates back to the past 13th decade when de Rey-Pailhade first found that a substance contained in yeast and some other cells reacts spontaneously with elemental sulfur to yield hydrogen sulphide (Meister, 1988). This substance was later to be characterized, however erroneously, as a dipeptide consisting of cysteine and glutamine residues more than 3 decades later by Sir FG Hopkins and other workers (Simoni *et al.*, 2002). Because of the substance affinity for sulfur, de Rey-Pailhade initially named the compound "*philothion*" which

he took from the Greek words for love and sulfur (Meister, 1988). Furthermore, the presence of philothion was noted in many animal tissues such as liver, sheep brain, lamb intestine, fish muscle, fresh sheep blood and fresh egg white but scarcely was demonstrable in tendons, adipose tissue, fresh bile, normal urine and defibrinated blood (Meister, 1988). Additionally, philothion bleached various dyes as carmine, indigo and litmus whereas chlorine, iodine and bromine destroyed philothion instantly (Meister, 1988). These observations taken together led de Rey-Pailhade to conclude that solutions of philothion reacts with oxygen and consumed in the reaction (Meister, 1988). He further noted that despite consumption of philothion on reaction with oxygen, cells somehow always maintain a constant amount of philothion. He concluded that philothion is regenerated in cells as soon as it is consumed and thus must play important biological role because of its ubiquity in living cells (Meister, 1988). Several other workers reports including Heffter and Arnold, Hunter and Eagles and later Hopkins, until 1927, led to the structural characterization and isolation of the compound, initially controversially as a dipeptide and later as a tripeptide consisting of glutamine, cysteine and glycine residues and the name glutathione was later unanimously adopted as the name of the biological substance (Meister, 1988; Simoni *et al.*, 2002).

2.21.1.2 *The origin of glutathione in eukaryotic cells.*

Intracellular thiols such as glutathione (GSH), homoglutathione, γ-glutamylcysteine (γ-Glu-Cys), γ-glutamylcysteinylserine and mycothiol are produced in aerobic organisms for protection against ROS produced as by-products of aerobic metabolism (Copley & Dhillon, 2002). They protect the cell by buffering the redox status of cell cytoplasm and protecting biomolecules against oxidative damage. GSH, is the most common of these thiols, additionally provides reducing equivalents to several enzymes (such as ribonucleotide reductase, 3'-phosphoadenosine 5-phosphosulfate reductase and arsenate reductase) (Muri *et al.*, 2019) as well as serves as substrate for glutathione-S-transferases (Fujikawa *et al.*, 2019) which enzymatically detoxify toxic electrophiles.
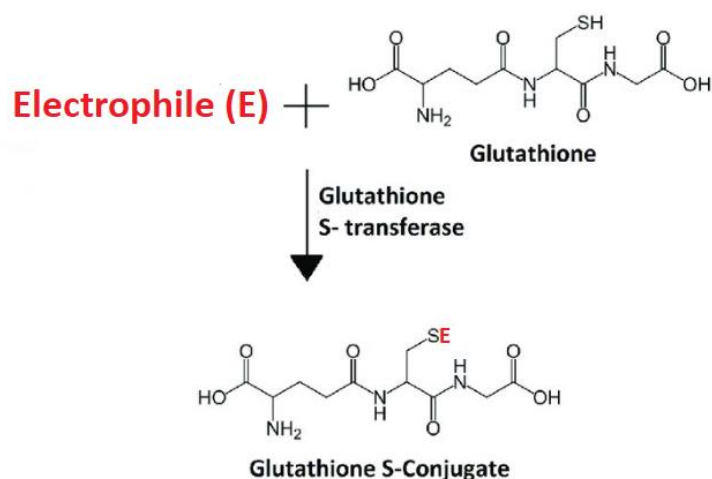
Figure 2.11: Enzymatic detoxification of electrophiles by glutathione-S transferases using reduced glutathione as substrate.

GST catalyses the formation of a thioester bond between reduced glutathione and the electrophile to form a glutathione S conjugate of the electrophile. Fate of the conjugate include sequestration into vacuole or direct export from the cell by ATP-dependent membrane pumps. GST, glutathione S-transferase.

Presence of GSH has been noted primarily in Gram-negative bacteria and eukaryotes (Marcén *et al.*, 2019; Pophaly *et al.*, 2017). It is rarely found in Gram-positive bacteria, and not present at all in the Archaea and in amitochondrial eukaryotes such as *Entamoeba histolytica* (Ondarza *et al.*, 1999), and *Trichomonas vaginalis* (Sena-Lopes *et al.*, 2019). This characteristic pattern suggests that the genes involved in GSH biosynthesis may have been transferred to eukaryotes from bacterial ancestry via mitochondrial progenitor. The biosynthesis of GSH involves activity of two enzymes γ -glutamine-cysteine ligase (GGCL) and GSH synthetase. GGCL catalyses the formation of peptide bond between the γ -carboxylate of glutamate and cysteine following which GSH synthetase catalyses the formation of the bond between the cysteinyl carboxylate of γ -glutamylcysteine and glycine (GGC) and the amino group of glycine (Copley & Dhillon, 2002). In each stage of the reactions, ATP hydrolysis is required to drive peptide bond formation (Copley & Dhillon, 2002). Much information regarding the evolutionary origin of GSH has been obtained from genetic analysis of its biosynthetic enzymes GGCL and GSH synthetase (GSS). Analysis of genetic sequences of the two enzymes of GSH synthesis suggests that the two enzymes are acquired independently (Copley & Dhillon, 2002). Further, the most probable source of the GGCL gene is cyanobacteria with this gene being later transferred to eukaryotes and other bacteria (Copley & Dhillon, 2002). After the acquisition of the GGCL

gene, to further strengthen protection against ROS each eukaryotes and most bacteria apparently recruited a protein with the ATP-grasp superfamily structural fold that is glutathione synthetase, to catalyse synthesis of glutathione from GGC (Copley & Dhillon, 2002). The eukaryotic GSS_e did not evolve directly from the bacterial GSS_b but in each of the bacterial and eukaryotic domain GSS was independently recruited (Copley & Dhillon, 2002).

2.21.2 Cellular abundance of glutathione.

GSH content ranging between 0.5-10mM/L is the major low molecular weight thiol in animal cells (Wu *et al.*, 2004). The proportion of cellular GSH in the cytosol ranges between 85-90% while the remainder is distributed among cellular organelles such as the mitochondria, nuclear matrix and peroxisomes (Winterbourn, 2019). Net cellular loss of GSH is contributed to by GSSG efflux which accumulates as by product from utilization of GSH in redox buffering. Additionally, marked reduction of cellular GSH occurs in protein malnutrition, following OS and in many pathological conditions (Lu, 2009). The GSH+2GSSG concentration is usually denoted as 'total glutathione' in cells whereas up to 15% additional pool may be bound to proteins (Sies, 1999). The [GSH]:[GSSG] ratio is often used as an indicator of cellular redox status and this ratio is usually more > 10 under normal physiological conditions. GSH/GSSG being the major redox couple in cells determines the cellular anti-oxidative capacity, however, its value can be affected by the presence of other redox couples such as $NADPH/NADP^+$ and thioredoxin$_{red}$ /thioredoxin$_{ox}$.

2.21.3 Cellular biosynthesis of glutathione.

Reduced or free GSH is synthesized in the cytosol and involves a two-sequence reaction with each step requiring ATP, catalysed by GCL and GS, occurring in virtually all cell types. First, GCL catalyse the formation of a peptidic-γ linkage between the γ-carboxyl group of glutamate and the amino group of cysteine which protects GSH from hydrolysis by intracellular peptidases (Guilford & Hope, 2014). GS in animal cells is highly active and show great affinity for the γ-glutamyl-cysteine intermediate thus favouring the forward reaction leading to the formation of GSH (Wu *et al.*, 2004). GCL is composed of a catalytic (GCLC) and a modifier (GCLM) subunit and these subunits are encoded by different genes in rodents and humans (Dalton *et al.*, 2004). While catalytic activity and feedback inhibition reside in the GCLC subunit of the isolated enzyme, modifier or regulatory function is found in the GCLM subunit which lowers the K_m of GCL for glutamate and raises the K_i for GSH (Lu, 2013). These properties when taken together made the holoenzyme catalytically more efficient and less

subject to inhibition by GSH than GCLC alone (Yang *et al.*, 2002). Redox status can modulate GCL activity by favouring the formation of the holoenzyme (Yang, 2018). Under physiological conditions, the regulators of GSH synthesis include feedback inhibition by GSH, and the availability of cysteine which in turn depends on nutritional status (Wu *et al.*, 2004). The second step in GSH synthesis involves the activity of GSH synthetase (GS), an enzyme composed of two identical subunits, not subject to feedback inhibition by GSH (Lu, 2013). Because the γ-glutamyl-cysteine product of GCL is present at very low concentrations in the presence of GS, and that overexpression of GS does not experimentally increase GSH level whereas overexpression of GCL increases GSH levels (Lu, 2013), GCL is considered rate-limiting in GSH biosynthesis (Lu, 2013). During oxidative stress there is increased GSH oxidation and it is an important aspect of GSH homeostasis that there is usually an increase in the total glutathione pool due to upregulation of *de novo* synthesis of GSH (Li *et al.*, 2012).
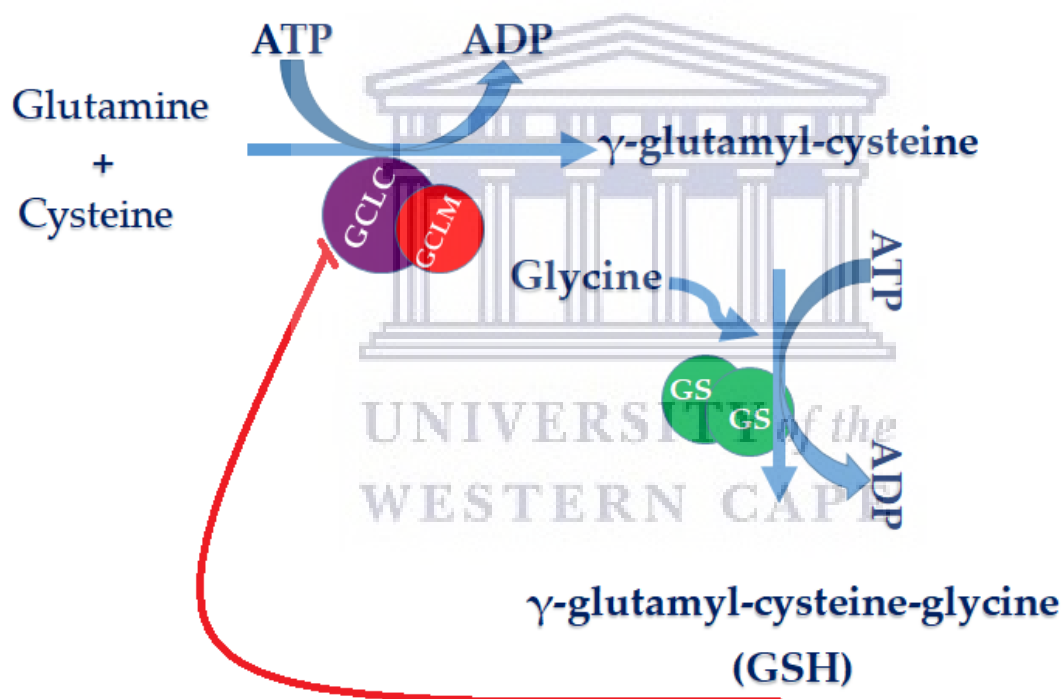
Figure 2.12: *De novo* synthesis of glutathione.

Synthesis involves ATP requiring 2-step reaction catalysed by γ-glutamylcysteine ligase (GCL) composed of catalytic (GCLC) and modifier (GCLM) subunits and glutathione synthetase made up of two identical subunits. GCLC is subject to feedback inhibition by GSH.

2.21.4 Role played by glutathione in cellular functions

Functions served by GSH in cells include antioxidant defence, detoxification of xenobiotics, regulation of cell cycle progression and apoptosis, cell differentiation, maintenance of redox potential, modulation of immune function and redox signalling.

2.21.4.1 Antioxidant function

Antioxidant function of GSH is largely by the reaction of glutathione peroxidase (GPx) which reduces H_2O_2 and lipid peroxides while oxidizing GSH to GSSG. Glutathione reductase enzyme recycles GSSG to GSH in a redox cycle involving the use of NADPH. Additionally, catalase is also present in the cell to reduce H_2O_2, however, it is present only in peroxisomes. Thus GSH is of critical importance in the mitochondria for the purpose of buffering oxidative stress. Given that GSH is the determinant of the intracellular redox potential, it follows that to prevent a major shift in the redox equilibrium when OS overcomes the ability of the cell to recycle GSSG, active GSSG export from the cell or its reaction with sulfhydryl group to form mixed disulphide is necessary. The implication is that severe OS depletes cellular GSH.

2.21.4.2 Cell signalling

GSH plays critical roles in redox-mediated signalling by mitigating the redox state of important protein redox-active cysteine residues (Forman, 2016). By its reversible binding to the -SH of protein cysteinyl residues, a process called glutathionylation, it generates either active or inactive glutathionylated proteins (Li *et al.*, 2012). This mechanism serves to protect sensitive protein thiols from irreversible oxidation and also to store GSH under oxidative conditions. Reversal or deglutathionylation occurs through the action of glutaredoxin and sulfiredoxin that use GSH as reductant (Lu, 2013). Oxidisable critical cysteine residues are important features of several signalling proteins and transcription factors, and glutathionylation therefore offers an important mechanism for modulation by GSH the regulatory functions of ROS on protein functions(Li *et al.*, 2012). Specifically, GSH is known to exert intense effects on vascular endothelial functions including endothelial barrier permeability, apoptosis, and angiogenesis by its ROS scavenging function through which it modulates the second messenger effect of ROS in many endothelial functions (Li *et al.*, 2012). Studies have shown GSH to ameliorate H_2O_2-induced reduction in transendothelial electrical resistance (TEER) via negative regulation of the activation of p38 MAP kinase. Further, GSH was shown to act as cofactor for the detoxification of methylglyoxal, thus preventing carbonyl stress-induced brain endothelial barrier dysfunction.

2.21.4.3 Cell proliferation

Increase in GSH has been linked to positive proliferative response in many cell types including normal brain microvascular endothelial cells and is thus essential for cell cycle progression (Markovic *et al.*, 2009). One important mechanism of GSH promotion of DNA synthesis relates to the maintenance of reduced glutaredoxin and thioredoxin which are required for the activity of ribonucleotide reductase which in turn is the enzyme that sets the pace in DNA synthesis (Forman, 2016). Furthermore, it has been reported that GSH co-localizes to the nucleus at the beginning of cell proliferation and this can affect the activity of nuclear proteins including histones, and many other factors that drive cell cycle progression (Markovic *et al.*, 2007). Taken together, these findings suggest that a reducing condition is vital for cell cycle progression.

2.21.4.4 Cell survival *and death*

GSH is also involved in the regulation of cell death such as occur via apoptosis and necrosis (Shen *et al.*, 2018). Apoptosis features chromatin condensation, fragmentation and internucleosomal DNA cleavage while necrosis is characterized by rupture or fragmentation of the plasma membrane and ATP depletion (Shlomovitz *et al.*, 2018). Both share a common pathway such as involvement of the mitochondrial and can also occur together (Shlomovitz *et al.*, 2018). During apoptosis in a variety of cells, GSH levels fall due to accumulating ROS, GSH efflux and decreased GCL activity (Circu & Aw, 2012). It may appear that GSH efflux compromises the normal protective role of the biomolecule, yet without it apoptosis may not occur in many cell types (Circu & Aw, 2012). Intense GSH depletion, however, blurs the distinction between apoptosis and necrosis inferring that very high levels of ROS may overwhelm the apoptotic machinery (Shlomovitz *et al.*, 2018). Severe GSH depletion particularly in the mitochondrial leads to high level accumulation of ROS, mitochondrial functional abnormalities and ATP depletion causing cells to bypass apoptosis into necrosis (Circu & Aw, 2012; Lu, 2013).

2.21.5 Regulation of GSH synthesis.

De novo synthesis is crucial to the homeostatic control of cellular GSH content and this is catalysed by heterodimeric GCL composed of GCLC and GCLM (Guilford & Hope, 2014). All catalytic activity of the enzyme resides in the GCLC subunit with heterodimerization serving only to increase its activity (Lu, 2009). Regulation of GCL activity could occur by metabolic of transcriptional means. Metabolic GCL regulation is effected through protein

phosphorylation at serine and threonine moieties leading to the inhibition of enzyme activity, while transcriptional control of GCL activity goes through the expression of the catalytic and modulatory subunits (Li *et al.*, 2012).

The promoters of the two subunits of GCL have certain elements in common such that coordinate transactivation can occur which leads to overall increase in subunit expression (Li *et al.*, 2012). Redox-sensitive transcription factors such as nuclear factor kappa B (Nf-kB, Sp-1, activator protein-1 and 2 (AP-1, AP-2) and nuclear factor E2-related factor 2 (Nrf2) mediate GCL expression (Lu, 2013). The human GCLC gene promoter features consensus binding sites for transcription factors such as AP-1, NF-kB, and Nrf2 as well as for the antioxidant response elements (ARE) (Li *et al.*, 2012; Lu, 2013; Raghunath *et al.*, 2018). There are four AREs identified in the human GCLC promoter denoted by ARE1, 2, 3 and 4 which show selectivity in binding of transcription factors. The number of identified AREs shows specie variability as there are only three AREs in the rat GCLC promoter of which ARE3 involvement in Nrf2-dependent expression of GCLC has been reported (Raghunath *et al.*, 2018).

Further contribution to the control of GCLC activity occur through constitutive and induced posttranslational phosphorylation of GCLC. This is evidenced by kinase-mediated phosphorylation of GCLC by stress hormones such as glucagon in contrast to insulin and hydrocortisone which induce GCLC expression. Kinases involved include PKA, PKC, and Ca2+-calmodulin kinase with resultant decrease in GCLC activity upon phosphorylation (Zhang *et al.*, 2017).

The transcriptional regulation of GCLM is yet poorly understood, however, the human GCLM has been shown to contain an ARE site that mediated Nrf2-dependent GCLM upregulation by β-naphthoflavone and lipid peroxidation products (Li *et al.*, 2012; Zhang *et al.*, 2007).
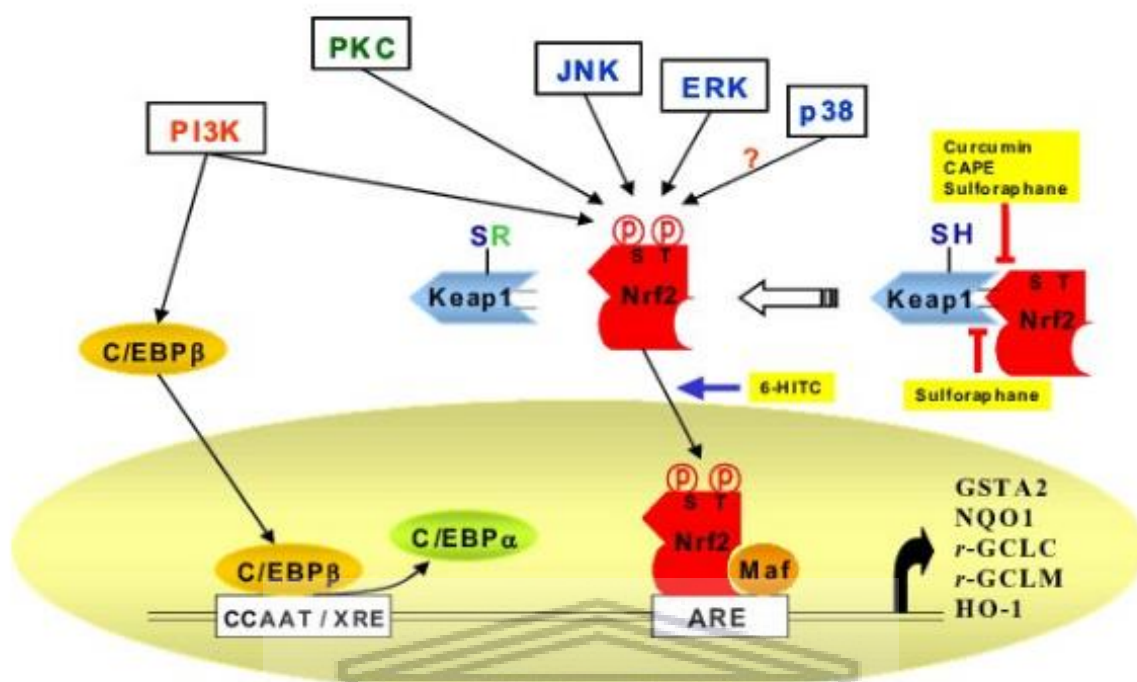
Figure 2.13: Transcriptional regulation of glutathione synthesis.

Kelch-like-ECH-associated protein 1(Keap1) is a cytoplasmic repressor of Nrf2 which inhibits its translocation to the nucleus and thus inhibits transactivation of ARE. Keap1 contains oxidisable cysteine residues which can be modified by oxidants leading to Nrf2 release from its repressor and subsequent translocation to the nucleus. Alternative route for Nrf2 dissociation include phosphorylation of Nrf2 by kinases such as MAPK, PKC or PI3 (Surh, 2004)

2.21.6 Chapter Summary

In this chapter, existing scientific information regarding the structure and function of the blood-brain barrier under physiological and pathological conditions are extensively discussed. The various events in cellular physiology and pathophysiology that interplay to give rise to BBB dysfunction and in turn neurological diseases, as well as scientific interventions already established and ongoing are reviewed. These include the concept of ROS and the homeostatic balance of ROS production within cells and oxidative stress, their effects on the physiology and pathophysiology of the BBB. Despite the several new knowledge of the nature of the BBB using different species and the advances in research methodology, therapeutic manipulations of the BBB remains largely unsuccessful. It is suggestive of lack of standardisation of the parameters used to study the cellular changes in the BBB under various conditions such as OS. In this study therefore, it was hypothesised that different cells, though taken from the same

animal source, responds differently to ROS challenge. The next chapter will focus on the research methodology and materials designed to drive this study.

3   CHAPTER 3: Materials and Methods

3.1   Research Design

The study is designed to study the capacity of BECs to survive 24hr exposure to increasing concentrations of H_2O_2 with and without application of exogenous antioxidants. The survival capacity of the two types of mouse-derived endothelial cells will be compared and further experiments will be carried out on either of these cell lines. Furthermore, the effect of exposure to escalating ROS on cell proliferation will be investigated in the two types of cell lines and compared. Subsequent experiments will include the study of the mechanism of cellular death and /or inhibition or promotion of cellular proliferation due to exposure to the varying concentrations of H_2O_2. Data will be analysed and interpreted in line with existing reports with respect to the ROS-induction of BBB dysfunction.

The schematic below summarises the study design.
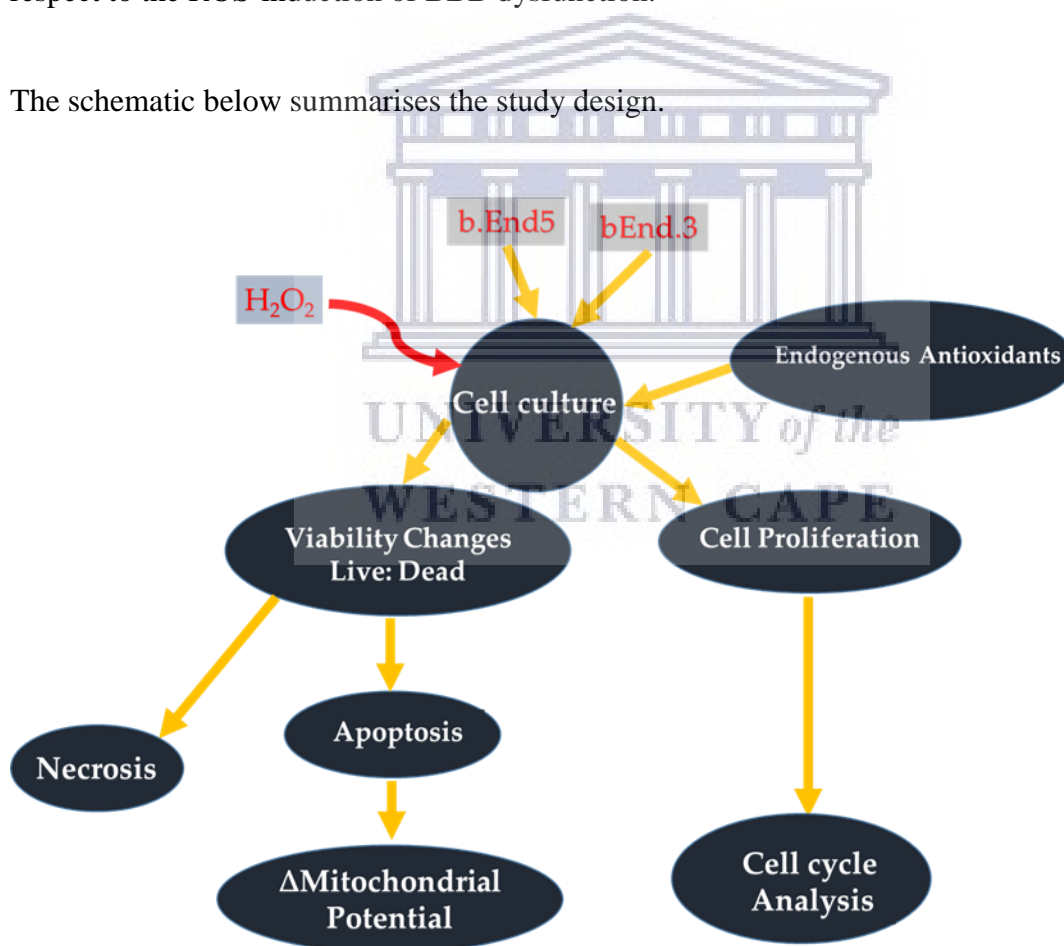
Figure 3.1: Schematic summary of the research design to study effects of ROS in BBB dysfunction.

3.2 Materials

3.2.1 Cells and cell culture

Immortalized mouse-derived brain endothelioma cell lines of two types, b.End5 and bEnd.3 were used for our studies.

The b.End5 type, previously described by Reiss et al 1998 (Reiss *et al.*, 1998) was purchased from ECACC (Sigma-Aldrich, 96091930), and were cultured in Dulbecco's modified Eagle's medium (DMEM, Lonza, BE 12-719F) supplemented with 10% (v/v) fetal bovine serum (FBS, biowest, S12010S181G), 100units/ml penicillin/streptomycin (Lonza, DE17-602E), 1% sodium pyruvate solution (Lonza, BE13-115E), and 1% non-essential amino acids (NEAA Lonza, BE 13-114E) at 37˚C and 5% CO_2 in a humidified atmosphere. For all experiments b.End5 cells between passages 5-20 were used and culture medium was changed every 2-3 days. Prior to experimentation, cells were rinsed with 1X phosphate buffer solution (PBS). The adherent cells were detached by the addition of TrypLE™ Express, a recombinant trypsin enzyme preparation, after which equal volume of complete media was added and aspirated into 15ml conical tubes. The cells in suspension were further pelleted by centrifugation for 5 minutes at rpm of 2,500. Supernatant was then aspirated to remove the effects of trypsin and thereafter, known volume of fresh media added to bring the cells into suspension.

The bEnd.3 (ATCC® CRL-2299) cell line as previously characterized (Montesano *et al.*, 1990; Williams *et al.*, 1989) was purchased from American Type Culture Collection (ATCC) and was maintained in Dulbecco's modified Eagle's medium (Gibco™ 11320074) supplemented with 10% (v/v) fetal bovine serum (FBS, Biowest S12010S181G), 100U/ml penicillin/streptomycin (Lonza, DE17-602E) and L-glutamine to a final concentration of 4.1mM (ThermoFisher 25030081) and at 37˚C and 5% CO_2 in a humidified atmosphere. For all experiments, bEnd.3 cells used were between passages 5-20 and culture medium was changed every 2-3 days. Prior to cell seeding for experiments, adherent bEnd.3 cells were brought into suspension as described for bEnd5 cells above.

3.2.2 Bio-reagents

Analytical grade reagents were used for all experiments. These include Monochlorobimane (Molecular Probe M1381MP), Trypan blue, (Gibco 1520-061), Tris (2-carboxyethyl) phosphine hydrochloride, TCEP (Sigma C4706), GSH-Glo™ Glutathione Assay Kit (Promega V6911/2), Trolox ((±)-6-Hydroxy-2, 5, 7, 8-tetramethylchromane-2-carboxylic acid,

Sigma 238813), Cell Proliferation Kit II (XTT) (Roche, Sigma 11465015001), Hydrogen Peroxide (30%, Merck Millipore 107209), Tetramethylrhodamine, Ethyl Ester, Perchlorate (TMRE) (Invitrogen™ T669), Hoechst 33342, Trihydrochloride, Trihydrate (Molecular probes, H3570), FxCycle™ PI/RNase Staining Solution (Invitrogen F10797), Annexin V, FITC conjugate (molecular probes A13199), L-Glutathione reduced (Merck, CAS Number 70-18-8), Bicinchoninic Acid solution (Merck CAS Number 1245-13-2), Bovine Serum Albumin (Merck CAS Number 9048-46-8), TrypLE™ Express Enzyme (1X), no phenol red (Gibco 12604013), 1, 4-diazobicyclo-[2, 2, 2]-octane (DABCO, Merck CAS Number 280-57-9)

3.3 Methods

3.3.1 Determination of comparative ROS-buffering capacity of b.End5 and bEnd.3 cells

3.3.1.1 Hydrogen Peroxide Treatments

A stock solution of hydrogen peroxide (H_2O_2, 9.8M, Merck Millipore) was diluted to the required concentrations in complete media. Cultured b.End5 and bEnd.3 cells were divided into labelled treatment wells exposed to H_2O_2 concentrations ranging between 10µM to 2mM and cells that were unexposed to H_2O_2 served as control. To determine the antioxidant capacity of cultured cells both b.End5 and bEnd.3 cells were seeded in separate transparent 96 well plates at $1x\,10^4$ cells per well in 200µL of normal media and allowed to attach overnight. Media were then aspirated and replaced with either 100µL of fresh media to serve as control or 100µL of media dosed with the appropriate concentrations of H_2O_2 for another 24hrs. Experiments were repeated thrice and average values of parameters were recorded. Viability of the cells exposed to different concentrations of hydrogen peroxide were then analysed and compared against viability measures for the control cells under same duration in culture.

3.3.1.2 Antioxidants treatments

To study the effects of exogenous antioxidant treatment on the capacity for survival of b.End5 and bEnd3 cells exposed to H_2O_2 concentrations of increasing strength, either solutions of reduced glutathione or Trolox (each 25µM final concentration) in combination with the IC_{75} concentrations of H_2O_2 were added as additional test groups

3.3.1.3 Viability assay: cell proliferation

Cells were cultured in a transparent 96 well plate as described for hydrogen peroxide treatments. Equal numbers of b.End5 cells were seeded into eighteen treatment wells in triplicate (n=3). Control wells were not exposed to H_2O_2 while experimental wells were treated with H_2O_2 concentrations in multiples of 50µM up to a maximum of 850µM. For cultured bEnd.3 cells, equal numbers of cells were seeded into sixteen sets of 3 wells (n=3) with control wells not exposed to H_2O_2, while treatment wells were exposed to H_2O_2 in multiples of 10µM up to 100µM and then in multiples of 100µM up to a maximum of 500µM. A blank column of 3 wells was also included in both treatment plates to facilitate the determination of relative absorbance units. The XTT (Kazaks *et al.*, 2019) viability assay kit (Roche) was used to quantify cell viability after treatment for 24hr. The XTT reagent was reconstituted by mixing 100µL of electron-coupling reagent (0.383mg/ml) with 5ml of XTT labelling reagent (1mg/ml) to activate it as per manufacturer's recommendation. Reconstituted XTT, 50µL, was then added to each well containing 100µL of cell culture and incubated for 4hrs at 37˚C in a CO_2 incubator. Absorbance was then read for each well at 450nm and blank-corrected values obtained using a GloMax–Multi Detection System (Promega). The absorbance measures directly correlate with the viability of the cells in each well.
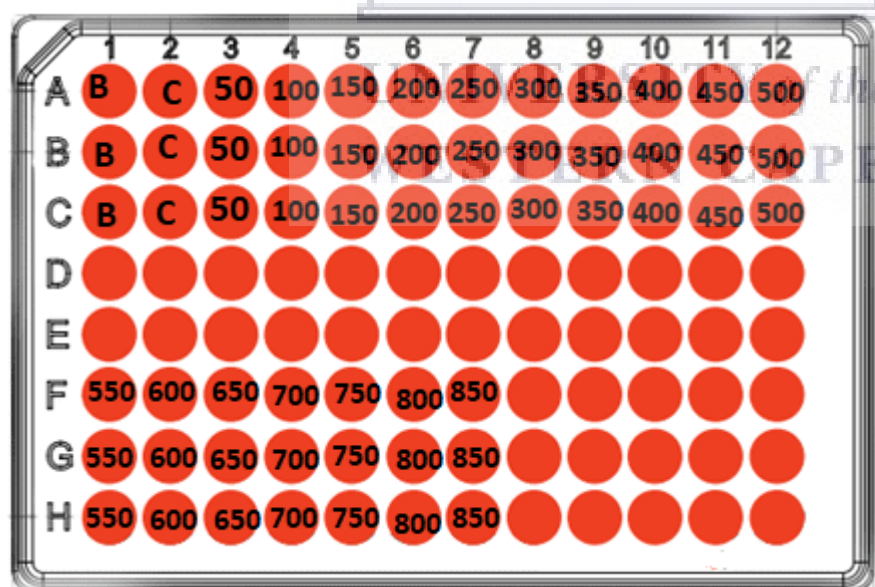
Figure 3.2: Plate layout for XTT cell proliferation/ viability assay. 'B' represents a blank well while 'C' represents a treatment control well. Figures indicated in wells are the µM concentrations of H_2O_2 treatments for each well.

3.3.1.4 Trypan Blue viability assays

Cultured b.End5 and bEnd.3 cells proliferate while getting attached under culture condition and it was required to quantify glutathione content of specific numbers of cells in order to determine the quantity per unit cell. We determined the 24hr proliferation rate for both b.End5 and bEnd.3 cells and estimated the number of cultured cells that gives 10,000 cells at 24hrs in culture. Glutathione quantity in 10,000 cells were then determined and from this value was the amount per unit cell calculated.

1×10^6 cells were seeded into $25 cm^2$ flasks in groups of 5 (n=3; day=0). Cells were incubated at 37°C and 5% CO_2. At 24hr of the incubation bEnd5 cells were washed, trypsinated, centrifuged, and resuspended in media to get cells into suspension in preparation to perform the Trypan Blue (TB) staining for cell counting. Cells were counted, using the Neubauer hemocytometer. The TB cell suspension was made up of 10μl cells suspension and 10μl TB. TB-cell suspension, 10μl, was added to the each section of the hemocytometer and a minimum of 100 cells were counted under an inverted phase contrast microscope (Zeiss). This process was performed for each flask of cells at each time point to obtain a controlled b.End5 cells number targeting 1×10^4 cells per well in 24hr for cellular glutathione quantification. The bEnd5 cell proliferation rate in 24-32hrs was determined using the plot of the number of cells against duration of cells in culture. All experiments were performed in triplicate. Similarly, TB assay was performed to determine the viability of cultured cells exposed to 24hr of ROS challenge using ratio of live to dead cell counts. This served to evaluate the cell depletion observed on treatment of the endothelial cells with higher ranges of H_2O_2 concentrations.

3.3.1.5 Clonogenic Cell Survival Assay

It is of importance to know the status of the b.End5 cells that remained with un-depleted GSH in the highest $[H_2O_2]$ treatment. The same group of cells still retained some absorbance of XTT thereby making it needful to find out if these cells are actually dead or alive. A standard clonogenic assay was then performed with cells seeded in 6 well plates and exposed to the selected inhibitory $[H_2O_2]$. Following treatment for 24hr, cells were trypsinated and cell stocks of equal seeding density were diluted 1: 1000. These cells were then seeded into 10mmX 35mm Petri dishes and colonies were allowed to grow for 10-14days before staining with crystal violet 0.1% [w/v] in 10% EtOH. The density of cell re-growth in each well were then observed and compared for the different treatments.

3.3.2 Fluorescent detection of glutathione in cultured cells

Equal numbers of b.End5 and bEnd.3 cells were cultured under standard conditions on microscopic glass coverslips in separate 10 X 35mm Petri dishes. Prior to cell culture, the glass cover slips were sterilized and cleaned with 70% ethanol (EtOH) and inserted into Petri dishes. The cover slips in the Petri dishes were then further sterilized under UV light for 1-2hr. The cells were then seeded on the coverslips and allowed to attach overnight in all Petri dishes and cells on each cover slip were used to demonstrate the presence of glutathione in the cultured cells. Briefly, the medium was removed from the attached cells and were rinsed twice with PBS solution at pH, 7.4 and then incubated with Monochlorobimane solution (mBCl, Molecular Probe™ M1381MP) 60μM in complete DMEM in a humidified incubator at 37°C and 5% CO_2 for 30 minutes (Chatterjee *et al.*, 1999). Following incubation with mBCl, cells on the cover slips were fixed using a mixture of 4% paraformaldehyde (PFA) and 0.2% glutaraldehyde (GA) in PBS solution at pH 7.4 for 10min and following fixation, samples were rinsed with PBS and excess PBS aspirated from the Petri dishes. The cells were then nuclear-counterstained for by incubating slides in the dark with 20μg/ml propidium iodide (PI) solution for 15min at room temperature (RT). DABCO (1, 4-diazobicyclo-[2, 2, 2]-octane) mountant, 20μl, was added to microscope glass slides and the cover slips with stained cells were inverted and mounted on the glass slides. Cells on each slide mount were then viewed and imaged under a fluorescent microscope equipped with a Nikon Eclipse 50i camera using a triband filter.

3.3.3 Quantification of total cellular glutathione in b.End5 and Bend.3 cells

To accurately quantify the total amount of glutathione in a single b.End5/bEnd.3 cell, a GSH-Glo™ Glutathione Assay Kit was used which works by a luminescence assay to detect and quantify glutathione (Scherer *et al.*, 2008). The assay is based on the conversion of a luciferin derivative into luciferin in the presence of glutathione, catalyzed by glutathione-S-transferase (GST). The reaction is further coupled with a firefly luciferase which leads to the generation of luminescence signal proportional to the amount of glutathione in the sample. To estimate glutathione fairly accurately in 1 x 10^4 cells, according to manufacturer's recommendation and to control for cell proliferation occurring alongside cell attachment, cells were plated in white 96 well plates and incubated at 37˚C and 5% CO_2 at a density of 4 x 10^3 cells per well for the b.End5 cells and 4.5 x 10^3 cells per well for the bEnd.3 cells, based on an optimized number of the respective cells that give the target density at 24hrs in culture (based on the data obtained from proliferation study). Cells were plated in columns of 4 wells (n=4) in a 96-well white bottom plate and 100μl of prepared 1X GSH-Glo reagent were transferred to each well. In

order to measure the total glutathione (GSH + GSSG), 100µl of 1mM Tris (2-Carboxyethyl) Phosphine (TCEP) was added to a group of 4 wells in addition to the GSH-Glo reagent according to GSSG recycling method (Tietze, 1969). The sensitivity of the GSSG measurement using this method is between 0.5-0.6µM. The contents of the wells were agitated briefly on an orbital shaker before incubation at room temperature for 30 minutes. 100µl of reconstituted Luciferin detection reagent was then transferred to each well, and the plate was mixed briefly on an orbital shaker before incubation at room temperature for 15minutes. Luminescence values were then read using a GloMax –Multi Detection System (Promega). Luminescence readings were converted to GSH concentration using a standard curve generated from a 5mM GSH standard supplied by the manufacturer. Similarly, cellular GSH quantity changes were determined to study the trend in the cellular glutathione during exposure of both b.End5 and bEnd.3 cells to escalating concentrations of H_2O_2 for 24hr.

3.3.4 Cell cycle analysis

In order to further investigate changes in cell viability and /or proliferation observed when cultured BECs are exposed to increasing concentrations of H_2O_2, analysis of cell cycle was carried out. Culture of b.End5 cells were maintained in a $25cm^2$ flasks and were exposed to selected concentrations of H_2O_2 for 24hr. The treatment media was then removed from the cells and they were rinsed once with 1ml of PBS, following which 500µl of TrypLE™ Express enzyme was added to each sample and incubated for 5min in a humidified incubator. After incubation, 500µl of media was added to each sample and cells were brought to suspension in a 15ml conical tube. Each cell suspension was then centrifuged at rpm 2500 for 5min to obtain cell pellets and the supernatant were carefully discarded. The samples were then each resuspended in 500µl of PBS and immediately fixed with a dropwise addition of ice-cold 70 % EtOH to a final volume of 5 ml and were then placed at -20°C for a minimum of 2 h. Prior to analysis, cell samples were first centrifuged at 1,000 rpm for 5 min at RT to pellet the cells, EtOH was carefully removed and the pellet resuspended in 1 ml PBS. The resuspended pellet was again centrifuged at 1000rpm for 5min and the supernatant carefully decanted. The pellet obtained were then resuspended in 1ml of FxCycle™ PI/RNase Staining Solution and incubated at RT for 30min prior to flow cytometric analysis. After 30min of incubation in FxCycle™ PI/RNase Staining Solution, the samples were then analysed with BD Accuri C6 flow cytometer. Samples were analysed in triplicates and data analysis was done using the FlowJo_v10.6.1 analysis software.

3.3.5   Determination of changes in the mitochondrial membrane potential (Δψm)

To evaluate changes in mitochondrial membrane potential (Δψm) in cells exposed to increasing concentrations of H_2O_2, transparent glass cover slips were sterilized as described earlier and cells were grown on cover slips placed in 10 x 35mm Petri dishes. Cultured cells were then incubated with media dosed with H_2O_2 concentrations corresponding to the IC_{25}, IC_{50}, and IC_{75}, values, prior determined, and another group consisting of cells treated with IC_{75} value with added antioxidant (25µM each of either GSH and/or Trolox) while untreated cell cultures served as control. All treatment were for a duration of 24hr before analysis. At the end of treatment, the treatment medium was removed and attached cells were incubated with medium containing 50nM TMRE and 7.5µM Hoechst 33342 solution for 30min in the dark at 37°C. TMRE is a cell-permeant, cationic red-orange fluorescent dye that accumulates in active mitochondrial while Hoechst 33342 is a cell membrane-permeable dye that binds to DNA to generate a blue fluorescence. After staining for 30min, cells were washed twice with PBS, pH 7.4 and immediately analysed using the triband filter of a fluorescence microscope equipped with a Nikon Eclipse 50i camera (Bova *et al.*, 2005).

Alternatively, cells were grown in a 6-well culture plate and treated with H_2O_2 concentrations as described previously for 24hr. At the end of treatment, cells were scraped with a cell scraper and lysed in lysis buffer composed of SDS (0.1%v/v) in 0.1M Tris-HCl buffer. Subsequently, 200µl samples of the lysate were transferred into 96-well culture plates and TMRE fluorescence was measured using a microplate reader at Ex/Em wavelengths of 508±20nm/580±40nm. The fluorescence intensity from each sample was normalized to the protein concentration of the corresponding lysate. To ensure that mitochondrial uptake of TMRE was related to membrane potential, a control study was included in the experiment composed of cells treated with an uncoupling agent (CCCP, 100µM) known to abolish Δψm. For microplate determination of TMRE fluorescence, protein concentrations were assayed using the BCA protein assay kit and the fluorescence measurement recorded for each well normalized to protein concentration in corresponding cell lysate (Oubrahim *et al.*, 2001).

Additionally, culture of b.End5 cells were maintained in a $25cm^2$ flasks and were exposed to selected concentrations of H_2O_2 as described earlier for 24hr. The treatment media was then removed from the cells and they were rinsed once with 1ml of PBS, following which 500µl of

TrypLE™ Express enzyme was added to each sample and incubated for 5min in a humidified incubator. After incubation, 500µl of media was added to each sample and cells were brought to suspension in a 15ml conical tube. Each cell suspension was then centrifuged at rpm 2500 for 5min to obtain cell pellets and the supernatant were carefully discarded. Cell pellets in each sample were then resuspended in 500µl of media containing 100nM TMRE solution and incubated in the dark in a humidified incubator at 37°C and 5% CO_2 for 30min. Following incubation with TMRE, cell suspension were centrifuged at 1000rpm for 5min and supernatant were carefully discarded and the samples were washed once by suspension in 500µl of cold PBS, centrifuged at 1000rpm for 5min and pellets were resuspended in 500µl PBS and analysed using a BD Accuri C6 flow cytometer. Samples were processed as triplicates and data acquisition and analysis were carried out using the BD Accuri C6 analysis software (Crowley, Christensen*, et al.*, 2016).

3.3.6   Annexin V/Propidium Iodide analysis of cell death

In order to determine the nature of cellular death induced in brain endothelial cell culture exposed to escalating ROS concentrations, cell death by apoptosis and necrosis were analysed using Annexin V coupled with propidium iodide by flow cytometry (Crowley, Marfell*, et al.*, 2016).

Briefly, b.End5 cells were cultured in 25cm^2 flasks and allowed to attach and grow to 60-70% confluence. Cells were then treated for a duration of 24hr in triplicates with inhibitory concentrations of H_2O_2 in growth medium prior determined viz, IC_{25}, IC_{50}, and IC_{75}. Further, another two groups were treated with IC_{75} concentration in combination with either of 25µM GSH or Trolox solution in growth medium while a group of cultures were incubated only in normal growth medium to serve as control. After treatment for 24hr, cell cultures were rinsed once with cold PBS and 500µl of TrypLE™ Express enzyme was added to each culture flask and incubated for 5min to detach the cells. After cells were detached, 500µl of culture medium was added to neutralize the TrypLE™ Express enzyme and cells were brought into suspension. The suspended cells were then centrifuged at rpm 2500 for 5min and cell pellets obtained were kept on ice and washed twice by resuspension in cold PBS (pH 7.4) followed by centrifugation and removal of the supernatant and then finally resuspended in 100µl of cold Annexin-binding buffer (ABB) 1X. Annexin-binding buffer 10X consisted of 0.1M HEPES (pH 7.4), 1.4M NaCl and 25mM $CaCl_2$ in double distilled water (ddH_2O) and was diluted to 1X by adding 1 volume of the 10X ABB to 9 volume of ddH_2O. To the 100µl of cold cell suspension in ABB was added 5µl of FITC Annexin V and then 20µl of FxCycle™ PI/RNase Staining Solution. The

cell suspension was then gently vortexed and then allowed to incubate for 15min at room temperature in the dark. After 15min of incubation in the dark, additional 400µl of ABB 1X was added and each sample analysed with a BD Accuri C6 flow cytometer. Both the acquisition and analysis of obtained data were carried out using the BD Accuri C6 software (Fernandez-Gil *et al.*, 2019; Martin *et al.*, 1995).

3.4   Statistical Analysis

Data were presented as mean ± standard error of the mean (Mean±SEM) and statistical software, Graph Pad Prism was used to analyse numerical data. Significant data were accepted at p values <0.05

4 CHAPTER 4

4.1 Experimental Results

4.1.1 Introduction

In this chapter, the findings and analysis of results from the experiments carried out using the methods described in the previous chapter are presented and explained in details. Tabulations, graphical presentations and statistical analysis of the data obtained are presented. The results are arranged to relate the survival capacity of the two cell lines used under ROS duress, H_2O_2, and the comparative capacity of the two cell lines for survival with respect to the duration of exposure, and the magnitude of the ROS stressor. The assay for cell survival also included a standard clonogenic assay on cells after 24hr treatment with selected inhibitory concentrations of the ROS stressor. Data presented in this regards represents analysis of live and dead cells as well as changes in cell proliferation under ROS duress in the presence and absence of an exogenous antioxidant. Next presented is the fluorescent microscopic detection of the endogenous antioxidant, GSH, in the two cell lines followed by comparison of spectrophotometric estimation of GSH quantity per unit cell in each cell lines. Further, changes in the cellular contents of GSH as the cells are exposed to increasing H_2O_2 concentrations was studied for the cell lines. Results from investigations of the mechanism of cell inhibition with ROS treatment were then presented; first was the analysis of cell death by apoptosis and necrosis studied by flow cytometry using combination of FITC Annexin V and propidium iodide. Supporting data for apoptotic cell death were presented using marker of mitochondrial membrane depolarization studied by fluorescent microscopy, fluorescent spectrophotometry and flow cytometry of cells that take up the cationic tetramethyl rhodamine ethyl ester into their mitochondria under physiologic conditions. Finally presented is the analysis of cell cycle changes during exposure to ROS. Numerical data were presented as means ± standard error of the mean.

4.2 Cell viability/ cell survival studies

In order to approximate the levels of ROS that inhibit cell proliferation or induce cellular death in 25, 50, and 75% of cultured cells, cells in culture were exposed to increasing concentrations of H_2O_2 and their viability by XTT cell proliferation assay and the Trypan blue assay for the number of live and dead cells were studied.

4.2.1 XTT Cell proliferation assay

Results of XTT assays done with treatment of b.End5 and bEnd.3 cell cultures with increasing concentrations of H_2O_2 showed dose-dependent decline in cell viability for both b.End5 and bEnd.3 cells. A non-linear regression analysis of the 50% inhibitory concentrations, IC_{50}, showed marked differences in values for both cells. Statistical comparison showed that b.End5 has statistically higher IC_{50} value than bEnd.3 cell line (Fig. 4.5).
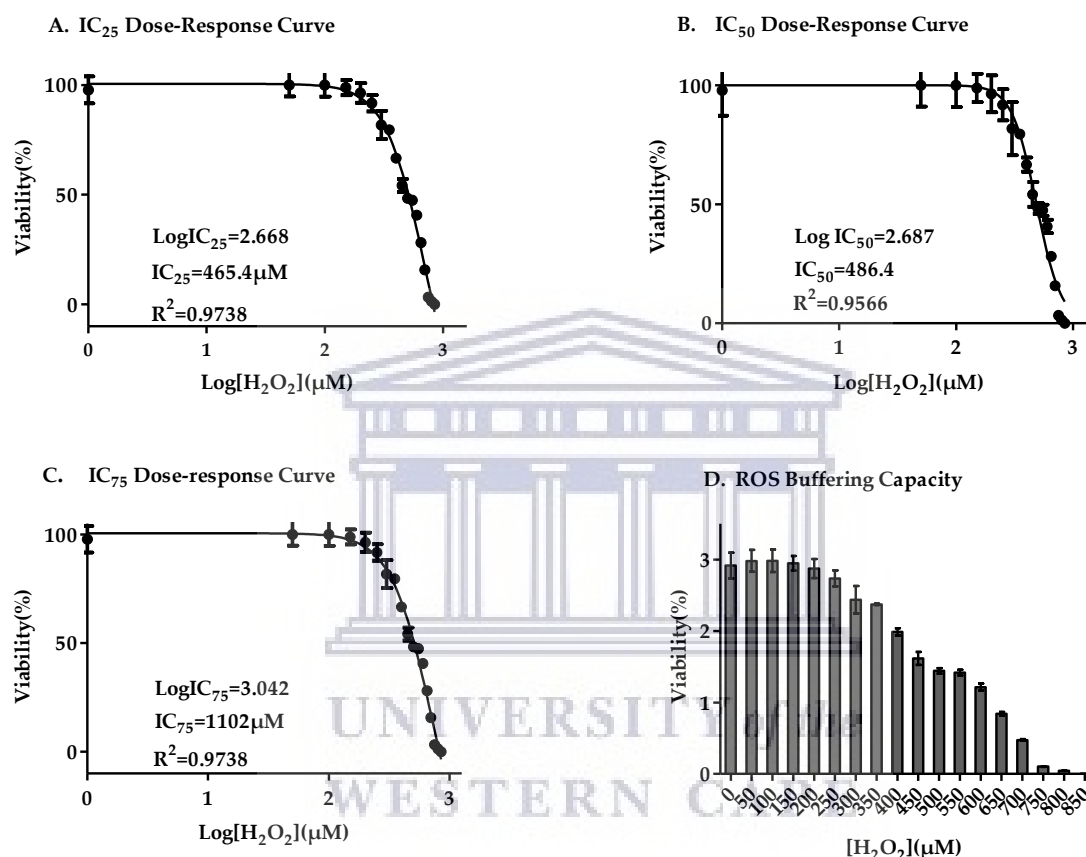
Figure 4.1: ROS buffering capacity of b.End5 cell line: Cells were exposed to [H_2O_2] between 0-1000µM for 24hrs and absorbance of XTT (plotted on the Y-axis as percentage of absorbance from the control experiment) from each test well at different concentrations was used for a non-linear regression analysis to determine the [H_2O_2] for 25%, 50% and 75% cell viability inhibition. The respective inhibitory concentrations are: 465.4, 486.4 and 1102µM H_2O_2 represented by charts A, B, and C respectively. Chart D shows a bar chart presentation of the varying measures of the cells at the [H_2O_2] used. Between [H_2O_2] of 50-250µM, viability values were either above or at par with the control (unexposed cells) values.

A. IC$_{25}$ Dose-Response Curve

Log IC$_{25}$ =42.46μM
IC$_{25}$ =42.46μM
R^2 =0.9843

B. IC$_{50}$ Dose-Response Curve

Log IC$_{50}$=1.872
IC$_{50}$ =74.55μM
R^2 = 0.9687

C. IC$_{75}$ Dose-response Curve

Log IC$_{75}$ =2.478μM
IC$_{75}$ =300.4μM
R^2 = 0.9843

D. ROS Buffering Capacity
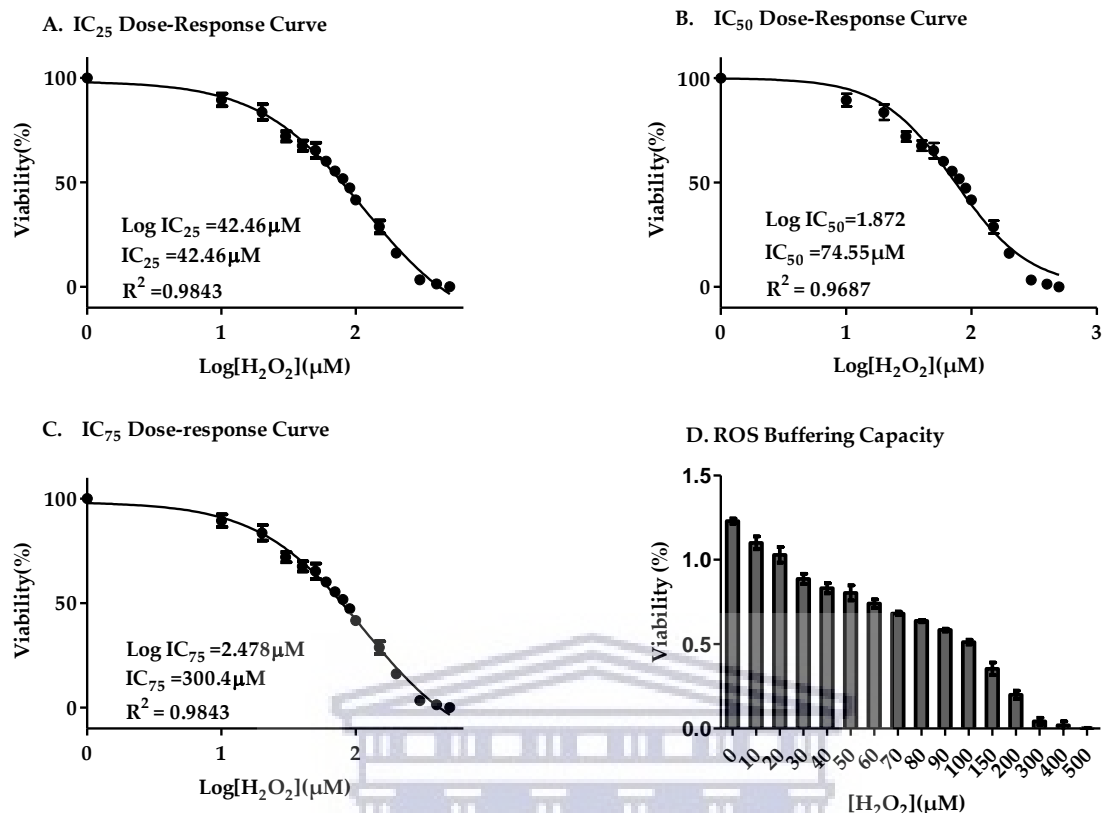
Figure 4.2: ROS buffering capacity of bEnd.3 cells: Cells exposed to [H$_2$O$_2$] between 0-500μM for 24hrs and absorbance of XTT(plotted on the Y-axis as percentage of absorbance from the control experiment) from each test well at different concentrations was used for non-linear regression analysis and the 25%, 50% and 75% cell viability inhibitory concentrations for [H$_2$O$_2$] were determined. The respective inhibitory concentrations are: 42.46, 74.55 and 300.4μM H$_2$O$_2$ represented by charts A, B, and C respectively. Chart D shows a bar chart presentation of varying measures of the cell viability for bEnd.3 cells at the [H$_2$O$_2$] used. The cells showed a steady, dose-dependent decline in viability with successive increment in [H$_2$O$_2$] relative to the viability of the control group. Viability measures become statistically significant relative to the control from [H$_2$O$_2$] of 20μM (P<0.05).
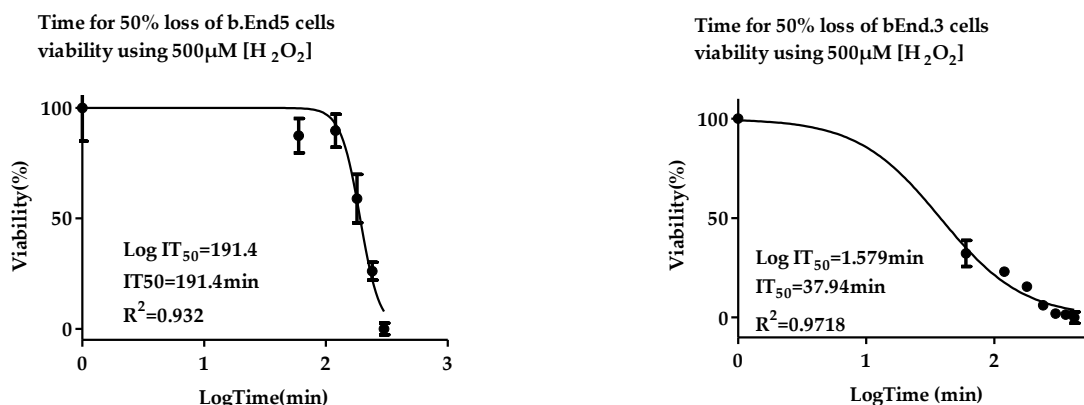
Figure 4.3: Temporal inhibition of b.End5 and bEnd.3 cell lines on exposure to equal magnitude of ROS: Growing cells were exposed to 500µM [H_2O_2] and XTT absorbance measured hourly until absorbance values approach values obtained for blank media. Non-linear regression analysis was then used to determine the time for half maximal viability based on XTT absorbance. A longer time was taken for half maximal inhibition of b.End5 cells than for bEnd.3 cells. Half maximal viability times were 191.4 and 37.94 min respectively for b.End5 and bEnd.3 cell lines.

Though the two cell lines were cultured in this study using the media recommendation of the manufacturers for the optimum survival of each cell in culture, a difference of 0.5mM sodium pyruvate was noted in the composition of the media with b.End5 media having the higher content of sodium pyruvate. Since sodium pyruvate can serve as an additional source of energy, we hypothesised that the observed higher survival capacity of the b.End5 cells was due to higher energy sources from higher supplementation of its medium with sodium pyruvate. We therefore investigated the effect of the differences in media composition for the growth of each cell lines, particularly the difference in sodium pyruvate content by attempting to grow the cells in interchanged media while repeating the cell viability experiment with exposure to the previously studied ROS magnitude. The result showed that each of the cell line does not attach as usually observed for these cells when seeded in the interchanged media. Alternatively, cells were seeded in their recommended medium for 24hr to allow cell attachment after which media in each cell lines were removed and culture rinsed once with PBS. Medium in each cell line culture was then interchanged and cell cultures were observed in 24hrs. Results showed cell detachment and attenuation of their characteristic dendritic extensions as shown below:
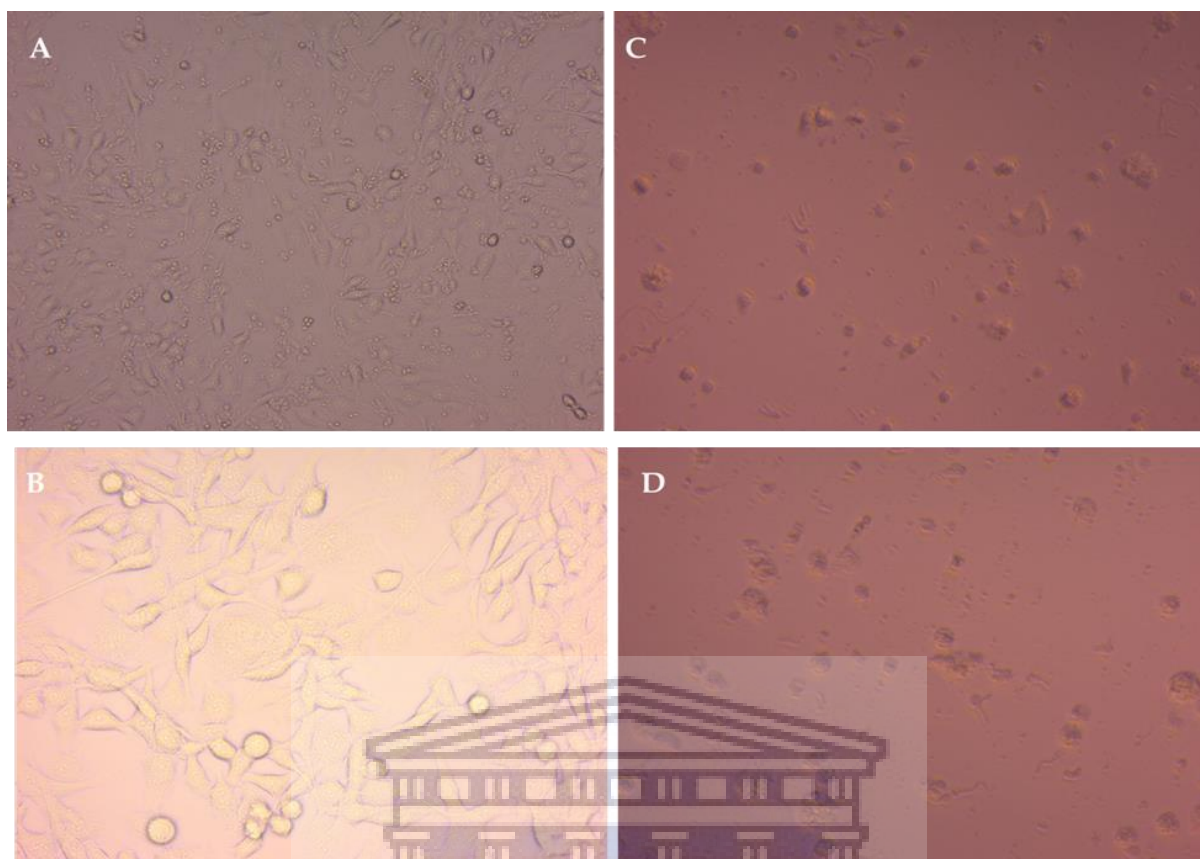
Figure 4.4: Micrographs showing the effect of interchanging cell culture media on the growth of cell lines. Plates A and B represents bEnd.3 and b.End5 cell cultures in their recommended media respectively, while Plates C and D shows bEnd.3 and b.End5 cells, grown respectively in interchanged media. Cell rounding and attenuation of dendritic cytoplasmic extensions are observable in both plates C and D.

4.2.2 Comparison of the half maximal inhibition hydrogen peroxide concentrations (IC$_{50}$) for b.End5 and bEnd.3 cell lines.

Statistical comparison of the values of the IC$_{50}$ (half maximal inhibitory concentration of H$_2$O$_2$) data obtained for the two cell lines are as presented below. Statistically significant difference was observed for the magnitude of the IC$_{50}$ between b.End5 and bEnd.3 cell line. The IC$_{50}$ concentration for b.End5 cell line was higher than that for bEnd.3 cells and thus the b.End5 cells showed a higher survival capability under ROS duress than bEnd.3
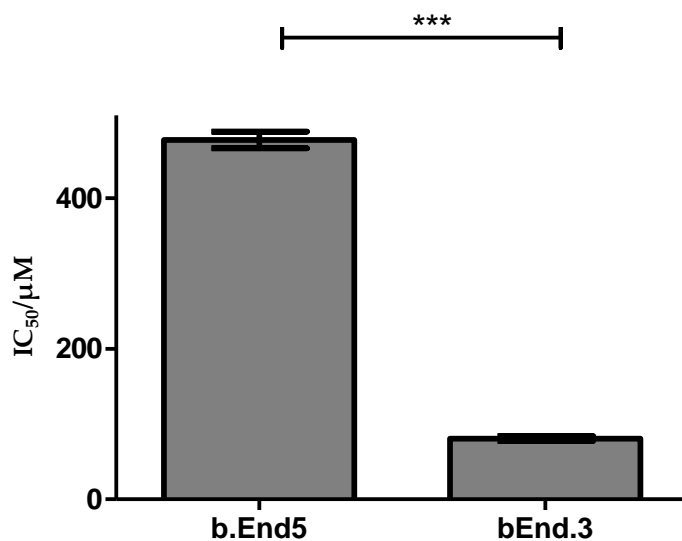
IC_{50} for b.End5 higher than bEnd.3 (p<0.0001)

Figure 4.5: Graph shows the values of the IC_{50} concentrations of hydrogen peroxide obtained for b.End5 and bEnd.3 cell lines. The values were statistically compared using a Student's t test which showed that b.End5 have a significantly higher IC_{50} than bEnd.3 cell line (P<0.0001)

4.2.3 Evaluation of live and dead cell counts using Trypan Blue exclusion assay

The changes in the number of live and dead cells with 24hr exposure to H_2O_2 was studied using b.End5 cell line. Results showed that the initial increase in the concentration of H_2O_2 leads to increase in the total number of live cells while minimal increase in the number of dead cells was observed. Specifically below and at the IC_{50} (486.4µM)ranges of H_2O_2 concentrations, the mean total number of live cells stayed significantly higher than that for the control whereas after the IC_{50} concentration is exceeded, the mean total live cell number decreased to values significantly lower than for the control group of cells. Similarly observed was increase in the number of dead cells in a dose-dependent pattern. The number of dead cells at H_2O_2 concentrations below the IC_{50} values for the b.End5 cells was slightly but insignificantly higher than the control group. When the data for live and dead cells were analysed together, it was observable that the combination of the number of live and dead cells cannot clearly evaluate the dynamics of the changes, either increase or decrease, in the total number of cells in the assays. The previous experiment using the XTT cell proliferation kit showed clearly that there was increase in the number of cells treated with some levels of ROS (<300µM of H_2O_2) and this result was again observed here using the Trypan Blue exclusion assay. However, to further

elucidate the mechanism of cell depletion, cell cycle analysis was carried out. Additionally, an Annexin V/PI analysis of apoptosis and/or necrosis was proposed in subsequent experiment to evaluate the involvement of apoptosis and cell cycle enhancement or arrest in the process of H_2O_2-induced endothelial cell depletion.
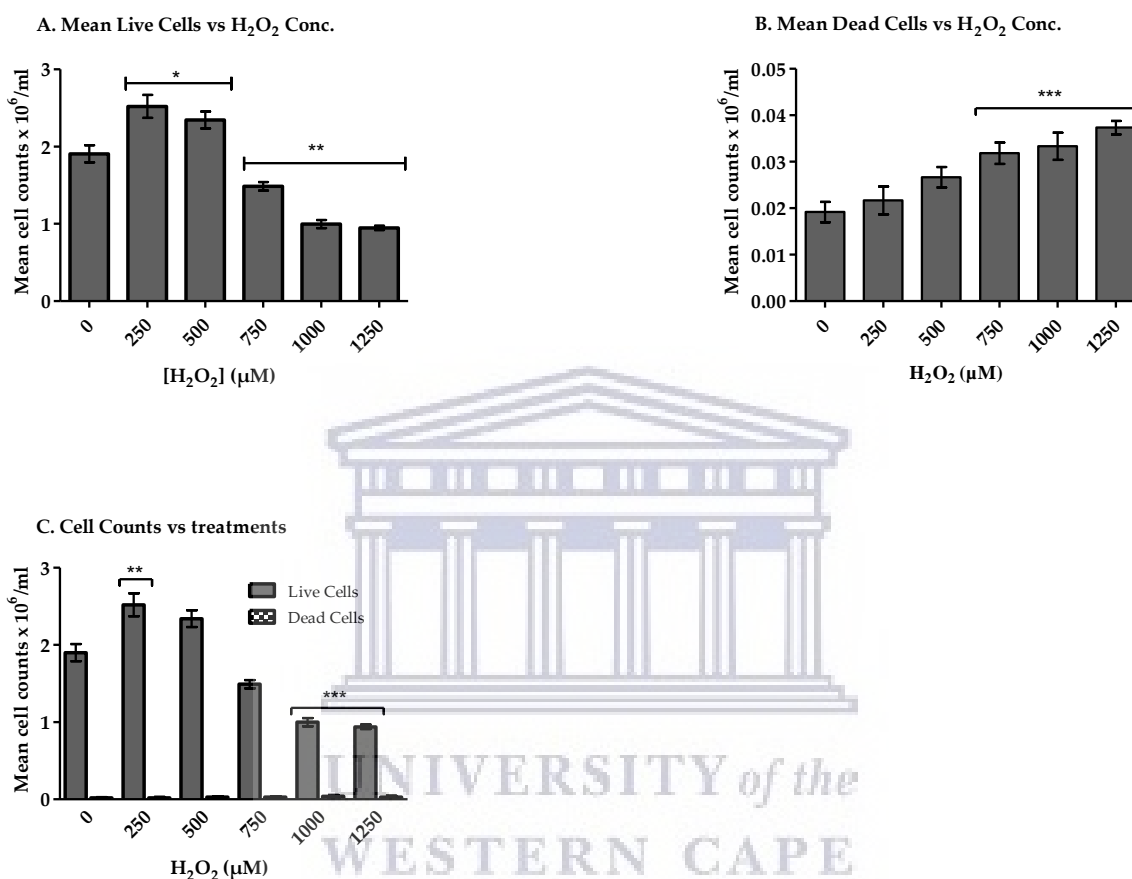
Figure 4.6: Cultured b.End5 cells were treated with $[H_2O_2]$ ranging between 250 to 1250µM for 24hrs and trypan blue exclusion assay were done to count the number of live and dead cells. Number of live cells at 250µM were significantly higher than control (P<0.05) while the numbers of live cells at 1000 and 1250µM while significantly lower than control (P<0.001). Dead cell numbers were significantly higher compared to the control at $[H_2O_2]$ range between 750µM and 1250µM in a dose dependent fashion (P<0.05). Despite the absolute number of live cells, at hydrogen peroxide concentrations between 1000 and 1250µM, showing significant reduction the absolute number of dead cells were not correspondingly low.

4.2.4 Effect of combined treatment of hydrogen peroxide with 25μM Trolox on b.End5 cells.

To determine if the viability of cells exposed to H_2O_2 will be improved if combined with selected dose of an exogenous antioxidant, Trolox (25μM), results using the XTT proliferation assay showed that cell viability was enhanced to comparable values as that of the control at H_2O_2 concentration 750μM and only slightly lower than the control even at 1000μM. This was contrary to significantly lower values for similar H_2O_2 concentrations without Trolox treatment. Thus administration of exogenous antioxidant enhanced survival of b.End5 cells under ROS duress.
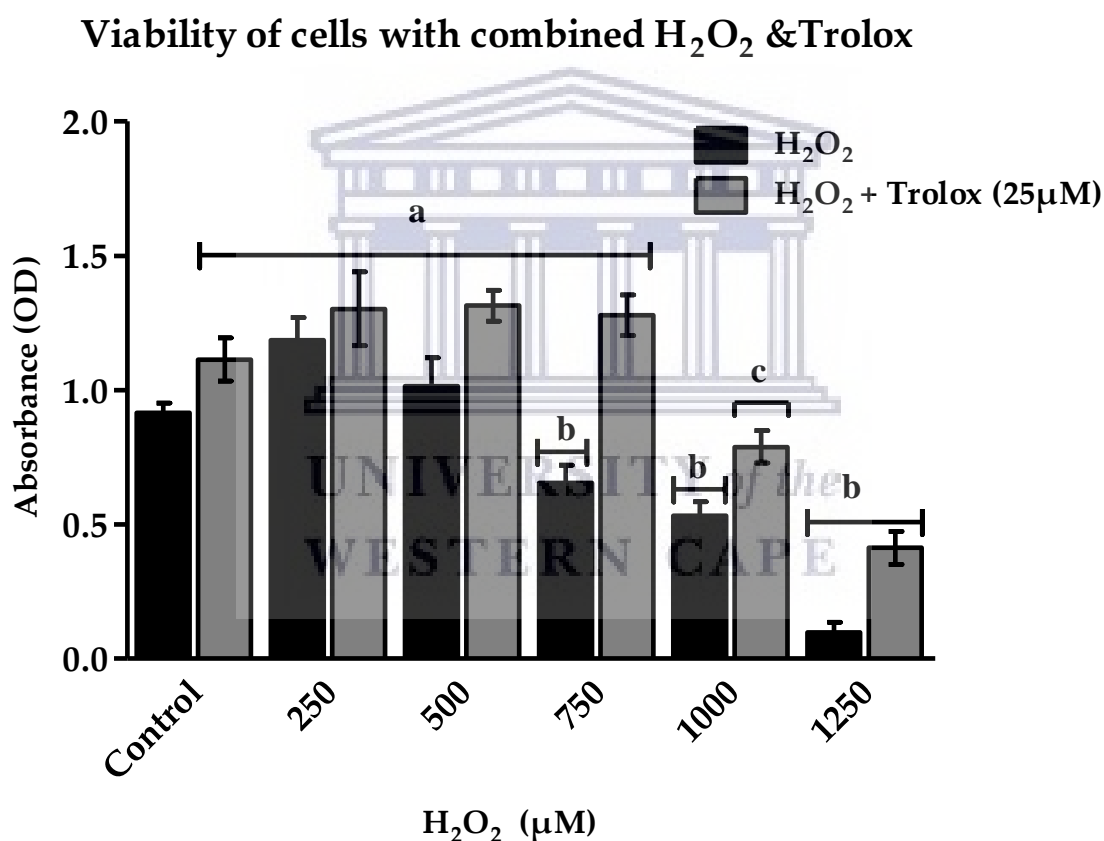
Figure 4.7: Cell proliferation assay with and without antioxidant treatment. Culture of bEnd5 cells were plated in 96 well as previously described and cells were treated with escalating concentrations of H_2O_2 with or without combination of 25μM Trolox. Viability directly correlated with the absorbance of XTT and showed enhanced viability for Trolox-treated cells when compared with the control for concentrations of 750 and 1000μM H_2O_2. Annotations 'a, b and c' denote data values significantly higher, lower and at par with the control respectively.

4.3   Detection and quantification of GSH in BECs

To study the presence of a selected endogenous antioxidant, GSH, in the two cell lines and also to quantify the amount in each cell line, both fluorescence microscopy utilising Monochlorobimane fluorescence and a luminescence spectrophotometric assay using GSH Glo assay kit were respectively used. Both of these methods were also used to monitor changes in the cellular GSH contents when the cells were exposed to ROS.

In the detection experiments, GSH specific fluorochrome, mBCl was used to mark the presence of GSH in the cells on fluorescent microscopy. The fluorochrome, binds to GSH to form GSH-bimane adduct which fluoresces blue light when excited at wavelengths between 365 and 400nm. This allowed a micrographic, though subjective, appraisal of the quantity of GSH in both normal and ROS-treated cells (refer to chapter 3, section 3.2).

Data presented in this study include experimental detection and confirmation of the presence of GSH in the cell lines used, quantity of GSH per unit cell for each line and both micrographic and quantitative data for cellular changes in GSH when the cells are subjected to ROS duress.

4.3.1   Detection and confirmation of GSH presence in b.End5 and bEnd.3 cells

Both b.End5 and bEnd.3 cells showed variable blue fluorescence on microscopy which confirms the presence of GSH in the cell lines used (Figure 4.8). The micrograph suggests that b.End5 cell culture emitted a slightly higher intensity of blue fluorescence than bEnd.3 cells which suggests a higher GSH content for b.End5. Additionally, the ration of nuclear volume to that of the cytoplasm, the nucleo-cytoplasmic ratio, appear higher for bEnd.3 cells which suggests that GSH which is mostly cytoplasmic in location is less for bEnd.3 than for b.End5 cells. These assessment were, subjective and thus further experiments to quantify the amount of GSH in each cell type were carried out.
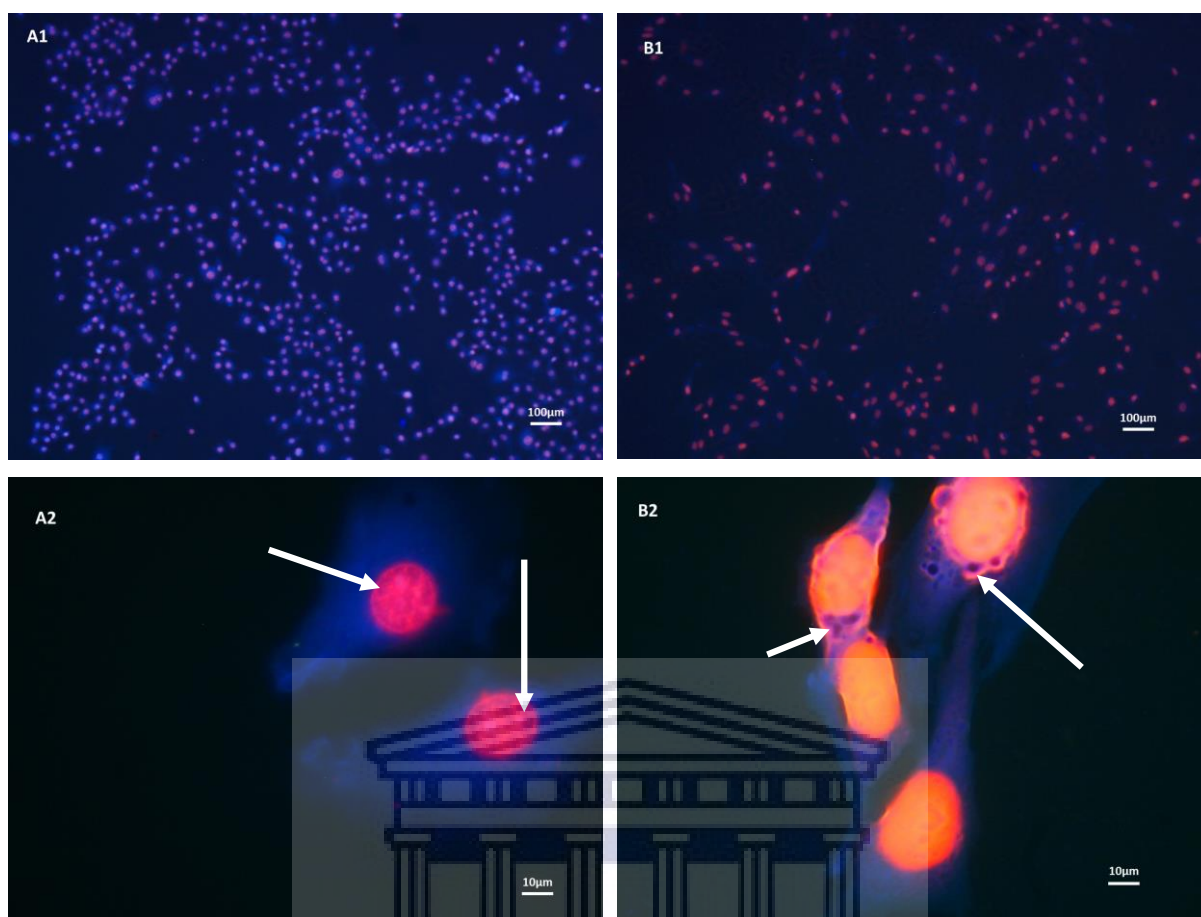
Figure 4.8: Micrographs show fluorescent images of b.End5 (A1, A2) and bEnd.3 cells (B1, B2) in normal culture. Both cells showed blue mBCl fluorescence (due to binding with GSH) in their cytoplasm, though at the higher magnification b.End5 appeared more deeply stained. Furthermore, plate A2 revealed a lower nucleo-cytoplasmic ratio in b.End5 cells suggesting more cytoplasmic GSH content than in bEnd.3 cells. Importantly also, multiple segments and rings of blue fluorescence (white arrows) indicative of glutathione were observed within the nuclei and at the nucleo-cytoplasmic interfaces in both cell types (Plates A2 and B2).

4.3.2 Quantification of cellular GSH for b.End5 and bEnd.3 cells

Using the GSH-Glo™ assay kit, the quantity of GSH in 10,000 cells of each type of cell lines were measured and data used to calculate the average quantity contained in a single b.End5 and bEnd.3 cell. First, optimization assay to control for the number of cells per assay recommended by the manufacturer of the kit used was done. Each cell type was cultured to determine the rate of proliferation for the specific cell in 24hr which was the targeted duration for cell culture at the time of GSH measurement. Seeding cell density for each cell line was then calculated from the data obtained for the proliferation assay. Based on the data obtained from the optimisation assay, a seeding density of 4 X 10^3 and 4.5 X 10^3 cells per well of a 96

well cell culture plate were used for b.End5 and bEnd.3 cells respectively, targeted at 1×10^4 cells at the end of 24hr in normal culture. By the technique described in the previous chapter 3, the quantity of GSH and GSSG fractions in a single cell of each cell line was determined first in arbitrary luminescence units which was then converted to actual GSH quantity, using a standard curve generated with a 5mM GSH standard supplied with the GSH-Glo™ assay kit (Figure 4.9). The data obtained was then used to determine the GSH: GSSG oxidant status of each cell in normal culture. The quantity of GSH in each cell type was then compared statistically and the results are as shown in the figures that follow:
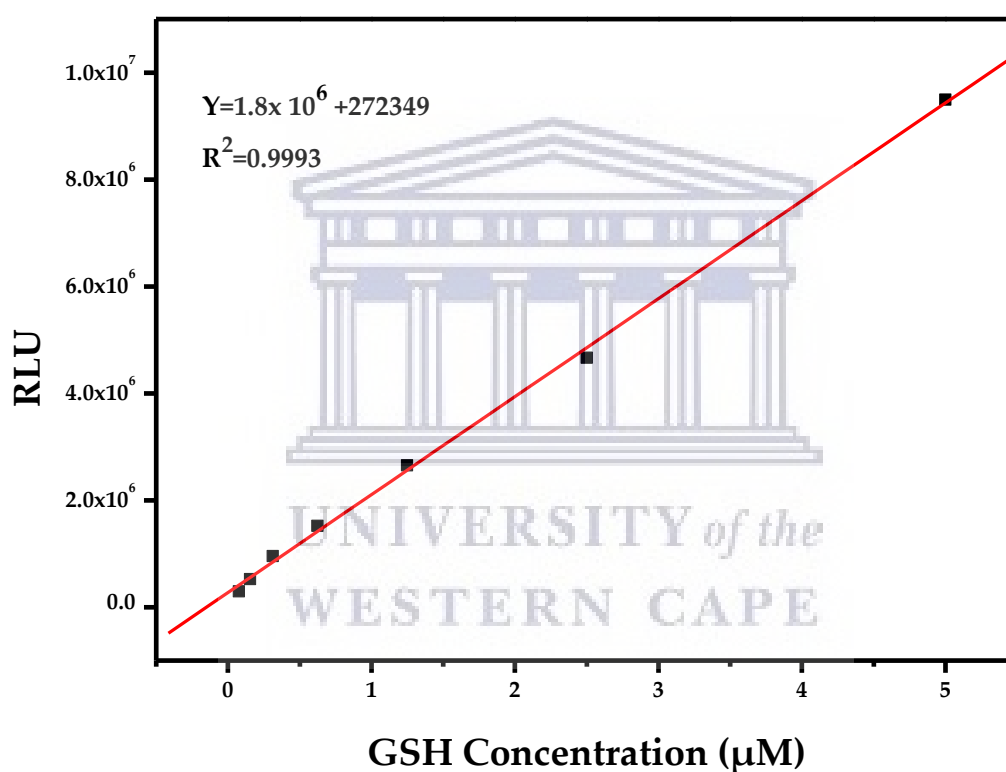
Figure 4.9: Standard curve for GSH estimation using the GSH-Glo™ assay kit. The R^2 value of 0.9993 suggests acceptability of the accuracy of the estimation using this kit.

Mean GSH quantity per single b.End5 cell was estimated as 2.769±0.113 fMol with similar estimation of its GSSG content as 0.139±0.006 fMol while in a single bEnd.3 cell, mean GSH quantity amounts to 2.305±0.219 fMol and GSSG was 0.115±0.011. Thus there is a higher GSH content in b.End5 cell with a mean difference of 0.464±0.106fMol, however, statistical

analysis showed that the difference was not statistically significant, P>0.005 (actual P value =0. 1325). (Figure 4.10)

4.3.3 Cellular GSH response to increasing hydrogen peroxide concentrations.

Both b.End5 and bEnd.3 cells were treated with increasing concentrations of hydrogen peroxide within the range between their respectively determined inhibitory concentrations. After treatment for 24hr, the mean GSH content at each concentrations were measured using the GSH-Glo™ assay kit. Data values for the mean GSH were then plotted against the hydrogen peroxide concentrations for each of the b.End5 and bEnd.3 cells to show the trend in cellular GSH changes as hydrogen peroxide concentration increases. Analysis from the trend plot showed a marked difference in the reactive changes in the cellular GSH content within b.End5 and bEnd.3 cells during ROS duress. At low $[H_2O_2]$, b.End5 cell GSH content is increased in the cell in quantity higher than the values for the control group to reach a peak value at about 250µM H_2O_2. These higher values were maintained until $[H_2O_2]$ exceeded 500µM and a steady decline in the GSH content was then observed until $[H_2O_2]$ of about 1000µM. Thereafter, increase in $[H_2O_2]$ only cause minimal, negligible decline in the GSH content of the b.End5 cells. At no $[H_2O_2]$ was the GSH content of b.End5 cells completely depleted. Similar trend plot for the bEnd.3 cells showed a steady and steep fall in the GSH content to zero.

In order to investigate whether the apparent increase in the GSH content of b.End5 cells are due to actual synthesis of GSH or simply the effects of increased cell numbers due to cell proliferation, experiments are done with ROS treatments that targeted the points of GSH elevation and decline when H_2O_2 treatment was combined with Trolox antioxidant which antioxidant mechanism differ from that of GSH. Additionally, parallel experiment was carried out with identical treatment but cell proliferation data, instead of GSH, was taken and analysed against GSH trends. Analysis showed that GSH decline followed the initial pattern at hydrogen peroxide concentrations where Trolox enhanced cell proliferation. At these points in $[H_2O_2]$ GSH reduction and preservation of cell proliferation coexisted. The data in these experiments are represented by graphs C and D in the figure below. This clearly showed that the increased GSH content observed in b.End5 cells between the control and 500µM $[H_2O_2]$ was certainly due to upregulation of the *de novo* GSH synthesis in response to ROS duress incident on these cells. Similarly, the graph B, showed that the bEnd.3 cells either has virtually no capacity for reactive synthesis of GSH under conditions of increasing ROS or that its rate of *de novo* synthesis of GSH cannot match the rate of consumption at the tested H_2O_2 concentrations .
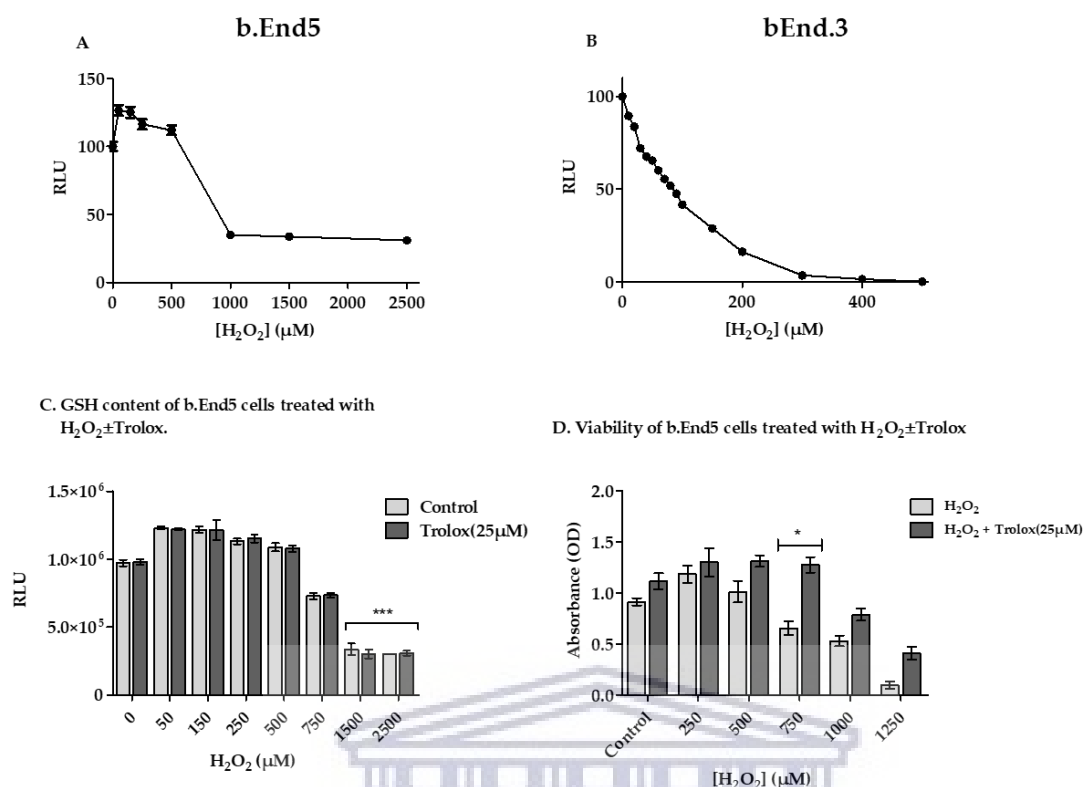
Figure 4.10: Changes in cellular GSH content of endothelial cells under ROS duress. Graphs A and B present trends in the cellular GSH for b.End5 and bEnd.3 on exposure to increasing $[H_2O_2]$ respectively. In A, GSH quantity was higher than control until $[H_2O_2]$ was well above 500µM and from the point of decline in GSH, a steady downward trend was observed until $[H_2O_2]$ of 1000µM. From this point a fairly horizontal trend was seen denoting minimal or no change, such that at no $[H_2O_2]$ was the GSH content completely depleted. This is the graph that represents the GSH trend for b.End5 cell line. In graph B, the cellular GSH content decline steadily from the level for the control until the values for the GSH content of the bEnd.3 cells amounts to zero. Graphs C and D showed the GSH response and cell proliferation changes with co-administration of $[H_2O_2]$ and an exogenous antioxidant, Trolox. RLU denotes a relative luminescence unit. In graph C, there was no difference observed in GSH content between the control and trolox-treated groups at $[H_2O_2]$ 1000µM and above. In graph D, detectable differences were shown in the GSH contents of cells treated with either H_2O_2 alone or in combination with trolox between $[H_2O_2]$ 1000 and 1250µM.

4.3.4   Cell recovery assessment

It is of importance to know the status of the b.End5 cells that remained with un-depleted GSH in the highest $[H_2O_2]$ treatment. The same group of cells still retained some absorbance of XTT

thereby making it needful to find out if these cells are actually dead or alive. A standard clonogenic assay was then performed with cells seeded in 6 well plates and exposed to the selected inhibitory [H_2O_2]. Following treatment for 24hr, cells were trypsinated and cell stocks of equal seeding density were diluted 1: 1000. These cells were then seeded into 10mmX 35mm Petri dishes and colonies were allowed to grow for 10-14days before staining with crystal violet 0.1% [w/v] in 10% EtOH. Results showed the control and the IC_{50} groups regrow back almost to a monolayer while the IC_{75} with and without Trolox antioxidant combination treatment showed obviously few colonies, however, the Trolox treated dish showed a higher number of colonies than the IC_{75} without Trolox.

Control IC_{50}

IC_{75} IC_{75} Trolox
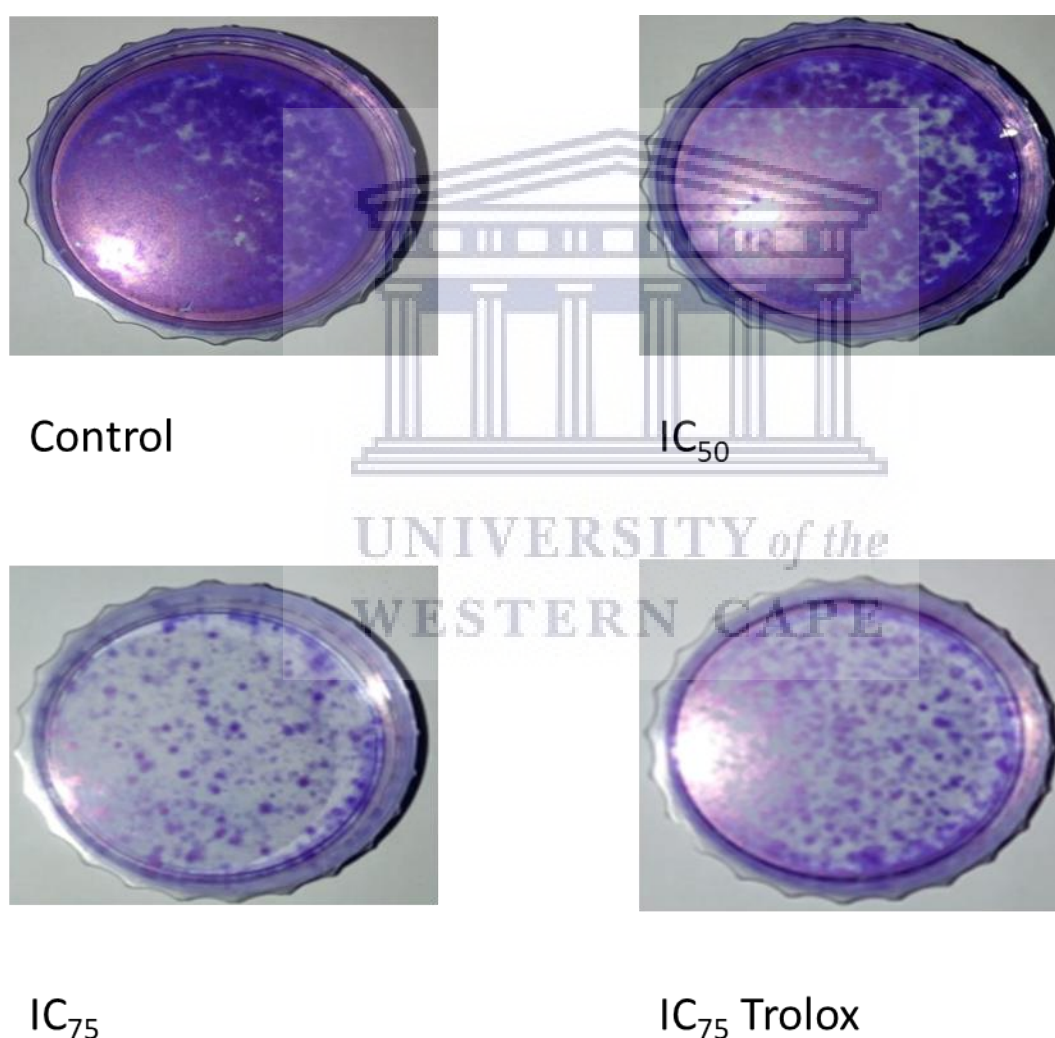
Figure 4.11: Clonogenic assay for cell survival after ROS stress. Photographs showed lowest colonies growing in cells treated with IC_{75} concentrations of $H_2O_2 \pm$ Trolox (25µM) while the control and the IC_{50} group showed virtually monolayers. Though the rate of growth is low in

the IC_{75} groups, it is observed that the population of cells in these categories are not entirely composed of dead cells.

4.3.5   GSH depletion in b.End5 cells under ROS stress: studies by fluorescent microscopy.

Experiment was carried out using fluorescent microscopy as described in chapter 3 for visual micrographic assessment of the depletion in cellular GSH within b.End5 cells under ROS treatment as an addendum to the quantitative studies above. [H_2O_2] used correspond to the inhibitory concentrations earlier determined for b.End5 cells. Micrographic data showed a slight difference in GSH-bimane fluorescent until concentrations are above the IC_{50} which is fairly in agreement with the quantitative data presented earlier.
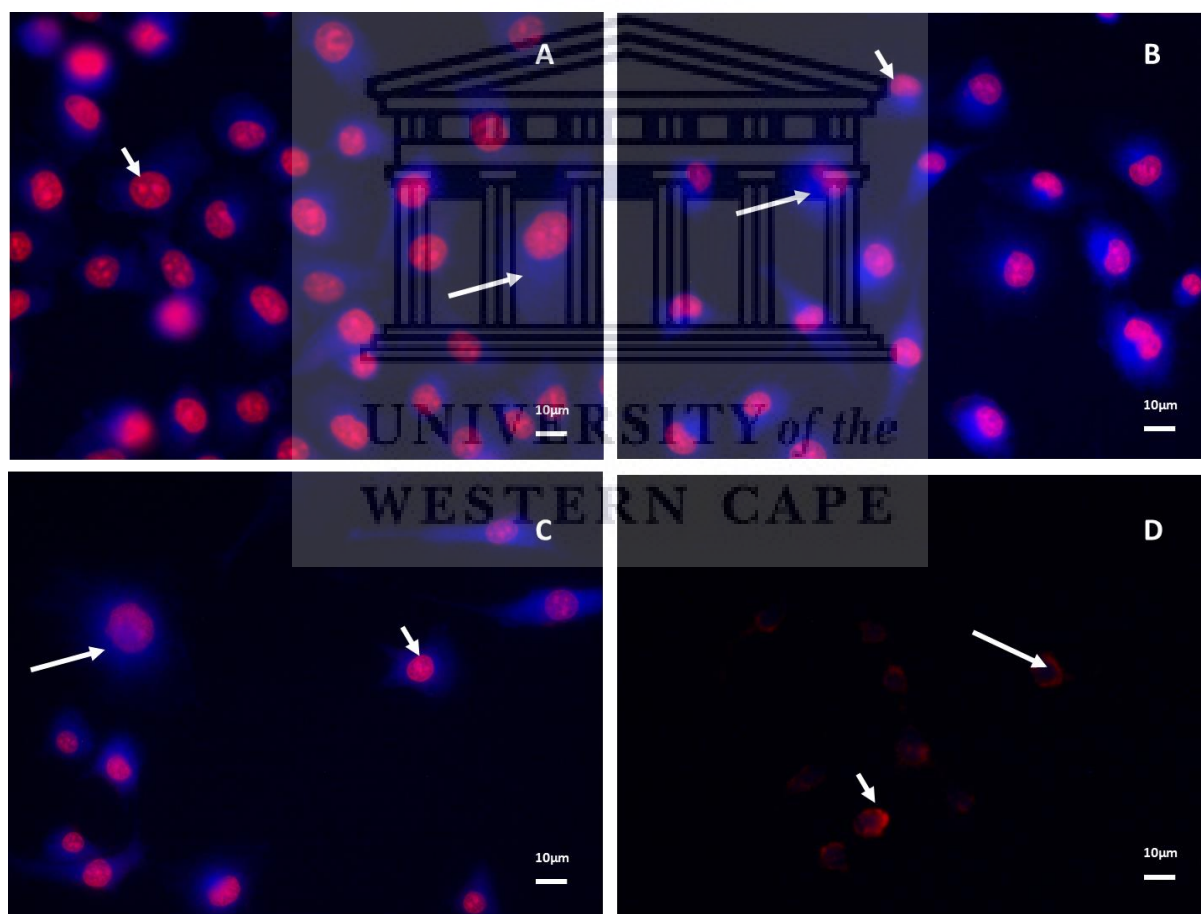
Figure 4.12: Micrograph Plates A, B, C, and D represents [H_2O_2] 0μM (control), 465μM (IC_{25}), 486μM (IC_{50}) and 1100μM (IC_{75}) respectively using b.End5 cell line. Long arrows point at cytoplasmic fluorescence of glutathione-bound mBCl while short arrows point at PI-bound nuclear fluorescence. The mBCl fluorescence is sensitive to the presence of GSH. Micrographs show dose dependent weakness in GSH-bimane fluorescence which was maximal at IC_{75} H_2O_2

concentration but not completely absent. This qualitative studies corroborate the downward trend in the quantity of GSH within cells treated with increasing ROS load.

4.4   Mechanisms for H₂O₂-induced brain endothelial cell inhibition.

Assay are done in order to account for the reduction of cell numbers that was observed in cell cultures and are associated with increasing concentrations of H_2O_2. In previous assay for cell viability with respect to number of live and dead cells in cultures, differences were observed in the ratio of live to dead cells (with floaters included and counted) but which could not account for the total loss of cells relative to the control and the groups which showed increased cell numbers due to cell proliferation. Additionally, an important limitation of the Trypan blue exclusion assay earlier used is that it cannot account for apoptotic cells if present. In order to account for the differences in cell viability observed, two assays were carried out to determine the contribution of apoptosis and necrosis on the one hand, and cell cycle disorder on the hand to the changes in cell numbers observed on treatment of b.End5 cells with increasing concentrations of H_2O_2.

4.4.1   Flow cytometric analysis of Apoptosis and necrosis

Apoptotic and necrotic cellular changes were evaluated using Annexin V-FITC/Propidium Iodide based protocols for flow cytometry as described in chapter 3. Using Annexin V-FITC/PI fluorochrome, the population of cells in the studies were sorted into live, early apoptotic, late apoptotic and necrotic cells were analysed.

In this study, background necrosis and late apoptosis contributed to 5.2% and 5.6% respectively of total cell population while early apoptotic and live cells were 0.2% and 89% respectively in the control (Figure 4.13). With exposure to 465.4µM which represent IC$_{25}$ concentration of H_2O_2, there was an increase in the ratio of dead cell in which late apoptotic cell population increased 3 folds while necrotic cell populations increased 6 folds which therefore doubled the rate of increase in the number of apoptotic cells. Also, early apoptotic cell population increased 9 folds (Figure 4.14).
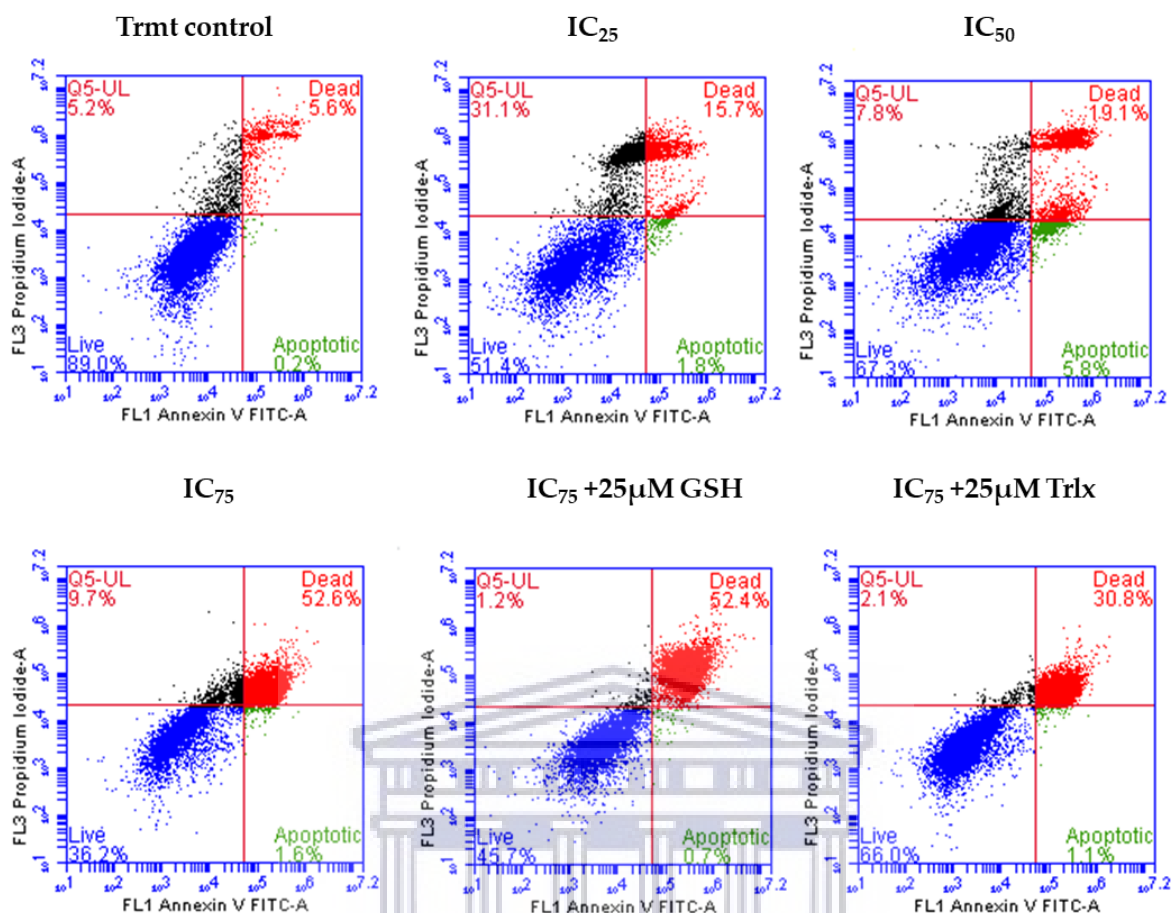
Figure 4.13: Shows dot plot presentation of the unstained cell position (left) against the stained treatment control group (right).

Statistical analysis of the live, apoptotic and necrotic components of the population of cells at the different inhibitory concentrations of H_2O_2 showed significant variations in the characteristic of cell death encountered and further differences were observed at concentrations co-administered with 25µM GSH and/ or Trolox. Reduction in the number of live cells peaked at the IC_{75} concentration (P<0.0001) remaining about 30% of the total cell count but with 25µM Trolox co-administration the number of live cells was comparable to the IC_{25} concentration which though was significantly lower than control yet contributes above 60% of total cell count. IC_{50} concentration and IC_{75} co-administered with 25µM GSH showed highly significant reduction in live cells each remaining only about 50% total cell population.

Apoptotic cells are sorted into early and late apoptosis populations. Early apoptotic cells population was significantly higher at IC_{25} and IC_{50} with IC_{25} as the peak, however, the overall number was less than 6% of total cell count (Figure 4.15 and 4.16). For the rest of the

treatments, early apoptotic populations remained indifferent from the control group. Highly significant increases in the late apoptotic cell populations was highest at IC_{75} (P<0.0001) with values above 60% and at antioxidant co-administered treatments (with GSH, about 50% and with Trolox, about 30% of total cell populations). Other concentrations are either slightly significantly lower than control (IC_{50}) or not statistically different (IC_{25}). Necrosis was significantly highest at IC_{50} concentration of H_2O_2 contributing about 27% of total cell population and it is the only concentration that produced significant increase in the population of necrotic cells whereas other concentrations showed no significant differences compared to the control. Thus administration of exogenous antioxidants to b.End5 cells under ROS stress protects cell population from cellular death by sparing significant number of live cells while also creating preference for apoptotic change rather than necrotic cellular death. With the observation of significant apoptotic change, involvement of mitochondrial contribution was next investigated using fluorescent microscopy of TMRE cationic dye as well as fluorescent spectroscopy and flow cytometry of TMRE stained cells.

Statistical analysis of the results further lead to the summary that the highest depletion of live cells in the samples of b.End5 cells occurred at IC_{50} and IC_{75} concentrations and the highest figure of late apoptosis was obtained at IC_{75} concentration (Figure 4.20). Proportion of live cells was highest compared to the control at IC_{25} concentration and the samples treated with antioxidants. Also, necrotic cells recorded highest figure at the IC_{50} concentration. With this summary, OS could be conveniently defined as occurring at between IC_{50} and IC_{75} concentrations.
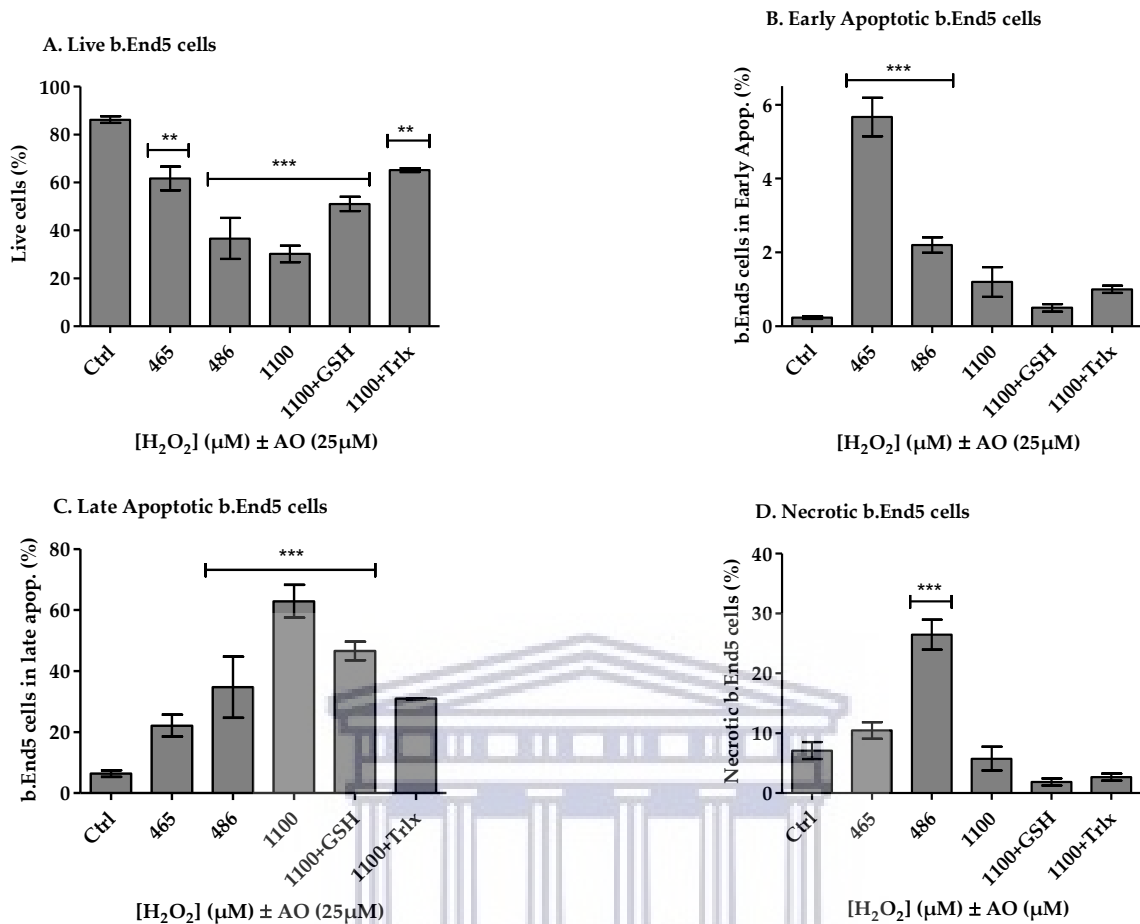
Figure 4.14: Analysis of cell populations that account for the changes in cell numbers during at 24hr treatment of b.End5 cells with H_2O_2 ROS of selected concentrations alone and when 25μM of selected antioxidants are co-administered. In viability experiments (Fig.4.7), cells showed complete recovery when treated with exogenous antioxidants hence in this experiment IC_{75} dose was used to test the efficacy of antioxidant protection in order to further examine effects of antioxidant at doses where cell viability decompensated. Annotations * denotes statistical difference compared with the treatment control and the number of * is an indication of magnitude of the differences. Multiples of * represent $p < 0.05$, 0.01 and 0.001 respectively.
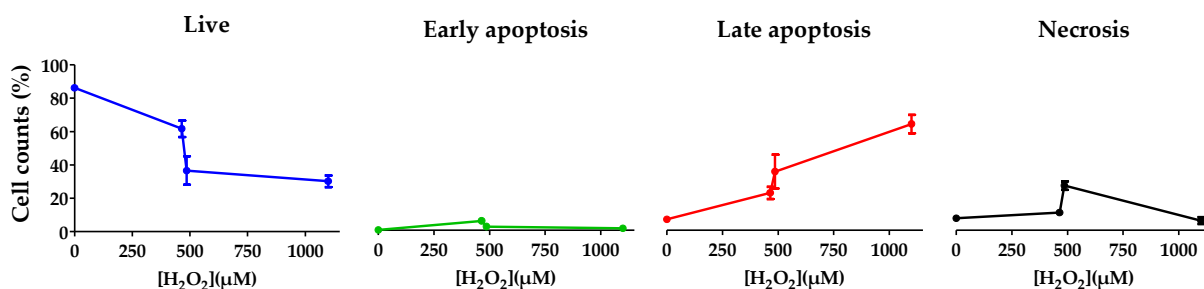
Figure 4.15: Trends in the survival status of b.End5 cells under conditions of increasing magnitude of ROS stress. The survival statuses presented in the graphs are aligned to share a common y-axis for comparison.
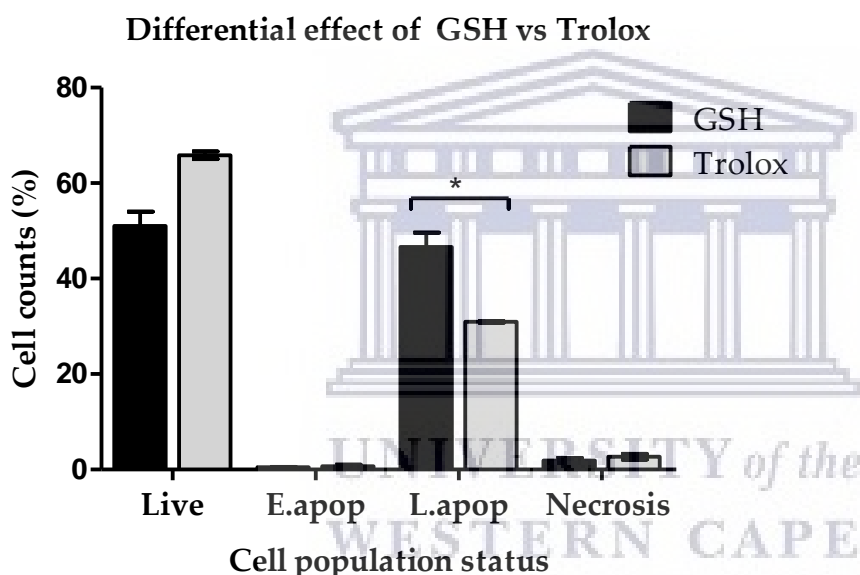
Figure 4.16: Graph shows the differential effects of two exogenously administered antioxidants on the survival status of b.End5 cells undergoing redox stress at IC_{75} level of stress. The two major populations of cells are with live and late apoptosis statuses while early apoptosis and necrosis contribute negligible fraction of the total cell counts. GSH treatment showed slightly significant increase in the number of cells in apoptosis than Trolox. (* denotes statistical significance at $p < 0.05$). Cellular pretreatment with GSH to determine GSH loading was not considered having first established in previous experiment an adequate GSH contents in the cells as well as a normal GSH/GSSG ratio. E.apop, early apoptosis; L.apop, late apoptosis.

4.4.2 Evaluation of changes in the mitochondrial membrane potential (Δψm)

Fluorescent detection of the changes in mitochondrial membrane potential was carried out while b.End5 cells undergo ROS stress using fluorescent microscopy, fluorescent spectrophotometry and flow cytometry. This studies were done to determine if mitochondrial membrane depolarization was contributory to the apoptotic changes observed in the endothelial cells under ROS stress.

Micrographic results showed significant reduction in the red fluorescence of TMRE dye indicative of depolarized mitochondrial at IC_{50} concentration and virtually no mitochondrial fluorescence at IC_{75} concentration.
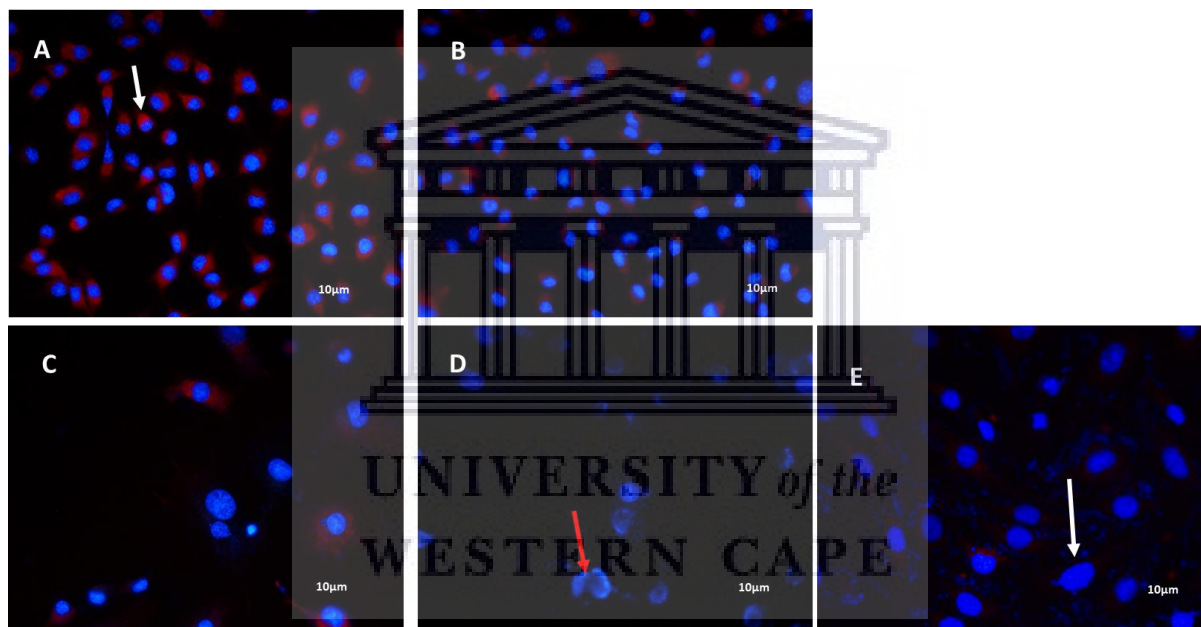
Figure 4.17: Micrograph Plates A, B, C, and D showed cells at redox levels [H_2O_2] 0µM (control), 465µM (IC_{25}), 486µM (IC_{50}) and 1100µM (IC_{75}) respectively. Micrograph E showed cells treated with CCCP. White arrow points at a normal mitochondrion with normal mitochondrial membrane potential while red arrow points at a depolarized mitochondrion. Micrographs show dose dependent decrease in TMRE mitochondrial fluorescence which was completely absent at IC_{75} H_2O_2 concentration.

Microplate assay was alternatively carried out as described in chapter 3 section 3.5. Results showed that mitochondrial depolarization of variable magnitude occurred at all concentrations with significant reduction in mitochondrial fluorescent for all concentrations. However, mitochondrial TMRE fluorescent showed dose-response reduction with the highest

mitochondrial depolarization occurring at IC$_{75}$ concentration which was virtually at par with the negative control group which was treated with an optimized concentration of a known mitochondrial uncoupler, CCCP (100μM)'

A. Δψ$_m$ vs ROS
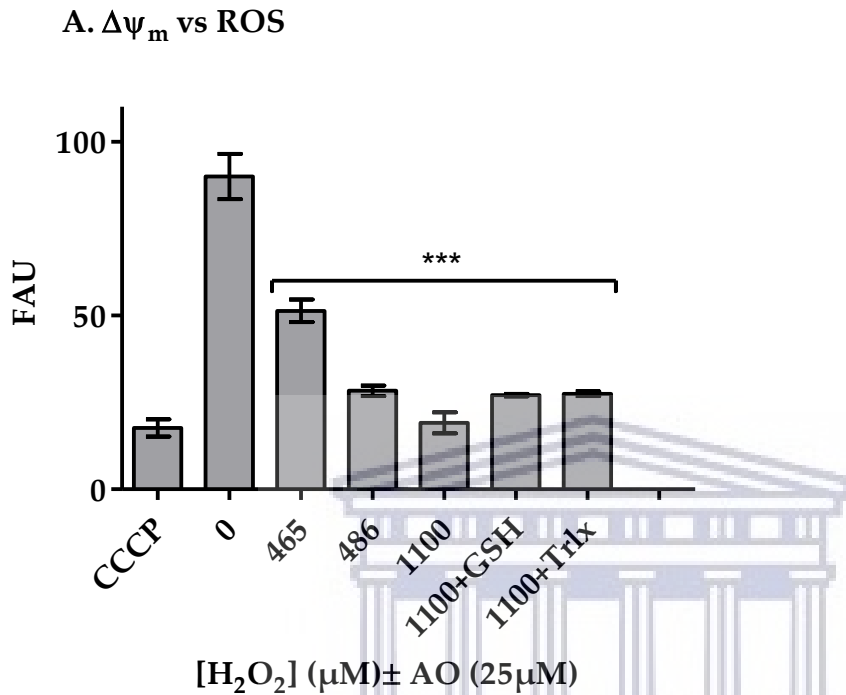
Figure 4.18: Shows TMRE fluorescence of ROS-treated b.End5 cells. Fluorescence from all treatment groups are significantly lower than the control with dose-dependent inter-group differences lowest at IC$_{75}$ concentration which was virtually at par with the negative control data value. With co-administration of antioxidants, a partial but insignificant recovery of mitochondrial fluorescence was observed at the IC$_{75}$ [H$_2$O$_2$] tested. FAU denotes fluorescent arbitrary unit.

Comparisons of the treatment groups using histogram data from flow cytometry study also gave similar results with mitochondrial fluorescent waning as H$_2$O$_2$ concentrations increases.
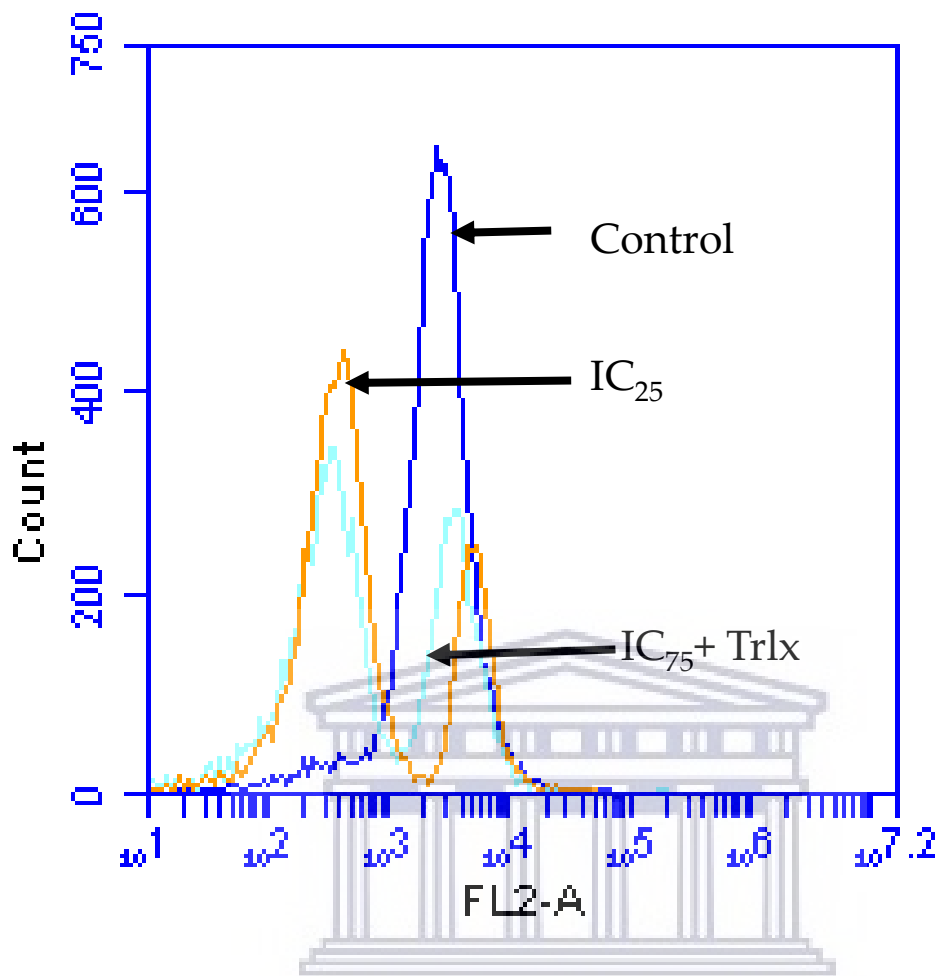
Figure 4.19: Shows overlay histogram of two treatment groups against the treatment control. TMRE fluorescence in the control group lies to the right of others and also occur in higher population of cells than the IC_{25} and the Trolox-treated IC_{75} concentration. The more aligned to the right of the histogram the higher the fluorescence of TMRE.

4.4.3 Analysis of cell cycle in b.End5 cells subjected to exogenously incident escalating ROS concentrations

In order to further evaluate the changes in cell number and/or viability of b.End5 cells under conditions of exogenously incident ROS of increasing strength, cells were cultured and subjected to H_2O_2 treatments as described earlier for a duration of 24hr. Following treatments, the cells of various treatment groups and the control were trypsinated and processed for cell cycle analysis by flow cytometry with propidium iodide used as the fluorochrome for the analysis of DNA synthesis. Changes in the DNA contents of the various treatment groups were

statistically compared with that of the treatment control group for analysis of the different phases of the cell cycle.
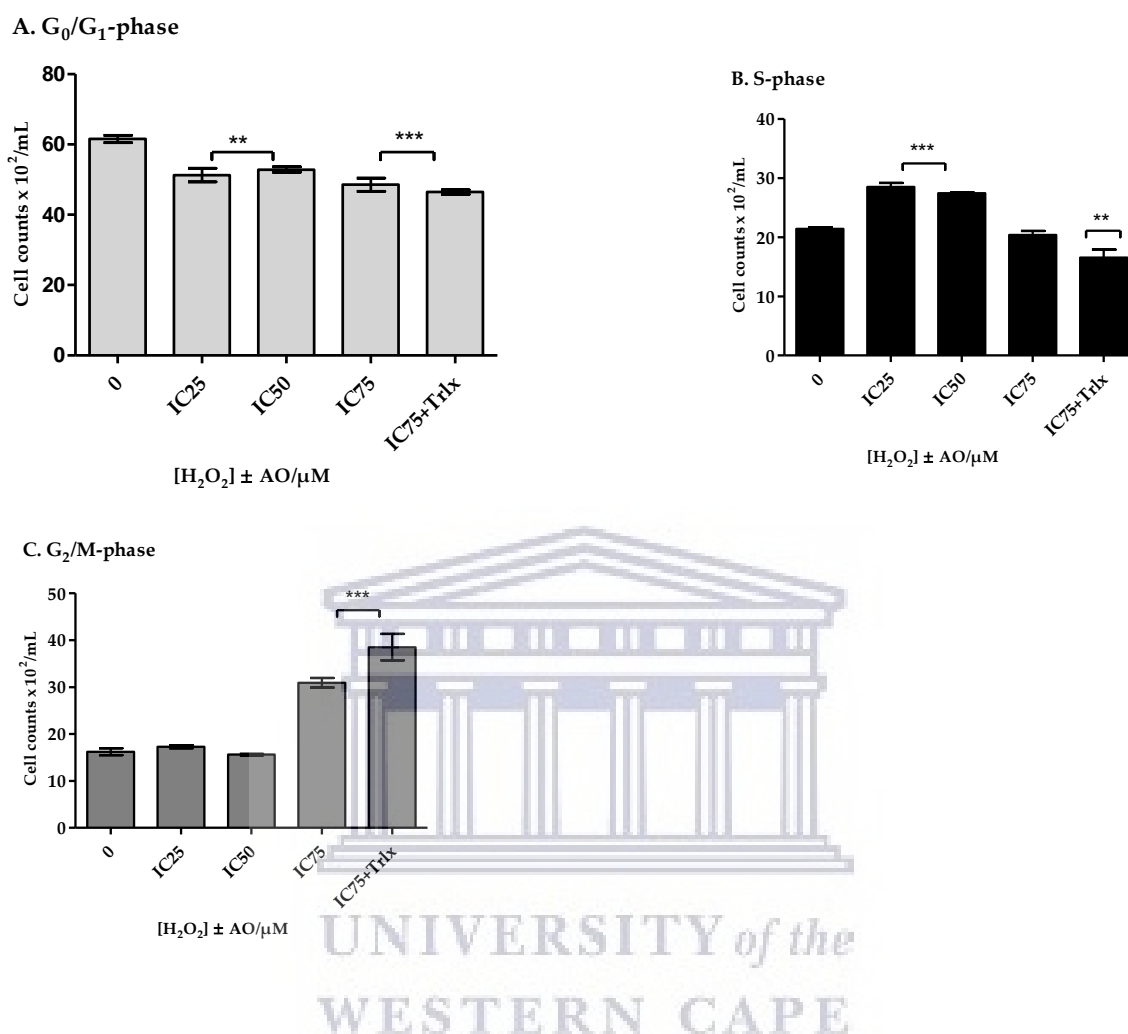
Figure 4.20: Graph shows b.End5 cell cycle analysis during escalating ROS challenge. Graphs A, B and C present the G_0G_1, S and G_2/M phases of the cell cycle. Annotations * denote statistically different data at P<0.05 (compared to the control group) with multiple annotations reflecting the magnitude of the differences in the data.
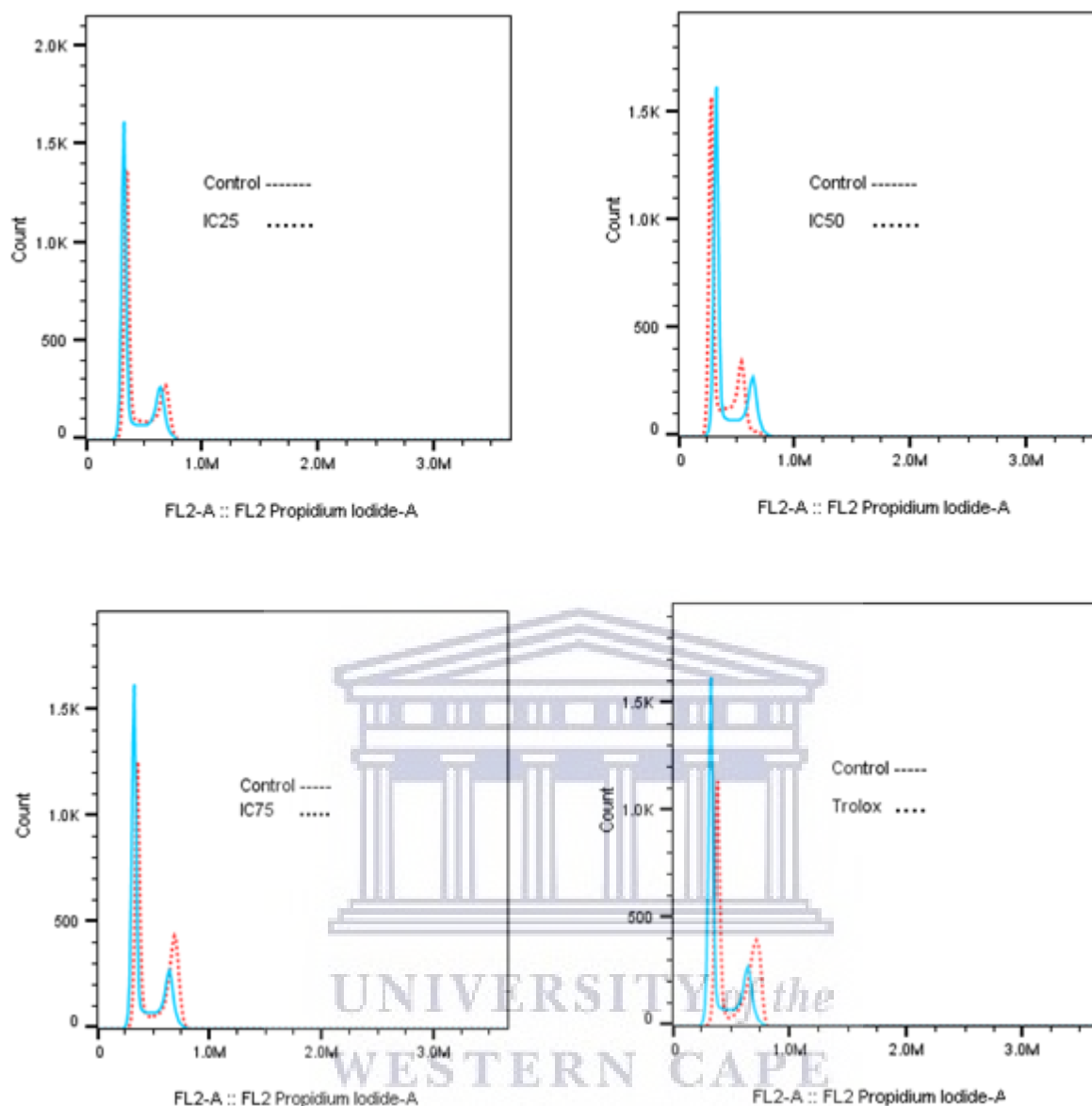
Figure 4.21: Shows histogram presentation for the cell cycle changes at each H_2O_2 concentrations overlaid with the control. At IC_{25} and IC_{50} concentrations, cell counts was different compared to the control but at IC_{75} concentration with and without trolox, G_2/M phase was significantly higher in the number of cells than the control. Higher peaks in the histogram represent peak of the population of cells in the G_0/G_1 phase while the lower peaks represent cell populations in the G_2/M phases of cell division.

5 Chapter 5

5.1 Discussion.

5.1.1 Introduction.

Cell culture systems have, to date, offered valuable tools for the study of the effects of oxidative stress on cellular toxicity as well as adaptive cellular responses. It appears that understanding the processes involved in oxidative stress-mediated cellular responses is obligatory to the full comprehension of several physiological and/or pathological conditions such as aging, degenerative neuropathies, cardiovascular diseases and several others. Aging has been scientifically characterised as a condition of diminishing cellular functions in consequence of accumulating subcellular damage mostly caused by ROS (Jeong, 2017; Madonna *et al.*, 2016).

This study looks into the roles played by ROS and OS on the toxic and adaptive changes in the endothelial cells of the BBB culminating in BBB dysfunction which in turn has been established as a component of several neurological pathologies (Nation *et al.*, 2019; Sweeney *et al.*, 2018).

ROS are normally produced as an inevitable consequence of aerobic life and they pose a very present threat to cellular functions (Sies *et al.*, 2017). Interestingly, most of the damaging effects of ROS are offset by the antioxidant defence system of the cell, composed of a very complex and finely modulated system (Sies *et al.*, 2017). This system consists of a number of enzymes with ample capability for detoxification of oxygen radicals and an additional complement of low molecular weight antioxidants (Sies *et al.*, 2017). Furthermore, repair and turnover processes also help to minimise subcellular damage caused by free radical attack (Birben *et al.*, 2012; Sies *et al.*, 2017). With a perfectly functioning antioxidant system, no cellular damage persists. However, with increase in the ROS load or decrease in the effectiveness of the antioxidant system, a situation of unbalanced redox status in favour of oxidation, known as OS, may arise (Birben *et al.*, 2012; Sies *et al.*, 2017).

The concept that ROS-mediated cellular dysfunctions are due to accumulating subcellular damage presents opportunity for *in vitro* studying of cells in culture under defined conditions of ROS/OS. Such studies can accommodate the use of various types of cells ranging from highly differentiated (primary) cells with a finite *in vitro* life span to permanent (immortalised)

cell lines with an infinite life span to assess the effect of OS in post-mitotic versus cycling cells (Gille & Joenje, 1992).

In inducing OS, given the foregoing, disturbance of the prooxidant-antioxidant balance can be alternatively achieved by either increasing the radical load or inhibiting the antioxidant defences (Gille & Joenje, 1992; Park, 2013; Salvi *et al.*, 2016).

Models using free radical load either increase the load from outside using cellular exposure to γ-irradiation (Kawamura *et al.*, 2018), elevated O_2 tension (Bai *et al.*, 2017), extracellular O_2^- or H_2O_2 (Jacobi *et al.*, 2005; Park, 2013) or by inducing radical production from inside using free radical-generating drugs such as paraquat (Senejani *et al.*, 2019) and menadione (Smith *et al.*, 2017). Antioxidant defences can be compromised by inhibiting catalase and superoxide dismutase using 3-aminotriazole (So *et al.*, 2017) and diethyldithiocarbamate (Lushchak *et al.*, 2005), respectively, or by depleting glutathione using buthionine sulphoximine (Salvi *et al.*, 2016).

5.2   Discussion of findings

5.2.1   Selection of hydrogen peroxide as a source of ROS

In this study, immortalised brain endothelial cells of two types were used for *in vitro* redox experiments by exposure to extracellular H_2O_2. These two cell lines were derived from primary brain endothelial cells of two different mouse strains, BALB/c and SV129 respectively, by infection with a retrovirus coding for the Polyoma middle T-antigen (Montesano *et al.*, 1990; Williams *et al.*, 1989). Both have been used extensively to study BBB function (Helms *et al.*, 2016; Yang *et al.*, 2017; Yang *et al.*, 2007), all with the underlying assumption, that there is physiological parity between these cell lines. The importance of NADPH oxidases (Nox) as a major source of ROS in addition to mitochondria has been well reported in endothelial cells (Konior *et al.*, 2014). Nox enzymes are localized to the cell membrane and generate superoxide radicals from the plasma membrane into the cytoplasm where SOD converts the superoxide to H_2O_2 (Schröder, 2019). In addition, extracellularly added H_2O_2 is freely permeable across cell membranes and will interact at subcellular level. Taken together, these characteristics of endothelial Nox and the cellular accessibility of H_2O_2 motivated the use of extracellularly added H_2O_2 (added to culture media) in this study.

5.2.2 Comparative study of endothelial ROS-Buffering Capacity

In order to define the concentrations of H_2O_2 that simulate OS in the cell lines used, viability assays were done in 96 well culture plates for each cell line with respect to cell proliferation and ratio of live to dead cells using the XTT (Figure 3.2) and Trypan blue exclusion methods respectively. Assay was done in each case by culturing cells in media until cells were attached after which media was replaced with media containing determined concentrations of H_2O_2, which were varied from 0µM in the control treatment group to between 1-1.5mM for a duration of 24hr.

Results showed significantly different capacities of the two cell lines, b.End5 and bEnd.3 cells for survival under the condition of escalating ROS. Using the IC_{50} H_2O_2 concentrations experimentally determined for both cells as a basis for comparison, values of the IC_{50} concentrations for b.End5 cells (486.4µM) (Figure 4.0.) significantly exceeded the values (74.55µM) (Figure 4.1) obtained for the bEnd.3 cell line (P< 0.0001) (4.4). While the b.End5 cell line survived fairly comparably with the control at concentrations of H_2O_2 up to 350µM and attained an IC_{50} value at 486.4µM, the bEnd.3 cell line showed significant decline in viability right from the minimal H_2O_2 concentrations compared to the control which implies a greater sensitivity of the bEnd.3 cell line to ROS stress. Comparison of the viability values at the various [H_2O_2] with the control, using one-way ANOVA, showed that significant decline in viability commenced at 20µM for bEnd.3 cell line. Because targeted changes for study in the OS-induced BBB dysfunction represent adaptive changes of the cells to the condition of OS, an important inference from this finding is that bEnd.3 cells lack the adaptive capability to buffer ROS suggesting that it is unsuitable for *in vitro* redox studies. However, neither this important finding nor the comparative adaptability of the b.End5 and bEnd.3 to OS been reported in scientific literature. BECs, including bEnd.3 cells are routinely used to study characteristics of the BBB under both physiological, pathological conditions, as well as studying processes such as the expression, redistribution and functionality of tight junction proteins depends on redox status of the cell. Thus (using incremental concentrations of H_2O_2) the findings obtainable from the use of bEnd.3 which has no adaptive capability for ROS buffering may mislead scientists into the wrong conclusion that the BBB has no ability to withstand even the slightest change in environmental redox perturbations. Thus, despite that the two cell lines were derived from same species of mammals, they differ markedly in their ability to buffer extracellularly incident ROS. In order to further investigate whether the differences in their culture media composition could have imparted a more redox stability to

the b.End5 cells due to a difference of 0.5mM in the pyruvate content of the culture media recommendation for the two cells, the cells were grown and allowed to attach after which their media were interchanged. Results further showed that the two cell lines could not grow optimally in the swapped media as evidenced by variable degree of cell rounding and cell detachments in the culture of the two cells after 24hr incubation in swapped media (Figure 4.3).

The observed differences, however, could be due to inter-strain differences as has been reported for varying characteristics in some other cells of same animal origin but of divergent strains. Zhai et al, 2019, reported strain specific differences in the anti-inflammatory characteristics of strain 139 and ATCC of a probiotic *Akkermansia municiphila*, showing that the ATCC strain has a stronger anti-inflammatory effects in mice with chronic colitis (Zhai *et al.*, 2019). Another study compared the development of neuronal excitability in the ventral nucleus of the trapezoid body (VNTB) between two strains of mice, CBA and C57, which have different progression rate for age-related hearing loss and reported that VNTB neurons fire at a faster rate in CBA than C57 strains (Sinclair *et al.*, 2017). Furthermore, Gooch and Yee in 1999 examined seven strains of MCF-7 cell line for DNA fragmentation induced by doxorubicin. They found that sensitivity to doxorubicin-induced apoptosis differ between strains. Measure of DNA fragmentation was used to quantify apoptotic change and this was assayed for by DNA laddering and they found further that despite MCF-7 ATCC and MCF-7 MG cells induced similar fold of apoptotic change, the former showed no DNA ladder while the latter showed laddering of DNA. It was concluded that DNA laddering was not suitable for assessment of apoptosis in these cells due to strain-specific differences observed in DNA laddering (Gooch & Yee, 1999).

Despite these previous reports, researchers have largely ignored this important piece of evidence when choosing cell lines to model physiological functions. This is particularly evident in the use of cell lines modelling the BBB, where a variety of primary and immortalized cell lines have been used to study its physiological functions. In a real instance, controversial data have been published in terms of the concentrations of H_2O_2 used for induction of OS using bEnd.3 cells in some reports (Cao, Dai*, et al.*, 2019; Song *et al.*, 2014). Cao et al, 2019 utilised 2mM H_2O_2 for 1hr on bEnd.3 cells which is particularly contrary to the findings in this present study. When bEnd.3 cells were exposed to 0.5mM H_2O_2 half maximal cell death was observed only after approximately 38min (Figure 4.2) and with this finding it is probable that a 2mM H_2O_2 will result in the complete destruction of the bEnd.3 cells within a period of 1hr. In

addition, the surface protein expression such as the tight junction proteins will be completely undetectable (Gangwar *et al.*, 2017). Contrary to this finding with bEnd.3 cells, higher concentrations of H_2O_2 were not toxic to the b.End5 cells which continued to sustain viability measures virtually at par with the control for H_2O_2 concentrations up to 350µM. Another factor that may specify the differences in survival responses of the two cell lines to ROS stress could be due to the predominant cell death mechanism or pathway induced by ROS in the cells. The quick loss of cells in bEnd.3, though not exclusive of apoptotic mechanisms, is more suggestive of a predominantly necrotic pathway which usually features non-physiological disruption of cellular membrane. This in turn can be associated with strain-specific differences in the anti-apoptotic Bcl-2 proteins as has been documented by several reports (Ryter *et al.*, 2007) or even antioxidant responses. Additionally, results from this study showed that several concurrent processes are jointly responsible for the cellular inhibition that resulted the perturbations of cell viability observed, which include cellular death by necrosis and apoptosis as well as perturbations in cell proliferation. In the background of these observations are influences of cellular stress responses including upregulation of cellular antioxidants such as glutathione which in turn influences changes in the mitochondria Ca^{2+} metabolism as well as the formation of mitochondrial transition pore (MTP), mitochondrial membrane depolarization, cytochrome c release and activation of the effectors of apoptotic and necrotic cell death (Li *et al.*, 2012; Okouchi *et al.*, 2009).

The link between OS and the initiation and/or propagation of several disease processes, including degenerative neuropathies, has led scientists to conduct clinical trials of antioxidants targeting the alleviation of these diseases (Angeles *et al.*, 2016; Martinc *et al.*, 2014; Mecocci & Polidori, 2012). Despite several trials conducted, the role of antioxidant treatment in several of the degenerative neuropathies has yet to be ascertained. Additionally, there is virtually no scientific report detailing the endogenous capacity of the BECs of the BBB to buffer ROS providing information which could guide scientists about the rational indications for the administration of exogenous antioxidants or the manipulation of the BECs to increase synthesis under the condition of OS. To evaluate the adaptive responses of the glutathione system, selected for our study amidst other cellular antioxidants, as a marker of endogenous antioxidant responses of BECs used in this study, assays were done to determine if the cell models possess any detectable quantity of GSH and to quantify the content of the GSH, if present, in each of the cell lines as well as determine the adaptive changes with respect to the quantity of glutathione content of the cells during oxidative challenge. Using a combination of fluorescent

microscopy (Stevenson *et al.*, 2002) and spectrometry (Scherer *et al.*, 2008), the presence of GSH was demonstrated and the quantity of GSH per unit cell was experimentally determined. Results of the fluorescent microscopy detection of GSH showed blue mBCl fluorescence in the nuclear and cytoplasmic compartments of b.End5 and bEnd.3 cells (Figure 4.7). Additionally, b.End5 cells showed a greater intensity of mBCl fluorescence as well as a lower nucleo-cytoplasmic ratio than the bEnd.3 cells which suggest that the b.End5 cells have more cytoplasmic GSH than bEnd.3. However, a compartmental GSH quantification would be more suggestive since GSH content may correlate with differential susceptibility to ROS. Because of the subjective nature of the fluorescent microscopy detection, a further GSH quantification assay was done to objectively measure the actual amount of GSH in a unit of each cell lines. The quantitative data of the glutathione content of the b.End5 and bEnd.3 cell types substantiated our visual observations and, although b.End5 cells had a slightly higher mean glutathione content, statistically no significant difference in glutathione quantity was found between the respective cell lines (Figure 4.9). Calculations from data indicated that the GSH concentration per unit cell for the b.End5 and bEnd.3 cell types were within the range of 2.769 ± 0.113 fMol and 2.305 ± 0.219 fMol respectively. Both cell types also have GSH/GSSG ratio of approximately 95%/5% which indicated that both cells were redox-stable in normal culture (Table 4.1). Comparisons of the average cellular glutathione per single cell for both the b.End5 and bEnd.3 cell lines predict that these cells are well suited for OS resistance in that their GSH contents are in the range of cells specialized for detoxification, such as the liver cancer cell line, HepG2 with GSH content of 2.9 fMol/cell (Yuan *et al.*, 2013). Furthermore, these data, considered on their own endorses the use of these cell lines for BBB modeling. However, it is presumptuous to assume that simply on the basis that the cell lines have similar basal levels of endogenous antioxidants that these cells may indeed respond to incremental ROS stress in a similar manner. This is all the more convoluted from a research point of view given the arbitrary concentrations of ROS stressors used in experiments to demonstrate OS on the BBB (Cao, Dai*, et al.*, 2019; Song *et al.*, 2014). It is noteworthy that scientists have been unable to measure absolute magnitude of ROS nor are able to determine the quantitative amount of physiological or pathophysiological ROS but instead measure products of ROS reactions in order to assess levels of ROS in biological tissues.

To evaluate the response of the endogenous antioxidant glutathione to incremental concentrations of H_2O_2 in each cell-line, the relative levels of OS that causes decompensation of the GSH/GSSG antioxidant system in the cell after 24 h exposure were then determined

(Figure 4.10 A, B). In this study the cell lines were profiled using the glutathione system which has been reported as a reliable and sensitive marker of oxidative cellular status (Bains & Bains, 2015; Kranner *et al.*, 2006). Furthermore, because the physiological variable of cell viability was used as a general indicator of the response of the cells to ROS (H_2O_2), it is scientifically plausible that viability changes will be a reliable indicator of the total cellular antioxidant capacity, and therefore, a singular marker (glutathione) would provide enough insight on the differences in the total antioxidant capacities of the two cell lines. Using the IC_{50} (Doroshow & Juhasz, 2019) values as a comparator, this study provides here for the first time documented evidence of the significantly greater capability of the b.End5 cells to neutralize higher ROS concentrations of H_2O_2 than the bEnd.3 cells ([$p < 0.0001$] Figure 4.4). Experimental data from analysis of the trend in GSH depletion within cells exposed to increasing ROS load, showed that the bEnd3 cell type has a very limited ability for *de novo* upregulation of glutathione synthesis under condition of increased ROS accumulation (Figure 4.10 B), whereas the b.End5 cell type showed ability to sustain adequate levels of glutathione, to elevate levels of GSH in response to initial low concentration of ROS, and to maintain this sustained endogenous GSH levels despite several subsequent increases in the concentration of ROS (Figure 4.10 A). Because of the possibility that the increase in the cellular GSH observed in the b.End5 cells may be due to increases in cell number (due to proliferation), the assay was repeated with the combination of H_2O_2 and 25µM trolox treatment for all treatment points. Trolox is a vitamin E analogue that exhibits an antioxidant effect by scavenging for lipid peroxides and thus protects cell membranes (Niki & Noguchi, 2004). The data showed an identical pattern of GSH depletion, while cell proliferation was preserved at concentrations well above 500µM (Figure 4.10 C and D) which conclusively establishing that cell proliferation does not necessarily correlate to the increments in total cellular GSH content observed. Furthermore, it was observed that cellular GSH was never completely depleted in the b.End5 cells despite exposure to H_2O_2 concentrations up to 2.5mM. Thus it is of interest to know the status of the cells with maximal GSH depletion whether live or completely dead. A clonogenic assay was performed using the cells at this position of GSH depletion with or without combination treatment with 25µM trolox and compared with control and IC_{50} groups. Result showed that the cells at the base of GSH depletion trend are live cells but have a very slow rate of re-growth compared with the control and IC_{50} groups (Figure 4.11). Implication of this finding is that cellular inhibition by OS in these cells are reversible, and as such if the stressor is relieved they will regrow, though slowly. Similar corroborative result was obtained using fluorescent microscopy

which show dose dependent reduction in the mBCl fluorescence in response to treatment with incremental concentrations of H_2O_2 (Figure 4.12).

The mechanism for this divergent reaction of the glutathione system in the two cell types against increasing concentration of ROS is not clear, and requires further study. However, this observed difference is suggestive of inter-strain differences in the system that regulates ROS accumulation within these cells, as has been reported for several diverse physiological characteristics in different strains of cells from the same species of animal (Doroshow & Juhasz, 2019; Shidara *et al.*, 2019; Sinclair *et al.*, 2017). In addition, differentially expressed genes in specific domains of the system that regulate ROS in intracellular *milieu* or perhaps strain-specific genetic alteration following viral oncogenic transformation of the primary cells could be responsible (Sandberg *et al.*, 2000). The foregoing is supported by the earlier mentioned reports of mouse strain-specific differences in neuro-behavior, neuronal excitability, susceptibility to fibrosis, anti-inflammatory response, and bone density that have been previously reported (Shidara *et al.*, 2019). These previous reports have strengthened the position that strain-specific genes are very important in shaping the phenotypic differences in the two cell types investigated with respect to their glutathione system plasticity to OS. This finding has an important bearing on experimental designs aimed at studying effects of OS on the BBB. However, whether these two mouse cells respond differently to OS *in vivo* is not known. It is suggestive here that a genome-wide genetic screen in the cells for evaluating the physiological variables of the BBB may be necessary to identify important differences in the genes that control several key functions of the BBB (Cao, Poddar*, et al.*, 2019). Also, further research is required to determine these properties in primary cells of the mouse brain endothelial cells with the potential for unraveling the true behavior of the mouse brain endothelial cells during OS conditions with respect to capacity for ROS neutralization and the glutathione system response. Conclusively though the catalase status of brain ECs is unclear, the glutathione system responses and ROS buffering capacities are clearly linked and they are thus partial determinants of the magnitude of ROS that induces OS in the b.End5 and bEnd.3 mouse brain endothelial cell line models of the BBB. Strain-specific differences in the different cells will result in different definitions of OS in different models of different animal strains within the same species. Thus it is important to establish experimental parameters that best define OS for each endothelial cell model of the BBB for reproducibility. Such information will avail researchers of opportunity to verify and select appropriate models of BBB endothelial

cells for specific redox investigations and enable them to draw comparable and reproducible conclusions.

5.3   Discussion of findings of mechanism of OS-induced BBB dysfunction.

Having established that b.End5 features the adaptive responses necessary to respond to the effects of ROS and /or OS, changes in the BECs that underlie OS-mediated BBB dysfunction, were investigated using the b.End5 cells.

Analysis of the results of trypan blue exclusion viability assay on b.End5 cells (Figure 4.5 and 4.6) was considered together with similar assay by XTT proliferation kit. Both results showed that the process of cell proliferation and cell death were concurrently occurring throughout the period of H_2O_2 exposure. Evidence of this include the finding that 50% of live cells remained at H_2O_2 concentration of 486.4µM in the XTT assay (IC_{50}) while the total number of live cells were significantly lower than control at concentrations above 500µM in the trypan blue exclusion assay. However, in the trypan blue assay (despite controlling for floating cells in the media) analysis of the number live and dead cells at high H_2O_2 concentrations (>500µM) showed that the addition of the number of live and dead cells does equal the total number of cells in the control. This implies there are other mechanisms for the H_2O_2-mediated depletion in the number of cultured b.End5 cells in the samples. In addition to molecular alterations, cell death also presents with macroscopic morphological changes. These morphological manifestations together with the mechanisms for the disposal of cell fragments have been used to classify cell death into three different forms such as apoptosis, autophagy and necrosis (Galluzzi *et al.*, 2018). While the former two types have a common component involving vesicular or cytoplasmic vacuolisations that are efficiently taken up by neighbouring cells with phagocytic activities and degraded within lysosomes, the necrotic type disposes dead cells without involvement of phagocytic or lysosomal activities (Galluzzi *et al.*, 2018). Though apoptosis features retention of plasma membrane integrity, however, the end-stage apoptosis subsequently incorporates a complete breakdown of the plasma membrane and the acquisition of a necrotic morphology due to the lack of phagocytic activity in cultured cells *in vitro*. Furthermore, the trypan blue exclusion assay works on the principle that the dye does not penetrate an intact cell membrane and so live cells exclude the dye. This becomes a limitation of the assay in that apoptotic cells will be undetectable due to non-disruption of their cell membranes in the various stages of apoptotic change (Strober, 1997, 2015). Induction of

apoptotic change in cells treated with H_2O_2 has been well reported (Park, 2013; Sun *et al.*, 2012). Further experiments were therefore carried out to investigate the possible involvement of cellular apoptotic changes in the depletion of b.End5 cells following treatment with incremental concentrations of H_2O_2. Using annexin V/propidium iodide assay by flow cytometry, evaluation of the number of cells undergoing apoptotic and necrotic death was done in comparison to live cells in the treated samples compared to the control. Results showed that apoptosis contribute largely to the cell depletion that occur during exposure to H_2O_2 concentrations that define IC_{50} and above (Figure 4.15-4.17). Stress-driven physiological cell death as well as adaptive stress responses both represents a grand plan for the preservation of biological equilibrium, however, adaptive response relates to cellular level of operation while physiological cell death operates at the level of the organism (Galluzzi *et al.*, 2018). In essence, it features a homeostatic function that represents the elimination of useless and potentially dangerous cells with additional ability of dying cells to expose or release molecules that alert the organism about a potential threat (Galluzzi *et al.*, 2018). Danger signals such as these has been described as damage-associated molecular patterns (DAMPs) or alarmins (Galluzzi *et al.*, 2018). From the control position of cell population ratio, it appeared that the necrotic cell population represents a transition from late apoptosis status to completely dead or necrotic change due to the fact that in the *in vitro* setting, there are no immune cells to scavenge for the late apoptotic cells as occur in the *in vivo* situation. As such this transition represents a false mimicry of normal senescence that is usually associated with aging in an entire population of cells including endothelial cells (Faragher & Kipling, 1998). However, with application of IC_{50} H_2O_2 concentration, the changes observed are suggestive of more actively mediated changes. First it showed there is a rapid transition from live cells towards more cells in the necrotic quadrant of the total cell population. Cells may have been stimulated to undergo more apoptotic changes with resultant increase in the population of necrotic cells. Alternatively, direct damage to the cell membranes by the H_2O_2 at high concentrations may have led to necrotic changes in the cell population without going through the cycle of early and late apoptosis. However, the former has been reported in several other studies which summarized that H_2O_2 of low concentrations induced more apoptotic change with subsequent increase in necrotic cell population (Kim *et al.*, 2003; Luo & Xia, 2006). In one of these reports, H_2O_2-effected change through the caspase 3-dependent apoptosis pathway was described; while other reports suggested enhanced TNF-α toxicity causing activation of downstream effectors of apoptosis (Luo & Xia, 2006). When the cells are exposed to IC_{50} H_2O_2 concentration, there was a relative

increase in the proportion of early and late apoptotic cells with relative reduction in the ratio of necrotic cells while there was marginal increase in the number of live cells. Early apoptotic cells showed about a 29 fold increase which implies that a greater number of live cells were undergoing transition to apoptosis. At the concentration corresponding to the IC_{75} (1100µM) more cells pooled in the late apoptosis (52.6%) category and it appeared that only a minimal transition into necrotic cells took place in treated samples (Figure 4.16). However, at IC_{75} the number of live cell population reached its minimum value of about 36%. Also the proportion of early apoptotic cells was still about 8 fold compared to the control. So under this condition, which can be described as severe oxidative stress, apoptotic endothelial cells constitute the major component of the entire cell population and thus it becomes evidently clear that apoptosis is the major morphological change resulting from exposure of brain endothelial cells to H_2O_2-induced OS. When antioxidants GSH and trolox (25µM each) were exogenously administered in combination with H_2O_2 treatment, it was observed that the population of necrotic cells in each of the antioxidants was reduced to levels lower than control while the total cell population gained more proportion in live cells. These findings for GSH and trolox suggest that exogenously administered antioxidants have direct ameliorative effects on the endothelial cell death characteristic of endothelial OS (Figures 4.17 and 4.18).

Initiation of apoptosis may follow either of intrinsic, mitochondrial-mediated or extrinsic, death receptor-mediated pathways and factors that trigger either pathway of apoptosis have been well studied (Bonora *et al.*, 2015). The intrinsic apoptosis pathway is triggered by microenvironmental perturbations, including but not limited to, ROS overload (Galluzzi *et al.*, 2018). The critical step in intrinsic apoptosis is the irreversible and widespread mitochondrial outer membrane permeabilisation, MOMP, which is controlled by pro-apoptotic and anti-apoptotic members of the Bcl2, apoptosis regulator members of the Bcl2 protein family (Bonora *et al.*, 2015; Galluzzi *et al.*, 2018). MOMP directly promotes the cytosolic release of apoptogenic factors which normally reside in the mitochondrial intermembrane space and include cytochrome c, somatic (CYCS), diablo IAP-binding mitochondrial protein (DIABLO) also known as second mitochondrial activator of caspases (SMAC). The release of these two factors is associated with mitochondrial cristae remodelling (Gottlieb *et al.*, 2003). MOMP subsequently leads to the dissipation of the MMP, mainly as a consequence of the respiratory impairment imposed by the loss of CYCS and thus the cessation of mitochondrial membrane

potential (MMP)-dependent mitochondrial functions, such as ATP synthesis. Catalytic activity of executioner caspases then precipitates cellular death and many of the morphological and biochemical correlates of apoptosis (Bonora *et al.*, 2015; Galluzzi *et al.*, 2018). Thus mitochondria can be a source of energy generation for cellular use under aerobic conditions but it can also be a source of signals initiating cell death (Ly *et al.*, 2003).

In studying the molecular pathway of H_2O_2-induced apoptosis and necrosis, mitochondrial involvement was investigated using mitochondrial membrane potential changes as marker for cytochrome c release. Cultured b.End5 cells were divided into groups according to predetermined concentrations of H_2O_2 for 24hr and then incubated with cationic dye tetramethylrhodamine ester (TMRE) for 20-30min. Stained cells were then analysed by either of fluorescent microscopy, microplate spectrometry and flow cytometry. Micrographic results showed dose dependent reduction in the number of cells showing TMRE fluorescence which is suggestive of reduction in mitochondrial membrane potential (Figure 4.22). Analysis in microplate (Figure 4.23) showed significantly lower TMRE fluorescence at all concentrations of H_2O_2 used when compared with the control. The lowest value of measured TMRE fluorescence was observed at the IC_{75} concentration which is statistically at par with the negative control data consisting of wells of cells treated with a known mitochondrial uncoupler, 100μM CCCP. Additionally, flow cytometry assay also showed gradual dose-dependent reduction in the TMRE fluorescent in the cells. The observed reduction in the mitochondrial membrane potential with increase in the concentration of H_2O_2 correlates with MOMP and release of cytochrome c which are the major events preceding the activation of apoptogenic caspases that are responsible for the increased number of apoptotic cells in the treated samples (Crowley, Christensen*, et al.*, 2016).

The last potential source of end-point reduction in the total number of cells under conditions of incremental H_2O_2 concentrations is alteration in the cell cycle dynamics leading to cell cycle arrest. Cell cycle arrest in cells treated with H_2O_2 has also been documented in scientific reports (Correia *et al.*, 2017; Santa-Gonzalez *et al.*, 2016). In this study, data from cell cycle assay using flow cytometry analysis of b.End5 cells treated with incremental H_2O_2 concentrations and PI staining showed variations in the number of cells in the G_0/G_1, S and G_2/M phases at different H_2O_2 concentrations. In the G_0/G_1 phase, H_2O_2 concentrations representing IC_{75} with and without antioxidant treatment (trolox) showed a significant reduction in the number of cells compared to the control group of cells (P<0.05). In the S-phase, H_2O_2 concentrations

representing IC_{25} and IC_{50} showed statistically significant increase in cell counts compared to the control ($P<0.05$) and finally in the G_2/M phase H_2O_2 concentrations representing IC_{75} with and without antioxidant treatment (trolox) showed statistically significant increase compared to the control. These data when considered together showed that H_2O_2 concentrations in the range of IC_{25} and IC_{50} stimulate increased rates of endothelial cell proliferation, while endothelial proliferation is inhibited at the IC_{75} concentration which is at level of severe OS precipitating the arrest of cell cycle at the G_2/M phase. Further, the application of exogenous antioxidant trolox does not inhibit the effects of the ROS overload in causing cell cycle arrest. A number of reports gave accounts of cell cycle arrest in the G_2/M phase caused by treatments of various cancer cells with agents such as resveratrol (Yu *et al.*, 2016), *Dendrobium candidum* (Sun *et al.*, 2016), coptisine (Rao *et al.*, 2017) and hesperidine (Pandey *et al.*, 2019). A number of these reports postulated an association of the G_2/M arrest with ROS and apoptosis as also found in the present study (Chaudhary *et al.*, 2013; Shendge *et al.*, 2020). The data obtained from this study showed that effects of incremental ROS on endothelial cells of the BBB include cell proliferation, necrosis and apoptosis with cell cycle arrest occurring concurrently. However, at ROS levels indicative of OS, data suggest that the major events culminating in BBB dysfunction are increased level of endothelial cell apoptosis and cell cycle arrest characteristically in the G_2/M phase of the cell cycle. It is clearly observed from this study that cell cycle arrest and apoptosis greatly contributed to cell depletion under condition of OS. Increased cell proliferation at low to moderate doses of H_2O_2 is another interesting finding with more cells driven to G_0-S phase and thus cell cycle progression. This implies that moderate oxidative shift in redox equilibrium causes increased EC proliferation and thus favors angiogenesis.

With the simulation of ROS conditions in cells used in this study, our investigations did not include an attempt to measure ROS because our source of ROS and magnitude are predetermined and as such any attempt to measure ROS is expected to yield the same magnitude as the experimentally incident ROS. Furthermore, with the use of immortalized cells in this study, it is acknowledged that the findings discussed may or may not represent what holds in the primary cells from the same animal source.

5.3.1 Conclusion and recommendation

The use of non-physiologically defined concentrations of hydrogen peroxide for simulation of oxidative stress in many *in vitro* research studies, especially experiments designed to study the

BBB leave a substantial gap in technicality. This present study has provided useful insight into the need for caution in assuming parity between different cells available for the various studies, even when they are of same species. Finding here has shown significant difference between two cell lines b.End5 and bEnd.3, both of murine origin, in their sensitivity to toxicity induced by incremental concentration of hydrogen peroxide. There is therefore need to define what concentration of hydrogen peroxide that constitute oxidative stress in each of these cell prior to real experiments so a reproducible and reliable conclusion can be drawn from the findings from such studies. However, this has not been the case for many researchers who used different concentrations of hydrogen peroxide on bEnd.3 to produce results that seems to agree despite these divergence in the protocols. The findings of the present study clearly contradict the use of such random experimental protocols as published by these previous works. In the cell lines studied in this work, the suggested causes of the disparity in the capacities of the cell for ROS buffering was that despite content of comparable amount of glutathione in the two cells, adaptive GSH synthesis via the *de novo* synthetic pathway differ significantly, a finding which in turn is probably due to strain-specific differences in physiological characteristics. It is therefore a recommendation from this study that researchers determine first the maximum capacity of the cells of choice to withstand the challenge being studied, for the different models of the BBB, before embarking on definitive experiments.

Furthermore, the study concludes that under conditions of varying severity of oxidative stress, some of the pathological events that leads to abnormal BBB function are going on at the same time. These events include endothelial cell death of different modalities viz necrosis but mainly apoptosis with some significant arrest of cell proliferation. However, at a very low amount of ROS accumulation, endothelial proliferation was enhanced. The rapid endothelial proliferation could lead to increased proportion of ECs with immature characteristics, such as poorly expressed tight junction proteins, resulting in the abnormal permeability of the oxidative-stressed BBB. Use of exogenous antioxidant assist the endothelial cells in the preservation of a pool of active cells ready for the process of angiogenesis and can speed up the timeline of new blood vessel maturity (i.e., the development of all components required for the characteristics of the blood vessels at the different locations in the, such as tight junction proteins, efflux proteins etc). This is so because it takes longer time for residual endothelial cells after severe oxidative stress without antioxidant use to regrow when compared to residual cells with antioxidant co-administered. It is recommendable from this study, therefore, further

studies to strongly suggest the use of antioxidant as adjuvant therapy in the clinical management of neurological diseases and especially the degenerative neuropathies.

5.3.2 Limitations of the project

Due to defined scope of the project, this work could not incorporate the induction of internally generated ROS using drugs that could stimulate the cells to produce ROS from intracellular organelles. This could have required the use of techniques that measure the amount of ROS produced by individual subcellular organelles such as mitochondria, and endoplasmic reticulum. Also, predominant types of internal ROS would have need be identified and quantified using using a combination of immuno-electron microscopy as qualitative and ELISA as semi-quantitative methods

Additionally, investigation such as messenger RNA expression of endogenous antioxidant genes as well as transcription factors that regulate the stress response would have been done but for technical hindrance encountered during the course of this work.

A significant part of the thesis has been largely published while a portion of the literature review has been published as a book chapter (cf. addendum).
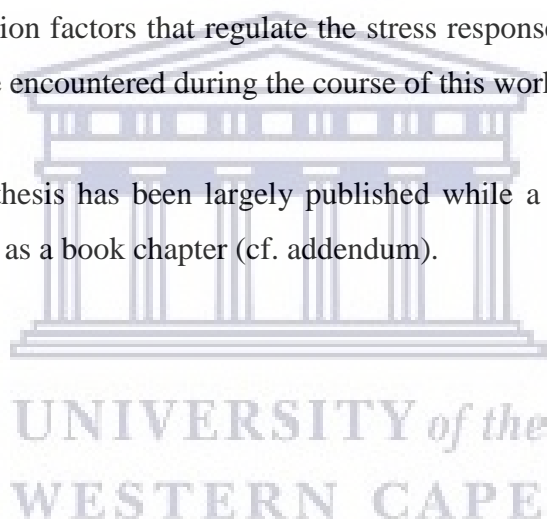
References

Abbott. (1992). Comparative physiology of the blood-brain barrier *Physiology and pharmacology of the blood-brain barrier* (pp. 371-396): Springer.

Abbott, Patabendige, A. A., Dolman, D. E., Yusof, S. R., & Begley, D. J. (2010). Structure and function of the blood-brain barrier. *Neurobiol Dis, 37*(1), 13-25. doi:10.1016/j.nbd.2009.07.030

Abbott, Rönnbäck, L., & Hansson, E. (2006). Astrocyte–endothelial interactions at the blood–brain barrier. *Nature Reviews Neuroscience, 7*(1), 41.

Abdullahi, W., Tripathi, D., & Ronaldson, P. T. (2018). Blood-brain barrier dysfunction in ischemic stroke: targeting tight junctions and transporters for vascular protection. *American Journal of Physiology-Cell Physiology, 315*(3), C343-C356.

Ahn, I., Ju, J., Lee, S., Park, J., Oh, H., Kim, H.*, et al.* (2012). Upregulation of Stromal Cell–Derived Factor By IL-17 and IL-18 Via a Phosphatidylinositol 3-Kinase-Dependent Pathway. *Scandinavian journal of immunology, 76*(4), 433-439.

Allen, L.-A. H., & Criss, A. K. (2019). Cell intrinsic functions of neutrophils and their manipulation by pathogens. *Current opinion in immunology, 60*, 124-129.

Angeles, D. C., Ho, P., Dymock, B. W., Lim, K. L., Zhou, Z. D., & Tan, E. K. (2016). Antioxidants inhibit neuronal toxicity in Parkinson's disease-linked LRRK 2. *Annals of clinical and translational neurology, 3*(4), 288-294.

Antony, A. N., Katona, M., Juskeviciute, E., Elrod, J. W., Hajnóczky, G., & Hoek, J. B. (2018). Fine-tuning of hepatocyte calcium signaling and liver regeneration by the mitochondrial calcium uniporter. *The FASEB Journal, 32*(1_supplement), 536.510-536.510.

Arias-del-Val, J., Santo-Domingo, J., Garcia-Casas, P., Alvarez-Illera, P., Galindo, A. N., Wiederkehr, A.*, et al.* (2019). Regulation of inositol 1, 4, 5-trisphosphate-induced Ca2+ release from the endoplasmic reticulum by AMP-activated kinase modulators. *Cell calcium, 77*, 68-76.

Armulik, A., Genové, G., & Betsholtz, C. (2011). Pericytes: developmental, physiological, and pathological perspectives, problems, and promises. *Dev Cell, 21*(2), 193-215.

Armulik, A., Genové, G., Mäe, M., Nisancioglu, M. H., Wallgard, E., Niaudet, C.*, et al.* (2010). Pericytes regulate the blood–brain barrier. *Nature, 468*(7323), 557.

Aslani, B. A., & Ghobadi, S. (2016). Studies on oxidants and antioxidants with a brief glance at their relevance to the immune system. *Life Sciences, 146*, 163-173.

Bai, Y.-x., Fang, F., Jiang, J.-l., & Xu, F. (2017). Extrinsic calcitonin gene-related peptide inhibits hyperoxia-induced alveolar epithelial type II cells apoptosis, oxidative stress, and reactive oxygen species (ROS) production by enhancing notch 1 and Homocysteine-induced endoplasmic reticulum protein (HERP) expression. *Medical science monitor: international medical journal of experimental and clinical research, 23*, 5774.

Bains, V. K., & Bains, R. (2015). The antioxidant master glutathione and periodontal health. *Dental research journal, 12*(5), 389.

Barnham, K. J., Masters, C. L., & Bush, A. I. (2004). Neurodegenerative diseases and oxidative stress. *Nature reviews Drug discovery, 3*(3), 205.

Bastianetto, S., Yao, Z. X., Papadopoulos, V., & Quirion, R. (2006). Neuroprotective effects of green and black teas and their catechin gallate esters against β-amyloid-induced toxicity. *European Journal of Neuroscience, 23*(1), 55-64.

Baxter, P. S., Bell, K. F., Hasel, P., Kaindl, A. M., Fricker, M., Thomson, D.*, et al.* (2015). Synaptic NMDA receptor activity is coupled to the transcriptional control of the glutathione system. *Nature communications, 6*, 6761.

Ben-Zvi, A., Lacoste, B., Kur, E., Andreone, B. J., Mayshar, Y., Yan, H*., et al.* (2014). Mfsd2a is critical for the formation and function of the blood–brain barrier. *Nature, 509*(7501), 507.

Bhat, A. H., Dar, K. B., Anees, S., Zargar, M. A., Masood, A., Sofi, M. A*., et al.* (2015). Oxidative stress, mitochondrial dysfunction and neurodegenerative diseases; a mechanistic insight. *Biomedicine & Pharmacotherapy, 74*, 101-110.

Biedl, A., & Kraus, R. (1898). Über eine bisher unbekannte toxische Wirkung der Gallensäure auf das Zentralnervensystem. *Zentralbl Inn Med, 19*, 1185-1200.

Birben, E., Sahiner, U. M., Sackesen, C., Erzurum, S., & Kalayci, O. (2012). Oxidative stress and antioxidant defense. *World Allergy Organ J, 5*(1), 9-19. doi:10.1097/WOX.0b013e3182439613

Blesa, J., Trigo-Damas, I., Quiroga-Varela, A., & Jackson-Lewis, V. R. (2015). Oxidative stress and Parkinson's disease. *Frontiers in Neuroanatomy, 9*(91). doi:10.3389/fnana.2015.00091

Boado, R. J., & Pardridge, W. M. (1991). A one-step procedure for isolation of poly (A)+ mRNA from isolated brain capillaries and endothelial cells in culture. *Journal of neurochemistry, 57*(6), 2136-2139.

Bolinger, M. T., Ramshekar, A., Waldschmidt, H. V., Larsen, S. D., Bewley, M. C., Flanagan, J. M*., et al.* (2016). Occludin S471 phosphorylation contributes to epithelial monolayer maturation. *Molecular and Cellular Biology, 36*(15), 2051-2066.

Bonora, M., Wieckowski, M. R., Chinopoulos, C., Kepp, O., Kroemer, G., Galluzzi, L*., et al.* (2015). Molecular mechanisms of cell death: central implication of ATP synthase in mitochondrial permeability transition. *Oncogene, 34*(12), 1475.

Booth, R., & Kim, H. (2012). Characterization of a microfluidic in vitro model of the blood-brain barrier (μBBB). *Lab on a Chip, 12*(10), 1784-1792.

Bova, M. P., Tam, D., McMahon, G., & Mattson, M. N. (2005). Troglitazone induces a rapid drop of mitochondrial membrane potential in liver HepG2 cells. *Toxicology letters, 155*(1), 41-50.

Bowman, P. D., Ennis, S. R., Rarey, K. E., Lorris Betz, A., & Goldstein, G. W. (1983). Brain microvessel endothelial cells in tissue culture: A model for study of blood-brain barrier permeability. *Annals of neurology, 14*(4), 396-402.

Brightman, M., & Reese, T. (1969). Junctions between intimately apposed cell membranes in the vertebrate brain. *J Cell Biol, 40*(3), 648-677.

Brightman, M. W. (1965). The distribution within the brain of ferritin injected into cerebrospinal fluid compartments: I. Ependymal distribution. *J Cell Biol, 26*(1), 99-123.

Brightman, M. W. (1968). The intracerebral movement of proteins injected into blood and cerebrospinal fluid of mice *Progress in brain research* (Vol. 29, pp. 19-40): Elsevier.

Brini, M., & Carafoli, E. (2011). The plasma membrane Ca2+ ATPase and the plasma membrane sodium calcium exchanger cooperate in the regulation of cell calcium. *Cold Spring Harbor Perspectives in Biology, 3*(2), a004168.

Butt, A. M., Jones, H. C., & Abbott, N. J. (1990). Electrical resistance across the blood-brain barrier in anaesthetized rats: a developmental study. *The Journal of physiology, 429*(1), 47-62.

Butterfield, D. A. (2018). Perspectives on Oxidative Stress in Alzheimer's Disease and Predictions of Future Research Emphases. *Journal of Alzheimer's Disease*(Preprint), 1-11.

Cabezas, R., Ávila, M., Gonzalez, J., El-Bachá, R. S., Báez, E., García-Segura, L. M*., et al.* (2014). Astrocytic modulation of blood brain barrier: perspectives on Parkinson's disease. *Frontiers in cellular neuroscience, 8*, 211.

Cai, R.-p., Xue, Y.-x., Huang, J., Wang, J.-h., Wang, J.-h., Zhao, S.-y.*, et al.* (2016). NS1619 regulates the expression of caveolin-1 protein in a time-dependent manner via ROS/PI3K/PKB/FoxO1 signaling pathway in brain tumor microvascular endothelial cells. *Journal of the neurological sciences, 369*, 109-118.

Campisi, M., Shin, Y., Osaki, T., Hajal, C., Chiono, V., & Kamm, R. D. (2018). 3D self-organized microvascular model of the human blood-brain barrier with endothelial cells, pericytes and astrocytes. *Biomaterials, 180*, 117-129.

Cantrell, D. A. (2001). Phosphoinositide 3-kinase signalling pathways. *J Cell Sci, 114*(8), 1439-1445.

Cao, Dai, L., Mu, J., Wang, X., Hong, Y., Zhu, C.*, et al.* (2019). S1PR2 antagonist alleviates oxidative stress-enhanced brain endothelial permeability by attenuating p38 and Erk1/2-dependent cPLA2 phosphorylation. *Cell Signal, 53*, 151-161.

Cao, Poddar, A., Magtanong, L., Lumb, J. H., Mileur, T. R., Reid, M. A.*, et al.* (2019). A genome-wide haploid genetic screen identifies regulators of glutathione abundance and ferroptosis sensitivity. *Cell reports, 26*(6), 1544-1556. e1548.

Cao, H., & Chen, X. (2012). Structures required of flavonoids for inhibiting digestive enzymes. *Anti-Cancer Agents in Medicinal Chemistry (Formerly Current Medicinal Chemistry-Anti-Cancer Agents), 12*(8), 929-939.

Carocho, M., & Ferreira, I. C. (2013). A review on antioxidants, prooxidants and related controversy: natural and synthetic compounds, screening and analysis methodologies and future perspectives. *Food and chemical toxicology, 51*, 15-25.

Chakraborty, A., De Wit, N., Van Der Flier, W., & De Vries, H. (2017). The blood brain barrier in Alzheimer's disease. *Vascular pharmacology, 89*, 12-18.

Chatterjee, S., Noack, H., Possel, H., Keilhoff, G., & Wolf, G. (1999). Glutathione levels in primary glial cultures: monochlorobimane provides evidence of cell type-specific distribution. *Glia, 27*(2), 152-161.

Chaudhary, P., Sharma, R., Sahu, M., Vishwanatha, J. K., Awasthi, S., & Awasthi, Y. C. (2013). 4-Hydroxynonenal induces G2/M phase cell cycle arrest by activation of the ataxia telangiectasia mutated and Rad3-related protein (ATR)/checkpoint kinase 1 (Chk1) signaling pathway. *Journal of Biological Chemistry, 288*(28), 20532-20546.

Chauhan, P. S., Singh, D., Dash, D., & Singh, R. (2018). Intranasal curcumin regulates chronic asthma in mice by modulating NF-κB activation and MAPK signaling. *Phytomedicine, 51*, 29-38.

Cheignon, C., Tomas, M., Bonnefont-Rousselot, D., Faller, P., Hureau, C., & Collin, F. (2018). Oxidative stress and the amyloid beta peptide in Alzheimer's disease. *Redox Biology, 14*, 450-464. doi:https://doi.org/10.1016/j.redox.2017.10.014

Chen, Lin, Y.-L., Chen, T.-L., Tai, Y.-T., Chen, C.-Y., & Chen, R.-M. (2016). Ketamine alleviates bradykinin-induced disruption of the mouse cerebrovascular endothelial cell-constructed tight junction barrier via a calcium-mediated redistribution of occludin polymerization. *Toxicology, 368*, 142-151.

Chen, Teng, H., Xie, Z., Cao, H., Cheang, W. S., Skalicka-Woniak, K.*, et al.* (2018). Modifications of dietary flavonoids towards improved bioactivity: an update on structure–activity relationship. *Critical reviews in food science and nutrition, 58*(4), 513-527.

Chin, J. H., & Vora, N. (2014). The global burden of neurologic diseases. *Neurology, 83*(4), 349-351.

Circu, & Aw, T. Y. (2010). Reactive oxygen species, cellular redox systems, and apoptosis. *Free Radic Biol Med, 48*(6), 749-762. doi:10.1016/j.freeradbiomed.2009.12.022

Circu, & Aw, T. Y. (2012). Glutathione and modulation of cell apoptosis. *Biochimica et Biophysica Acta (BBA)-Molecular Cell Research, 1823*(10), 1767-1777.

Citi, S. (2019). The mechanobiology of tight junctions. *Biophysical reviews*, 1-11.

Cobley, J. N., Fiorello, M. L., & Bailey, D. M. (2018). 13 reasons why the brain is susceptible to oxidative stress. *Redox Biology, 15*, 490-503. doi:https://doi.org/10.1016/j.redox.2018.01.008

Coelho-Santos, V., Socodato, R., Portugal, C., Leitao, R. A., Rito, M., Barbosa, M., *et al.* (2016). Methylphenidate-triggered ROS generation promotes caveolae-mediated transcytosis via Rac1 signaling and c-Src-dependent caveolin-1 phosphorylation in human brain endothelial cells. *Cellular and Molecular Life Sciences, 73*(24), 4701-4716.

Collaborators, G. N. (2019). Global, regional, and national burden of neurological disorders, 1990-2016: a systematic analysis for the Global Burden of Disease Study 2016.

Copley, S. D., & Dhillon, J. K. (2002). Lateral gene transfer and parallel evolution in the history of glutathione biosynthesis genes. *Genome Biol, 3*(5), research0025. doi:10.1186/gb-2002-3-5-research0025

Coronado-Velázquez, D., Betanzos, A., Serrano-Luna, J., & Shibayama, M. (2018). An In Vitro Model of the Blood–Brain Barrier: Naegleria fowleri Affects the Tight Junction Proteins and Activates the Microvascular Endothelial Cells. *Journal of Eukaryotic Microbiology, 65*(6), 804-819.

Correia, I., Alonso-Monge, R., & Pla, J. (2017). The Hog1 MAP kinase promotes the recovery from cell cycle arrest induced by hydrogen peroxide in Candida albicans. *Frontiers in microbiology, 7*, 2133.

Crowley, L. C., Christensen, M. E., & Waterhouse, N. J. (2016). Measuring mitochondrial transmembrane potential by TMRE staining. *Cold Spring Harbor Protocols, 2016*(12), pdb. prot087361.

Crowley, L. C., Marfell, B. J., Scott, A. P., & Waterhouse, N. J. (2016). Quantitation of apoptosis and necrosis by annexin V binding, propidium iodide uptake, and flow cytometry. *Cold Spring Harbor Protocols, 2016*(11), pdb. prot087288.

Dalleau, S., Baradat, M., Gueraud, F., & Huc, L. (2013). Cell death and diseases related to oxidative stress: 4-hydroxynonenal (HNE) in the balance. *Cell death and differentiation, 20*(12), 1615.

Dalton, T. P., Chen, Y., Schneider, S. N., Nebert, D. W., & Shertzer, H. G. (2004). Genetically altered mice to evaluate glutathione homeostasis in health and disease. *Free Radical Biology and Medicine, 37*(10), 1511-1526.

Daneman, R., & Prat, A. (2015). The Blood–Brain Barrier. *Cold Spring Harbor Perspectives in Biology, 7*(1), a020412. doi:10.1101/cshperspect.a020412

Daneman, R., Zhou, L., Agalliu, D., Cahoy, J. D., Kaushal, A., & Barres, B. A. (2010). The mouse blood-brain barrier transcriptome: a new resource for understanding the development and function of brain endothelial cells. *PLoS ONE, 5*(10), e13741.

Deane, Bell, R., Sagare, A., & Zlokovic, B. (2009). Clearance of amyloid-β peptide across the blood-brain barrier: implication for therapies in Alzheimer's disease. *CNS & Neurological Disorders-Drug Targets (Formerly Current Drug Targets-CNS & Neurological Disorders), 8*(1), 16-30.

Deane, Du Yan, S., Submamaryan, R. K., LaRue, B., Jovanovic, S., Hogg, E., *et al.* (2003). RAGE mediates amyloid-β peptide transport across the blood-brain barrier and accumulation in brain. *Nature medicine, 9*(7), 907.

Deane, Sagare, A., & Zlokovic, B. (2008). The role of the cell surface LRP and soluble LRP in blood-brain barrier Aβ clearance in Alzheimer's disease. *Current pharmaceutical design, 14*(16), 1601-1605.

Deane, & Zlokovic, B. V. (2007). Role of the blood-brain barrier in the pathogenesis of Alzheimer's disease. *Curr Alzheimer Res, 4*(2), 191-197.

DeBault, L. E., Kahn, L. E., Frommes, S. P., & Cancilla, P. A. (1979). Cerebral microvessels and derived cells in tissue culture: isolation and preliminary characterization. *In vitro, 15*(7), 473-487.

Del Pino, M. M. S., Hawkins, R. A., & Peterson, D. R. (1995). Biochemical discrimination between luminal and abluminal enzyme and transport activities of the blood-brain barrier. *Journal of Biological Chemistry, 270*(25), 14907-14912.

Dermietzel, R., Spray, D. C., & Nedergaard, M. (2007). *Blood-brain barriers: from ontogeny to artificial interfaces*: John Wiley and Sons.

Deshmukh, P., Unni, S., Krishnappa, G., & Padmanabhan, B. (2017). The Keap1–Nrf2 pathway: promising therapeutic target to counteract ROS-mediated damage in cancers and neurodegenerative diseases. *Biophysical reviews, 9*(1), 41-56.

Dickstein, D. L., Biron, K. E., Ujiie, M., Pfeifer, C. G., Jeffries, A. R., & Jefferies, W. A. (2006). Aβ peptide immunization restores blood-brain barrier integrity in Alzheimer disease. *The FASEB Journal, 20*(3), 426-433.

Dolman, D., Drndarski, S., Abbott, N. J., & Rattray, M. (2005). Induction of aquaporin 1 but not aquaporin 4 messenger RNA in rat primary brain microvessel endothelial cells in culture. *Journal of neurochemistry, 93*(4), 825-833.

Doroshow, J. H., & Juhasz, A. (2019). Modulation of selenium-dependent glutathione peroxidase activity enhances doxorubicin-induced apoptosis, tumour cell killing and hydroxyl radical production in human NCI/ADR-RES cancer cells despite high-level P-glycoprotein expression. *Free radical research, 53*(8), 882-891.

Ehrlich, P. (1885). *Das Sauerstoff-Bedürfniss des Organismus: eine farbenanalytische Studie*: August Hirschwald.

Eisenberg-Lerner, A., & Kimchi, A. (2012). PKD is a kinase of Vps34 that mediates ROS-induced autophagy downstream of DAPk. *Cell death and differentiation, 19*(5), 788.

Elahy, M., Jackaman, C., Mamo, J. C., Lam, V., Dhaliwal, S. S., Giles, C., *et al.* (2015). Blood–brain barrier dysfunction developed during normal aging is associated with inflammation and loss of tight junctions but not with leukocyte recruitment. *Immunity & Ageing, 12*(1), 2.

Erdő, F., Denes, L., & de Lange, E. (2017). Age-associated physiological and pathological changes at the blood–brain barrier: a review. *Journal of Cerebral Blood Flow & Metabolism, 37*(1), 4-24.

Erickson, M. A., & Banks, W. A. (2018). Neuroimmune axes of the blood–brain barriers and blood–brain interfaces: bases for physiological regulation, disease states, and pharmacological interventions. *Pharmacological reviews, 70*(2), 278-314.

Faragher, R. G., & Kipling, D. (1998). How might replicative senescence contribute to human ageing? *Bioessays, 20*(12), 985-991.

Feder, N. (1971). Microperoxidase: An ultrastructural tracer of low molecular weight. *J Cell Biol, 51*(1), 339.

Feno, S., Butera, G., Vecellio Reane, D., Rizzuto, R., & Raffaello, A. (2019). Crosstalk between Calcium and ROS in Pathophysiological Conditions. *Oxidative Medicine and Cellular Longevity, 2019*.

Fenstermacher, J. (1984). Volume regulation of the central nervous system: Edema. New York: Raven Press.

Fernandez-Gil, B. I., Guerra-Librero, A., Shen, Y.-Q., Florido, J., Martínez-Ruiz, L., García-López, S., *et al.* (2019). Melatonin enhances cisplatin and radiation cytotoxicity in head and neck squamous cell carcinoma by stimulating mitochondrial ROS generation, apoptosis, and autophagy. *Oxidative Medicine and Cellular Longevity, 2019*.

Festoff, B. W., Sajja, R. K., van Dreden, P., & Cucullo, L. (2016). HMGB1 and thrombin mediate the blood-brain barrier dysfunction acting as biomarkers of neuroinflammation

and progression to neurodegeneration in Alzheimer's disease. *Journal of neuroinflammation, 13*(1), 194.

Fettiplace, R., & Haydon, D. (1980). Water permeability of lipid membranes. *Physiol Rev, 60*(2), 510-550.

Fischer, R., & Maier, O. (2015). Interrelation of Oxidative Stress and Inflammation in Neurodegenerative Disease: Role of TNF. *Oxidative Medicine and Cellular Longevity, 2015*, 18. doi:10.1155/2015/610813

Fong, C. W. (2015). Permeability of the blood–brain barrier: molecular mechanism of transport of drugs and physiologically important compounds. *The Journal of membrane biology, 248*(4), 651-669.

Forman, H. J. (2016). Glutathione–From antioxidant to post-translational modifier. *Archives of Biochemistry and Biophysics, 595*, 64-67.

Forman, H. J., Maiorino, M., & Ursini, F. (2010). Signaling functions of reactive oxygen species. *Biochemistry, 49*(5), 835-842.

Freeman, L. R., & Keller, J. N. (2012). Oxidative stress and cerebral endothelial cells: regulation of the blood-brain-barrier and antioxidant based interventions. *Biochim Biophys Acta, 1822*(5), 822-829. doi:10.1016/j.bbadis.2011.12.009

Freyssin, A., Page, G., Fauconneau, B., & Bilan, A. R. (2018). Natural polyphenols effects on protein aggregates in Alzheimer's and Parkinson's prion-like diseases. *Neural regeneration research, 13*(6), 955.

Fujikawa, Y., Terakado, K., Nampo, T., Mori, M., & Inoue, H. (2019). 4-Bromo-1, 8-naphthalimide derivatives as fluorogenic substrates for live cell imaging of glutathione S-transferase (GST) activity. *Talanta*.

Galani, V., Varouktsi, A., Papadatos, S. S., Mitselou, A., Sainis, I., Constantopoulos, S., *et al.* (2019). The role of apoptosis defects in malignant mesothelioma pathogenesis with an impact on prognosis and treatment. *Cancer chemotherapy and pharmacology*, 1-13.

Galasko, D. R., Peskind, E., Clark, C. M., Quinn, J. F., Ringman, J. M., Jicha, G. A., *et al.* (2012). Antioxidants for Alzheimer disease: a randomized clinical trial with cerebrospinal fluid biomarker measures. *Archives of neurology, 69*(7), 836-841.

Galluzzi, L., Vitale, I., Aaronson, S. A., Abrams, J. M., Adam, D., Agostinis, P., *et al.* (2018). Molecular mechanisms of cell death: recommendations of the Nomenclature Committee on Cell Death 2018. *Cell Death & Differentiation, 25*(3), 486.

Gangwar, R., Meena, A. S., Shukla, P. K., Nagaraja, A. S., Dorniak, P. L., Pallikuth, S., *et al.* (2017). Calcium-mediated oxidative stress: a common mechanism in tight junction disruption by different types of cellular stress. *Biochemical Journal, 474*(5), 731-749.

Garcia-Castillo, M. D., Chinnapen, D. J.-F., & Lencer, W. I. (2017). Membrane transport across polarized Epithelia. *Cold Spring Harbor Perspectives in Biology*, a027912.

Gastfriend, B. D., Palecek, S. P., & Shusta, E. V. (2018). Modeling the blood–brain barrier: beyond the endothelial cells. *Current opinion in biomedical engineering, 5*, 6-12.

Gille, J., & Joenje, H. (1992). Cell culture models for oxidative stress: superoxide and hydrogen peroxide versus normobaric hyperoxia. *Mutation Research/DNAging, 275*(3-6), 405-414.

Glasauer, A., & Chandel, N. S. (2013). Ros. *Current Biology, 23*(3), R100-R102.

Goldmann, E. E. (1909). *Die äussere und innere skeretion des Gesunden organismus im lichte der" Vitalen Färbung"*: H. Laupp'schen Buchhandlung.

Goldmann, E. E. (1913). Vitalfarbung am zentralnervensystem. *Abhandl Konigl preuss Akad Wiss, 1*, 1-60.

Gooch, J. L., & Yee, D. (1999). Strain-specific differences in formation of apoptotic DNA ladders in MCF-7 breast cancer cells. *Cancer letters, 144*(1), 31-37.

Görlach, A., Bertram, K., Hudecova, S., & Krizanova, O. (2015). Calcium and ROS: a mutual interplay. *Redox Biology, 6*, 260-271.

Gottlieb, E., Armour, S., Harris, M., & Thompson, C. (2003). Mitochondrial membrane potential regulates matrix configuration and cytochrome c release during apoptosis. *Cell death and differentiation, 10*(6), 709.

Gräb, J., & Rybniker, J. (2019). The Expanding Role of p38 Mitogen-Activated Protein Kinase in Programmed Host Cell Death. *Microbiology insights, 12*, 1178636119864594.

Grillo, M. A., Grillo, S. L., Gerdes, B. C., Kraus, J. G., & Koulen, P. (2019). Control of neuronal ryanodine receptor-mediated calcium signaling by calsenilin. *Molecular neurobiology, 56*(1), 525-534.

Guilford, F. T., & Hope, J. (2014). Deficient glutathione in the pathophysiology of mycotoxin-related illness. *Toxins, 6*(2), 608-623.

Gürsoy-Özdemir, Y., & Tas, Y. C. (2017). Anatomy and Physiology of the Blood–Brain Barrier *Nanotechnology Methods for Neurological Diseases and Brain Tumors* (pp. 3-13): Elsevier.

Guzmán, D. C., Brizuela, N. O., Herrera, M. O., Peraza, A. V., Juárez-Olguín, H., & Mejía, G. B. (2019). Insulin plus zinc induces a favorable biochemical response effects on oxidative damage and dopamine levels in rat brain. *International journal of biological macromolecules, 132*, 230-235.

Haddad-Tóvolli, R., Dragano, N. R., Ramalho, A. F., & Velloso, L. A. (2017). Development and function of the blood-brain barrier in the context of metabolic control. *Frontiers in neuroscience, 11*, 224.

Haj-Yasein, N. N., Vindedal, G. F., Eilert-Olsen, M., Gundersen, G. A., Skare, Ø., Laake, P., *et al.* (2011). Glial-conditional deletion of aquaporin-4 (Aqp4) reduces blood–brain water uptake and confers barrier function on perivascular astrocyte endfeet. *Proceedings of the National Academy of Sciences, 108*(43), 17815-17820.

Halliwell, B. (1990). How to characterize a biological antioxidant. *Free radical research communications, 9*(1), 1-32.

Halliwell, B., & Gutteridge, J. M. C. (1995). The definition and measurement of antioxidants in biological systems. *Free Radical Biology and Medicine, 18*(1), 125-126. doi:https://doi.org/10.1016/0891-5849(95)91457-3

Hansen, A. J. (1985). Effect of anoxia on ion distribution in the brain. *Physiol Rev, 65*(1), 101-148. doi:10.1152/physrev.1985.65.1.101

Haorah, J., Knipe, B., Leibhart, J., Ghorpade, A., & Persidsky, Y. (2005). Alcohol-induced oxidative stress in brain endothelial cells causes blood-brain barrier dysfunction. *J Leukoc Biol, 78*(6), 1223-1232.

Haorah, J., Ramirez, S. H., Schall, K., Smith, D., Pandya, R., & Persidsky, Y. (2007). Oxidative stress activates protein tyrosine kinase and matrix metalloproteinases leading to blood–brain barrier dysfunction. *Journal of neurochemistry, 101*(2), 566-576.

Hawkins, R. A., O'kane, R. L., Simpson, I. A., & Vina, J. R. (2006). Structure of the blood–brain barrier and its role in the transport of amino acids. *The Journal of nutrition, 136*(1), 218S-226S.

Helms, H. C., Abbott, N. J., Burek, M., Cecchelli, R., Couraud, P.-O., Deli, M. A., *et al.* (2016). In vitro models of the blood–brain barrier: an overview of commonly used brain endothelial cell culture models and guidelines for their use. *Journal of Cerebral Blood Flow & Metabolism, 36*(5), 862-890.

Hladky, S. B., & Barrand, M. A. (2016). Fluid and ion transfer across the blood–brain and blood–cerebrospinal fluid barriers; a comparative account of mechanisms and roles. *Fluids and Barriers of the CNS, 13*(1), 19.

Hutami, I. R., Tanaka, E., & Izawa, T. (2018). Crosstalk between Fas and S1P1 signaling via NF-kB in osteoclasts controls bone destruction in the TMJ due to rheumatoid arthritis. *Japanese Dental Science Review*.

Ighodaro, O., & Akinloye, O. (2018). First line defence antioxidants-superoxide dismutase (SOD), catalase (CAT) and glutathione peroxidase (GPX): Their fundamental role in the entire antioxidant defence grid. *Alexandria Journal of Medicine, 54*(4), 287-293.

Jacobi, J., Kristal, B., Chezar, J., Shaul, S. M., & Sela, S. (2005). Exogenous superoxide mediates pro-oxidative, proinflammatory, and procoagulatory changes in primary endothelial cell cultures. *Free Radical Biology and Medicine, 39*(9), 1238-1248.

Jeong, S. (2017). Molecular and cellular basis of neurodegeneration in Alzheimer's disease. *Molecules and cells, 40*(9), 613.

Jomova, K., Vondrakova, D., Lawson, M., & Valko, M. (2010). Metals, oxidative stress and neurodegenerative disorders. *Molecular and cellular biochemistry, 345*(1-2), 91-104.

Kaisar, M. A., Sajja, R. K., Prasad, S., Abhyankar, V. V., Liles, T., & Cucullo, L. (2017). New experimental models of the blood-brain barrier for CNS drug discovery. *Expert opinion on drug discovery, 12*(1), 89-103.

Kalsi, K. K., Garnett, J. P., Patkee, W., Weekes, A., Dockrell, M. E., Baker, E. H.*, et al.* (2019). Metformin attenuates the effect of Staphylococcus aureus on airway tight junctions by increasing PKC ζ-mediated phosphorylation of occludin. *Journal of cellular and molecular medicine, 23*(1), 317-327.

Kamer, K. J., & Mootha, V. K. (2015). The molecular era of the mitochondrial calcium uniporter. *Nature Reviews Molecular Cell Biology, 16*(9), 545-553.

Karnovsky, M. J. (1967). The ultrastructural basis of capillary permeability studied with peroxidase as a tracer. *J Cell Biol, 35*(1), 213-236.

Kasner, S. E., & Sacco, R. L. (2013). Updating the Definition of Stroke: Seeing the Forest and the Trees.

Kawamura, K., Qi, F., & Kobayashi, J. (2018). Potential relationship between the biological effects of low-dose irradiation and mitochondrial ROS production. *Journal of radiation research, 59*(suppl_2), ii91-ii97.

Kazaks, A., Collier, M., & Conley, M. (2019). Cytotoxicity of Caffeine on MCF-7 Cells Measured by XTT Cell Proliferation Assay (P06-038-19): Oxford University Press.

Kidger, A. M., & Keyse, S. M. (2016). *The regulation of oncogenic Ras/ERK signalling by dual-specificity mitogen activated protein kinase phosphatases (MKPs).* Paper presented at the Seminars in Cell & Developmental Biology.

Kiess, T.-O., & Kockskämper, J. (2019). SERCA activity controls the systolic calcium increase in the nucleus of cardiac myocytes. *Frontiers in physiology, 10*.

Kim, Choi, T. G., Park, S., Yun, H. R., Nguyen, N. N. Y., Jo, Y. H.*, et al.* (2018). Mitochondrial ROS-derived PTEN oxidation activates PI3K pathway for mTOR-induced myogenic autophagy. *Cell Death & Differentiation, 25*(11), 1921.

Kim, Chung, J., Chung, S. M., Kwag, N. H., & Yoo, J. S. (2003). Hydrogen peroxide-induced cell death in a human retinal pigment epithelial cell line, ARPE-19. *Korean Journal of Ophthalmology, 17*(1), 19-28.

Kim, Kim, J. E., Rhie, S. J., & Yoon, S. (2015). The Role of Oxidative Stress in Neurodegenerative Diseases. *Exp Neurobiol, 24*(4), 325-340.

Konior, A., Schramm, A., Czesnikiewicz-Guzik, M., & Guzik, T. J. (2014). NADPH oxidases in vascular pathology. *Antioxidants & Redox Signaling, 20*(17), 2794-2814.

Konishi, H., Tanaka, M., Takemura, Y., Matsuzaki, H., Ono, Y., Kikkawa, U.*, et al.* (1997). Activation of protein kinase C by tyrosine phosphorylation in response to H2O2. *Proceedings of the National Academy of Sciences, 94*(21), 11233-11237.

Kranner, I., Birtić, S., Anderson, K. M., & Pritchard, H. W. (2006). Glutathione half-cell reduction potential: a universal stress marker and modulator of programmed cell death? *Free Radical Biology and Medicine, 40*(12), 2155-2165.

Krizbai, I. A., Bauer, H., Bresgen, N., Eckl, P. M., Farkas, A., Szatmari, E*., et al.* (2005). Effect of oxidative stress on the junctional proteins of cultured cerebral endothelial cells. *Cell Mol Neurobiol, 25*(1), 129-139.

Kruk, J. S., Vasefi, M. S., Heikkila, J. J., & Beazely, M. A. (2013). Reactive oxygen species are required for 5-HT-induced transactivation of neuronal platelet-derived growth factor and TrkB receptors, but not for ERK1/2 activation. *PLoS ONE, 8*(9), e77027.

Krzyzowska-Gruca, C. (1966). Histochemical studies on the localization of intravenously injected peroxidase in the rat brain. *Folia Histochem Cytochem, 4*, 205-210.

Lasbennes, F., & Gayet, J. (1984). Capacity for energy metabolism in microvessels isolated from rat brain. *Neurochemical research, 9*(1), 1-10.

Lee, Chen, M., & Pandolfi, P. P. (2018). The functions and regulation of the PTEN tumour suppressor: new modes and prospects. *Nature Reviews Molecular Cell Biology, 19*(9), 547.

Lee, & Loscalzo, J. (2020). Systems biology and network medicine: An integrated approach to redox biology and pathobiology *Oxidative Stress* (pp. 29-49): Elsevier.

Letts, J. A., & Sazanov, L. A. (2017). Clarifying the supercomplex: the higher-order organization of the mitochondrial electron transport chain. *Nature structural & molecular biology, 24*(10), 800.

Levental, K. R., & Levental, I. (2019). Homeoviscous Adaptation in Mammalian Cell Membranes in Response to Dietary Lipid Perturbations. *Biophysical Journal, 116*(3), 20a.

Levites, Y., Amit, T., Youdim, M. B., & Mandel, S. (2002). Involvement of protein kinase C activation and cell survival/cell cycle genes in green tea polyphenol,(-)-epigallocatechin-3-gallate neuroprotective action. *Journal of Biological Chemistry*.

Lewandowsky, M. (1900). Zur lehre von der cerebrospinalflussigkeit. *Z klin Med, 40*(480), 19.

Lewis, R. S. (2019). Store-Operated Calcium Channels: From Function to Structure and Back Again. *Cold Spring Harbor Perspectives in Biology*, a035055.

Li, W., Busu, C., Circu, M. L., & Aw, T. Y. (2012). Glutathione in cerebral microvascular endothelial biology and pathobiology: implications for brain homeostasis. *Int J Cell Biol, 2012*, 434971. doi:10.1155/2012/434971

Liebner, S., Dijkhuizen, R. M., Reiss, Y., Plate, K. H., Agalliu, D., & Constantin, G. (2018). Functional morphology of the blood–brain barrier in health and disease. *Acta Neuropathologica, 135*(3), 311-336. doi:10.1007/s00401-018-1815-1

Lin, B., Xu, J., Feng, D.-G., Wang, F., Wang, J.-X., & Zhao, H. (2018). DUSP14 knockout accelerates cardiac ischemia reperfusion (IR) injury through activating NF-κB and MAPKs signaling pathways modulated by ROS generation. *Biochemical and Biophysical Research Communications, 501*(1), 24-32.

Lu, S. C. (2009). Regulation of glutathione synthesis. *Molecular Aspects of Medicine, 30*(1-2), 42-59.

Lu, S. C. (2013). Glutathione synthesis. *Biochimica et Biophysica Acta (BBA)-General Subjects, 1830*(5), 3143-3153.

Luo, T., & Xia, Z. (2006). A small dose of hydrogen peroxide enhances tumor necrosis factor-alpha toxicity in inducing human vascular endothelial cell apoptosis: reversal with propofol. *Anesthesia & Analgesia, 103*(1), 110-116.

Lushchak. (2014). Free radicals, reactive oxygen species, oxidative stress and its classification. *Chemico-Biological Interactions, 224*, 164-175.

Lushchak, Semchyshyn, H., Lushchak, O., & Mandryk, S. (2005). Diethyldithiocarbamate inhibits in vivo Cu, Zn-superoxide dismutase and perturbs free radical processes in the yeast Saccharomyces cerevisiae cells. *Biochemical and Biophysical Research Communications, 338*(4), 1739-1744.

Ly, J. D., Grubb, D. R., & Lawen, A. (2003). The mitochondrial membrane potential (Δψ m) in apoptosis; an update. *Apoptosis, 8*(2), 115-128.

MacAulay, N., & Zeuthen, T. (2010). Water transport between CNS compartments: contributions of aquaporins and cotransporters. *Neuroscience, 168*(4), 941-956.

Madonna, R., Novo, G., & Balistreri, C. R. (2016). Cellular and molecular basis of the imbalance between vascular damage and repair in ageing and age-related diseases: as biomarkers and targets for new treatments. *Mechanisms of ageing and development, 159*, 22-30.

Mann, G. E., Yudilevich, D. L., & Sobrevia, L. (2003). Regulation of amino acid and glucose transporters in endothelial and smooth muscle cells. *Physiol Rev, 83*(1), 183-252.

Marcén, M., Cebrián, G., Ruiz-Artiga, V., Condón, S., & Mañas, P. (2019). Protective effect of glutathione on Escherichia coli cells upon lethal heat stress. *Food Research International, 121*, 806-811.

Marchi, S., & Pinton, P. (2016). Alterations of calcium homeostasis in cancer cells. *Current opinion in pharmacology, 29*, 1-6.

Marengo, B., Nitti, M., Furfaro, A. L., Colla, R., Ciucis, C. D., Marinari, U. M*., et al.* (2016). Redox homeostasis and cellular antioxidant systems: crucial players in cancer growth and therapy. *Oxidative Medicine and Cellular Longevity, 2016*.

Markovic, Borras, C., Ortega, A., Sastre, J., Vina, J., & Pallardo, F. V. (2007). Glutathione is recruited into the nucleus in early phases of cell proliferation. *J Biol Chem, 282*(28), 20416-20424. doi:10.1074/jbc.M609582200

Markovic, Mora, N. J., Broseta, A. M., Gimeno, A., de-la-Concepción, N., Viña, J*., et al.* (2009). The Depletion of Nuclear Glutathione Impairs Cell Proliferation in 3t3 Fibroblasts. *PLoS ONE, 4*(7), e6413. doi:10.1371/journal.pone.0006413

Martin, S., Reutelingsperger, C., McGahon, A. J., Rader, J. A., Van Schie, R., LaFace, D. M*., et al.* (1995). Early redistribution of plasma membrane phosphatidylserine is a general feature of apoptosis regardless of the initiating stimulus: inhibition by overexpression of Bcl-2 and Abl. *Journal of Experimental Medicine, 182*(5), 1545-1556.

Martinc, B., Grabnar, I., & Vovk, T. (2014). Antioxidants as a preventive treatment for epileptic process: a review of the current status. *Current neuropharmacology, 12*(6), 527-550.

Maryanovich, M., & Gross, A. (2013). A ROS rheostat for cell fate regulation. *Trends in cell biology, 23*(3), 129-134.

Mecocci, P., & Polidori, M. C. (2012). Antioxidant clinical trials in mild cognitive impairment and Alzheimer's disease. *Biochimica et Biophysica Acta (BBA)-Molecular Basis of Disease, 1822*(5), 631-638.

Meister, A. (1988). On the discovery of glutathione. *Trends Biochem Sci, 13*(5), 185-188. doi:10.1016/0968-0004(88)90148-x

Mentor, S., & Fisher, D. (2017). Aggressive antioxidant reductive stress impairs brain endothelial cell angiogenesis and blood brain barrier function. *Current neurovascular research, 14*(1), 71-81.

Mirończuk-Chodakowska, I., Witkowska, A. M., & Zujko, M. E. (2018). Endogenous non-enzymatic antioxidants in the human body. *Advances in medical sciences, 63*(1), 68-78.

Montagne, A., Barnes, S. R., Sweeney, M. D., Halliday, M. R., Sagare, A. P., Zhao, Z.*, et al.* (2015). Blood-brain barrier breakdown in the aging human hippocampus. *Neuron, 85*(2), 296-302.

Montagne, A., Zhao, Z., & Zlokovic, B. V. (2017). Alzheimer's disease: A matter of blood–brain barrier dysfunction? *Journal of Experimental Medicine, 214*(11), 3151-3169.

Montesano, R., Pepper, M., Möhle-Steinlein, U., Risau, W., Wagner, E., & Orci, L. (1990). Increased proteolytic activity is responsible for the aberrant morphogenetic behavior of endothelial cells expressing the middle T oncogene. *Cell, 62*(3), 435-445.

Montezano, A. C., De Lucca Camargo, L., Persson, P., Rios, F. J., Harvey, A. P., Anagnostopoulou, A.*, et al.* (2018). NADPH oxidase 5 is a pro-contractile Nox isoform and a point of cross-talk for calcium and redox signaling-implications in vascular function. *Journal of the American Heart Association, 7*(12), e009388.

Morris, D., Guerra, C., Khurasany, M., Guilford, F., Saviola, B., Huang, Y.*, et al.* (2013). Glutathione supplementation improves macrophage functions in HIV. *Journal of Interferon & Cytokine Research, 33*(5), 270-279.

Muri, J., Thut, H., Heer, S., Krueger, C. C., Bornkamm, G. W., Bachmann, M. F.*, et al.* (2019). The thioredoxin-1 and glutathione/glutaredoxin-1 systems redundantly fuel murine B-cell development and responses. *Eur J Immunol, 49*(5), 709-723.

Murray, C. J., Vos, T., Lozano, R., Naghavi, M., Flaxman, A. D., Michaud, C.*, et al.* (2012). Disability-adjusted life years (DALYs) for 291 diseases and injuries in 21 regions, 1990–2010: a systematic analysis for the Global Burden of Disease Study 2010. *The Lancet, 380*(9859), 2197-2223.

Nag, S., & David J, B. (2005). Blood Brain Barrier, Exchange of metabolites and gases (pp. 22-29). Basel: ISN Neuropath Press.

Nakagawa, S., Deli, M. A., Kawaguchi, H., Shimizudani, T., Shimono, T., Kittel, A.*, et al.* (2009). A new blood–brain barrier model using primary rat brain endothelial cells, pericytes and astrocytes. *Neurochemistry international, 54*(3-4), 253-263.

Nation, D. A., Sweeney, M. D., Montagne, A., Sagare, A. P., D'Orazio, L. M., Pachicano, M.*, et al.* (2019). Blood–brain barrier breakdown is an early biomarker of human cognitive dysfunction. *Nature medicine, 25*(2), 270.

Nguyen, L. N., Ma, D., Shui, G., Wong, P., Cazenave-Gassiot, A., Zhang, X.*, et al.* (2014). Mfsd2a is a transporter for the essential omega-3 fatty acid docosahexaenoic acid. *Nature, 509*(7501), 503.

Nič, M., Jirát, J., Košata, B., Jenkins, A., & McNaught, A. (2009). IUPAC compendium of chemical terminology. *IUPAC, Research Triangle Park, NC*.

Niedzwiecka, K., Tisi, R., Penna, S., Lichocka, M., Plochocka, D., & Kucharczyk, R. (2018). Two mutations in mitochondrial ATP6 gene of ATP synthase, related to human cancer, affect ROS, calcium homeostasis and mitochondrial permeability transition in yeast. *Biochimica et Biophysica Acta (BBA)-Molecular Cell Research, 1865*(1), 117-131.

Niki, E., & Noguchi, N. (2004). Dynamics of antioxidant action of vitamin E. *Accounts of Chemical Research, 37*(1), 45-51.

Nischwitz, V., Berthele, A., & Michalke, B. (2008). Speciation analysis of selected metals and determination of their total contents in paired serum and cerebrospinal fluid samples: An approach to investigate the permeability of the human blood-cerebrospinal fluid-barrier. *Anal Chim Acta, 627*(2), 258-269. doi:10.1016/j.aca.2008.08.018

Nissanka, N., & Moraes, C. T. (2018). Mitochondrial DNA damage and reactive oxygen species in neurodegenerative disease. *FEBS letters, 592*(5), 728-742.

Noell, S., Wolburg-Buchholz, K., Mack, A. F., Beedle, A. M., Satz, J. S., Campbell, K. P.*, et al.* (2011). Evidence for a role of dystroglycan regulating the membrane architecture of astroglial endfeet. *European Journal of Neuroscience, 33*(12), 2179-2186.

Oh, W. Y., & Shahidi, F. (2018). Antioxidant activity of resveratrol ester derivatives in food and biological model systems. *Food chemistry, 261*, 267-273.

Okouchi, M., Okayama, N., & Aw, T. Y. (2009). Preservation of cellular glutathione status and mitochondrial membrane potential by N-acetylcysteine and insulin sensitizers prevent carbonyl stress-induced human brain endothelial cell apoptosis. *Current neurovascular research, 6*(4), 267-278.

Ondarza, R. N., Iturbe, A., Hurtado, G., Tamayo, E., Ondarza, M., & Hernandez, E. (1999). Entamoeba histolytica: a eukaryote with trypanothione metabolism instead of glutathione metabolism. *Biotechnology and applied biochemistry, 30*(1), 47-52.

Oubrahim, H., Stadtman, E. R., & Chock, P. B. (2001). Mitochondria play no roles in Mn (II)-induced apoptosis in HeLa cells. *Proceedings of the National Academy of Sciences, 98*(17), 9505-9510.

Paloczi, J., Varga, Z. V., Hasko, G., & Pacher, P. (2018). Neuroprotection in Oxidative Stress-Related Neurodegenerative Diseases: Role of Endocannabinoid System Modulation. *Antioxid Redox Signal, 29*(1), 75-108. doi:10.1089/ars.2017.7144

Pan, T., Fei, J., Zhou, X., Jankovic, J., & Le, W. (2003). Effects of green tea polyphenols on dopamine uptake and on MPP+-induced dopamine neuron injury. *Life Sciences, 72*(9), 1073-1083.

Panahi, G., Pasalar, P., Zare, M., Rizzuto, R., & Meshkani, R. (2018). High glucose induces inflammatory responses in HepG2 cells via the oxidative stress-mediated activation of NF-κB, and MAPK pathways in HepG2 cells. *Archives of physiology and biochemistry, 124*(5), 468-474.

Pandey, P., Sayyed, U., Tiwari, R. K., Siddiqui, M. H., Pathak, N., & Bajpai, P. (2019). Hesperidin Induces ROS-Mediated Apoptosis along with Cell Cycle Arrest at G2/M Phase in Human Gall Bladder Carcinoma. *Nutrition and cancer, 71*(4), 676-687.

Pardridge, W. M. (1993). Transport of Insulin-Related Peptides and Glucose across the Blood-Brain Barrier a. *Annals of the New York Academy of Sciences, 692*(1), 126-137.

Pardridge, W. M. (1998). *Isolated brain capillaries: an in vitro model of blood-brain barrier research*: University Press, Cambridge.

Pardridge, W. M. (1999). Blood-brain barrier biology and methodology. *Journal of neurovirology, 5*(6), 556-569.

Park. (2013). The effects of exogenous H2O2 on cell death, reactive oxygen species and glutathione levels in calf pulmonary artery and human umbilical vein endothelial cells. *International Journal of Molecular Medicine, 31*(2), 471-476.

Park, & Suh, B.-C. (2018). Modulation mechanisms of voltage-gated calcium channels. *Current Opinion in Physiology, 2*, 77-83.

Patching, S. G. (2017). Glucose transporters at the blood-brain barrier: function, regulation and gateways for drug delivery. *Molecular neurobiology, 54*(2), 1046-1077.

Paulson, O. B., Hasselbalch, S. G., Rostrup, E., Knudsen, G. M., & Pelligrino, D. (2010). Cerebral blood flow response to functional activation. *Journal of Cerebral Blood Flow & Metabolism, 30*(1), 2-14.

Pophaly, S., Poonam, S., Pophaly, S., Kapila, S., Nanda, D., Tomar, S*., et al.* (2017). Glutathione biosynthesis and activity of dependent enzymes in food-grade lactic acid bacteria harbouring multidomain bifunctional fusion gene (gshF). *Journal of applied microbiology, 123*(1), 194-203.

Raffaello, A., Mammucari, C., Gherardi, G., & Rizzuto, R. (2016). Calcium at the center of cell signaling: interplay between endoplasmic reticulum, mitochondria, and lysosomes. *Trends in biochemical sciences, 41*(12), 1035-1049.

Raghunath, A., Sundarraj, K., Nagarajan, R., Arfuso, F., Bian, J., Kumar, A. P*., et al.* (2018). Antioxidant response elements: discovery, classes, regulation and potential applications. *Redox Biology, 17*, 297-314.

Rakkar, K., & Bayraktutan, U. (2016). Increases in intracellular calcium perturb blood–brain barrier via protein kinase C-alpha and apoptosis. *Biochimica et Biophysica Acta (BBA)-Molecular Basis of Disease, 1862*(1), 56-71.

Ramassamy, C. (2006). Emerging role of polyphenolic compounds in the treatment of neurodegenerative diseases: a review of their intracellular targets. *European journal of pharmacology, 545*(1), 51-64.

Rao, P. C., Begum, S., Sahai, M., & Sriram, D. S. (2017). Coptisine-induced cell cycle arrest at G2/M phase and reactive oxygen species–dependent mitochondria-mediated apoptosis in non-small-cell lung cancer A549 cells. *Tumor Biology, 39*(3), 1010428317694565.

Reese, T., & Karnovsky, M. J. (1967). Fine structural localization of a blood-brain barrier to exogenous peroxidase. *J Cell Biol, 34*(1), 207-217.

Reiss, Y., Hoch, G., Deutsch, U., & Engelhardt, B. (1998). T cell interaction with ICAM-1-deficient endothelium in vitro: essential role for ICAM-1 and ICAM-2 in transendothelial migration of T cells. *Eur J Immunol, 28*(10), 3086-3099. doi:10.1002/(sici)1521-4141(199810)28:10<3086::aid-immu3086>3.0.co;2-z

Reyskens, K. M., & Essop, M. F. (2014). HIV protease inhibitors and onset of cardiovascular diseases: A central role for oxidative stress and dysregulation of the ubiquitin–proteasome system. *Biochimica et Biophysica Acta (BBA)-Molecular Basis of Disease, 1842*(2), 256-268.

Ribatti, D., Nico, B., Crivellato, E., & Artico, M. (2006). Development of the blood-brain barrier: A historical point of view. *The Anatomical Record, 289*(1), 3-8.

Rodríguez-Morató, J., Boronat, A., Dierssen, M., & de la Torre, R. (2018). Neuroprotective properties of wine: Implications for the prevention of cognitive impairment *Role of the Mediterranean Diet in the Brain and Neurodegenerative Diseases* (pp. 271-284): Elsevier.

Rosenberg, G. A. (2012). Neurological diseases in relation to the blood–brain barrier. *Journal of Cerebral Blood Flow & Metabolism, 32*(7), 1139-1151.

Ryter, S. W., Kim, H. P., Hoetzel, A., Park, J. W., Nakahira, K., Wang, X*., et al.* (2007). Mechanisms of cell death in oxidative stress. *Antioxid Redox Signal, 9*(1), 49-89. doi:10.1089/ars.2007.9.49

Sakaki, J., Melough, M., Lee, S. G., Pounis, G., & Chun, O. K. (2019). Polyphenol-Rich Diets in Cardiovascular Disease Prevention *Analysis in Nutrition Research* (pp. 259-298): Elsevier.

Salvi, A., Patki, G., Khan, E., Asghar, M., & Salim, S. (2016). Protective effect of tempol on buthionine sulfoximine-induced mitochondrial impairment in hippocampal derived HT22 cells. *Oxidative Medicine and Cellular Longevity, 2016*.

Samieri, C. (2018). Epidemiology and Risk Factors of Alzheimer's Disease: A Focus on Diet *Biomarkers for Preclinical Alzheimer's Disease* (pp. 15-42): Springer.

Sánchez, G., Fernández, C., Montecinos, L., Domenech, R. J., & Donoso, P. (2011). Preconditioning tachycardia decreases the activity of the mitochondrial permeability transition pore in the dog heart. *Biochemical and Biophysical Research Communications, 410*(4), 916-921.

Sandberg, R., Yasuda, R., Pankratz, D. G., Carter, T. A., Del Rio, J. A., Wodicka, L*., et al.* (2000). Regional and strain-specific gene expression mapping in the adult mouse brain. *Proceedings of the National Academy of Sciences, 97*(20), 11038-11043.

Santa-Gonzalez, G. A., Gomez-Molina, A., Arcos-Burgos, M., Meyer, J. N., & Camargo, M. (2016). Distinctive adaptive response to repeated exposure to hydrogen peroxide associated with upregulation of DNA repair genes and cell cycle arrest. *Redox Biology, 9*, 124-133.

Saraiva, C., Praça, C., Ferreira, R., Santos, T., Ferreira, L., & Bernardino, L. (2016). Nanoparticle-mediated brain drug delivery: overcoming blood–brain barrier to treat neurodegenerative diseases. *Journal of Controlled Release, 235*, 34-47.

Scherer, C., Cristofanon, S., Dicato, M., & Diederich, M. (2008). Homogeneous Luminescence-Based Assay for Quantifying the Glutathione Content in Mammalian Cells. *EDITOR'S DESK*.

Schielke, G. P., Moises, H. C., & Betz, A. L. (1990). Potassium activation of the Na, K-pump in isolated brain microvessels and synaptosomes. *Brain research, 524*(2), 291-296.

Schönfeld, P., & Reiser, G. (2019). Energy Metabolism of Neural Cells Under the Control of Phospholipases A2 and Docosahexaenoic Acid *Omega Fatty Acids in Brain and Neurological Health* (pp. 131-141): Elsevier.

Schröder, K. (2019). NADPH oxidase-derived reactive oxygen species: Dosis facit venenum. *Experimental physiology, 104*(4), 447-452.

Segref, A., Kevei, E., Pokrzywa, W., Schmeisser, K., Mansfeld, J., Livnat-Levanon, N.*, et al.* (2014). Pathogenesis of human mitochondrial diseases is modulated by reduced activity of the ubiquitin/proteasome system. *Cell metabolism, 19*(4), 642-652.

Sena-Lopes, Â., das Neves, R. N., Alves, M. S. D., Perin, G., Alves, D., Casaril, A. M.*, et al.* (2019). Quinolines-1, 2, 3-triazolylcarboxamides exhibits antiparasitic activity in Trichomonas vaginalis. *Biotechnology Research and Innovation*.

Senejani, A. G., Magrino, J. M., Marston, A., Gregoire, M., & Dinh, K. D. (2019). Menadione Induces DNA Damage and Superoxide Radical Level In HEK293 Cells. *Cell Biology, 7*(2), 14.

Serlin, Y., Shelef, I., Knyazer, B., & Friedman, A. (2015). *Anatomy and physiology of the blood–brain barrier.* Paper presented at the Seminars in Cell & Developmental Biology.

Shen, T., Li, H.-Z., Li, A.-L., Li, Y.-R., Wang, X.-N., & Ren, D.-M. (2018). Homoeriodictyol protects human endothelial cells against oxidative insults through activation of Nrf2 and inhibition of mitochondrial dysfunction. *Vascular pharmacology, 109*, 72-82.

Shendge, A., Chaudhuri, D., Basu, T., & Mandal, N. (2020). A natural flavonoid, apigenin isolated from Clerodendrum viscosum leaves, induces G2/M phase cell cycle arrest and apoptosis in MCF-7 cells through the regulation of p53 and caspase-cascade pathway. *Clinical and Translational Oncology*, 1-13.

Shepro, D., & Morel, N. (1993). Pericyte physiology. *The FASEB Journal, 7*(11), 1031-1038.

Shidara, K., Mohan, G., Lay, Y.-A. E., Jepsen, K. J., Yao, W., & Lane, N. E. (2019). Strain-specific differences in the development of bone loss and incidence of osteonecrosis following glucocorticoid treatment in two different mouse strains. *Journal of orthopaedic translation, 16*, 91-101.

Shigetomi, K., & Ikenouchi, J. (2017). Regulation of the epithelial barrier by post-translational modifications of tight junction membrane proteins. *The Journal of Biochemistry, 163*(4), 265-272.

Shlomovitz, I., Zargarian, S., Erlich, Z., Edry-Botzer, L., & Gerlic, M. (2018). Distinguishing Necroptosis from Apoptosis *Programmed Necrosis* (pp. 35-51): Springer.

Shokouhi, S., Claassen, D., Kang, H., Ding, Z., Rogers, B., Mishra, A.*, et al.* (2013). Longitudinal Progression of Cognitive Decline Correlates with Changes in the Spatial Pattern of Brain 18F-FDG PET. *Journal of Nuclear Medicine, 54*(9), 1564-1569. doi:10.2967/jnumed.112.116137

Sies, H. (1999). Glutathione and its role in cellular functions. *Free Radical Biology and Medicine, 27*(9-10), 916-921.

Sies, H., Berndt, C., & Jones, D. P. (2017). Oxidative Stress. *Annual Review of Biochemistry, 86*(1), 715-748. doi:10.1146/annurev-biochem-061516-045037

Silva-Islas, C. A., & Maldonado, P. D. (2018). Canonical and non-canonical mechanisms of Nrf2 activation. *Pharmacological research, 134*, 92-99.

Simoni, R. D., Hill, R. L., & Vaughan, M. (2002). The discovery of glutathione by F. Gowland Hopkins and the beginning of biochemistry at Cambridge University. *Journal of Biological Chemistry, 277*(24), e13-e13.

Sinclair, J. L., Barnes-Davies, M., Kopp-Scheinpflug, C., & Forsythe, I. D. (2017). Strain-specific differences in the development of neuronal excitability in the mouse.

Singh, N., & Ghosh, K. K. (2019). Recent Advances in the Antioxidant Therapies for Alzheimer's Disease: Emphasis on Natural Antioxidants *Pathology, Prevention and Therapeutics of Neurodegenerative Disease* (pp. 253-263): Springer.

Smith, R. L., Tan, J. M., Jonker, M. J., Jongejan, A., Buissink, T., Veldhuijzen, S*., et al.* (2017). Beyond the polymerase-γ theory: Production of ROS as a mode of NRTI-induced mitochondrial toxicity. *PLoS ONE, 12*(11), e0187424.

So, K.-Y., Kim, S.-H., Jung, K.-T., Lee, H.-Y., & Oh, S.-H. (2017). MAPK/JNK1 activation protects cells against cadmium-induced autophagic cell death via differential regulation of catalase and heme oxygenase-1 in oral cancer cells. *Toxicology and applied pharmacology, 332*, 81-91.

Someya, E., Akagawa, M., Mori, A., Morita, A., Yui, N., Asano, D*., et al.* (2019). Role of Neuron–Glia Signaling in Regulation of Retinal Vascular Tone in Rats. *International journal of molecular sciences, 20*(8), 1952.

Song, J., Kang, S. M., Lee, W. T., Park, K. A., Lee, K. M., & Lee, J. E. (2014). Glutathione protects brain endothelial cells from hydrogen peroxide-induced oxidative stress by increasing nrf2 expression. *Exp Neurobiol, 23*(1), 93-103. doi:10.5607/en.2014.23.1.93

Sorokin, L. (2010). The impact of the extracellular matrix on inflammation. *Nature Reviews Immunology, 10*(10), 712.

Stevenson, D., Wokosin, D., Girkin, J., & Grant, M. (2002). Measurement of the intracellular distribution of reduced glutathione in cultured rat hepatocytes using monochlorobimane and confocal laser scanning microscopy. *Toxicology in vitro, 16*(5), 609-619.

Strober, W. (1997). Trypan blue exclusion test of cell viability. *Curr Protoc Immunol, 21*(1), A. 3B. 1-A. 3B. 2.

Strober, W. (2015). Trypan blue exclusion test of cell viability. *Curr Protoc Immunol, 111*(1), A3. B. 1-A3. B. 3.

Su, X., Ditlev, J. A., Hui, E., Xing, W., Banjade, S., Okrut, J*., et al.* (2016). Phase separation of signaling molecules promotes T cell receptor signal transduction. *Science, 352*(6285), 595-599.

Sun, Guo, Y., Fu, X., Wang, Y., Liu, Y., Huo, B*., et al.* (2016). Dendrobium candidum inhibits MCF-7 cells proliferation by inducing cell cycle arrest at G2/M phase and regulating key biomarkers. *OncoTargets and therapy, 9*, 21.

Sun, Yau, H.-Y., Wong, W.-Y., Li, R. A., Huang, Y., & Yao, X. (2012). Role of TRPM2 in H2O2-induced cell apoptosis in endothelial cells. *PLoS ONE, 7*(8), e43186.

Surh, Y.-J. (2004). Transcription factors in the cellular signaling network as prime targets of chemopreventive phytochemicals. *Cancer research and treatment: official journal of Korean Cancer Association, 36*(5), 275.

Sweeney, M. D., Sagare, A. P., & Zlokovic, B. V. (2018). Blood–brain barrier breakdown in Alzheimer disease and other neurodegenerative disorders. *Nature Reviews Neurology, 14*, 133. doi:10.1038/nrneurol.2017.188

Takagi, S., Ehara, K., & Finn, R. D. (1987). Water extraction fraction and permeability-surface product after intravenous injection in rats. *Stroke, 18*(1), 177-183.

Takeda, S., Sato, N., & Morishita, R. (2014). Systemic inflammation, blood-brain barrier vulnerability and cognitive/non-cognitive symptoms in Alzheimer disease: relevance to pathogenesis and therapy. *Frontiers in aging neuroscience, 6*, 171.

Thapa, N., Horn, H. T., & Anderson, R. A. (2019). Phosphoinositide spatially free AKT/PKB activation to all membrane compartments. *Advances in biological regulation*.

Tietze, F. (1969). Enzymic method for quantitative determination of nanogram amounts of total and oxidized glutathione: applications to mammalian blood and other tissues. *Anal Biochem, 27*(3), 502-522.

Tramutola, A., Lanzillotta, C., Perluigi, M., & Butterfield, D. A. (2017). Oxidative stress, protein modification and Alzheimer disease. *Brain Research Bulletin, 133*, 88-96. doi:https://doi.org/10.1016/j.brainresbull.2016.06.005

Tzeng, H.-P., Yang, T.-H., Wu, C.-T., Chiu, H.-C., Liu, S.-H., & Lan, K.-C. (2019). Benzo [a] pyrene alters vascular function in rat aortas ex vivo and in vivo. *Vascular pharmacology*, 106578.

Van Itallie, C. M., & Anderson, J. M. (2018). Phosphorylation of tight junction transmembrane proteins: many sites, much to do. *Tissue barriers, 6*(1), e1382671.

Viswanathan, B., & Razul, M. S. G. (2020). A Method for Teaching How to Balance Redox Reactions by Building Up Molecules. *World Journal of Chemical Education, 8*(2), 67-70.

Wang, Branicky, R., Noë, A., & Hekimi, S. (2018). Superoxide dismutases: dual roles in controlling ROS damage and regulating ROS signaling. *J Cell Biol, 217*(6), 1915-1928.

Wang, Wang, W., Li, L., Perry, G., Lee, H.-g., & Zhu, X. (2014). Oxidative stress and mitochondrial dysfunction in Alzheimer's disease. *Biochimica et Biophysica Acta (BBA) - Molecular Basis of Disease, 1842*(8), 1240-1247. doi:https://doi.org/10.1016/j.bbadis.2013.10.015

Weiss, N., Miller, F., Cazaubon, S., & Couraud, P.-O. (2009). The blood-brain barrier in brain homeostasis and neurological diseases. *Biochimica et Biophysica Acta (BBA)-Biomembranes, 1788*(4), 842-857.

Wentworth, C. C., Alam, A., Jones, R. M., Nusrat, A., & Neish, A. S. (2011). Enteric commensal bacteria induce extracellular signal-regulated kinase pathway signaling via formyl peptide receptor-dependent redox modulation of dual specific phosphatase 3. *Journal of Biological Chemistry, 286*(44), 38448-38455.

Westergaard, E. (1977). The blood-brain barrier to horseradish peroxidase under normal and experimental conditions. *Acta Neuropathologica, 39*(3), 181-187.

Wilhelm, I., Fazakas, C., & Krizbai, I. A. (2011). In vitro models of the blood-brain barrier. *Acta Neurobiol Exp (Wars), 71*(1), 113-128.

Williams, R. L., Risau, W., Zerwes, H.-G., Drexler, H., Aguzzi, A., & Wagner, E. F. (1989). Endothelioma cells expressing the polyoma middle T oncogene induce hemangiomas by host cell recruitment. *Cell, 57*(6), 1053-1063.

Winterbourn, C. C. (2019). Regulation of intracellular glutathione. *Redox Biology, 22*.

Wolburg, H., Noell, S., Mack, A., Wolburg-Buchholz, K., & Fallier-Becker, P. (2009). Brain endothelial cells and the glio-vascular complex. *Cell and tissue research, 335*(1), 75-96.

Wolburg, H., Wolburg-Buchholz, K., Fallier-Becker, P., Noell, S., & Mack, A. F. (2011). Structure and functions of aquaporin-4-based orthogonal arrays of particles *International review of cell and molecular biology* (Vol. 287, pp. 1-41): Elsevier.

Wu, Fang, Y.-Z., Yang, S., Lupton, J. R., & Turner, N. D. (2004). Glutathione metabolism and its implications for health. *The Journal of nutrition, 134*(3), 489-492.

Wu, C., Ivars, F., Anderson, P., Hallmann, R., Vestweber, D., Nilsson, P*., et al.* (2009). Endothelial basement membrane laminin α5 selectively inhibits T lymphocyte extravasation into the brain. *Nature medicine, 15*(5), 519.

Xie, & Chen, X. (2013). Structures required of polyphenols for inhibiting advanced glycation end products formation. *Current drug metabolism, 14*(4), 414-431.

Xie, Zu, X., Liu, F., Wang, T., Wang, X., Chen, H*., et al.* (2019). Purpurogallin is a novel mitogen-activated protein kinase kinase 1/2 inhibitor that suppresses esophageal squamous cell carcinoma growth in vitro and in vivo. *Molecular carcinogenesis*.

Yang. (2018). *Post-translational regulation of redox-sensitive glutamylcysteine ligase (GCL)-revisited.*

Yang, & Candelario-Jalil, E. (2017). Role of Matrix Metalloproteinases in Brain Edema *Brain Edema* (pp. 199-215): Elsevier.

Yang, Dieter, M. Z., Chen, Y., Shertzer, H. G., Nebert, D. W., & Dalton, T. P. (2002). Initial Characterization of the Glutamate-Cysteine Ligase Modifier Subunit Gclm (−/−) Knockout Mouse NOVEL MODEL SYSTEM FOR A SEVERELY COMPROMISED OXIDATIVE STRESS RESPONSE. *Journal of Biological Chemistry, 277*(51), 49446-49452.

Yang, Mei, S., Jin, H., Zhu, B., Tian, Y., Huo, J*., et al.* (2017). Identification of two immortalized cell lines, ECV304 and bEnd3, for in vitro permeability studies of blood-brain barrier. *PLoS ONE, 12*(10), e0187017.

Yang, Roder, K. E., & Abbruscato, T. J. (2007). Evaluation of bEnd5 cell line as an in vitro model for the blood–brain barrier under normal and hypoxic/aglycemic conditions. *Journal of pharmaceutical sciences, 96*(12), 3196-3213.

Yang, Ye, L., Hui, T.-Q., Yang, D.-M., Huang, D.-M., Zhou, X.-D*., et al.* (2015). Bone morphogenetic protein 2-induced human dental pulp cell differentiation involves p38 mitogen-activated protein kinase-activated canonical WNT pathway. *International journal of oral science, 7*(2), 95.

Yu, X.-D., Yang, J.-l., Zhang, W.-L., & Liu, D.-X. (2016). Resveratrol inhibits oral squamous cell carcinoma through induction of apoptosis and G2/M phase cell cycle arrest. *Tumor Biology, 37*(3), 2871-2877.

Yuan, Y., Zhang, J., Wang, M., Mei, B., Guan, Y., & Liang, G. (2013). Detection of glutathione in vitro and in cells by the controlled self-assembly of nanorings. *Anal Chem, 85*(3), 1280-1284. doi:10.1021/ac303183v

Zhai, R., Xue, X., Zhang, L., Yang, X., Zhao, L., & Zhang, C. (2019). Strain-Specific Anti-inflammatory Properties of Two Akkermansia muciniphila Strains on Chronic Colitis in Mice. *Frontiers in Cellular and Infection Microbiology, 9*, 239.

Zhang, Court, N., & Forman, H. J. (2007). Submicromolar concentrations of 4-hydroxynonenal induce glutamate cysteine ligase expression in HBE1 cells. *Redox Report, 12*(1-2), 101-106.

Zhang, Suen, C. L.-C., Yang, C., & Quek, S. Y. (2018). Antioxidant capacity and major polyphenol composition of teas as affected by geographical location, plantation elevation and leaf grade. *Food chemistry, 244*, 109-119.

Zhang, Wang, X., Vikash, V., Ye, Q., Wu, D., Liu, Y*., et al.* (2016). ROS and ROS-Mediated Cellular Signaling. *Oxid Med Cell Longev, 2016*, 4350965. doi:10.1155/2016/4350965

Zhang, Xiong, Y.-W., Zhu, T.-T., Xiong, A.-Z., Bao, H.-h., & Cheng, X.-S. (2017). MicroRNA let-7g inhibited hypoxia-induced proliferation of PASMCs via G0/G1 cell cycle arrest by targeting c-myc. *Life Sciences, 170*, 9-15. doi:https://doi.org/10.1016/j.lfs.2016.11.020

Zhao, Nelson, A. R., Betsholtz, C., & Zlokovic, B. V. (2015). Establishment and dysfunction of the blood-brain barrier. *Cell, 163*(5), 1064-1078.

Zhao, Sagare, A. P., Ma, Q., Halliday, M. R., Kong, P., Kisler, K., *et al.* (2015). Central role for PICALM in amyloid-β blood-brain barrier transcytosis and clearance. *Nature neuroscience, 18*(7), 978.

Zlokovic, B. V., Mackic, J. B., Wang, L., McComb, J. G., & McDonough, A. (1993). Differential expression of Na, K-ATPase alpha and beta subunit isoforms at the blood-brain barrier and the choroid plexus. *Journal of Biological Chemistry, 268*(11), 8019-8025.

UNIVERSITY *of the*

WESTERN CAPE

Appendix

Attached as addendum are the publications of original article and a book chapter from the work of this thesis

Addendum

Book chapter:

Fisher D, O. Alamu (2020). The relationship between the blood-brain barrier, degenerative neuropathy and oxidative stress. In: Martin CR, Preedy VR, editors. Oxidative Stress and Dietary Antioxidants in Neurological Diseases. San Diego: Academic Press. (Accepted).

Article

Differential Sensitivity of Two Endothelial Cell Lines to Hydrogen Peroxide Toxicity: Relevance for *In Vitro* Studies of the Blood–Brain Barrier

Olufemi Alamu [1,2], **Mariam Rado** [1], **Okobi Ekpo** [1] **and David Fisher** [1,*]

[1] Department of Medical Bioscience, University of the Western Cape, Cape Town 7530, South Africa; olufemialamu@gmail.com (O.A.); maryamadem99@gmail.com (M.R.); okobiekpo@yahoo.co.uk (O.E.)

[2] Anatomy Department, Ladoke Akintola University of Technology, Ogbomoso 210241, Nigeria

* Correspondence: dfisher@uwc.ac.za; Tel.: +27-21-959-2185

Abstract: Oxidative stress (OS) has been linked to blood–brain barrier (BBB) dysfunction which in turn has been implicated in the initiation and propagation of some neurological diseases. In this study, we profiled, for the first time, two endothelioma cell lines of mouse brain origin, commonly used as in vitro models of the blood–brain barrier, for their resistance against oxidative stress using viability measures and glutathione contents as markers. OS was induced by exposing cultured cells to varying concentrations of hydrogen peroxide and fluorescence microscopy/spectrometry was used to detect and estimate cellular glutathione contents. A colorimetric viability assay was used to determine changes in the viability of OS-exposed cells. Both the b.End5 and bEnd.3 cell lines investigated showed demonstrable content of glutathione with a statistically insignificant difference in glutathione quantity per unit cell, but with a statistically significant higher capacity for the b.End5 cell line for de novo glutathione synthesis. Furthermore, the b.End5 cells demonstrated greater oxidant buffering capacity to higher concentrations of hydrogen peroxide than the bEnd.3 cells. We concluded that mouse brain endothelial cells, derived from different types of cell lines, differ enormously in their antioxidant characteristics. We hereby recommend caution in making comparisons across BBB models utilizing distinctly different cell lines and require further prerequisites to ensure that in vitro BBB models involving these cell lines are reliable and reproducible.

Keywords: oxidative stress; blood–brain barrier; bEnd5; bEnd.3; glutathione; viability

1. Introduction

The blood–brain barrier (BBB) is a functional and morphological interface between the systemic blood circulation and the CNS. The central regulatory component is the brain capillary endothelial cell (BEC), which is assisted by a number of cellular entities, viz. pericytes and astrocytes, together forming an interface, described as the neuro-vasculo-glial unit (NVU). The NVU has the dynamic ability to respond to the homeostatic changes in the brain interstitium ensuring a stable environment for neuronal functionality(N. J. Abbott et al., 2010). From a research point of view, it is therefore of interest to understand the capability of the BEC to withstand oxidative stress (OS), and to scrutinize the BBB in vitro models used to study these physiological processes. However, from a therapeutic point of view the strict regulatory mechanisms for molecules to cross the barrier provide a serious clinical challenge to molecules of desired therapeutic interest to reach their neural target sites (Betzer, Shilo, Motiei, & Popovtzer, 2019; Ramirez et al., 2009; Zhao, Nelson, et al., 2015; Zhao, Sagare, et al., 2015).

Endothelial dysfunction-mediated vascular diseases such as BBB dysfunction have been well linked to excess production of reactive oxygen species (ROS) (Liebner et al., 2018; Nation et al., 2019).

A major source of ROS in these conditions is the upregulation of nicotinamide adenine dinucleotide phosphate oxidase (Nox, especially Nox2) activity (Breitenbach et al., 2018; Fan et al., 2017). Excess superoxide (O_2^-) produced primarily from increased Nox activity undergoes both spontaneous and enzymatic dismutation by superoxide dismutases (SOD), resulting in increase and/or accumulation of its dismutation product, hydrogen peroxide (H_2O_2) (Sies et al., 2017). Keeping vascular endothelial cells in redox balance involves the activities of several endogenous antioxidants whose activities may be enzymatic or non-enzymatic (Sies et al., 2017). Superoxide dismutase (SOD) is an enzymatic, first-line, intracellular antioxidant that catalyzes the conversion of superoxide to hydrogen peroxide (Mirończuk-Chodakowska et al., 2018). Other important enzymatic antioxidants such as glutathione peroxidase (GPx), and catalase (CAT), help to neutralize H_2O_2 to water and oxygen (Mirończuk-Chodakowska et al., 2018)

Endothelial nitric oxide synthase (eNOS) is another enzyme which normally plays a protective role in the vascular endothelial cell through its production of nitric oxide (NO) while oxidizing its substrate L-arginine to L-citrulline using molecular oxygen (O_2) (Forstermann & Munzel, 2006; Koch, Choi, Mace, & Stark, 2019). However, parallel upregulation of eNOS and Nox as occurs in many vascular diseases results in eNOS uncoupling with subsequent conversion of eNOS to an O_2^--producing enzyme that contributes to further vascular oxidative stress (Drummond, Cai, Davis, Ramasamy, & Harrison, 2000; Santhanam et al., 2015; Toda & Okamura, 2016). Furthermore, free radicals such as superoxide can attack polyunsaturated fatty acids (PUFAs) such as arachidonic acid in the cell membranes of vascular endothelial cells to yield advanced lipid peroxidation end products (ALEs) (Enciu, Gherghiceanu, & Popescu, 2013). One of ALEs of relevance is 4-hydroxynonenal (4-HNE), an electrophile that is highly reactive towards nucleophilic thiols and amino groups (Dalleau, Baradat, Gueraud, & Huc, 2013; Enciu et al., 2013). It readily reacts with proteins (4-HNE-protein adduction), lipids, and nucleic acids of DNA. Its reaction with proteins modifies their activity thus acting as a second messenger in various biologic activities including modification of enzymatic actions or transcription factor modulations that determine cell survival or death (Dalleau et al., 2013). Oxidative stress (OS) occurs in the cells when an unbalanced accumulation of ROS exists within the cell and/or in its immediate environment(Sies, 2018). BBB dysfunction in relation to OS has been implicated in the initiation and propagation of several neurological conditions such as epilepsy, stroke, and degenerative neuropathies such as Alzheimer's disease, Parkinson's disease, and multiple sclerosis (Dohgu et al., 2019; Solé et al., 2019). Thus, OS has been scientifically documented as a common factor to both the etiologies of these neurological disorders as well as abnormal BBB function. Cell modeling has, to date, provided a robust tool in the in vitro study of the BBB (Campisi et al., 2018; Gastfriend et al., 2018). The brain microvascular endothelial cells are the principal cells of the BBB which have had several cell models characterized for use as in vitro models in the study of the BBB (Linville et al., 2019). This study focused on two mouse-derived cell lines, b.End5 and bEnd.3, established for use as in vitro models of the BBB (He et al., 2010; Steiner, Coisne, Engelhardt, & Lyck, 2011). It is of interest to understand how the endothelial cells of the BBB respond to oxidative stress as well as the endothelial cell-specific events that underlie the abnormalities of BBB permeability. It is, however, disconcerting that most of the in vitro cell models in use for BBB studies have not been characterized for their oxidative/antioxidant features, which are necessary for the definition of OS, as well as for features that characterize changes in oxidative stress responsible for the observation of abnormal permeability under OS conditions. In this study, we profiled for the first time, b.End5 and bEnd.3 cells, both mouse-derived cell lines obtained after immortalizing primary mouse brain endothelial cells by infection with middle T antigen-expressing polyoma virus, for their resistance against a suitably-selected ROS, hydrogen peroxide (H_2O_2), which can permeate all intracellular membranes and thus exert its effects on organelles (Glasauer & Chandel, 2013). Cellular glutathione content (reduced/oxidized form [GSH/GSSG]), a well reported marker of cellular oxidative status, is a tripeptide, L-γ-glutamine-L-cysteinyl-glycine, that acts as an endogenous cellular antioxidant either by direct neutralization of ROS or as cofactor for the antioxidant enzyme, glutathione peroxidase (GPx) (Volodymyr I. Lushchak, 2012). [Hereafter, we refer to the full component of reduced and oxidized glutathione as 'total glutathione while GSH and GSSG

refer to the 'reduced glutathione' and 'glutathione disulfide/oxidized glutathione' fractions respectively]. This functional capability of GSH is conferred by its active thiol group residing in its cysteine residue (Jones et al., 2011). Glutathione exists within cells in either the reduced (GSH) form or in oxidized form as glutathione disulfide (GSSG). It is usually synthesized as GSH but oxidized to GSSG upon participating in a redox reaction. Changes in cellular reduced glutathione content as well as changes in cell viabilities were used to assess cellular capacities to respond to varying levels of ROS. This protocol is robustly useful whenever it is desired to use these cells to study oxidant effects on the BBB.

2. Materials and Methods

2.1. Bio-Reagents

Analytical grade reagents were used for all experiments. These included monochlorobimane (Molecular Probe M1381MP, Eugene, OR 97402, USA), trypan blue, (Gibco 1520-061, Gaithersburg MD 20877, USA), tris (2-carboxyethyl) phosphine hydrochloride, TCEP (Sigma C4706, Laramie, WY 82070, USA), GSH-Glo™ Glutathione Assay Kit (Promega V6911/2, Madison, WI 53711, USA), Trolox ((±)-6-Hydroxy-2,5,7,8-tetramethylchromane-2-carboxylic acid, Sigma 238813, Laramie, WY 82070, USA), Cell Proliferation Kit II (XTT) (Roche, Sigma 11465015001, Laramie, WY 82070, USA), and hydrogen peroxide (30%, Merck Millipore 107209, Feldbergstraße 80, 64293 Darmstadt, Germany)

2.2. Cell Cultures

Two mouse brain endothelioma cell lines (b.End5 and bEnd.3) were used in this study. The b.End5 (ECACC 96091930, Salisbury, Wiltshire SP4 0JG, UK) cells were cultured in Dulbecco's modified Eagle's medium (DMEM Lonza BE 12-719F, Salisbury, MD 21801, USA.) supplemented with 10% fetal bovine serum (FBS Biowest12010S181G, Rue du Vieux Bourg, 49340 Nuaillé, France), 100 U/mL penicillin/streptomycin (Lonza DE17-602E,), 1 mM sodium pyruvate solution (Lonza BE13-115E), and 1% non-essential amino acids (NEAA Lonza BE13-114E) at 37 °C and 5% CO_2 in a humidified incubator. For all experiments, b.End5 cells at passages 5–20 were used and culture medium was changed every 2–3 days. Prior to experimentation, cells were rinsed in 1× phosphate buffer solution (PBS). The adherent cells were detached by the addition of 0.25% trypsin-EDTA after which equal volume of fresh media was added and the cell suspension aspirated into 15 mL conical tubes. The cell suspensions were then centrifuged for 5 min at rpm of 2500 to obtain a cell pellet. The supernatant was then removed by gentle aspiration and thereafter, 5 mL of fresh media added to bring the cell pellets back in suspension. The bEnd.3 (ATCC® CRL-2299, Gaithersburg, MD 20877, United States) cells were cultured in Dubelcco's Eagle's medium (Gibco 11320074) supplemented with 10% fetal bovine serum (FBS Biowest S12010S181G), 100 U/mL penicillin/streptomycin (Lonza DE17-602E), and L-glutamine to a final concentration of 4.1 mM (Invitrogen 25030081, Camarillo, CA 93012, United States) and at 37 °C and 5% CO_2 in a humidified incubator. The bEnd.3 cells used for all experiments were at passages 5–20 and the medium was changed every 2–3 days. Prior to cell seeding for experiments, adherent bEnd.3 cells were similarly brought to suspension as described for the b.End5 cells.

2.3. Hydrogen Peroxide Treatments

A stock solution of H_2O_2 (9.8 M, Merck Millipore, Feldbergstraße 80, 64293 Darmstadt, Germany) was diluted to the required concentrations in complete media. Cultured b.End5 and bEnd.3 cells were divided into labelled treatment wells exposed to H_2O_2 concentrations ranging between 10 µM and 2 mM and cells that were unexposed to H_2O_2 served as control. To determine the antioxidant capacity of cultured cells both b.End5 and bEnd.3 cells were seeded in separate transparent 96-well plates at 1×10^4 cells per well in 200 µL of normal media and allowed to attach overnight. Media were then aspirated and replaced with either 100 µL of fresh media to serve as control or 100 µL of media dosed with the appropriate concentrations of hydrogen peroxide for another 24 h. Experiments were repeated thrice

and average values of parameters were recorded. Viability of the cells exposed to different concentrations of hydrogen peroxide were then analysed and compared against viability measures for the control cells under same duration in culture.

2.4. Viability Assay

Cells were cultured in a transparent 96-well plate as described for hydrogen peroxide treatments. Equal numbers of b.End5 cells were seeded into eighteen treatment (H_2O_2) wells ($n = 3$) starting from control (unexposed) and treatment with [H_2O_2] in multiples of 50 μM up to a maximum of 850 μM. For cultured bEnd.3 cells, equal numbers of cells were seeded into sixteen sets of 3 wells ($n = 3$) and treated as control (unexposed), then [H_2O_2] in multiples of 10 μM up to 100 μM and then in multiples of 100 μM up to a maximum of 500 μM. A blank column of three wells was also included in both treatment plates to facilitate the determination of relative absorbance units. The XTT (Kazaks et al., 2019) viability assay kit (Roche) was used to quantify cell viability after treatment for 24 h. The XTT reagent was reconstituted by mixing 100 μL of electron-coupling reagent (0.383 mg/mL) with 5 mL of XTT labelling reagent (1 mg/mL) to activate it as per manufacturer's recommendation. Reconstituted XTT, 50 μL, was then added to each well containing 100 μL of cell culture and incubated for 4 h at 37 °C in a CO_2 incubator. Absorbance was then read for each well at 450 nm and blank-corrected values obtained using a GloMax–Multi Detection System (Promega, Madison, WI 53711, USA). The absorbance measures directly correlated with the viability of the cells in each well.

2.5. Fluorescent Detection of Glutathione in Cultured Cells

Equal numbers of b.End5 and bEnd.3 cells were cultured under standard conditions on microscopic glass slides in separate Petri dishes. The cells were then allowed to attach overnight in all Petri dishes and cells on each slide were used to demonstrate glutathione. Briefly, the medium was removed from the attached cells and were rinsed twice with PBS solution, pH, 7.4, and then incubated with monochlorobimane solution (mBCl, Molecular Probe™ M1381MP) 60 μM in complete DMEM for 30 min (Chatterjee et al., 1999). Following mBCl loading, slides were fixed using a mixture of 4% paraformaldehyde (PFA) and 0.2% glutaraldehyde (GA) in PBS solution at pH 7.4 for 10 min and following fixation, cells were nuclear-counterstained by incubating slides with 20 μg/mL propidium iodide (PI) solution for 15 min. DABCO (1,4-diazobicyclo-[2,2,2]-octane) mountant, 20 μL, was added to each slide mounted with cover slips. Cells on each slide were then viewed and imaged under a Nikon Eclipse 50i fluorescent microscope at $\lambda_{ex}/\lambda_{em}$ of 365/490 nm and 439/636 nm for mBCl and PI, respectively.

2.6. Quantification of Total Cellular Glutathione in bEnd5 Cells

To accurately quantify the total amount of glutathione in a single b.End5/bEnd.3 cell, we used a GSH-Glo™ Glutathione Assay Kit which works by a luminescence assay to detect and quantify glutathione (SCHERER et al., 2008). The assay is based on the conversion of a luciferin derivative into luciferin in the presence of glutathione, catalyzed by glutathione-S-transferase (GST). The reaction is further coupled with a firefly luciferase which leads to the generation of luminescence signal proportional to the amount of glutathione in the sample. To estimate glutathione fairly accurately in 1 $\times$ 10^4 cells, according to manufacturer's recommendation and to control for cell proliferation occurring alongside cell attachment, cells were plated in white 96-well plates and incubated at 37 °C and 5% CO_2 at a density of 4×10^3 cells per well for the b.End5 cells and 4.5×10^3 cells per well for the bEnd.3 cells, based on an optimized number of the respective cells that gave the target density at 24 h in culture (based on our data from proliferation study, not shown). Cells were plated in columns of four wells ($n = 4$) in a 96-well white bottom plate and 100 μL of prepared 1X GSH-Glo reagent was transferred to each well. In order to measure the total glutathione (GSH + GSSG), 100 μL of 1 mM tris (2-carboxyethyl) phosphine (TCEP) was added to a group of four wells in addition to the GSH-Glo reagent according to the GSSG recycling method (Tietze, 1969). The contents of the wells were agitated briefly on an orbital

shaker before incubation at room temperature for 30 min. Then, 100 µL of reconstituted luciferin detection reagent was transferred to each well, and the plate was mixed briefly on an orbital shaker before incubation at room temperature for 15 min. Luminescence values were then read using a GloMax–Multi Detection System (Promega, Madison, WI 53711, USA). Luminescence readings were converted to GSH concentration using a standard curve generated from a 5 mM GSH standard supplied by the manufacturer.

2.7. Statistical Analysis

Statistical analysis was done using Graph Pad Prism.5 statistical analysis software. Data were expressed as mean ± SEM and significant differences in data were accepted at $p < 0.05$

3. Results

In this study differences in antioxidant capacities of two brain endothelial cell lines from the same animal species were observed. We firstly established baseline data for both cell lines in terms of their endogenous glutathione concentrations, and secondly, we profiled the response of these cell lines to an exogenous ROS stress, H_2O_2, with respect to the content of the endogenous antioxidant, glutathione, using fluorescent imaging, and fluoro-spectrometric quantification.

3.1. Both b.End5 and bEnd.3 Cells Demonstrated Glutathione Presence on Fluorescent Microscopy

We first investigated presence and distribution of glutathione in each of the selected cell lines. Monochlorobimane with propidium iodide nuclear counterstaining revealed blue fluorescence due to the presence of glutathione while the nuclei fluoresced red (Figure 1). Both cells appeared intensely fluorescent for glutathione, however, bEnd.3 showed less cytoplasmic glutathione possibly due to a higher nucleo-cytoplasmic ratio. Variable segments and rings of blue fluorescence were observed around the periphery of the nuclei in both cells (Figure 1, Plates A2 and B2) which are evidence of glutathione presence within the nuclear structure. This was more prominently observed at the nucleo-cytoplasmic interface in both cell types and especially in the bEnd.3 cell (Figure 1, Plate B2).
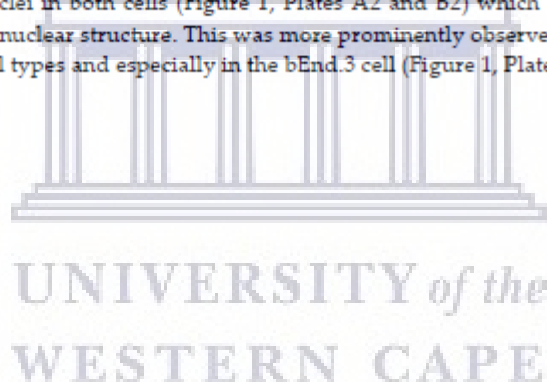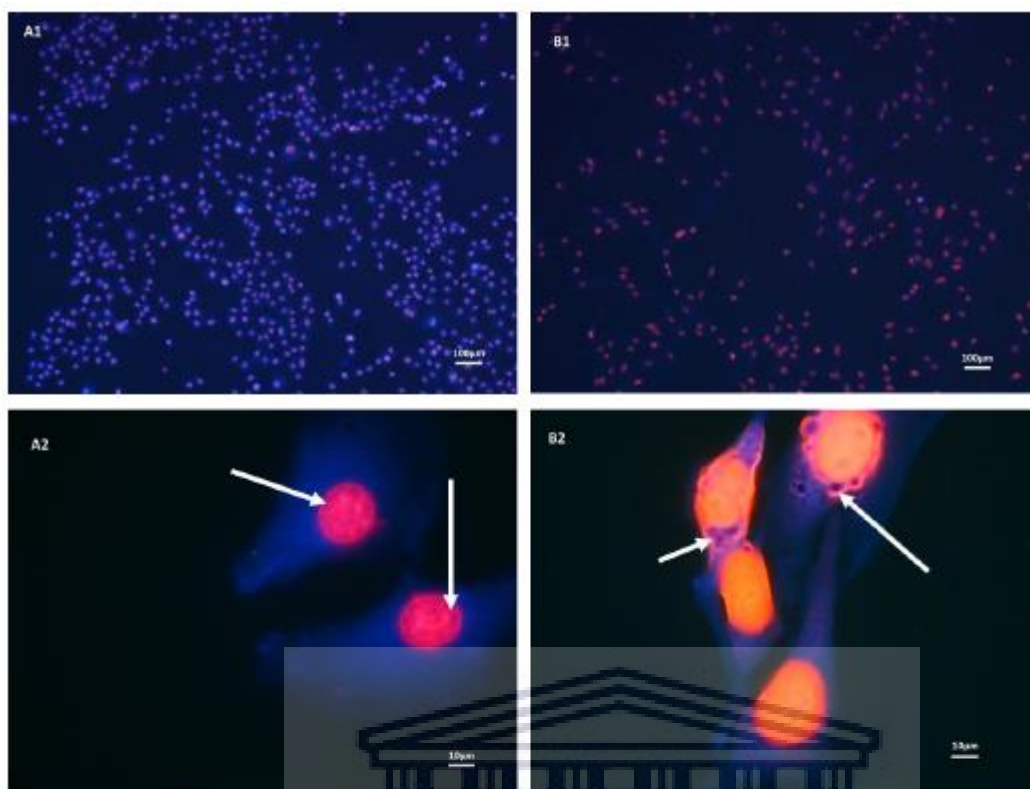
Figure 1. Micrographs show fluorescent images of b.End5 (**A1**) and (**A2**) and bEnd.3 cells (**B1**) and (**B2**) in normal culture. Both cells showed blue monochlorobimane solution (mBCl) fluorescence (due to binding with reduced glutathione (GSH)) in their cytoplasm, though at the higher magnification b.End5 appeared more deeply stained. Furthermore, plate A2 revealed a lower nucleo-cytoplasmic ratio in b.End5 cells suggesting more cytoplasmic GSH content than in bEnd.3 cells. Furthermore, multiple segments and rings of blue fluorescence (white arrows) were indicative of glutathione observed within the nuclei and nucleo-cytoplasmic interface in the cells of both cell types (Plates A2 and B2).

3.2. Glutathione Contents of Both b.End5 and bEnd.3 Cells Are Comparable in Normal Culture

The difference in blue fluorescence between the two cell types provided micrographical evidence for the presence and distribution of glutathione. The objective quantification of the levels of glutathione in each cell type was required to compare the cells' ability to respond to OS (Figure 2).
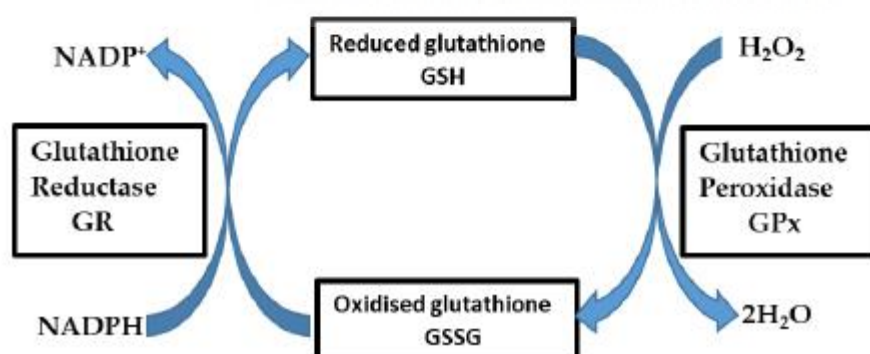
Figure 2. The above diagram illustrates the redox buffering reaction of the glutathione system. Glutathione peroxidase (GPx) enzymatically converts H_2O_2 to $2H_2O$ using reduced glutathione (GSH) as substrate which is then converted to its oxidized form, glutathione disulfide (GSSG) in the process. The GSSG in a second reaction involving glutathione reductase enzyme is converted back to GSH and thus GSH is recycled. The glutathione reductase reaction contributes significantly to the cellular maintenance of pooled reduced glutathione for redox defense.

Total and reduced fraction of the glutathione content in both cell types were experimentally determined while the content of oxidized glutathione was derived by deduction of the reduced glutathione values from the respective total glutathione values. The value of the total glutathione was obtained by reducing the GSSG fraction in each sample using TCEP which also has the ability to recover protein-bound GSH. However, because GSH exists within cells either freely or bound to proteins the recovered GSH still constituted a fraction of the total glutathione pool. In b.End5 cells the amount of glutathione per unit cell was higher than that of bEnd.3, however, the difference was not statistically significant ($p = 0.1325$) (Figure 3). Estimated values were 2.769 ± 0.113 fM/cell for b.End5 and 2.305 ± 0.219 fMol/cell for bEnd.3. Corresponding GSSG values for both b.End5 and bEnd.3 cells were respectively 0.139 ± 0.006 fM/cell and 0.115 ± 0.011 fM/cell. GSH/GSSG ratio in both cells approximated to 95%/5%.
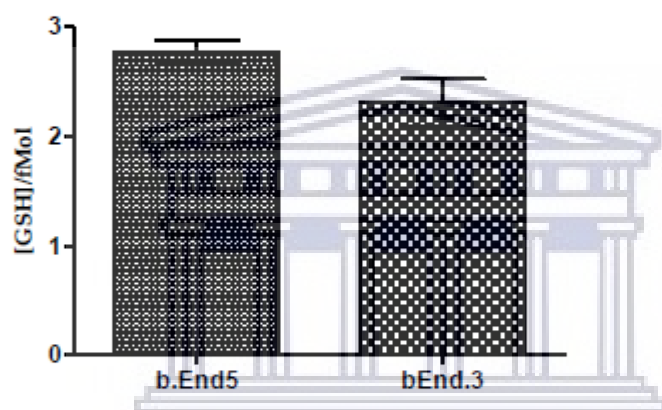
Figure 3. A comparison of GSH concentration in the two types of cells revealed no statistical difference between the two means (Student's t test; $p = 0.1325$).

3.3. Antioxidant Capacity is Higher in b.End5 Cells.

Although both cell lines tested showed that glutathione was abundantly present in both the cytoplasm and nucleoplasm, the response of these cell lines to ROS stress remains to be investigated. Both bEnd.3 and b.End5 cells treated with increasing concentrations of hydrogen peroxide showed changes in viability which correlated with the relative absorbance units obtained from XTT proliferation assay. The assay is based on the cleavage of the yellow tetrazolium salt, XTT, to form an orange formazan dye by mitochondrial dehydrogenases in metabolically active cells. Because an increase in the number of cells results in an increase in the overall activity of mitochondrial dehydrogenases in the samples, these changes correlated to the amount of orange formazan formed, a parameter that was monitored by the relative changes in the absorbance. The viability changes in both cells were normalized as percentages of the control, unexposed, cells and plotted against the logarithmic values of the various concentrations and the half-maximal inhibitory concentrations (IC_{50}) were determined and compared for the two cells (Figure 4A,B). Experiments were repeated three times and average values were analyzed. Results showed that the IC_{50} for the b.End5 cell was significantly higher than for the bEnd.3 cell (Figure 4C).

A. Log[H₂O₂] against viability (%) for b.End5

B. Log[H₂O₂] against viability (%) for bEnd.3

$IC_{50}=486.4\mu M$
$R^2=0.9566$

$IC_{50}=74.55\mu M$
$R^2=0.9687$

C. IC_{50} values compared for b.End5 and bEnd.3

****
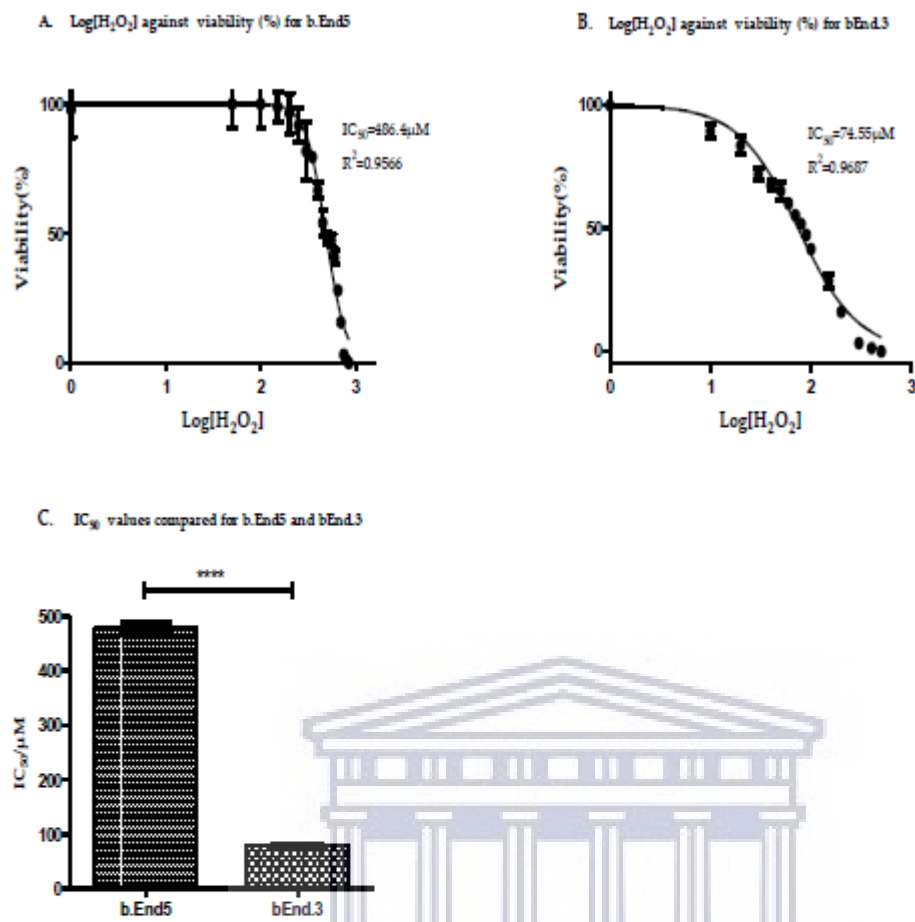
Figure 4. A non-linear regression analysis of logarithmic values of $[H_2O_2]$ against normalized viability was used to determine the hydrogen peroxide concentration that caused 50% inhibition of cell viability in b.End5 cells. Cells were exposed to $[H_2O_2]$ that ranged between 0 (control) and 850 μM for 24 h in flat-bottom transparent 96-well plates. Viability changes correlated to the absorbance measured at 450 nm from each well following incubation with XTT reagent for 4 h. (A) Results showed IC_{50} for b.End5 cell as equivalent of 486.4 μM at $r^2 = 0.9566$. (B) Data for bEnd.3 cells was obtained by exposing cultured bEnd.3 cells to $[H_2O_2]$ ranged from 0 (control) to 500 μM and non-linear regression analysis done as described above. Results showed IC_{50} for bEnd.3 cell to be 74.55 μM at $r^2 = 0.9687$ μM. (C). Graph of the IC_{50} values for the b.End5 compared with the same values for the bEnd.3 cells (annotation * denotes statistically significant difference between the values shown). IC_{50} values for b.End5 and bEnd.3 cells were statistically compared using the Student's *t* test. The analyzed data showed that the IC_{50} value was significantly higher for b.End5 cell than for the bEnd.3 cell ($p < 0.0001$).

3.4. Glutathione Was More Resistant to Oxidant Depletion in b.End5

Changes in the glutathione content of equal number of cells were plotted against the hydrogen peroxide concentrations. This allowed for the analysis of the physiological response (endogenous antioxidant response) of the two cell lines to increased H_2O_2 concentrations. The profile in glutathione depletion against increasing concentrations of hydrogen peroxide for the two cell lines was examined (Figure 5A,B). The data showed a steady decline in the glutathione content of the bEnd.3 cells (Figure

5B) while the b.End5 cells, in contrast, showed an initial significant increase in glutathione content and then a decline (Figure 5A). In b.End5 cells, glutathione increase was sustained either higher or at par with the control cells until about a concentration of 500 μM which was close to its IC$_{50}$ value (Figure 5A). Also, the glutathione content of b.End5 cells were observed to decline to a steady lowest value at about 1 mM hydrogen peroxide concentration and thereafter remained constant.
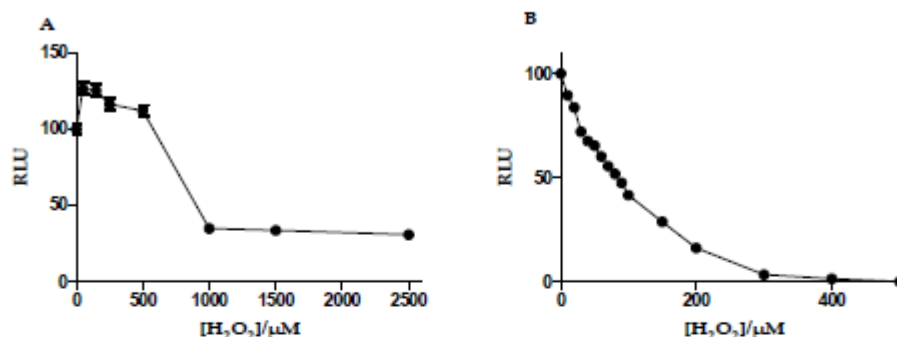

Figure 5. (A) and (B) show trends in the glutathione contents of b.End5 and bEnd3 cells with exposure to increasing [H$_2$O$_2$]. Cells were exposed to increasing concentrations of [H$_2$O$_2$] for 24 h and average cellular glutathione contents estimated using the GSH-Glo kit. Glutathione contents of the cells correlated directly to the relative luminescent values (RLU) obtained following incubation with the optimized reagents of the GSH-Glo assay kit described. Data in Figure 4A represents b.End5 cells and shows an upward trend in the glutathione content of the b.End5 cells upon exposure to [H$_2$O$_2$] of 0–250 μM. Above this concentration was observed a downward trend though values remained higher or at par with the starting point until [H$_2$O$_2$] higher than 500 μM. From this point a steady decline occurred until about 1 mM [H$_2$O$_2$] followed by a plateau but not a complete depletion. Data in Figure 4B represent the trend in bEnd.3 glutathione changes with increasing [H$_2$O$_2$]. A steady decline was observed until complete depletion at about 400 μM [H$_2$O$_2$].

4. Discussion

Although several previous reports have reported the existence of strain-specific genes in contributing to some differences in the physiological characteristics of different organs and/or systems in animals of the same species (Gooch & Yee, 1999; Sinclair et al., 2017; Zhai et al., 2019), researchers have largely ignored this evidence in choosing cell lines to model a physiological system. This is particularly evident in the use of cell lines modelling the BBB, where a variety of primary and immortalized cell lines have been used to study its physiological functions. This phenomenon creates un-necessary murkiness in comparing data between different studies. In this study, we were able to illustrate convincingly that differences in the antioxidant characteristics of the two cell lines (b.End5 and bEnd.3) (Figure 4A–C) of the same species, have distinctly different response profiles to an escalating ROS stressor. These two cells were derived from primary brain endothelial cells of two different mouse strains, BALB/c and SV129 respectively, by infection with a retrovirus coding for the Polyoma middle T-antigen (Montesano et al., 1990; Williams et al., 1989). Both have been used extensively to study BBB function (Helms et al., 2016; S. Yang et al., 2017; T. Yang et al., 2007), all with the underlying assumption, that there is physiological parity between these cell lines.

We investigated the cellular content of the glutathione antioxidant in the two cell types under normal culture conditions (as per the instructions provided by the suppliers), first by fluorescent microscopy, and although we easily established the cellular presence for glutathione, we were unable to distinguish clear quantitative differences between the two cell lines. Close examination of the fluorescence micrographs clearly illustrated the even distribution of glutathione throughout the

cytoplasm of both cell types, however, the higher ring of fluorescence just inside the nuclear membrane seem to suggest that glutathione plays an important role in neutralizing ROS entering into the nucleus. Given that DNA fragmentation is prone under conditions of OS (Agarwal, Cho, Esteves, & Majzoub, 2017; Homa et al., 2019), this provides solid circumstantial evidence as to the role of glutathione in protecting the nuclear material from ROS compromise. Although fluorescence demonstrated the presence of glutathione in both types of cells, the presence of blue fluorescence provided subjective evidence of increased cytoplasmic glutathione within b.End5 cells as evidenced by a lower nucleo-cytoplasmic ratio in the b.End5 cells with consequently more cytoplasmic content of glutathione.

Our quantitative data of the glutathione content of the b.End5 and bEnd.3 cell types substantiated our visual observations and, although b.End5 cells had a slightly higher mean glutathione content, statistically no significant difference in glutathione quantity was found between the respective cell lines (Figure 3). Calculations from data indicated that the GSH concentration per unit cell for the b.End5 and bEnd.3 cell types were within the range of 2.769 ± 0.113 fMol and 2.305 ± 0.219 fMol respectively. Both cell types also have GSH/GSSG ratio of approximately 95%/5% which indicated that both cells were redox-stable in normal culture. Comparisons of the average cellular glutathione per single cell for both the b.End5 and bEnd.3 cell lines predict that these cells are well suited for OS resistance in that their GSH contents are in the range of cells specialized for detoxification, such as the liver cancer cell line, HepG2 with GSH content of 2.9 fMol/cell (Yuan et al., 2013). These data, taken independently endorses the use of these cell lines for BBB modeling. It is presumptuous to assume that simply on the basis that the cell lines have similar basal levels of endogenous antioxidants that these cells may indeed respond to incremental ROS stress in a similar manner. This is all the more complicated given the arbitrary concentrations of ROS stressors used in experiments to demonstrate OS on the BBB (C. Cao et al., 2019; Song et al., 2014).

To evaluate the response of the endogenous antioxidant glutathione to incremental concentrations of H_2O_2 in each cell-line, we then determined the relative levels of OS that causes decompensation of the GSH/GSSG antioxidant system in the cell after 24 h exposure (Figure 4A,B). In this study we profiled the cell lines using the glutathione system which has been reported as a reliable and sensitive marker of oxidative cellular status (Bains & Bains, 2015; Kranner et al., 2006). Furthermore, because the physiological variable of cell viability was used as a general indicator of the response of the cells to ROS (H_2O_2), it is scientifically plausible that viability changes will be a reliable indicator of the total cellular antioxidant capacity, and therefore, a singular marker (glutathione) would provide enough insight on the differences in the total antioxidant capacities of the two cell lines. Using the IC$_{50}$ (Doroshow & Juhasz, 2019)values for comparison, we documented for the first time evidence of a significantly greater capability of the b.End5 cells to neutralize higher ROS concentrations than the bEnd.3 cells ([$p < 0.0001$] Figure 4C). When we studied the profile in the GSH depletion within the cells exposed to increasing ROS load the data showed that the bEnd3 cell type has a very limited ability for de novo upregulation of glutathione synthesis under condition of increased ROS accumulation (Figure 5B), whereas the b.End5 cell type showed ability to sustain adequate levels of glutathione, to elevate levels of GSH in response to initial low concentration of ROS, and to maintain this sustained endogenous GSH levels despite several subsequent increases in the concentration of ROS (Figure 5A). The mechanism for this divergent reaction of the glutathione system in the two cell types against increasing concentration of ROS is not clear, and requires further study. However, this observed difference is suggestive of inter-strain differences in the system that regulates ROS accumulation within these cells, as has been reported for several diverse physiological characteristics in different strains of cells from the same species of animal (Doroshow & Juhasz, 2019; Shidara et al., 2019; Sinclair et al., 2017). Differentially expressed genes in specific domains of the system that regulate ROS in intracellular milieu or perhaps strain-specific genetic alteration following viral oncogenic transformation of the primary cells could be responsible (Sandberg et al., 2000). Mouse strain-specific differences in neuro-behavior, neuronal excitability, susceptibility to fibrosis, anti-inflammatory response, and bone density have been previously reported (Shidara et al., 2019). These previous reports have strengthened our position that strain-specific genes are very important in shaping the phenotypic differences in the two cell types

investigated with respect to their glutathione system plasticity to OS. This finding has an important bearing on experimental designs aimed at studying effects of OS on the BBB. However, whether these two mouse cells respond differently to OS in the in vivo situation is not known. We propose here that a genome-wide genetic screen of the cells in use for evaluating the physiology of the BBB will identify important differences in the genes that control several key functions of the BBB (J. Y. Cao et al., 2019). Also, further research is required to determine these properties in primary cells of the mouse brain endothelial cells with the potential for the unraveling of the true behavior of the mouse brain endothelial cells during OS conditions with respect to capacity for ROS neutralization and the glutathione system response.

Given that under control conditions we are confident that the BECs would be in redox balance, it is, therefore, unimportant to localize the source of endogenous ROS production in response to exogenous ROS exposure, neither does it make scientific sense to measure ROS production from the cell organelles when the source of ROS was clearly defined as the experimental treatment (exogenous H_2O_2). Exogenous ROS treatment would gauge the physiological capacity of the cells to respond to ROS exposure from an exogenous source. Exogenous exposure would be additional to the normal ROS load generated by normal physiological cellular processes. Thus, the measuring of ROS levels while exposing cells to exogenous H_2O_2 in this study would be superfluous. Nevertheless, it might be assumed that the study largely ignored the spatiotemporal localization and quantification of endogenous ROS production, but we are aware of the lack of the use of these techniques, which is intended to be the focus of our future study, in which we propose to measure ROS produced endogenously by cellular organelles using a combination of immuno-electron microscopy as qualitative and ELISA as semi-quantitative methods (Grasso, Komatsu, & Axelsen, 2017; Jaganjac et al., 2019; Tanikawa & Torimura, 2006).

5. Conclusions

The glutathione system responses and ROS buffering capacities are clearly linked and they determine the magnitude of ROS that induces OS in the b.End5 and bEnd.3 mouse brain endothelial cell line models of the BBB. Strain-specific differences in the different cells will result in different definitions of OS in different models of different animal strains within the same species. Thus it is important to establish experimental parameters that best define OS for each endothelial cell model of the BBB for reproducibility. Such information will avail researchers of opportunity to verify and select appropriate models of BBB endothelial cells for specific redox investigations and enable them to draw comparable and reproducible conclusions.

Conflicts of Interest: The authors declare no conflict of interest.

References

Abbott, N.J.; Patabendige, A.A.; Dolman, D.E.; Yusof, S.R.; Begley, D.J. Structure and function of the blood-brain barrier. *Neurobiol. Dis.* **2010**, *37*, 13–25, doi:10.1016/j.nbd.2009.07.030.

Ramirez, S.H.; Potula, R.; Fan, S.; Eidem, T.; Papugani, A.; Reichenbach, N.; Dykstra, H.; Weksler, B.B.; Romero, I.A.; Couraud, P.O.; et al. Methamphetamine disrupts blood brain barrier function by induction of oxidative stress in brain endothelial cells. *J. Cereb. Blood Flow Metab.* **2009**, *29*, 1933–1945, doi:10.1038/jcbfm.2009.112.

Betzer, O.; Shilo, M.; Motiei, M.; Popovtzer, R. Insulin-coated gold nanoparticles as an effective approach for bypassing the blood-brain barrier. *Nanoscale Imaging, Sensing, and Actuation for Biomedical Applications XVI* **2019**, *10891*, 108911H.

Zhao, Z.; Nelson, A.R.; Betsholtz, C.; Zlokovic, B.V. Establishment and dysfunction of the blood-brain barrier. *Cell* **2015**, *163*, 1064–1078.

Zhao, Z.; Sagare, A.P.; Ma, Q.; Halliday, M.R.; Kong, P.; Kisler, K.; Winkler, E.A.; Ramanathan, A.; Kanekiyo, T.; Bu, G. Central role for PICALM in amyloid-β blood-brain barrier transcytosis and clearance. *Nat. Neurosci.* **2015**, *18*, 978–987.

Liebner, S.; Dijkhuizen, R.M.; Reiss, Y.; Plate, K.H.; Agalliu, D.; Constantin, G. Functional morphology of the blood–brain barrier in health and disease. *Acta Neuropathol.* **2018**, *135*, 311–336, doi:10.1007/s00401-018-1815-1.

Nation, D.A.; Sweeney, M.D.; Montagne, A.; Sagare, A.P.; D'Orazio, L.M.; Pachicano, M.; Sepehrband, F.; Nelson, A.R.; Buennagel, D.P.; Harrington, M.G. Blood–brain barrier breakdown is an early biomarker of human cognitive dysfunction. *Nat. Med.* **2019**, *25*, 270–276.

Fan, Lampson M.; Cahill-Smith, S.; Geng, L.; Du, J.; Brooks, G.; Li, J.-M. Aging-associated metabolic disorder induces Nox2 activation and oxidative damage of endothelial function. *Free Radic. Biol. Med.* **2017**, *108*, 940–951, doi:https://doi.org/10.1016/j.freeradbiomed.2017.05.008.

Breitenbach, M.; Rinnerthaler, M.; Weber, M.; Breitenbach-Koller, H.; Karl, T.; Cullen, P.; Basu, S.; Haskova, D.; Hasek, J. The defense and signaling role of NADPH oxidases in eukaryotic cells. *Wien. Med. Wochenschr.* **2018**, *168*, 286–299, doi:10.1007/s10354-018-0640-4.

Sies, H.; Berndt, C.; Jones, D.P. Oxidative Stress. *Annu. Rev. Biochem.* **2017**, *86*, 715–748, doi:10.1146/annurev-biochem-061516-045037.

Mirończuk-Chodakowska, I; Witkowska, A.M.; Zujko, M.E. Endogenous non-enzymatic antioxidants in the human body. *Adv. Med. Sci.* **2018**, *63*, 68–78.

Forstermann, U.; Munzel, T. Endothelial nitric oxide synthase in vascular disease: From marvel to menace. *Circulation* **2006**, *113*, 1708–1714.

Koch, S.R.; Choi, H.; Mace, E.H.; Stark, R.J. Toll-like receptor 3-mediated inflammation by p38 is enhanced by endothelial nitric oxide synthase knockdown. *Cell Commun. Signal.* **2019**, *17*, 33.

Santhanam, A.V.R.; d'Uscio, L.V.; He, T.; Das, P.; Younkin, S.G.; Katusic, Z.S. Uncoupling of endothelial nitric oxide synthase in cerebral vasculature of Tg2576 mice. *J. Neurochem.* **2015**, *134*, 1129–1138.

Drummond, G.R.; Cai, H.; Davis, M.E.; Ramasamy, S.; Harrison, D.G. Transcriptional and posttranscriptional regulation of endothelial nitric oxide synthase expression by hydrogen peroxide. *Circ. Res.* **2000**, *86*, 347–354.

Toda, N.; Okamura, T. Cigarette smoking impairs nitric oxide-mediated cerebral blood flow increase: Implications for Alzheimer's disease. *J. Pharmacol. Sci.* **2016**, *131*, 223–232.

Enciu, A.-M.; Gherghiceanu, M.; Popescu, B.O. Triggers and Effectors of Oxidative Stress at Blood-Brain Barrier Level: Relevance for Brain Ageing and Neurodegeneration. *Oxidative Med. Cell. Longev.* **2013**, *2013*, 1–12. doi:10.1155/2013/297512.

Dalleau, S.; Baradat, M.; Gueraud, F.; Huc, L. Cell death and diseases related to oxidative stress: 4-hydroxynonenal (HNE) in the balance. *Cell Death Differ.* **2013**, *20*, 1615–1630.

Sies, H. On the history of oxidative stress: Concept and some aspects of current development. *Curr. Opin. Toxicol.* **2018**, *7*, 122–126.

Dohgu, S.; Takata, F.; Matsumoto, J.; Kimura, I; Yamauchi, A.; Kataoka, Y. Monomeric α-synuclein induces blood–brain barrier dysfunction through activated brain pericytes releasing inflammatory mediators in vitro. *Microvasc. Res.* **2019**, *124*, 61–66.

Solé, M.; Esteban-Lopez, M.; Taltavull, B.; Fábregas, C.; Fadó, R.; Casals, N.; Rodríguez-Álvarez, J.; Miñano-Molina, A.J.; Unzeta, M. Blood-brain barrier dysfunction underlying Alzheimer's disease is induced by an SSAO/VAP-1-dependent cerebrovascular activation with enhanced Aβ deposition. *Biochim. Et Biophys. Acta (BBA)-Mol. Basis Dis.* **2019**.

Gastfriend, B.D.; Palecek, S.P.; Shusta, E.V. Modeling the blood–brain barrier: Beyond the endothelial cells. *Curr. Opin. Biomed. Eng.* **2018**, *5*, 6–12.

Campisi, M.; Shin, Y.; Osaki, T.; Hajal, C.; Chiono, V.; Kamm, R.D. 3D self-organized microvascular model of the human blood-brain barrier with endothelial cells, pericytes and astrocytes. *Biomaterials* **2018**, *180*, 117–129.

Linville, R.M.; DeStefano, J.G.; Sklar, M.B.; Xu, Z.; Farrell, A.M.; Bogorad, M.I.; Chu, C.; Walczak, P.; Cheng, L.; Mahairaki, V. Human iPSC-derived blood-brain barrier microvessels: Validation of barrier function and endothelial cell behavior. *Biomaterials* **2019**, *190*, 24–37.

Steiner, O.; Coisne, C.; Engelhardt, B.; Lyck, R. Comparison of immortalized bEnd5 and primary mouse brain microvascular endothelial cells as in vitro blood–brain barrier models for the study of T cell extravasation. *J. Cereb. Blood Flow Metab.* **2011**, *31*, 315–327, doi:10.1038/jcbfm.2010.96.

He, F.; Yin, F.; Peng, J.; Li, K.Z.; Wu, L.W.; Deng, X.L. [Immortalized mouse brain endothelial cell line Bend.3 displays the comparative barrier characteristics as the primary brain microvascular endothelial cells]. *Zhongguo Dang Dai Er Ke Za Zhi = Chin. J. Contemp. Pediatrics* **2010**, *12*, 474–478.

Glasauer, A.; Chandel, N.S. Ros. *Curr. Biol.* **2013**, *23*, R100–R102.

Lushchak, V.I. Glutathione Homeostasis and Functions: Potential Targets for Medical Interventions. *J. Amino Acids* **2012**, *2012*, 1–26, doi:10.1155/2012/736837.

Jones, D.P.; Park, Y.; Gletsu-Miller, N.; Liang, Y.; Yu, T.; Accardi, C.J.; Ziegler, T.R. Dietary sulfur amino acid effects on fasting plasma cysteine/cystine redox potential in humans. *Nutrition* **2011**, *27*, 199–205.

Kazaks, A.; Collier, M.; Conley, M. Cytotoxicity of Caffeine on MCF-7 Cells Measured by XTT Cell Proliferation Assay (P06-038-19). *Curr. Dev. Nutr.* **2019**, *3*.

Chatterjee, S.; Noack, H.; Possel, H.; Keilhoff, G.; Wolf, G. Glutathione levels in primary glial cultures: Monochlorobimane provides evidence of cell type-specific distribution. *Glia* **1999**, *27*, 152–161.

SCHERER, C.; CRISTOFANON, S.; DICATO, M.; DIEDERICH, M. HOMOGENEOUS LUMINESCENCE-BASED ASSAY FOR QUANTIFYING THE GLUTATHIONE CONTENT IN MAMMALIAN CELLS. *Cells Nots* **2008**, *20*.

Tietze, F. Enzymic method for quantitative determination of nanogram amounts of total and oxidized glutathione: Applications to mammalian blood and other tissues. *Anal. Biochem.* **1969**, *27*, 502–522.

Zhai, R.; Xue, X.; Zhang, L.; Yang, X.; Zhao, L.; Zhang, C. Strain-Specific Anti-inflammatory Properties of Two Akkermansia muciniphila Strains on Chronic Colitis in Mice. *Front. Cell. Infect. Microbiol.* **2019**, *9*, 239.

Sinclair, J.L.; Barnes-Davies, M.; Kopp-Scheinpflug, C.; Forsythe, I.D. Strain-specific differences in the development of neuronal excitability in the mouse ventral nucleus of the trapezoid body. *Hear. Res.* **2017**, *354*, 28–37.

Gooch, J.L.; Yee, D. Strain-specific differences in formation of apoptotic DNA ladders in MCF-7 breast cancer cells. *Cancer Lett.* **1999**, *144*, 31–37.

Montesano, R.; Pepper, M.; Möhle-Steinlein, U.; Risau, W.; Wagner, E.; Orci, L. Increased proteolytic activity is responsible for the aberrant morphogenetic behavior of endothelial cells expressing the middle T oncogene. *Cell* **1990**, *62*, 435–445.

Williams, R.L.; Risau, W.; Zerwes, H.-G.; Drexler, H.; Aguzzi, A.; Wagner, E.F. Endothelioma cells expressing the polyoma middle T oncogene induce hemangiomas by host cell recruitment. *Cell* **1989**, *57*, 1053–1063.

Helms, H.C.; Abbott, N.J.; Burek, M.; Cecchelli, R.; Couraud, P.-O.; Deli, M.A.; Förster, C.; Galla, H.J.; Romero, I.A.; Shusta, E.V. In vitro models of the blood–brain barrier: An overview of commonly used brain endothelial cell culture models and guidelines for their use. *J. Cereb. Blood Flow Metab.* **2016**, *36*, 862–890.

Yang, S.; Mei, S.; Jin, H.; Zhu, B.; Tian, Y.; Huo, J.; Cui, X.; Guo, A.; Zhao, Z. Identification of two immortalized cell lines, ECV304 and bEnd3, for in vitro permeability studies of blood-brain barrier. *PLoS ONE* **2017**, *12*, e0187017.

Yang, T.; Roder, K.E.; Abbruscato, T.J. Evaluation of bEnd5 cell line as an in vitro model for the blood–brain barrier under normal and hypoxic/aglycemic conditions. *J. Pharm. Sci.* **2007**, *96*, 3196–3213.

Agarwal, A.; Cho, C.-L.; Esteves, S.C.; Majzoub, A. Reactive oxygen species and sperm DNA fragmentation. *Transl. Androl. Urol.* **2017**, *6*, S695.

Homa, S.T.; Vassiliou, A.M.; Stone, J.; Killeen, A.P.; Dawkins, A.; Xie, J.; Gould, F.; Ramsay, J.W. A comparison between two assays for measuring seminal oxidative stress and their relationship with sperm DNA fragmentation and semen parameters. *Genes* **2019**, *10*, 236.

Yuan, Y.; Zhang, J.; Wang, M.; Mei, B.; Guan, Y.; Liang, G. Detection of glutathione in vitro and in cells by the controlled self-assembly of nanorings. *Anal. Chem* **2013**, *85*, 1280–1284, doi:10.1021/ac303183v.

Cao, C.; Dai, L.; Mu, J.; Wang, X.; Hong, Y.; Zhu, C.; Jin, L.; Li, S. S1PR2 antagonist alleviates oxidative stress-enhanced brain endothelial permeability by attenuating p38 and Erk1/2-dependent cPLA2 phosphorylation. *Cell. Signal.* **2019**, *53*, 151–161.

Song, J.; Kang, S.M.; Lee, W.T.; Park, K.A.; Lee, K.M.; Lee, J.E. Glutathione protects brain endothelial cells from hydrogen peroxide-induced oxidative stress by increasing nrf2 expression. *Exp Neurobiol* **2014**, *23*, 93–103, doi:10.5607/en.2014.23.1.93.

Bains, V.K.; Bains, R. The antioxidant master glutathione and periodontal health. *Dent. Res. J.* **2015**, *12*, 389–405.

Kranner, I.; Birtić, S.; Anderson, K.M.; Pritchard, H.W. Glutathione half-cell reduction potential: A universal stress marker and modulator of programmed cell death? *Free Radic. Biol. Med.* **2006**, *40*, 2155–2165.

Doroshow, J.H.; Juhasz, A. Modulation of selenium-dependent glutathione peroxidase activity enhances doxorubicin-induced apoptosis, tumour cell killing and hydroxyl radical production in human NCI/ADR-RES cancer cells despite high-level P-glycoprotein expression. *Free Radic. Res.* **2019**, *53*, 882–891.

Shidara, K.; Mohan, G.; Lay, Y.-A.E.; Jepsen, K.J.; Yao, W.; Lane, N.E. Strain-specific differences in the development of bone loss and incidence of osteonecrosis following glucocorticoid treatment in two different mouse strains. *J. Orthop. Transl.* **2019**, *16*, 91–101.

Sandberg, R.; Yasuda, R.; Pankratz, D.G.; Carter, T.A.; Del Rio, J.A.; Wodicka, L.; Mayford, M.; Lockhart, D.J.; Barlow, C. Regional and strain-specific gene expression mapping in the adult mouse brain. *Proc. Natl. Acad. Sci.* **2000**, *97*, 11038–11043.

Cao, J.Y.; Poddar, A.; Magtanong, L.; Lumb, J.H.; Mileur, T.R.; Reid, M.A.; Dovey, C.M.; Wang, J.; Locasale, J.W.; Stone, E. A genome-wide haploid genetic screen identifies regulators of glutathione abundance and ferroptosis sensitivity. *Cell Rep.* **2019**, *26*, 1544–1556.e8.

Tanikawa, K.; Torimura, T. Studies on oxidative stress in liver diseases: Important future trends in liver research. *Med. Mol. Morphol.* **2006**, *39*, 22–27.

Grasso, G.; Komatsu, H.; Axelsen, P. Covalent modifications of the amyloid beta peptide by hydroxynonenal: Effects on metal ion binding by monomers and insights into the fibril topology. *J. Inorg. Biochem.* **2017**, *174*, 130–136.

Jaganjac, M.; Milkovic, L.; Gegotek, A.; Cindric, M.; Zarkovic, K.; Skrzydlewska, E.; Zarkovic, N. The relevance of pathophysiological alterations in redox signaling of 4-hydroxynonenal for pharmacological therapies of major stress-associated diseases. *Free Radic. Biol. Med.* **2019**.
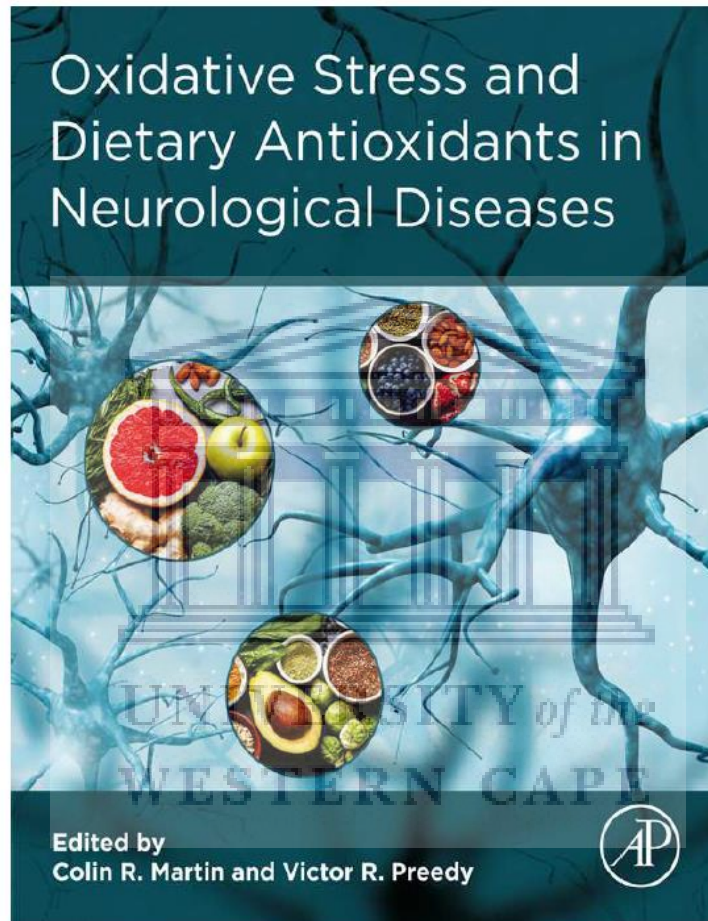
UNIVERSITY *of the* WESTERN CAPE

Oxidative Stress and Dietary Antioxidants in Neurological Diseases

Edited by
Colin R. Martin and Victor R. Preedy

CHAPTER 2

The relationship between the blood-brain barrier, degenerative neuropathy, and oxidative stress

David Fisher, Olufemi A. Alamu
Department of Medical Bioscience, Faculty of Natural Science, University of the Western Cape, Bellville, Cape Town, South Africa

Abbreviations

ATP	adenosine triphosphate
AO	antioxidants
AD	Alzheimer's disease
Aβ	amyloid beta peptide
APP	amyloid precursor protein
ALS	amyotrophic lateral sclerosis
ApoE-Ɛ4	apolipoprotein E (epsilon 4)
ApoJ	apolipoprotein J
BM	basement membrane
Bax	Bcl-2-associated X protein
Bad	Bcl-2-associated death promoter
BBB	blood-brain barrier
CNS	central nervous system
CSF	cerebrospinal fluid
CLU	clusterin
DM	diabetes mellitus
ETC	electron transport chain
EC	endothelial cell
eNOS	endothelial nitric oxide synthase
EGCG	epigallocatechin-3-gallate
ECM	extracellular matrix
FADH$_2$	flavin adenine dinucleotide
Gadd45	growth arrest and DNA damage 45
HPLC	high-performance liquid chromatography
LRP1	low-density lipoprotein receptor-related protein 1
MRI	magnetic resonance imaging
MMP	matrix metalloproteinases
MCI	mild cognitive impairment
MAPK	mitogen-activated protein inases
MPTP	N-methyl-4-phenyl-1,2,3,6-tetrahydropyridine
MS	multiple sclerosis
Nox	NADPH oxidases
NDD	neurodegenerative disease

17

NFT	neurofibrillary tangles
NVU	neuro-glial-vascular unit
NADPH	nicotinamide adenine dinucleotide phosphate
OS	oxidative stress
PD	Parkinson's disease
PC	pericyte
PTP	permeability transition pore
PI3K	phosphatidylinositol-3 kinase
PICALM	phosphatidylinositol-binding clathrin assembly protein
ROS	reactive oxygen species
RAGE	receptors for advanced glycation end products
6-OHDA	6-hydroxydopamine
SNP$_C$	substantia nigra pars compacta
SOD	superoxide dismutase
TJP	tight junction proteins
TRAIL	tumor necrosis factor-related apoptosis-inducing ligand
UV	ultraviolet light
VaD	vascular dementia

Introduction: Purpose and function of the blood-brain barrier

The functional integrity of the central nervous system (CNS) is largely dependent on neuronal wiring into reflex arcs and neuronal circuitry. These neuronal circuits transmit impulses as electrical and chemical signals and as such, obligatory control of the milieu around the axons and synapses that form these circuits becomes a necessity for consistency and continuity in neural signaling.[1] The brain has evolved a structural mechanism for regulating the composition of the neural microenvironment, the blood-brain barrier (BBB). The BBB is the key interface between blood and neural tissue and is vital to this regulation.[1,2]

Structure of the BBB

Endothelial component

The microvessels of the brain consist of two main cell types, the endothelial cells (ECs) that line the blood vessels and the mural cells (astrocytes) that sleeve the abluminal surface of the ECs.[3] The BBB properties, conferred by the ECs, are stimulated and maintained by intricate interactions with the astrocyte cells, immune cells, glial cells, and neural cells which are known as the neuro-glial-vascular unit (NVU).[1,3] The ECs of the BBB are modified simple squamous epithelial cells that line the walls of blood capillaries. They are held together by tight junctions that tightly restrict paracellular transit of solutes.[2] The BBB ECs also exhibit extremely low rates of transcytosis which limits vesicular transcellular transit of molecules and cells. These two barrier systems polarized the EC into

distinct luminal and abluminal membrane compartments regulating the movement of molecules between the blood and the brain.[3] Exclusion of some lipophilic molecules from the brain, while selectively transporting similar molecules of obligatory importance, is achieved by the expression of two modalities of transporters which appear to recognize molecules as either wanted or unwanted.[3,4] Efflux transporters transport lipophilic molecules that can freely diffuse through the cell membrane back into the blood. The highly specific nutrient transporters ferry specific nutrients across the BBB into the CNS and remove specific waste products from the brain into the blood. Other properties of the brain ECs include possession of higher mitochondrial density than ECs elsewhere in the body used for adenosine triphosphate (ATP) generation needed to drive and maintain the ion gradient that is crucial to neuronal homeostasis. Expression of extremely low levels of leukocyte adhesion molecules greatly restrict the access of immune cells from the circulation.[5] Furthermore, the presence of metabolic enzymes that alter the physical properties of molecules in transit across the EC constitutes the metabolic or enzymatic barrier by influencing its reactivity, solubility, and transport properties.[6] These barrier facets combine to afford the ECs a dynamic regulation of the CNS homeostasis[3,4,6] (Fig. 1).

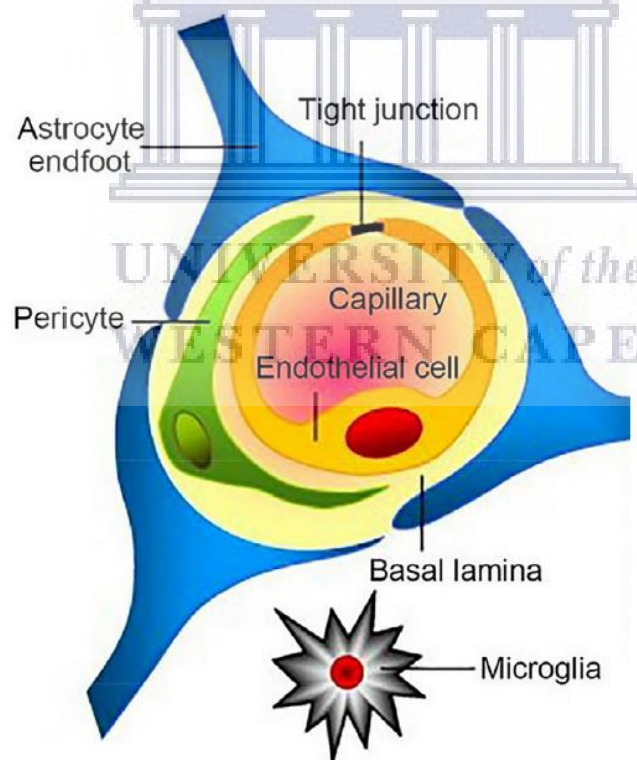**Fig. 1** Components of the blood-brain barrier. The BBB consists of specialized capillary endothelial cells that are lined by the basal lamina, astrocytic endfeet, pericytes, and microglial cells. *(From He Q, Liu J, Liang J, Liu X, Li W, Liu Z, Ding Z, Tuo D. Towards Improvements for Penetrating the Blood–Brain Barrier—Recent Progress from a Material and Pharmaceutical Perspective. Cells 2018;**7**(24).)*

Nonendothelial components

Mural cells in microvessels that form the BBB include the pericytes (PCs) which form an incomplete enclosure around the endothelial walls. They are localized to the abluminal surface of the microvascular endothelial tube, embedded in the basement membrane (BM).[7] PCs contain contractile proteins that serve to control the diameter of the capillaries by their contractile activities. In addition to a higher density of PCs in CNS microvasculature than elsewhere in the body, CNS PCs have a neural crest origin whereas elsewhere in the body PCs are of mesodermal origin.[7] Their roles include regulation of angiogenesis, deposition of extracellular matrix (ECM), wound healing, regulation of immune cell infiltration, and blood flow regulation in response to neural signals and also possibly acts as multipotent stem cells of the CNS.[8] Well documented is also their regulatory role in BBB development as well as its maintenance function in adulthood and aging.[5]

The BM forms the outer covering of the vascular tube and has two layers including the vascular layer and the outer parenchymal layer.[3,9] The vascular layer is secreted by the ECs and PCs while the parenchymal BM is secreted by astrocytic endfeet that extends to the vasculature.[3] The secreted molecular components of the BM include type IV collagens, laminin, nidogen, heparin sulfate, proteoglycans, and other glycoproteins.[3] The vascular and parenchymal layers differ in composition: the vascular layer contains laminins α4 and α5 while the parenchymal layer contains α1 and α2.[9] The BM serves as an anchor for signaling processes at the vasculature as well as provide an additional barrier against the access of the neural tissue by transiting molecules.[9] Disruption of the BM by matrix metalloproteinases (MMPs) has been documented as an important component of several neurological disorders.[10,11]

Astrocytes are glial cells with polarized cellular processes. The endfeet of their basal processes sheaths the vascular tube containing the BBB. They feature proteins such as dystroglycan, dystrophin, and aquaporin 4. The astrocytic endfeet binds to the BM through protein interaction between dystroglycan-dystrophin-agrin binding and by this linkage a process that regulates water homeostasis in the CNS is established.[3,12] Astrocytes couple neuronal circuits to the blood vessels and by so doing relay signals that regulate blood flow in response to neuronal activity. They are also recognized as an important stabilizer of the BBB phenotype.[3]

Function of the BBB

The functions of BBB are to keep the ionic composition of the CNS optimal for neural signaling, exclude neuro-excitatory amino acid from causing neuro-excitatory neuronal damage, protect the brain from the damaging effects of circulating plasma proteins, and shield the CNS from circulating endogenous or exogenous neurotoxic substances.[1]

The BBB exhibits low passive permeability to many water-soluble nutrients and metabolites needs of nervous tissue and thus specific transporters are expressed by ECs to ensure an adequate supply of essential nutrients.[1] Because of the low passive permeability of the BBB to many essential water-soluble nutrients and metabolites needs of the CNS, specific transport systems are expressed in the BBB to enable the adequate supply of these molecules. The differential expression of specific transporter proteins in the luminal and abluminal membranes results in the polarity of the ECs.[12] In summary, the Interactions of the ECs with PCs, microglia and nerve terminals are crucial for supporting BBB induction, maintenance, and function.[13]

Contribution of BBB dysfunction to the pathogenesis of NDDs

Effects of aging and oxidative stress

Fluxes of molecules between the peripheral circulation and the CNS, and vice versa, are finely controlled by the BBB which is composed primarily of ECs, which in turn is regulated by astrocytes and pericytes. These interactions between EC and astroglial cells at the BBB, regulate and maintain the homeostasis of the brain metabolism.[1-3]

The BBB is sensitive to OS-induced damage and disruption, which in turn compromises the homeostasis of neural function and may be responsible for triggering neural pathogenesis. OS has been strongly associated with a number of physiological conditions, such as neural aging, vascular disorders, genetic risks, molecular irregularities, arising anatomical pathologies, and topographical incidences which relate to neurodegenerative disease (NDD).

Aging is an important contributing risk factor in the development of neurodegeneration and BBB disruption, occurring early in the aging human brain. Research has indicated that a higher incidence of age-related neurodegeneration begins in the hippocampus, a brain region associated with cognitive functions.[14,15] MRI quantification of regional BBB permeability in the living human brain indicated an age-dependent BBB breakdown in the hippocampus, a brain region affected early in AD.[16] The cognitive impairment associated with hippocampal BBB breakdown correlates with injury to BBB-associated pericytes.[1,17] The association of the stage at which the BBB breaks down and whether it causatively impacts cognitive impairment, is however, unsettled.

There is increasing evidence to support the contribution of BBB breakdown in the pathogenesis of NDDs such as PD, AD, ALS (amyotrophic lateral sclerosis), and MS (multiple sclerosis) as well as typical neurovascular disorders such as stroke and vascular dementia (VaD).[18] One of the implications of the number of vascular disorders such as hypertension, cerebrovascular disorder, and dysfunctional BBB is the increased permeability associated with neurodegeneration. Data from mouse transgenic models with BBB breakdown studies support the initiation and or contribution to neurodegeneration by

the accumulation of circulating proteins, free iron, iron-containing hemosiderin, and/or plasmin in the CNS neurons.[19] Emerging research on the overlap between the pathogenesis of VaD and AD is now found in the epidemiological studies that revealed that vascular risk factors such as diabetes mellitus (DM), hypertension, and atherosclerosis, which play an important role in the progression of AD but the mechanisms of these associations are yet unclear. Putative theories include the possibility that the cerebrovascular damage induced by these diseases could cause impaired cognitive function.[15] Examining the effects of hypertension on the pathological amyloid accumulation in mouse brain models demonstrated Aβ (amyloid-β peptide) deposition in the hypertensive brain which was associated with impaired BBB integrity. There is also evidence that some antihypertensive drugs restored cerebrovascular dysfunction via the reduction of OS and improved cognitive function in an AD mouse model.[15] Another study using diabetic AD mouse models showed that coexistence of the diabetic condition could lead to accelerated Aβ-related vascular alterations which were associated with induction of receptors for advanced glycation end products (RAGE) in the cerebral blood vessels. Many studies suggest that cerebrovascular dysfunction does not only play a role in VaD but also in the AD brain.[15]

Immuno-genetic factors

ApoE-Ɛ4 is a strong genetic factor for sporadic AD although the mechanism of how it impacts AD pathogenesis is not clear. The ApoE-Ɛ4 allele increases the accumulation of senile plaques in AD subjects as well as cognitively normal people. Recent findings showed that ApoE regulates cerebrovascular function via the cyclophilin A–nuclear factor-κB–matrix metalloproteinase-9 pathway in pericytes.[16] Some evidence is available to support the compromise of BBB integrity in AD preceding the development of amyloid plaques and cognitive impairment. Thus, functional changes in the BBB could be one of the earliest signs of AD.[15] It was also demonstrated that Aβ immunization therapy can restore BBB integrity in some mouse models and improve typical AD brain pathological features such as plaques and microgliosis. This suggests the possibility of a BBB-focused strategy for AD treatment.[15]

Postmortem tissue analysis of the AD brain showed evidence of BBB damage including accumulation of blood-derived proteins in the hippocampus and cortex of human subjects with AD and ALS, and degeneration of BBB-associated pericytes, which indicated BBB breakdown.[15,19] Tight junction protein function and transmembrane components are also affected in neurodegenerative disorders: occludin being vulnerable to degradation by MMPs, while the molecular connections of adherens junctions and tight junction proteins (TJPs) to the actin cytoskeleton are also disrupted by tau leading to tau-induced neurotoxicity. TJPs are also reported to be involved in RAGE-mediated Aβ cytotoxicity to the BBB ECs with subsequent damaged BBB structural integrity.[14]

There is the early development of neurovascular dysfunction in AD associated with the accumulation of Aβ peptide and NFTs in the brain.[19] Depending on the stage of the disease, AD affects all cell types of the NVU including EC and mural cells, glial, and neurons.[19] Faulty Aβ clearance from the brain leads to elevated Aβ in the brain of patients with sporadic AD.[19] Research data has shown from various animal models that Aβ is cleared from the brain primarily by trans-vascular clearance across the BBB.[20] The molecular mechanism involves the Aβ produced in the brain binding to LRP1 (low-density lipoprotein receptor-related protein-1) at the abluminal side of the BBB leading to its rapid internalization into ECs and subsequent clearance through the blood.[21] PICALM (phosphatidylinositol-binding clathrin assembly protein) plays a critical role in the molecular mechanism of Aβ clearance by directing the internalization, trafficking, and sorting of LRP1-Aβ complexes for exocytosis at the luminal side of the BBB.[19,21,22] Aβ is then cleared in the plasma by binding to soluble plasma LRP1 and subsequent transport via blood to the excretory organs (kidney and liver).[14,19] Other contributions to CNS clearance of Aβ peptide include enzymatic degradation by neprilysin, an insulin-degrading enzyme, MMPs plasmin, and tissue plasminogen activator.[19,22] Recent research data has suggested that PICALM variants, as well as mutation of Clusterin (CLU, apoJ), are also associated with the pathogenesis of sporadic AD.[19,22]

Role of OS in the development of neurodegenerative diseases

OS is a condition of unbalanced cellular and/or tissue redox states to which the brain is especially vulnerable because of its high oxygen demand, possession of abundant peroxidation-susceptible lipid cells, and modest content of antioxidant and related enzymes.[23] NDD is a heterogeneous group of neurological disorders characterized by a slow progressive neuronal loss.[23] Although the definitive cause of the NDD is yet uncertain, OS has been strongly implicated in playing a critical role in its initiation as well as progression. NDD has been strongly linked with aging and has thus been largely described as a disease of abnormal aging.[24] Alzheimer's disease, Parkinson's disease, Huntington's disease, and Friedreich's ataxia are well-known examples of NDD. The critical role played by OS has been reported in the pathogenesis of virtually all these diseases and thus OS appears to be a common denominator in their pathogenesis. Several mechanisms of OS regarding the initiation and/or its propagation have been reported for NNDs, especially for Alzheimer's disease (AD) and Parkinson's disease (PD).[18,24]

OS as an early event in the initiation and progression of AD

The evolution of AD incorporates an intermediate transient phase of mild cognitive impairment (MCI) during which there is no significant increase in senile plaques or neurofibrillary tangles (NFTs). Data from MCI subjects provided strong correlated evidence

that OS usually precedes the development of clinically demonstrable AD.[18,24] Significantly, elevated levels of oxidized biomolecular markers of OS, compared with age-matched control subjects, were found in MCI subjects.[11] Furthermore, in the urine, plasma, and CSF of MCI subjects elevated levels of specific isoprostanes were found, while CSF levels of markers such as Aβ peptides, and tau protein remain unchanged compared with controls with age-matched subjects.[23,24] Evidence of significantly increased levels of protein peroxidation and oxidative modification of specific proteins in the hippocampus, superior, and middle temporal gyri of MCI subjects has been documented.[18] Furthermore, several other studies also showed significantly decreased levels of nonenzymatic antioxidants such as uric acid, vitamin C, E, and A, zeaxanthin, β-cryptoxanthin, and α-carotene as well as reduced activity of antioxidant enzymes such as SOD, glutathione peroxidase, and glutathione reductase in MCI subjects.[15,23] Some of these biomolecules, especially the isoprostane (8,12-isoiPF2α-VI) is correlated with the severity of AD.[24] All these findings preceding the neuropathological findings in AD suggest that OS is a very early contributor to AD and is likely to play a critical role in the progression of the disease and probably other NDDs.

Sources of excess ROS production in NDDs

In spite of the telltale evidence of OS pathology in the brain, neither the specific origin of increased reactive oxygen species (ROS) nor the mechanisms for the dysfunction of endogenous antioxidant system or the disturbance of redox balance in AD and other NDDs are certain. However, both extracellular and subcellular accumulation of Aβ peptide and the presence of trace metal ions such as copper and iron have been suggested to cause increased ROS production.[18,23] Further, reduced activities of α-secretase can cause a decrease in β and γ-secretase activities which can further enhance Aβ peptide accumulation.[24] As the mitochondria are itself vulnerable to OS, increased ROS is associated with oxidation of mitochondrial proteins resulting in consequent mitochondrial dysfunction and energy production failure. Mitochondrial dysfunction and disordered glucose metabolism have been supported by overwhelming research data as a critical factor in the pathogenesis of AD.[18,24] Glucose is the primary source of energy in the brain, and the oxidation of enzymes involved in glucose metabolism leads to the consequential decline in glucose metabolism in AD.[18,24] Much evidence supports the hypothesis that the oxidation of crucial metabolic enzymes such as pyruvate kinase, phosphoglucomutase-1, enolase-1, triose phosphate isomerase, ATP-synthase, glyceraldehyde-3 phosphate dehydrogenase, malate dehydrogenase, leads to the reduced activities of these enzymes.[18] Parallel observations point to an OS-induced reduction in neuronal expression of genes encoding for subunits of the mitochondrial respiratory chain; reduced complex IV activity (Fig. 2) observed in the hippocampus and platelets of AD subjects.[18,23,24] The overall result is a dysfunctional glucose metabolism and reduced ATP generation in the AD brain which
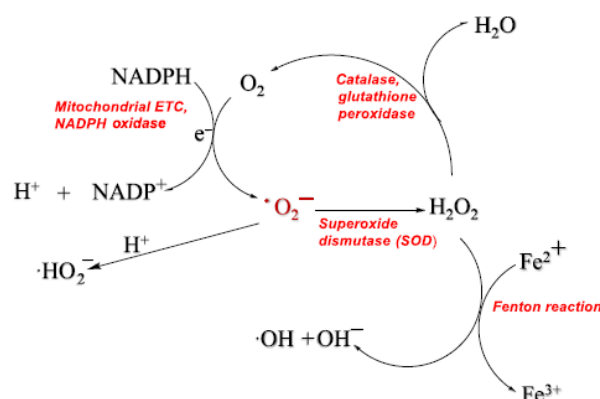
Fig. 2 Downstream propagation of ROS from primary ROS, the superoxide radical. Superoxide radical is the first free radical generated from the ETC and the cellular oxidases. Its reactivity results in the generation of several other species.

further leads to increased mitochondrial ROS generation. Furthermore, Aβ-induced mitochondrial dysfunction has also been reported as a cause of impaired calcium homeostasis in AD brain.[23] This may be associated with intracellular calcium overload and decreased calcium reuptake which is related to increased ROS, and the opening of the permeability transition pore (PTP) which is an important step in the ferrying of proapoptotic molecules across the mitochondria into the cytosol, triggering subsequent apoptosis. In PD, accumulation of α-synuclein aggregates which interferes with vesicular dopamine storage, leading to a build-up of cytosolic dopamine which interacts with trace metal ions, such as iron, to generate ROS.[16,17] Further, supporting this school of thought, a number of reports indicate the metabolism of dopamine into semiquinones, auto-oxidation into ROS, as well as the deficiency of complex I enzyme of the mitochondrial respiratory chain.[17,18,23]

Evidence of OS involvement in the development of NDDs

Research has demonstrated that an increase in oxidized biomolecules generated by ROS as well as changes in cellular content of antioxidant molecules as corroborative evidence of OS in several NDDs including AD and PD. This line of action is premised on the difficulty in measuring ROS, which is usually short lived and are kept at modestly low concentrations by a dynamic balance between the rates of cellular production and neutralization by endogenous antioxidants, leaving empirically either excessive ROS production or impaired antioxidant systems to cause OS. Alterations in the levels of antioxidants and antioxidant enzyme activities were also reported in AD and other NDDs.[24] Significantly low plasma levels of antioxidants such as glutathione, albumin, lycopene, bilirubin, vitamin A, C, and E, were reported in AD patients compared with age-matched control subjects.[24] Furthermore, different brain areas in AD also showed significant

decreases in the activity of endogenous antioxidant enzymes such as superoxide dismutase (SOD), catalase, glutathione peroxidase, and heme-oxygenase despite increased gene expression of some of these enzymes.[23,24]

Reactive oxygen species

ROS are generated as by-products of the incomplete reduction of an oxygen molecule, an inevitable occurrence in all aerobic cells. They are therefore defined as a group of highly reactive chemical species containing oxygen with various numbers of unpaired valence electrons.[23,25] They generally have a short half-life, 1 ns for the hydroxyl radical,[26] due to their high reactivity conferred by the presence of unpaired electron(s). Free radicals such as the superoxide molecule ($^{\bullet}O_2^-$) and hydroxyl radical ($^{\bullet}OH$) as well as nonradicals such as hydrogen peroxide (H_2O_2) are examples of ROS. The superoxide radical is the primary ROS generated in cells while other molecules, inclusive of the list of ROS, are all secondary derivatives of downstream reactions involving the superoxide radical and other biomolecules.

The presence of ROS in the cell produces effects reminiscent of a double-edged sword: under physiological conditions, it can serve a number of beneficial roles such as cell signaling that mediates growth, differentiation, proliferation, and ROS-mediated microbial killing.[27] On the other hand, its accumulation under conditions of oxidative stress (OS) mediates modification of cellular biomolecules with consequent functional aberrations causing pathological programmed cell death (PCD), atherosclerosis, diabetes, dysfunctional cell proliferation, neurodegeneration, inflammation, and aging.[27] These oxidants were originally thought to be host defender molecules, released by neutrophils to destroy infective microbial organisms such as bacteria, but in the light of current knowledge, they play critical roles in the determination of the cell's fate as they act as second messengers which modify cell-signaling molecules.[27]

Most aerobic cells have evolved with an antioxidant defense system responsible for neutralizing ROS and so prevent its accumulation such that a dynamic equilibrium is maintained between ROS production and neutralization within the cell. However, under various circumstances, this equilibrium may be disturbed, which, when in favor of a net increase in ROS results in OS. OS causes ROS-mediated damage to cellular biomolecules such as proteins, nucleic acids, and lipids as implicated in cancer initiation and progression, neurodegeneration and aging, atherosclerosis, and diabetes.[27]

Generation of reactive oxygen species

All aerobic cells, including neuron and ECs, produce ROS, mediated mainly by enzymes. The generation of cellular ROS involves both endogenous and exogenous sources. In vascular ECs, the main endogenous sources of ROS include NADPH

oxidases (Nox), the mitochondrial electron transport chain (ETC), xanthine oxidase, cytochrome P450, and uncoupled endothelial NO synthase (eNOS).[28] The importance of each of the proteins varies with the physiological state of specific tissues.[29] Exogenous generation in general involves cellular interaction with exogenous sources such as xeno-biotics, radiation, UV light, air pollution, cytokines, bacterial invasion, and cigarette smoking[28] (Fig. 3).

Role of antioxidant therapy in neurologic disorders

In view that OS has been a well-documented factor in the initiation and progression of neurological diseases including NDDs, it becomes rational to propose the use of exogenous antioxidants for the amelioration of the cumulative effects of OS.

What are antioxidants?

An antioxidant is defined as any substance that, when present at low concentrations compared to an oxidizable substrate, significantly delays or prevents oxidation of that substrate.[30] Several distinct dietary compounds with antioxidant properties have been identified and studied such as polyphenols (flavonoids), β-carotene, vitamin C, and vitamin E (α-tocopherol).

Evidence of the ameliorative effects of dietary antioxidants on neurodegenerative diseases

Dietary polyphenols

Epidemiological and clinical studies have demonstrated that polyphenols and flavonoids exert a protective effect against NDDs.[31] Several authors have reported that diets enriched with fruits and vegetables rich in antioxidants (carrots, blueberries, strawberries, spinach) can produce a beneficial effect in old rats against age-related decline in cognitive functions.[16] Polyphenols are naturally present in fruits and vegetables (olive oil, red wine, tea) with flavonoids being the largest group of the polyphenols with more than 2000 distinct flavonoids known.[32] They naturally occur as glycosylated, hydroxylated, and methoxylated phenol derivatives.[33] The glycosylated form either contains glucose or rhamnose as the sugar moiety.[32] By glycosylation, the chemical, physical and biological properties of the flavonoids are moderated as well as their absorption by the small intestine.[34] Their antioxidant potency is related to the number of hydroxyl groups present such that the most potent of flavonoids contains 3–6 hydroxyl groups.[35] There is a paucity of data on the bioavailability of phenolics after oral intake, however, the increase in the serum antioxidant levels following consumption of food and beverages rich in
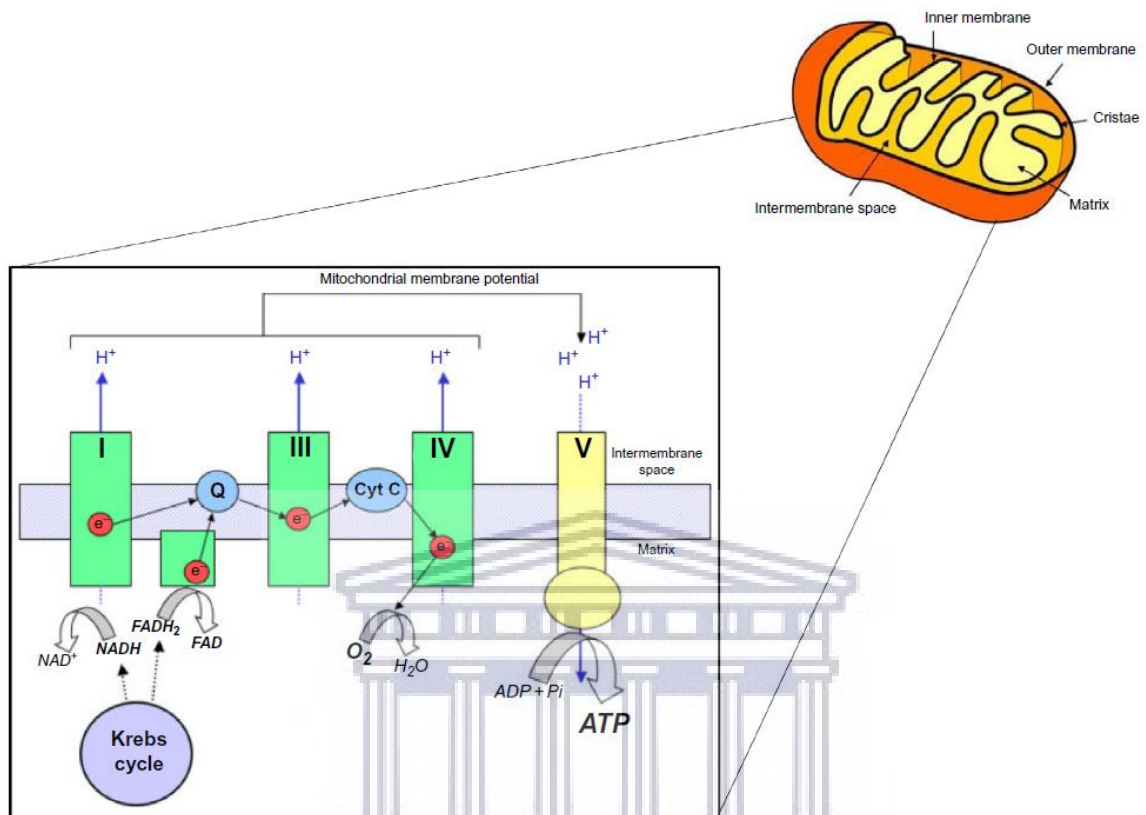
Fig. 3 The electron transport chain generates ATP while producing superoxide as a by-product. The electron transport chain (ETC) in the mitochondria is the site of oxidative phosphorylation in mammalian cells. The ETC is a series of electron transporters in the inner mitochondria membrane which transfer electrons from NADH and FADH$_2$ to molecular O$_2$. At the same time, protons are pumped from the mitochondrial matrix to the intermembrane space while O$_2$ is reduced to form water.

polyphenols has been reported.[36] Taken together, these findings suggest that the consumption of polyphenolic compounds could have beneficial effects against OS-induced damages.

Ameliorative effects of dietary polyphenols

For the purposes of this chapter, we discussed the widely used exemplar of exogenous AOs, green tea. The flavonoids in green tea have attracted considerable research interest because of its potential to prevent or treat cancer.[32,37] Bioactive constituents of green tea include flavonoids (catechins and their derivatives) and it constitutes about 30% of the dry weight of a leaf.[37] Analysis of green tea using HPLC yields mainly epigallocatechin-3-gallate (EGCG) as the polyphenolic constituent (more than 60% of total catechins).[37] Other compounds in green tea are the flavonols (quercetin, kaempferol, and rutin), caffeine, phenolic acids, and theanine.[37,38]

Reports from nutritional and epidemiological studies as well as an animal model of PD revealed risk reduction for Parkinson's disease by the consumption of teas with high AO content such as green and black teas. These effects have been ascribed to EGCG, which is the most potent component of green tea.[39,40] Green tea compounds also act as a chelator of ferric ion which could also explain the green tea-induced-protection against MPTP[40] since MPTP is known to increase iron levels in the substantia nigra pars compacta of mice, rats, and monkeys. While there is no significant benefit with regard to tea consumption in AD, several in vitro studies showed that green tea could protect against Aβ-induced neuronal damages.[40,41]

In the last decade, studies have provided multiple confirmations that EGCG is able to regulate the proteolytic processing of amyloid-precursor protein in both in vivo and in vitro studies.[41] In neuronal cell cultures, it promotes the nonamyloidogenic α-secretase pathway[41] and reduces the formation of Aβ fibrils.[41] EGCG-mediated promotion of neuronal protection has also been linked to its ability to modulate a number of intracellular signaling pathways such as MAPK, protein kinase C, and phosphatidylinositol-3-kinase (PI3K).[32,42] These pathways play important roles in neuronal protection against a variety of redox insults and are essential to cell survival.[27] EGCG also lowers the expression of the proapoptotic genes Bax, Bad, cell cycle inhibitor Gadd45, Fas ligand, and tumor necrosis factor-related apoptosis ligand (TRAIL) in SH-SY5Y neuroblastoma cells.[43]

Beneficial effects were mediated via antioxidant potential, through modulation of different pathways such as signaling cascades, antiapoptotic processes, and synthesis or degradation of Aβ peptide.[32]

Overindulgence of dietary AOs: Reductive stress

Under physiologic conditions, the redox system within the cells and the entire body is maintained at a redox balance by the action of the endogenous antioxidant system that

neutralizes excess ROS. Under pathologic conditions resulting from redox imbalance, the endogenous antioxidant system either fails to contain the challenge of ROS production or the rate of ROS production becomes excessive.[23] Research data has supported the use of exogenous antioxidants (such as vitamin C and vitamin E, and polyphenols) supplementation of diet as beneficial in the treatment and/or amelioration of diseases conditions mechanistically impacted by redox imbalance.[37] However, several reports have documented the adverse effects of exogenous AO treatment on cellular physiology, which include modulatory effects on cell signals involved in critical cell functions such as proliferation, senescence, cell growth, and apoptosis.[27] The overzealous use of antioxidants therefore, has the potential to impact negatively the normal and beneficial effects of ROS in biologic systems which can lead to undesirable conditions of reductive stress.[44] Furthermore, because the beneficial effects of antioxidant clinical trials on many clinical conditions had largely yielded modest benefit, some authors have suggested the overuse of exogenous AOs may indeed cause a "prooxidant" effect (reductive stress).[44]

Conclusion

It is not completely clear whether it is NDD that causes BBB dysfunction or vice versa, but what is conspicuous is that the two conditions are inextricably related. It is also very clear that OS is a physiological trigger that is linked to NDD and that it is also capable of causing the compromise of BBB function. The compromise of BBB function is linked to irregular permeability between the blood and brain, and this relates to homeostatic instability within the brain. Together with the co-effects of OS on the BBB and neurons, this may be responsible for the progressive nature of NDD. The benefits of dietary foods rich in antioxidants in delaying the progression of NDDs must be carefully weighed against the prooxidant (reductive stress) effects of overdosing with exogenous AOs, especially pharmaceuticals.

Summary points

- The BBB regulates the transport of molecules between the brain and the circulation and is sensitive to oxidative stress.
- Aging is an important risk factor for degenerative neuropathy which has in turn been linked to oxidative stress and blood-brain barrier disruption.
- Oxidized biomarkers accumulate long before the development of cognitive impairment in AD and suggest that OS is an early component of neurodegeneration.
- The specific source of increased ROS and the focus of redox imbalance in NDD are not clearly defined.
- Dietary antioxidants have been demonstrated to ameliorate the process of neurodegeneration.

References

1. Abbott NJ, Patabendige AA, Dolman DE, Yusof SR, Begley DJ. Structure and function of the blood-brain barrier. *Neurobiol Dis* 2010;**37**(1):13–25.
2. Liebner S, Dijkhuizen RM, Reiss Y, Plate KH, Agalliu D, Constantin G. Functional morphology of the blood-brain barrier in health and disease. *Acta Neuropathol* 2018;**135**(3):311–36.
3. Daneman R, Prat A. The blood-brain barrier. *Cold Spring Harb Perspect Biol* 2015;**7**(1):a020412.
4. Serlin Y, Shelef I, Knyazer B, Friedman A, editors. Anatomy and physiology of the blood-brain barrier. In: *Seminars in cell & developmental biology*. Elsevier; 2015.
5. Blanchette M, Daneman R. Formation and maintenance of the BBB. *Mech Dev* 2015;**138**:8–16.
6. Haddad-Tóvolli R, Dragano NR, Ramalho AF, Velloso LA. Development and function of the blood-brain barrier in the context of metabolic control. *Front Neurosci* 2017;**11**:224.
7. Shepro D, Morel N. Pericyte physiology. *FASEB J* 1993;**7**(11):1031–8.
8. Armulik A, Genové G, Betsholtz C. Pericytes: developmental, physiological, and pathological perspectives, problems, and promises. *Dev Cell* 2011;**21**(2):193–215.
9. Sorokin L. The impact of the extracellular matrix on inflammation. *Nat Rev Immunol* 2010;**10**(10):712.
10. Yang C, Candelario-Jalil E. Role of matrix metalloproteinases in brain edema. In: *Brain edema*. Elsevier; 2017. p. 199–215.
11. Montagne A, Zhao Z, Zlokovic BV. Alzheimer's disease: a matter of blood-brain barrier dysfunction? *J Exp Med* 2017;**214**(11):3151–69.
12. Wolburg H, Wolburg-Buchholz K, Fallier-Becker P, Noell S, Mack AF. Structure and functions of aquaporin-4-based orthogonal arrays of particles. In: *International review of cell and molecular biology*. **287**. Elsevier; 2011. p. 1–41.
13. Nakagawa S, Deli MA, Kawaguchi H, Shimizudani T, Shimono T, Kittel A, et al. A new blood-brain barrier model using primary rat brain endothelial cells, pericytes and astrocytes. *Neurochem Int* 2009;**54**(3–4):253–63.
14. Erdő F, Denes L, de Lange E. Age-associated physiological and pathological changes at the blood-brain barrier: a review. *J Cereb Blood Flow Metab* 2017;**37**(1):4–24.
15. Takeda S, Sato N, Morishita R. Systemic inflammation, blood-brain barrier vulnerability and cognitive/non-cognitive symptoms in Alzheimer disease: relevance to pathogenesis and therapy. *Front Aging Neurosci* 2014;**6**:171.
16. Nissanka N, Moraes CT. Mitochondrial DNA damage and reactive oxygen species in neurodegenerative disease. *FEBS Lett* 2018;**592**(5):728–42.
17. Blesa J, Trigo-Damas I, Quiroga-Varela A, Jackson-Lewis VR. Oxidative stress and Parkinson's disease. *Front Neuroanat* 2015;**9**(91).
18. Tramutola A, Lanzillotta C, Perluigi M, Butterfield DA. Oxidative stress, protein modification and Alzheimer disease. *Brain Res Bull* 2017;**133**:88–96.
19. Zhao Z, Nelson AR, Betsholtz C, Zlokovic BV. Establishment and dysfunction of the blood-brain barrier. *Cell* 2015;**163**(5):1064–78.
20. Deane R, Bell R, Sagare A, Zlokovic B. Clearance of amyloid-β peptide across the blood-brain barrier: implication for therapies in Alzheimer's disease. *CNS Neurol Disord Drug Targets* 2009;**8**(1):16–30.
21. Garcia-Castillo MD, Chinnapen DJ-F, Lencer WI. Membrane transport across polarized epithelia. *Cold Spring Harb Perspect Biol* 2017.
22. Zhao Z, Sagare AP, Ma Q, Halliday MR, Kong P, Kisler K, et al. Central role for PICALM in amyloid-β blood-brain barrier transcytosis and clearance. *Nat Neurosci* 2015;**18**(7):978.
23. Kim GH, Kim JE, Rhie SJ, Yoon S. The role of oxidative stress in neurodegenerative diseases. *Exp Neurobiol* 2015;**24**(4):325–40.
24. Wang X, Wang W, Li L, Perry G, Lee H-g, Zhu X. Oxidative stress and mitochondrial dysfunction in Alzheimer's disease. *Biochim Biophys Acta (BBA)—Mol Basis Dis* 2014;**1842**(8):1240–7.
25. Circu ML, Aw TY. Reactive oxygen species, cellular redox systems, and apoptosis. *Free Radic Biol Med* 2010;**48**(6):749–62.
26. Singh R, Devi S, Gollen R. Role of free radical in atherosclerosis, diabetes and dyslipidaemia: larger-than-life. *Diabetes Metab Res Rev* 2015;**31**(2):113–26.

27. Zhang J, Wang X, Vikash V, Ye Q, Wu D, Liu Y, et al. ROS and ROS-mediated cellular signaling. *Oxid Med Cell Longev* 2016;**2016**.

28. Alom-Ruiz SP, Anilkumar N, Shah AM. Reactive oxygen species and endothelial activation. *Antioxid Redox Signal* 2008;**10**(6):1089–100.

29. Galadari S, Rahman A, Pallichankandy S, Thayyullathil F. Reactive oxygen species and cancer paradox: to promote or to suppress? *Free Radic Biol Med* 2017;**104**:144–64.

30. Halliwell B, Gutteridge JMC. The definition and measurement of antioxidants in biological systems. *Free Radic Biol Med* 1995;**18**(1):125–6.

31. Samieri C. Epidemiology and risk factors of Alzheimer's disease: a focus on diet. In: *Biomarkers for pre-clinical Alzheimer's disease*. Springer; 2018. p. 15–42.

32. Ramassamy C. Emerging role of polyphenolic compounds in the treatment of neurodegenerative diseases: a review of their intracellular targets. *Eur J Pharmacol* 2006;**545**(1):51–64.

33. Xie Y, Chen X. Structures required of polyphenols for inhibiting advanced glycation end products formation. *Curr Drug Metab* 2013;**14**(4):414–31.

34. Cao H, Chen X. Structures required of flavonoids for inhibiting digestive enzymes. *Anti-Cancer Agents Med Chem* 2012;**12**(8):929–39.

35. Chen L, Teng H, Xie Z, Cao H, Cheang WS, Skalicka-Woniak K, et al. Modifications of dietary flavonoids towards improved bioactivity: an update on structure–activity relationship. *Crit Rev Food Sci Nutr* 2018;**58**(4):513–27.

36. Oh WY, Shahidi F. Antioxidant activity of resveratrol ester derivatives in food and biological model systems. *Food Chem* 2018;**261**:267–73.

37. Sakaki J, Melough M, Lee SG, Pounis G, Chun OK. Polyphenol-rich diets in cardiovascular disease prevention. In: *Analysis in nutrition research*. Elsevier; 2019. p. 259–98.

38. Zhang C, Suen CL-C, Yang C, Quek SY. Antioxidant capacity and major polyphenol composition of teas as affected by geographical location, plantation elevation and leaf grade. *Food Chem* 2018;**244**:109–19.

39. Pan T, Fei J, Zhou X, Jankovic J, Le W. Effects of green tea polyphenols on dopamine uptake and on MPP+-induced dopamine neuron injury. *Life Sci* 2003;**72**(9):1073–83.

40. Bastianetto S, Yao ZX, Papadopoulos V, Quirion R. Neuroprotective effects of green and black teas and their catechin gallate esters against β-amyloid-induced toxicity. *Eur J Neurosci* 2006;**23**(1):55–64.

41. Singh N, Ghosh KK. Recent advances in the antioxidant therapies for Alzheimer's disease: emphasis on natural antioxidants. In: *Pathology, prevention and therapeutics of neurodegenerative disease*. Springer; 2019. p. 253–63.

42. Rodríguez-Morató J, Boronat A, Dierssen M, de la Torre R. Neuroprotective properties of wine: implications for the prevention of cognitive impairment. In: *Role of the Mediterranean diet in the brain and neurodegenerative diseases*. Elsevier; 2018. p. 271–84.

43. Levites Y, Amit T, Youdim MB, Mandel S. Involvement of protein kinase C activation and cell survival/cell cycle genes in green tea polyphenol (−)-epigallocatechin-3-gallate neuroprotective action. *J Biol Chem* 2002;**277**(34):30574–80.

44. Mentor S, Fisher D. Aggressive antioxidant reductive stress impairs brain endothelial cell angiogenesis and blood brain barrier function. *Curr Neurovasc Res* 2017;**14**(1):71–81.

Further reading

Hendricks BK, Cohen-Gadol AA, Miller JC. Novel delivery methods bypassing the blood-brain and blood-tumor barriers. *Neurosurg Focus* 2015;**38**(3):E10.